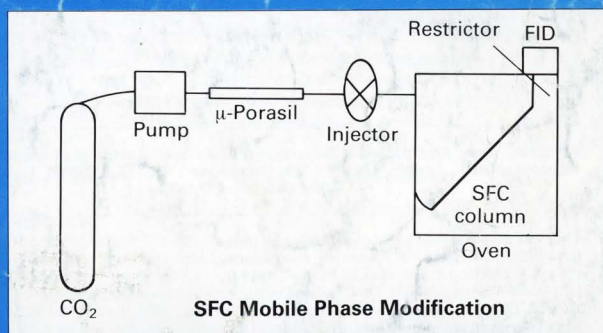THE ROYAL SOCIETY OF CHEMISTRY
PRUDENTIA HUMANITATE
Founded 1841

The
Analyst

An international journal dealing with all branches of

the theory and practice of analytical chemistry

SFC Mobile Phase Modification

The Analyst

The Analytical Journal of The Royal Society of Chemistry

Information for Authors

Full details of how to submit material for publication in *The Analyst* are given in the Instructions to Authors in the January issue. Separate copies are available on request.

The Analyst publishes papers on all aspects of the theory and practice of analytical chemistry, fundamental and applied, inorganic and organic, including chemical, physical, biochemical, clinical, pharmaceutical, biological, environmental, automatic and computer-based methods. Papers on new approaches to existing methods, new techniques and instrumentation, detectors and sensors, and new areas of application with due attention to overcoming limitations and to underlying principles are all equally welcome. There is no page charge.

The following types of papers will be considered:

Full research papers.

Communications, which must be on an urgent matter and be of obvious scientific importance. Rapidity of publication is enhanced if diagrams are omitted, but tables and formulae can be included. Communications receive priority and are usually published within 5–8 weeks of receipt. They are intended for brief descriptions of work that has progressed to a stage at which it is likely to be valuable to workers faced with similar problems. A fuller paper may be offered subsequently, if justified by later work. Although publication is at the discretion of the Editor, communications will be examined by at least one referee.

Full critical reviews, which must be a critical evaluation of the existing state of knowledge on a particular facet of analytical chemistry.

Every paper (except Communications) will be submitted to at least two referees, by whose advice the Editorial Board of *The Analyst* will be guided as to its acceptance or rejection. Papers that are accepted must not be published elsewhere except by permission. Submission of a manuscript will be regarded as an undertaking that the same material is not being considered for publication by another journal.

Regional Advisory Editors. For the benefit of potential contributors outside the United Kingdom and North America, a Group of Regional Advisory Editors exists. Requests for help or advice on any matter related to the preparation of papers and their submission for publication in *The Analyst* can be sent to the nearest member of the Group. Currently serving Regional Advisory Editors are listed in each issue of *The Analyst.*

Manuscripts (four copies typed in double spacing) should be addressed to:

H. S. Minhas, Editor, *The Analyst* or J. F. Tyson, US Associate Editor, *The Analyst*

Particular attention should be paid to the use of standard methods of literature citation, including the journal abbreviations defined in Chemical Abstracts Service Source Index. Wherever possible, the nomenclature employed should follow IUPAC recommendations, and units and symbols should be those associated with SI.

All queries relating to the presentation and submission of papers, and any correspondence regarding accepted papers and proofs, should be directed either to the Editor, or Associate Editor, *The Analyst* (addresses as above). Members of the Analytical Editorial Board (who may be contacted directly or via the Editorial Office) would welcome comments, suggestions and advice on general policy matters concerning *The Analyst.*

Fifty reprints are supplied free of charge.

Editorial

Any scientific research or investigation must be based on two foundations.

1. Careful observation of a well designed experiment.
2. Truthful reporting of those observations.

The intention here is to discuss only the second of these points, taking the first as read. Traditionally, scientific observations are reported in scientific journals such as this one. The editorial management has to walk a tightrope, ensuring that on the one hand all papers containing sound work, which falls within the remit of the journal, are included, and on the other that the size and content of the journal are such as to justify commercial publication. In order to ensure soundness of work, all respectable journals make use of referees.

A referee's task is to vet papers in terms of scientific content and general fitness for publication. No referee wants to reject a paper unless it fails to come up to standard. Nevertheless some standards must be set. As recent guidelines put it,

'A referee . . . should judge objectively the quality of the manuscript, of its experimental and theoretical work, of its interpretations and its exposition, with due regard to the maintenance of high scientific and literary standards. A referee should respect the intellectual independence of the authors'.

Unfortunately, the increase in higher education and the insistence, whether explicit or implied, that no aspiring postgraduate will receive his or her doctorate without at least one publication, has led to an enormous explosion in papers being submitted for publication. Equally unfortunately, the majority of such papers, however well written, are of little interest to the scientific world at large. The problem is especially pronounced with papers reporting spectrophotometric methods for metals and this aspect was discussed by Colin Watson seven years ago.[2] This was followed by an Editorial Board decision broadly in line with the aforementioned article, which was communicated to referees but not in its entirety to prospective authors, that such papers should be rejected

'unless the work constitutes a highly significant development in the field of analysis'.

The problem is, how to cope with such vast numbers of papers within the confines of the publication system, and this poses a considerable problem for the referee. It used to be generally accepted that any piece of sound scientific work that had not been previously reported was acceptable for publication. Indeed I have heard the argument (seriously put) that even negative results should be published in order to avoid other workers wasting their time. Unfortunately, the number of papers submitted has continued to rise and clearly the need to limit the number of such publications is important. As a referee, I am often distressed by the quality of some of the papers offered. Referees like to see good scientific work crowned by a solid, worthwhile publication, yet many a good piece of research is spoilt by the quality of its presentation to the potential publisher.

In my view, in order to justify publication the submitted script needs to meet the following criteria.

(a) The work must be novel. One assumes that no one commences bench work without first conducting a thorough literature search. At the same time, a research project which merely substitutes a reagent analogous to, but different from, one in a published paper ought not to be accepted unless there is a substantial gain in analytical performance.

(b) The work should either be of fundamental scientific interest or it should be of practical use, filling a clear need.

(c) The methodology used should be appropriate and up to date. A 'new' reagent for an analyte, for which many other good reagents are already available, or where perhaps most workers would use an alternative technique, is not worth publishing unless there are sound justifications for its use. However, there may be some justification in work on a new reagent for which adequate alternatives exist, if the new reagent has some special merit, e.g., use in the field in remote or primitive areas, and where there is a genuine need to meet that requirement. This feature of the work should then be made clear in the text.

(d) The paper should include a full discussion of alternative methods, explaining why this 'new' method is being offered.

(e) It should include adequate statistical detail, including correlation with at least one, preferably the most commonly used, of the accepted 'standard' methods. A paper where the experimental work is minimal and which contains no comparative study of existing methods can not be acceptable.

(f) It should be presented logically, clearly and in reasonable English. Of course editors and referees will and do make allowances for authors whose primary language is not English.

It follows therefore, that automatic rejection should result from one or more of the following faults (other referees may wish to extend this list):

(a) 'Me-tooism'—papers which follow so predictably and logically from previous work that they didn't need to be written.

(b) Papers which claim improvements in method, simplicity, sensitivity or selectivity without producing any evidence of this, or where the claimed 'improvements' are vanishingly small.

(c) Papers which quote no comparison with other, more generally accepted methods.

(d) Papers which quote no applications data.

(e) Papers in which a method is developed for the sake of producing a publication, where there is no possibility of the method being used in any other laboratory.

Finally, with the exception of methods for use in the field, spectrophotometric methods should only be published if they can be automated, either using specifically built equipment or by utilizing flow injection methodology.

Dr. M. A. Russell

References

1 Ethical Guidelines to Publication of Chemical Research, *Anal. Chem.*, 1992, **64**, 109.
2 Watson, C., *Analyst*, 1986, **111**, 1353.

EIRELEC 1993
Electrochemistry to the year 2000

September 11–15
Adare, Co. Limerick, Ireland

Scientific Programme

An international conference dealing with recent advances in electrochemical methodology, technology and sensors will be held at the Dun Raven Arms Hotel, Adare, Co. Limerick, Ireland. The programme will consist of plenary, invited and contributed oral papers and posters, and will be organized to allow for maximum discussion of papers.

Plenary lectures will be given by:

Professor A. Bard (USA)
Professor J.O.M. Bockris (USA)
Professor J. Wang (USA)

A strong programme of invited and contributed lectures is currently being organized.

Location

Adare is a small, picturesque, historical village located just a short drive from Shannon International Airport (approx. 35 min). The village has been chosen because of the large range of activities it can provide, both cultural and sporting, and ample opportunity will be given to savour the local environment.

The conference will be based in the "Olde Worlde" atmosphere of the Dun Raven Arms Hotel; a large range of accommodation is available within and close to Adare, ranging from the world renowned Adare Manor to pleasant bed and breakfast type lodgings. An option has been taken on several family holiday cottages within the town and these will be available to those delegates wishing to be accompanied by their families.

Publication

We have planned to publish a Special Issue of *The Analyst* based on the papers and posters that will be presented at this conference, and authors of invited and contributed papers will be encouraged to submit their papers to Professor M.R. Smyth at the address given below before, or at, the meeting.

Those wishing to submit abstracts (1 page A4) or to obtain further details of the meeting should contact Professor Smyth.

The second circular for this meeting will be available in April 1993 and will contain full details of registration fees, accommodation, *etc*.

Contact Address :   Professor M.R. Smyth,
School of Chemical Sciences, Dublin City University,
Dublin 9, Ireland.
Tel: +353-1-7045308; Fax: +353-1-7045503

Efficacy of Robust Analysis of Variance for the Interpretation of Data From Collaborative Trials

Michael Thompson, Bart Mertens and Margalith Kessler
Department of Chemistry, Birkbeck College, Gordon House, 29 Gordon Square, London, UK WC1H 0PP
Tom Fearn
Department of Statistical Science, University College London, Gower Street, London, UK WC1E 6BT

The Analytical Methods Committee (AMC) robust analysis of variance method has been compared with the Harmonized Protocol for the interpretation of data from collaborative trials. Many data sets, representing the extremes of concentration and precision, have been selected from published studies and subjected to the two methods for calculating estimates of the mean and the variances of repeatability and reproducibility. In addition the variabilities of the statistics have been investigated by the bootstrap method. The conclusion is that the AMC robust procedure is considerably more reliable than the Harmonized Protocol. Although the two methods give quite close results generally, the variability of the estimates produced by the Harmonized Protocol is considerably greater because of the masking of outliers. Even the robust method gives estimates that are more variable than expectations based on normal distribution theory.

Keywords: *Collaborative trial; Harmonized Protocol; robust statistics; outlier; analysis of variance; bootstrap*

The collaborative trial has long been recognized as an essential step in validating an analytical method and establishing its performance characteristics prior to its recognition as a standard method. The collaborative trial is nominally a randomized replicated experiment, although in practice the participating laboratories are rarely selected on a random basis. Analysis of variance (ANOVA) is the obvious method of interpreting the results of collaborative trials, in terms of a grand mean, μ, a between-laboratory effect with variance, σ_L^2, and a within-laboratory variance, σ_r^2. These parameters are conventionally regarded as properties of the analytical method. In recent times σ_r^2 has been called the variance of repeatability and $\sigma_R^2 = \sigma_L^2 + \sigma_r^2$ called the variance of reproducibility. A knowledge of σ_r for an analytical system permits the prediction of differences between the results obtained in one laboratory, while σ_R provides corresponding information for results obtained from two different laboratories. The corresponding relative standard deviations, RSD_r and RSD_R, are also in common use.

A number of variant approaches to the interpretation of data from collaborative trials have been proposed[1-7] and various bodies[8-10] including the International Organization for Standardization (ISO)[11] have issued protocols for conducting and interpreting them. By far the greatest controversy surrounds the question of the treatment of outlying results. Recent international activity by ISO, the International Union of Pure and Applied Chemistry (IUPAC) and the Association of Official Analytical Chemists (AOAC) has resulted in the adoption of the Harmonized Protocol,[12] which *inter alia* prescribes the exclusion of outliers by Grubb's and Cochrane's tests. Despite this, outlier exclusion is not universally accepted within the analytical community.[7]

A modern approach to the treatment of data containing outliers is called robust statistics.[13-14] Robust statistics are applied to data that are essentially normally distributed, but are contaminated with a minor proportion of outliers, or with 'heavy tails'. These features are typical of analytical data, where the accumulation of numerous, small independent errors in the various stages of the analytical procedure tends to give rise to a normal distribution, but the occasional large errors (perhaps due to contamination, mistakes in procedure or transcription errors) give rise to outliers. Therefore, robust methods seem to be ideally suited to the treatment of analytical data.

Robust statistics such as means and variances are estimated by accommodating, rather than by excluding, outlying results and, therefore, no tests of significance are required as part of the estimation procedure. The estimates are descriptors of the 'good' part of the data. The most effective of the robust estimators have to be calculated by the iterative application of an algorithm. Although the procedure is not difficult, a computer is needed for this task because the convergence is inconveniently slow for manual calculation.

The use of robust ANOVA for the interpretation of collaborative trial data has been proposed by Lischer[15] and the Analytical Methods Committee (AMC).[16] The AMC paper provides a FORTRAN program for executing robust ANOVA on collaborative trial data.

The properties of a particular method of robust ANOVA are inherent in the algorithm, but can also be explored by simulation or by the bootstrap method.[17] In simulation tests the AMC program gives good results and can eliminate the effect of reasonable proportions of both analytical outliers (*i.e.*, discordant replicates within a laboratory) and outlying laboratories. However, reassuring as simulation results are there is always some fear that 'real' data sets, with all of their peculiarities, may cause complex problems that give rise to incorrect information.

In this paper the statistics produced by the AMC program are compared with those produced by the Harmonized Protocol approach, making use of a substantial amount of representative 'real data'. The data were taken from the reports of two trials and were selected to represent the extremes of analyte concentration range. Data for crude protein determined by the Kjeldahl method represented the upper concentration ranges (10–100% m/m) and good precision ($RSD_R \approx 2\%$ and $RSD_r \approx 1.5\%$). Data for aflatoxins represented the lowest concentrations for which trial data were available (0–12 ppb) and poor precisions ($RSD_R \approx 40\%$ and $RSD_r \approx 20\%$, typically).

Experimental

Data Sources

Kane[18] described a double collaborative trial in which 26 animal feedstuffs and related materials were analysed for Kjeldahl protein in duplicate in 22 laboratories by two variants of the procedure. The results of one procedure (using a copper sulfate catalyst) are used here. A collaborative trial of a method for the determination of aflatoxins[19] was also used. The results obtained at each individual level of analyte in both

of these trials were subjected to separate comparison of the statistical methods.

Basic Statistics

Data were entered manually from the original papers into a statistical spreadsheet on a personal computer and subjected to a number of tests for reliable transcription. The data sets were then subjected to classical one-way ANOVA, to the Harmonized Protocol, and to robust one-way ANOVA in their original states. Calculations were performed with an authentic copy of the FORTRAN program provided by the AMC.[16]

Bootstrap Method

The variability of the results from the three methods was assessed using bootstrap samples drawn from the Kjeldahl protein data sets. The calculations were programmed in GAUSS (Aptech Systems, Maple Valley, WA 98038, USA). The GAUSS routine was used to calculate the robust estimates and the results were compared with those obtained with the AMC FORTRAN program, and found to give identical results (apart from round-off errors).

The bootstrap is a useful and established method of obtaining the standard errors and distributions of complex statistics, such as robust estimates, that cannot be calculated analytically. In the context of collaborative trials, the bootstrap method reveals the likely outcome of repeating the trial a large number of times (often about 1000 times), with random selection each time from an infinite population of laboratories of comparable ability. While the bootstrap method can occasionally give aberrant results due to an atypical original data set, the conclusions in this paper are based on data from 46 separate examples, and so can safely be regarded as typical of collaborative trials.

Results and Discussion

Basic Statistics

Kjeldahl protein

Estimates of the grand mean $\hat{\mu}$, the standard deviation of repeatability ($\hat{\sigma}_r$) and the standard deviation of reproducibility ($\hat{\sigma}_R$) were produced by classical ANOVA (no outliers removed), by the robust procedure (Rob) and by the Harmonized Protocol (HP) and are presented in Table 1. Where no outliers are removed the HP gives the same result as classical ANOVA. Generally the robust method gave similar results to HP, but there are some noticeable differences.

The standard deviation of repeatability estimates ($\hat{\sigma}_r$) are compared in Fig. 1. When no outliers were excluded by the HP, the robust method tended to give the slightly lower value, with an average value of $\hat{\sigma}_r(HP)/\hat{\sigma}_r(Rob)$ of 1.3. This effect was smaller when one or more outliers were excluded by the HP, giving an average value of $\hat{\sigma}_r(HP)/\hat{\sigma}_r(Rob)$ of 1.1. The difference between the results of the two methods is largely attributed to the conservative nature of the outlier tests used in HP, which use the 1% point for rejection of a laboratory's results. The robust method accommodates any marginal outliers that the HP ignores. However, when outliers are removed by the HP, the two methods give results that agree more closely.

The standard deviation of reproducibility estimates ($\hat{\sigma}_R$) show a similar pattern (Fig. 2), although the deviation between them is smaller. The ratio $\hat{\sigma}_R(HP)/\hat{\sigma}_R(Rob)$ had an average value of 1.1 when no outliers were rejected by the HP and 1.0 when one or more were rejected. Again the slightly high tendency of the HP is due to its conservatism in treating marginal outliers.

The grand mean estimates ($\hat{\mu}$) produced by the robust method and the HP are very similar. Fig. 3 shows the relative difference between the estimates $[(\hat{\mu}(HP)-\hat{\mu}(Rob))/\hat{\mu}(Rob)]$ plotted against the analyte concentration $[\hat{\mu}(Rob)]$. The mean relative difference is not significantly different form zero (p =

Table 1 The statistics $\hat{\sigma}_r$, $\hat{\sigma}_R$, and $\hat{\mu}$ for 26 materials analysed for Kjeldahl protein (% m/m) in a collaborative trial using 22 laboratories. The statistics were produced by the Harmonized Protocol (HP) classical ANOVA (Clas) and the AMC robust ANOVA (Rob); H is the number of laboratories rejected by the Harmonized Protocol

$\hat{\sigma}_r$			$\hat{\sigma}_R$			$\hat{\mu}$			
HP	Clas	Rob	HP	Clas	Rob	HP	Clas	Rob	H
0.79	0.79	0.62	1.47	1.47	1.22	90.17	90.17	90.21	0
1.13	1.13	0.76	1.42	1.42	1.37	88.79	88.79	88.81	0
0.57	0.99	0.61	1.21	1.35	1.08	87.85	87.91	87.92	1
0.62	3.00	0.87	1.02	3.11	1.43	85.80	85.65	85.84	4
0.47	1.14	0.48	0.97	1.55	1.07	84.82	84.93	84.84	3
0.69	0.68	0.40	1.39	2.41	1.08	80.63	81.05	80.73	1
0.53	0.52	0.44	0.68	0.89	0.65	54.26	54.13	54.22	1
0.80	0.80	0.63	0.93	0.93	0.79	53.90	53.90	53.93	0
0.75	1.23	0.57	0.78	1.23	0.75	44.46	44.52	44.51	1
0.44	1.02	0.49	0.44	1.02	0.59	44.08	44.12	44.08	4
0.82	0.82	0.89	1.17	1.17	0.92	40.54	40.54	40.52	0
0.93	0.93	0.55	0.96	0.96	0.69	39.42	39.42	39.40	0
0.30	0.30	0.29	0.56	0.56	0.51	29.79	29.79	29.76	0
0.26	0.39	0.23	0.39	0.54	0.36	29.26	29.33	29.31	1
0.22	0.40	0.20	0.43	0.48	0.33	28.15	28.15	28.17	1
0.32	0.78	0.20	0.46	0.80	0.46	27.00	26.91	26.97	1
0.43	0.43	0.23	0.48	0.48	0.44	18.71	18.71	18.72	0
0.22	0.35	0.22	0.24	0.39	0.30	17.93	17.96	17.95	3
0.31	0.70	0.22	0.39	0.75	0.33	17.76	17.86	17.80	1
0.29	0.44	0.22	0.33	0.45	0.33	17.76	17.81	17.78	1
0.17	0.46	0.21	0.25	0.46	0.30	17.02	17.01	17.02	2
0.29	0.29	0.20	0.36	0.36	0.31	16.86	16.86	16.86	0
0.34	0.48	0.31	0.34	0.48	0.32	16.25	16.16	16.20	3
0.18	0.35	0.17	0.29	0.38	0.26	15.71	15.74	15.73	1
0.19	0.19	0.21	0.19	0.34	0.24	13.37	13.37	13.38	0
0.14	0.51	0.17	0.25	0.51	0.25	10.16	10.24	10.20	3

0.09). The median absolute difference from zero is 0.0005 in instances where no outliers were removed by the HP and 0.0011 where one or more outliers were removed.

Overall, for these data, the AMC robust ANOVA gave similar basic statistics to those of the HP and both methods coped well with the data sets. The tendency of the HP to produce higher estimates of the standard deviation is due to its failure to reject marginal outliers.

Aflatoxin data

The estimates $\hat{\mu}$, $\hat{\sigma}_r$ and $\hat{\sigma}_R$ produced by classical ANOVA, robust ANOVA and by the Harmonized protocol are presented in Table 2. Again, the results produced by the HP were similar to those produced by robust ANOVA.

The $\hat{\sigma}_r$ values are compared in Fig. 4. There is a tendency for the HP estimates to be slightly higher and, with an average value of $\hat{\sigma}_r(HP)/\hat{\sigma}_r(Rob)$ of 1.1, no obvious distinction based on the number of outliers removed.

The $\hat{\sigma}_R$ values are compared in Fig. 5. The robust estimates are similar to the HP estimates when no outliers were rejected, with an average value of $\hat{\sigma}_R(HP)/\hat{\sigma}_R(Rob)$ of 1.0. In instances when one or more laboratories were rejected as outliers by the HP, the average was smaller at 0.8.

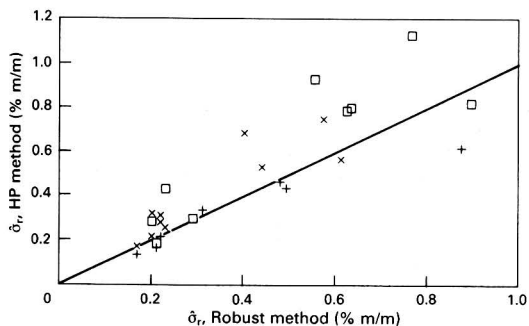The grand mean estimates are compared in Fig. 6, which

shows the difference between the estimates $[\hat{\mu}(HP)-\hat{\mu}(Rob)]$ plotted against the analyte concentration $[\hat{\mu}(Rob)]$. The mean difference is not significantly different from zero. The median absolute difference from zero is 0.02 ng g^{-1} for instances where all laboratories were included by the HP and 0.20 ng g^{-1} where one or more laboratories were rejected.

Fig. 2 Standard deviation of reproducibility estimated by robust ANOVA and the Harmonized Protocol for the determination of Kjeldahl protein (% m/m). The number of laboratories rejected by the Harmonized Protocol are shown as zero ($\square$), one ($\times$) or two or more ($+$)

Fig. 1 Standard deviation of repeatability estimated by robust ANOVA and the Harmonized Protocol for the determination of Kjeldahl protein (% m/m). The number of laboratories rejected by the Harmonized Protocol are shown as zero ($\square$), one ($\times$) or two or more ($+$). The line represents equality between the methods

Fig. 3 Relative differences between the grand mean estimated by robust ANOVA and the Harmonized Protocol, for the determination of Kjeldahl protein (% m/m). The number of laboratories rejected by the Harmonized Protocol are shown as: zero ($\square$) or one or more ($\times$)

Table 2 The statistics $\hat{\sigma}_r$, $\hat{\sigma}_R$ and $\hat{\mu}$ for 20 peanut butters analysed for aflatoxins (ng g^{-1}) in a collaborative trial. The statistics were produced by the Harmonized Protocol (HP), classical ANOVA (Clas) and the AMC robust ANOVA (Rob). L is the number of laboratories in the trial and H is the number of laboratories rejected by the Harmonized Protocol

$\hat{\sigma}_r$			$\hat{\sigma}_R$			$\hat{\mu}$				
HP	Clas	Rob	HP	Clas	Rob	HP	Clas	Rob	L	H
5.77	5.77	6.36	11.61	11.61	13.10	25.84	25.84	25.81	12	0
2.59	4.58	2.22	5.30	5.83	5.66	11.42	11.67	11.70	13	1
0.54	2.55	0.62	3.53	4.03	4.11	8.53	8.29	8.29	12	2
0.79	1.95	0.70	3.80	3.89	4.15	7.14	6.96	6.96	12	1
1.67	1.67	1.38	2.16	2.16	2.27	5.99	5.99	5.99	13	0
0.83	0.83	0.80	3.04	3.04	3.37	5.89	5.89	5.92	12	0
1.50	1.50	1.20	1.68	1.68	1.70	5.34	5.34	5.34	13	0
0.71	0.71	0.81	1.63	1.63	1.59	4.84	4.84	4.96	12	0
0.50	1.39	0.62	1.90	2.16	2.18	4.22	4.42	4.44	12	1
0.56	1.21	0.32	1.66	1.78	1.78	3.85	3.78	3.78	12	1
0.44	0.44	0.49	1.07	1.07	1.16	2.88	2.88	2.90	13	0
0.32	0.32	0.36	1.14	1.14	1.26	2.62	2.62	2.64	12	0
0.73	0.73	0.53	0.94	0.94	0.93	2.59	2.59	2.58	13	0
0.26	3.56	0.36	0.75	3.56	1.03	1.89	2.62	2.16	13	2
0.58	0.58	0.61	1.01	0.69	1.07	1.98	1.98	1.95	13	0
0.44	0.44	0.29	0.51	0.51	0.46	0.94	0.94	0.96	12	0
0.35	0.35	0.20	0.38	0.38	0.29	0.58	0.58	0.56	13	0
0.26	0.26	0.24	0.40	0.40	0.42	0.54	0.54	0.54	13	0
0.12	3.05	0.13	0.21	3.07	0.27	0.26	0.84	0.29	13	1
0.08	0.20	0.14	0.06	0.23	0.14	0.03	1.05	0.05	13	2

Fig. 4 Standard deviation of repeatability estimated by robust ANOVA and the Harmonized Protocol, for the determination of aflatoxins (ng g^{-1}). The number of laboratories rejected by the Harmonized Protocol are shown as: zero ($\square$) or one or more ($\times$). The line represents equality between the methods
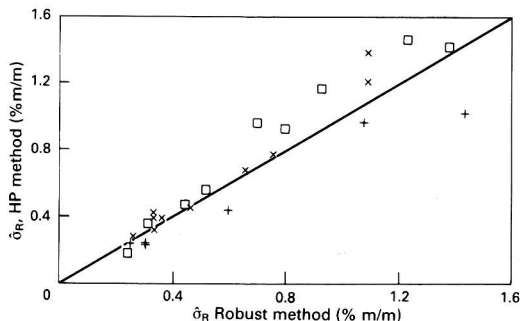

Fig. 5 Standard deviation of reproducibility estimated by robust ANOVA and the Harmonized Protocol, for the determination of aflatoxins (ng g^{-1}). The number of laboratories rejected by the Harmonized Protocol are shown as: zero ($\square$) or one or more ($\times$). The line represents equality between the methods

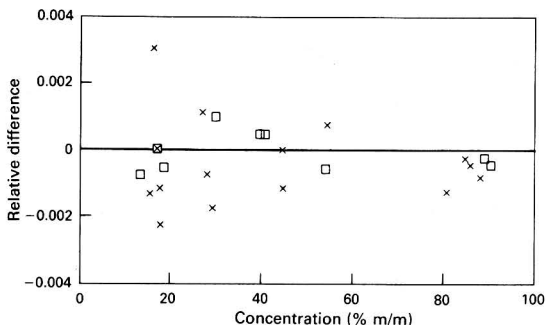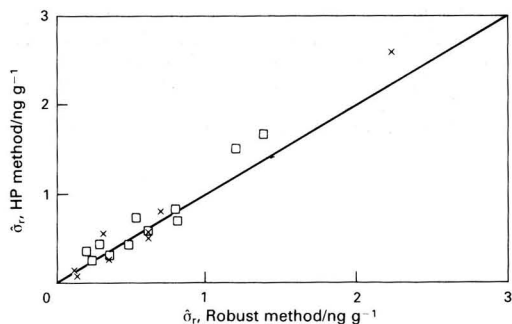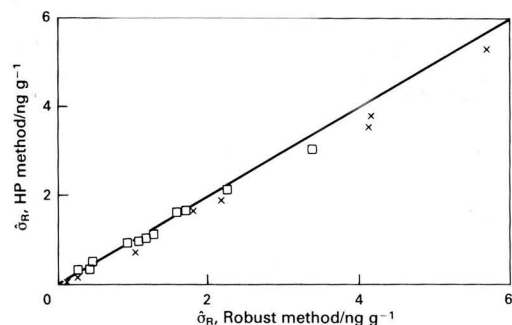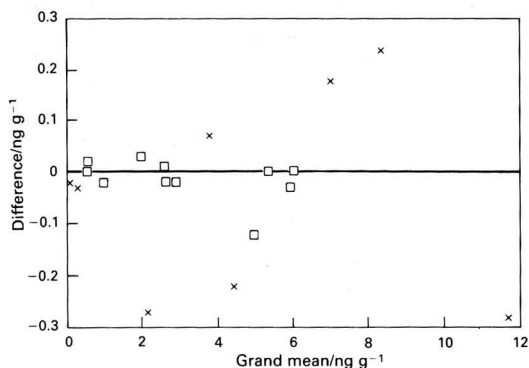**Fig. 6** Differences between the grand means estimated by robust ANOVA and the Harmonized Protocol, for the determination of aflatoxins (ng g^{-1}). The number of laboratories rejected by the Harmonized Protocol are shown as: zero ($\square$) or one or more ($\times$)

Variability of Estimates

To compare the variability of the estimates from the three methods a bootstrap exercise was performed using the 26 Kjeldahl protein data sets. Bootstrap samples[17] were generated from a given data set as follows: generate 22 laboratory means by sampling, randomly with replacement, from the 22

Table 3 Crude protein data used for detailed illustration of the bootstrap methods results. The corresponding statistics are in row 17 of Table 1

Laboratory	Duplicate results (% m/m)	
1	22.63	27.36
2	26.86	26.88
3	26.50	26.93
4	26.89	27.18
5	26.01	26.81
6	27.39	27.42
7	27.33	27.16
8	27.03	27.14
9	26.69	26.50
10	27.29	27.38
11	26.72	26.79
12	27.13	26.25
13	25.99	26.17
14	26.85	26.95
15	27.16	27.07
16	27.74	27.85
17	27.28	27.42
18	27.00	27.76
19	26.68	26.63
20	26.72	28.03
21	27.40	27.30
22	26.92	26.84

observed means; generate 22 differences between duplicates by sampling, randomly with replacement, from the 22 observed differences; pair means and differences in the order drawn to construct a data set of the same structure as the original. This procedure was repeated 1500 times for each of the 26 data sets and $\hat{\mu}$, $\hat{\sigma}_r$ and $\hat{\sigma}_R$ were calculated by each of the three methods for each bootstrap sample. The variability of the estimates over the generated samples is a natural estimate of their variability over repetitions of the trial that produced the original data. This approach was preferred to the alternative of simulation because it avoids possibly inappropriate distributional assumptions; the bootstrap samples look like real data because they are drawn directly from real data.

The method of drawing the bootstrap samples merits some discussion. In drawing means and differences independently, it fails to preserve any tendency in the original data for outlying laboratory means and large differences between duplicates to occur in the same laboratory. This may adversely affect the performance of the 'Harmonized Protocol which benefits from any such tendency. However, the obvious alternative approach, which is to sample 22 laboratories with replacement and use the original duplicates for these laboratories as the bootstrap sample, may also be criticized on the grounds that it under-represents the variability. On balance the method described first was preferred. As a check, part of the bootstrap excercise was repeated using the alternative sampling method. The results obtained were quantitatively but not qualitatively different.

Figs. 7–9 show the results of the bootstrap method for one of the 26 data sets (Table 3). These three sets of histograms show the distribution over the 1500 bootstrap samples of $\hat{\sigma}_r$, $\hat{\sigma}_R$ and $\hat{\mu}$ produced by the three ANOVA methods and the results are typical of the data as a whole.

The three histograms for the mean (Fig. 9) are quite similar, but those for the two standard deviations ($\hat{\sigma}_r$ and $\hat{\sigma}_R$) reveal marked differences between the methods. Consider the repeatability, $\hat{\sigma}_r$ (Fig. 7). The first laboratory produced a very large difference between its duplicate observations. In the bootstrap samples this difference, if it is present at all, may occur more than once. The five clumps of values in the histogram for the classical method correspond (left to right) to 0, 1, 2, 3 and 4 occurrences. An example of more than two
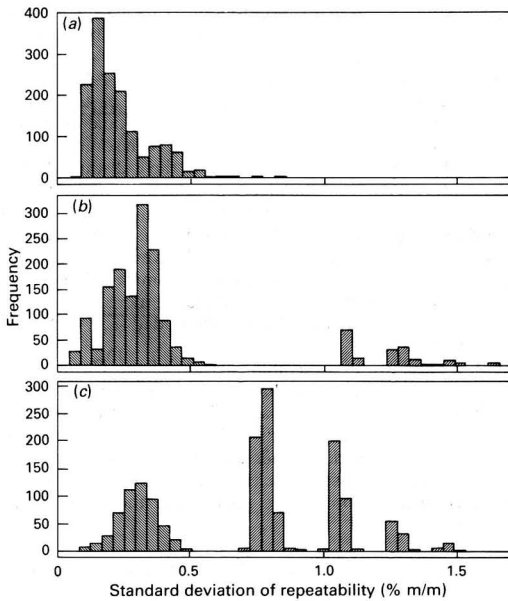
Fig. 7 Distribution over 1500 bootstrap samples from a single protein data set of the estimate of repeatability obtained by (*a*) the robust procedure, (*b*) the Harmonized Protocol and (*c*) the classical procedure

Fig. 8 Distribution over 1500 bootstrap samples from a single protein data set of the estimate of reproducibility obtained by (*a*) the robust procedure, (*b*) the Harmonized Protocol and (*c*) the classical procedure
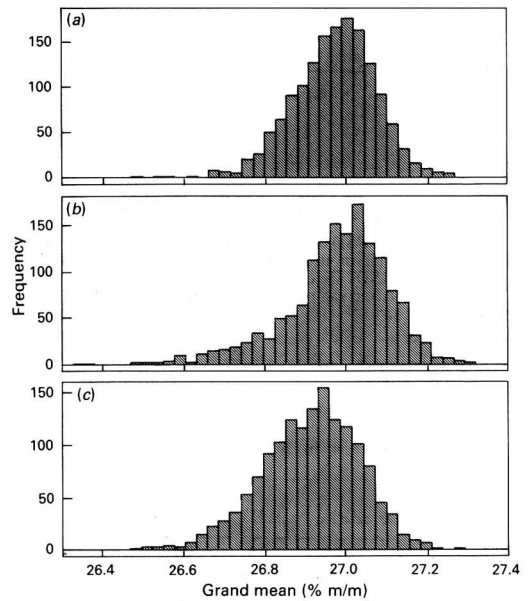
Fig. 9 Distribution over 1500 bootstrap samples from a single protein data set of the estimate of grand mean obtained by (*a*) the robust procedure, (*b*) the Harmonized Protocol and (*c*) the classical procedure
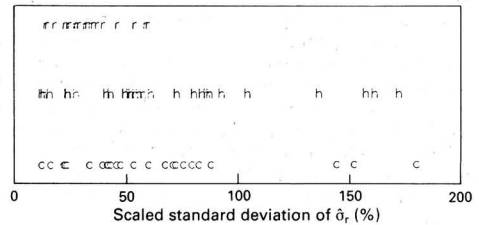
Fig. 10 Plots of the RSD of the $\hat{\sigma}_r$ estimated by the three methods (r, robust analysis; h, Harmonized Protocol; and c, classical analysis) for 26 data sets. The RSDs are calculated as $100\times$ (standard deviation of $\hat{\sigma}_r$ over 1500 bootstrap samples)/(robust estimate of σ_r from original data set)

occurrences is a rare event, but has a considerable impact on the estimate of repeatability when it happens. The Harmonized Protocol rejects a single outlier when it is present, thus merging the second clump into the first and sometimes, but not always, rejects both of two outliers. It cannot cope with more than two, the problem of multiple outliers masking each

other being well known. The reason why the two histograms do not match exactly on the right hand side, despite being based on the same bootstrap sample, is that the Harmonized Protocol also rejects laboratories with outlying means. Thus the same three outlying differences may represent a larger proportion of the total data for the Harmonized Protocol estimate of σ_r than for the classical estimate. The robust procedure is able to accommodate even four outliers and produces a histogram with a long right-hand tail but no detached clumps of values.

The histograms obtained for the standard deviation of reproducibility ($\hat{\sigma}_R$) tell a similar story (Fig. 8), with the Harmonized Protocol only partly coping with outliers and the robust procedure successfully accommodating even multiple outliers. The situation is now more complicated because outlying laboratory means also affect $\hat{\sigma}_R$ and various combinations of outlying means and differences are possible.

Figs. 10–12 summarize the variability of the estimates for all 26 sets of protein data. The plots are based on the standard deviations, calculated over 1500 bootstrap samples, of $\hat{\mu}$, $\hat{\sigma}_r$ and $\hat{\sigma}_R$. To make these standard deviations comparable
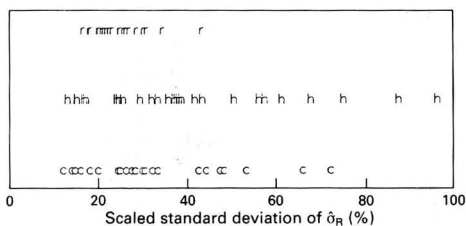
Fig. 11 Plots of the RSD of the $\hat{\sigma}_R$ estimated by the three methods (r, robust analysis; h, Harmonized Protocol; and c, classical analysis) for 26 data sets. The RSDs are calculated as $100\times$ (standard deviation of $\hat{\sigma}_R$ over 1500 bootstrap samples)/(robust estimate of σ_R from original data set)

Fig. 12 Plots of the RSD of the $\hat{\mu}$ estimated by the three methods (r, robust analysis; h, Harmonized Protocol; and c, classical analysis) for 26 data sets. The RSDs are calculated as $100\times$ (standard deviation of $\hat{\mu}$ over 1500 bootstrap samples)/(robust estimate of μ from original data set)

between data sets they have been scaled by dividing by the corresponding (robust) parameter estimate from the original data set and multiplying by 100. The points plotted may thus be interpreted as the RSD of the statistic in question.

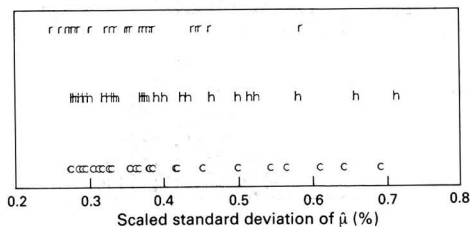Two features deserve comment. Firstly, the Harmonized Protocol gives estimates at least as variable as the classical method, whereas those from the robust procedure are far less variable. Secondly, most of the RSDs are alarmingly large. This is not an artifact of the bootstrap procedure: a bootstrap exercise with data generated from the normal theory model underlying the classical ANOVA produced RSDs of 11 and 10% for $\hat{\sigma}_r$ and $\hat{\sigma}_R$ respectively, in agreement with theoretical values. The large RSDs are a consequence of the non-normality of the real data used to generate the bootstrap samples.

Conclusions

The AMC robust ANOVA gave values of $\hat{\mu}$, $\hat{\sigma}_r$ and $\hat{\sigma}_R$ that were close to those provided by the Harmonized Protocol (in comparison with the likely standard errors) and the method could be used with equal facility. On those grounds alone the robust method must be regarded as a powerful alternative for interpreting collaborative trials. However, there are further reasons, based on the standard errors of the precision estimates, that show the robust method to be clearly preferable.

The bootstrap method showed that the standard deviations of the robust estimates of σ_r and σ_R are smaller than those of the Harmonized Protocol by an average factor of about two. The individual studies (e.g., Figs. 7–9) show the distribution of the HP estimate to be strongly skewed to high values, which in

practice would result in a substantial proportion of collaborative trials giving unrepresentatively high results. This is due to the limitations of outlier rejection procedures.

The bootstrap procedure also revealed that the AMC robust ANOVA has larger standard errors for $\hat{\sigma}_r$ and $\hat{\sigma}_R$ than those calculated from classical normal theory. Individual estimates of σ_r and σ_R must therefore be interpreted with some caution. Analytical chemists must be aware of the substantial confidence interval that must be placed around these estimates. In practice this variability of individual results is mitigated somewhat by the fact that collaborative trials involve studies on six or more separate materials. However, the results suggest that the number of laboratories and materials used in a collaborative trial could, with advantage, be increased beyond the minimum number currently recommended (i.e., eight and five respectively).

With a view towards possible revision of the Harmonized Protocol, it is recommended that the results from AMC robust ANOVA should be reported alongside those of the Harmonized Protocol in future published reports of collaborative trials. This will provide further information for comparison purposes and any discrepancies would alert users to the possibility of an inappropriate result from the Harmonized Protocol.

References

1 Youden, W. J., *Statistical Techniques for Collaborative Tests*, Association of Official Analytical Chemists, Washington, DC, 1969.
2 Zaalberg, J., *J. Assoc. Off. Anal. Chem.*, 1989, **72**, 34.
3 Kelly, P. C., *J. Assoc. Off. Anal. Chem.*, 1990, **73**, 58.
4 Malanoski, A. J., *J. Assoc. Off. Anal. Chem.*, 1990, **73**, 231.
5 Malanoski, A. J., *J. Assoc. Off. Anal. Chem.*, 1990, **73**, 235.
6 Malanoski, A. J., *J. Assoc. Off. Anal. Chem.*, 1990, **73**, 411.
7 Mandel, J., *Chemom. Intell. Lab. Syst.*, 1991, **11**, 109.
8 *Standard Practice for Conducting an Interlaboratory Study to Determine the Precision of a Test Method*. ASTM E691-87. American Society for Testing and Materials, Philadelphia, PA, 1988.
9 *Determination and Application of Precision Data in Relation to Methods of Test for Petroleum Products*. IP 367/84 in *Institute of Petroleum Standard Methods for the Analysis and Testing of Petroleum and Related Products*, Wiley, Bognor Regis, 1992.
10 *Guidelines for the Development of Standard Methods by Collaborative Study*, Laboratory of the Government Chemist, London, 4th edn., 1988.
11 *Precision of Test Methods—Determination of Repeatability and Reproducibility for a Standard Test Method by Interlaboratory Tests*. ISO 5725-1986, International Organization for Standardization, Geneva, 1986.
12 Horwitz, W., *Pure Appl. Chem.*, 1988, **60**, 855.
13 Analytical Methods Committee, *Analyst*, 1989, **114**, 1693.
14 Rousseeuw, P. J., *J. Chemom.*, 1991, **5**, 1.
15 Lischer, P., *Lebensm. Wiss. Technol.*, 1987, **20**, 167.
16 Analytical Methods Committee, *Analyst*, 1989, **114**, 1699.
17 Efron, B., and Tibshirani, R., *Stat. Sci.*, 1986, **1**, 54.
18 Kane, P. F., *J. Assoc. Off. Anal. Chem.*, 1984, **67**, 869.
19 Patey, A. L., Sharman, M., and Gilbert, J., *J. Assoc. Off. Anal. Chem.*, 1991, **74**, 76.

Detection of Aluminium(III) Binding to Citrate in Human Blood Plasma by Proton Nuclear Magnetic Resonance Spectroscopy

Jimmy D. Bell
NMR Unit, Hammersmith Hospital, Du Cane Road, London, UK W12 0HS
Gina Kubal, Stojan Radulovic, Peter J. Sadler* and Alan Tucker
Department of Chemistry, Birkbeck College, University of London, Gordon House and Christopher Ingold Laboratories, 29 Gordon Square, London, UK WC1H 0PP

Reactions of Al^{3+} (50–500 µmol l^{-1}) with intact blood plasma and its low relative molecular mass ultrafiltrate (<5 kDa) have been studied by proton nuclear magnetic resonance spectroscopy. Binding to citrate was detected and was reversed by addition of desferrioxamine. The use of combined exponential and sine-bell functions for the resolution enhancement of spectra of plasma is illustrated.

Keywords: *Proton nuclear magnetic resonance spectroscopy; aluminium; citrate; desferrioxamine; blood plasma*

There is a great deal of current interest in the speciation of Al^{3+} in the body. Aluminium is not thought to be an essential element for mammals, and has only toxic effects.[1,2] The speciation of Al^{3+} determines its biological availability,[3] and there is a need to understand the processes by which Al^{3+} is absorbed into the blood stream and either excreted, or, when the kidneys do not function efficiently, is deposited in the brain.[4] The main carriers of Al^{3+} in blood plasma are thought to be citrate, transferrin and possibly albumin.[5–10]

Calculations of the distributions of Al^{3+} species are usually based on thermodynamic stability constants and do not take kinetic factors into account.[11] Speciation *via* the separation and isolation of complexes can be complicated by changes in the equilibria during the separation process. We have therefore used nuclear magnetic resonance (NMR) spectroscopic methods to study Al^{3+} complexation as intact blood plasma can be studied, and kinetic measurements can be made.

Blood plasma is a complicated heterogeneous mixture of fat particles (the lipoproteins), proteins (such as immunoglobulins, albumin and transferrin), and small molecules and ions.[12] The lipoproteins are organized particles consisting of triacylglycerols, phospholipids, free and esterified cholesterol and proteins; some of the lipids are relatively mobile within the core of the particles. The smallest and densest particle HDL (high density lipoprotein) contains the highest protein and phospholipid content. Several plasma proteins are involved in binding functions. For example, albumin (66 kDa), the major plasma protein (concentration approximately 0.65 mmol l^{-1}), binds fatty acids, metal ions such as Zn^{2+} and Ca^{2+}, hormones and various drugs,[13] and transferrin (an 80 kDa glycoprotein) transports iron as Fe^{3+} along with carbonate anions.[14] The details of many of these biologically-important binding processes, including the mechanisms of metal ion and small molecule uptake and release by plasma proteins, are currently poorly understood.

Proton (¹H) NMR spectra of blood plasma consist of a complicated mixture of broad and sharp resonances, and normal single-pulse spectra are often difficult to interpret. Previously the broad resonances have been filtered out using Hahn or CPMG (Carr–Purcell—Meiboom–Gill) spin-echo sequences. This leaves the resonances from the mobile small molecules and a few highly mobile parts of macromolecules.[12,15,16] We have assigned resonances for the *N*-acetyl groups of mobile glycan chains of acute-phase plasma proteins,[17] and resonances for the mobile parts of chylomicrons, very low density lipoproteins (VLDL), low density

lipoproteins (LDL) and HDL.[18] It is even possible to distinguish between these various classes of lipoproteins. In some situations the peaks for these mobile protons are relatively intense and can be used, for example, to monitor disease states such as diabetes or lipidaemia,[19] and to investigate the binding of paramagnetic Cu^{2+} ions.[20]

In this paper the reactions of Al^{3+} with intact blood plasma and a low relative molecular mass (M_r) ultrafiltrate, and the reversal of the binding processes with the clinically-used chelating agent desferrioxamine, are studied. The use of combined exponential and sine-bell functions for resolution enhancement of ¹H NMR spectra is illustrated and discussed.

Experimental

Materials

Blood plasma samples were prepared from freshly drawn heparinized venous blood taken from normal healthy volunteers. Cells were removed by centrifugation at 277 K. Sodium hydrogen carbonate (25 mmol l^{-1}) was added to maintain the pH at 7.4. Protein-free low M_r ultrafiltrates (<5 kDa) were prepared using Amicon Centrifree filtration devices, which had been thoroughly washed with water (5×) to remove preservatives, and centrifugation for 1 h at 277 K. Aluminium was added in microlitre aliquots of an aqueous stock solution of $AlCl_3$ (Fluka). Desferrioxamine (Desferral) was obtained from Ciba-Geigy and trisodium citrate was purchased from Aldrich.

NMR Spectroscopy

The ¹H NMR spectra were recorded on Bruker AM500 and JEOL GSX500 instruments at 500 MHz, using 0.55 ml of solution in a 5 mm tube, ambient temperature, 128 transients, 45° pulses, relaxation delay 1.6 s, 16 k data points (zero-filled to 32 k), 6 kHz spectral width, and gated or continuous secondary irradiation of HOD.

For Hahn spin-echo spectra a 90°-τ-180°-τ-collect free induction decay (FID) (typically τ = 60 ms) sequence was used.[21] Exponential functions equivalent to a line-broadening of 0.5–2 Hz were used for processing where necessary.

For resolution enhancement, FIDs were typically processed using exponential functions equivalent to line-broadenings of 1–2 Hz combined with unshifted sine-bell functions. Data processing was carried out on a Bruker Aspect 1000, or SUN SPARC2 (Varian VNMR software), or Silicon Graphics personal IRIS 4D35TG using FELIX software (D. Hare).

---

* To whom correspondence should be addressed.

The effect of enhancement functions on peak heights was investigated using the PANIC simulation program (Bruker Spectrospin). Spectra containing single lines of different widths at half height were simulated followed by inverse Fourier transformation to produce the FIDs.

Results and Discussion

In Fig. 1, 500 MHz ^{1}H NMR spectra of the methyl and methylene regions of heparinized human blood plasma are compared. In the normal, single-pulse spectrum [Fig. 1(A)], some sharper resonances superimposed on a broad envelope of resonances can just be discerned. The broad peaks arise predominantly from fatty acids (triacylglycerols and phospholipids) and the major protein albumin. Two methods of filtering out the broad peaks are shown. First, the Hahn
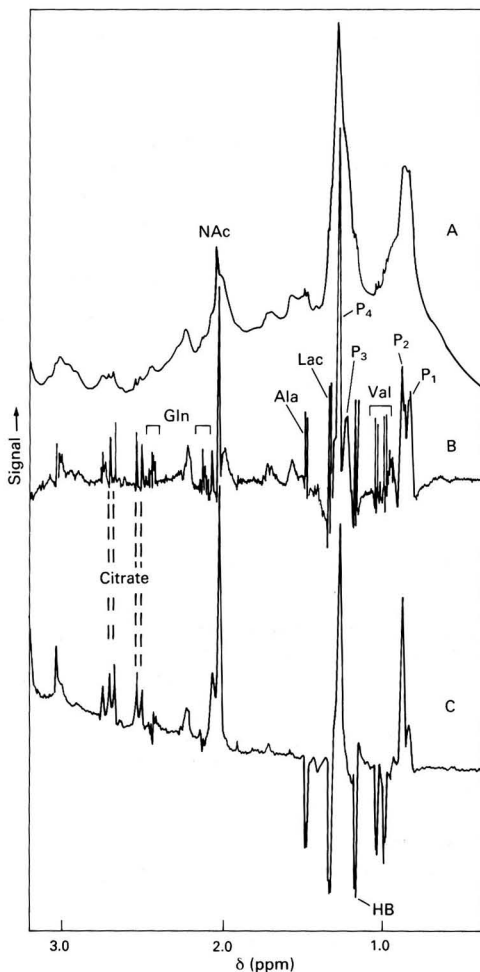

Fig. 1 Aliphatic region of 500 MHz ^{1}H NMR spectra of human blood plasma. A, Single-pulse spectrum: FID multiplied by an exponential function (equivalent to a line broadening of 1 Hz) prior to Fourier transformation. B, Resolution-enhanced single-pulse spectrum: FID multiplied by an exponential function (equivalent to a line broadening of 2 Hz) followed by an unshifted sine-bell function prior to Fourier transformation. C, Hahn spin-echo spectrum: $\tau = 60$ ms, FID multiplied by an exponential function (equivalent to a line broadening of 2 Hz) prior to Fourier transformation. NAc = N-acetyls of glycoproteins; Gln = glutamine; Val = valine; HB = hydroxybutyrate; and Lac = lactate. P = lipoprotein peaks: P_1, HDL and LDL CH$_3$; P_2, VLDL and chylomicron CH$_3$; P_3, HDL and LDL CH$_2$; and P_4, VLDL and chylomicron CH$_2$

spin-echo spectrum Fig. 1(C). With this procedure the contribution of magnetic field inhomogeneity to linewidths is removed, but linewidths are not otherwise reduced. Broad resonances are filtered out because the magnetization associated with them decays before acquisition begins (spin–spin relaxation times, T_2, short compared with the total delay 2 × τ). Intensities are also reduced by diffusion in local inhomogeneous fields in the sample during the delay,[22] and by phase modulation of the multiplets.[23] The choice of τ is a compromise between removing sufficient of the broad signals to achieve the simplification required, and retaining interpretable phase modulation.[16] With τ = 60 ms, most of the doublets are inverted (τ = 1/2 J). The largest peaks (P) are those for the CH$_3$ (P$_2$) and CH$_2$ (P$_4$) groups of chylomicrons and VLDL,[18] and the N-acetyl groups of the glycan chains of acute-phase glycoproteins such as α$_1$-acid glycoprotein.[17] Well-resolved sharp multiplets include those for valine, hydroxybutyrate, lactate, alanine and citrate. Secondly, a normal spectrum is shown after enhancement using combined exponential and sine-bell functions. The over-all appearance of this is similar to the spin-echo spectrum, except that there is no phase modulation, and partly as a result of this, some peaks are enhanced in intensity, e.g., P$_1$ and P$_3$. The peaks for glutamine are now interpretable, whereas in the spin-echo spectrum they are severely distorted. The advantage of resolution enhancement is that it can be carried out after the single-pulse spectrum has been acquired, and does not require acquisition of further experimental data.

Resolution enhancement is a well-known procedure in NMR spectroscopy,[24,25] but the combined application of exponential and sine-bell functions, although proposed,[26,27] has been little used in the past. The sine-bell function[26] is a commonly used window function, especially for studies of proteins. In the simplest use of this function, the FID is multiplied by a half cycle of a sine function with a period of twice the acquisition time. However, the improvement in resolution obtained with this function is often accompanied by an excessive degradation of the signal-to-noise ratio and distortion of baselines. We have countered this problem by pre-multiplication of the FID by a line-broadening exponential function, a procedure that we have found useful for the study of the large plasma proteins albumin and transferrin.[28–30] The function begins at zero (ensuring suppression of the broadest lines), rises to a maximum, which might be at an earlier point in the time domain than for the sine-bell (depending on the exponential function used), and then decays smoothly to zero. Mathematically the sine-bell function produces an FID that, after Fourier transformation, is equivalent to the discrete differential of the dispersion spectrum,[27] yielding a spectrum with inherently narrower lines, but with a poorer signal-to-noise ratio than the absorption spectrum. The introduction of either a phase-shift of the sine-bell function or pre-multiplication by an exponential function effectively adds a fraction of the absorption spectrum to the dispersion differential, improving the signal-to-noise ratio and broadening the lines slightly. The phase-shifted sine-bell does not begin at zero and is not as effective in suppression of broad resonances.

We investigated the effect of sine-bell and exponential sine-bell resolution enhancements on the intensity of resonances using simulated spectra. The FIDs for Lorentzian lines of varying widths at half height (2–30 Hz) were simulated and transformed with and without pre-multiplication with enhancement functions. The reduction of peak heights in enhanced spectra resulting from linewidth changes was determined. The curve for exponential sine-bell enhancement was much shallower than that for sine-bell, i.e., enhanced spectra are less affected by linewidth changes. For example, if a spectrum is enhanced using the sine-bell function, then an increase in peak width from 2 to 5 Hz leads to a 45% reduction in peak intensity, and an increase from 2 to 10 Hz to a 71%
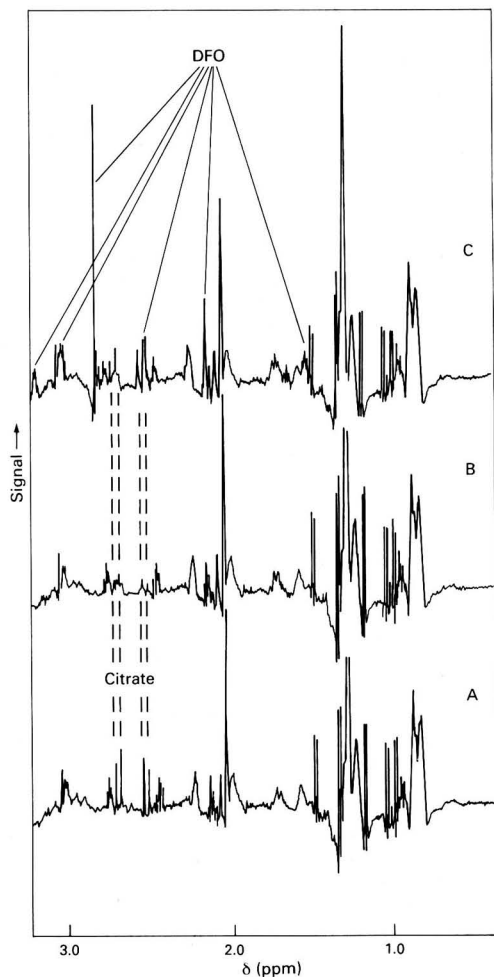
Fig. 2 Aliphatic region of resolution-enhanced 500 MHz ^{1}H NMR spectra of human blood plasma. A, Control; B, after addition of Al^{3+} (50 µmol l^{-1}); and C, after further addition of desferrioxamine (100 µmol l^{-1}). Exponential functions (equivalent to a line broadening of 2 Hz) followed by unshifted sine-bell functions were applied to the FIDs prior to Fourier transformation. DFO = desferrioxamine

Fig. 3 Aliphatic region of 500 MHz ^{1}H NMR spectra of a low M_r ultrafiltrate (<5 kDa) of human blood plasma. A, Control; B, after addition of 50 µmol l^{-1} Al^{3+}; and C, after further addition of desferrioxamine (100 µmol l^{-1}). Most of the multiplets between 3.2 and 3.9 ppm are assignable to glucose

reduction, whereas the corresponding reductions in peak intensity are 28% (increase in linewidth from 2 to 5 Hz) and 56% (from 2 to 10 Hz), respectively, as a result of using exponential sine-bell enhancement. The choice of acquisition time greatly affects the enhancement procedure when sine-bell functions are used, as the period of the function is normally set to twice that of the acquisition time, *i.e.*, the maximum of the function is at half the acquisition time. Hence the choice of acquisition time determines the portion of the FID that is maximally enhanced.

The effect of Al^{3+} on the resolution-enhanced spectrum of blood plasma is shown in Fig. 2. After addition of 50 µmol l^{-1} Al^{3+} the intensities of the peaks forming the AB quartet for citrate near 2.6 ppm, present at a concentration of 0.11 mmol l^{-1} in this sample of plasma (*i.e.*, within the normal range), markedly and selectively decrease intensity [Fig. 2(B)]. No further change was observed in the spectrum for the next 24 h. The citrate peaks disappear from the spectrum completely after addition of 200 µmol l^{-1} Al^{3+}, and no other resonances were affected up to a concentration of 500 µmol l^{-1}

Al^{3+} (data not shown). Addition of desferrioxamine to the plasma sample containing 50 µmol l^{-1} Al^{3+} led to the rapid (minutes) reappearance of citrate peaks, Fig. 2(C), although in a slightly broader form than they were originally. Addition of desferrioxamine alone to plasma had no effect on the peaks for plasma components.

Single-pulse ^{1}H NMR spectra of the low M_r (<5 kDa) ultrafiltrate of blood plasma are shown in Fig. 3. Now there are no broad peaks in the spectrum because the high M_r macromolecules have been separated out. It can be seen that addition of Al^{3+} (50–300 µmol l^{-1}) causes a specific decrease in intensity of the citrate peaks, whilst there is little effect on peaks for other small molecules such as lactate and alanine. Addition of desferrioxamine restored the intensity of the citrate peaks again, Fig. 3(C).

The ^{1}H NMR spectra of model systems containing Al^{3+} and citrate were studied. The spectrum of a 0.75 + 1.0 mixture of Al^{3+} and citrate at pH* 6.6 (pH* = pH meter reading in D$_2$O solution; adjusted with NaDCO$_3$) for example, gave rise to about 20 quartets covering the range 2.2–3.5 ppm. Evidently

there are a large number of different coordination modes for citrate in Al^{3+}–citrate complexes. This conclusion has already been drawn by others from ^{13}C NMR work,[31] and from X-ray crystallography of isolated complexes,[32] and appears to explain why new peaks for an aluminium citrate complex are not readily observable in spectra of plasma or its ultrafiltrate. The crystalline trinuclear complex $[Al_3(H_{-1}Cit)_3(OH)-(H_2O)]^{4-}$ isolated from $1 + 1$ mixtures of Al^{3+} and citrate (Cit) in the pH range 7–9,[32] contains three similar but distinct six-coordinate Al^{3+} ions bridged by tetradentate citrate anions; the hydroxyl and carboxyl groups are deprotonated. Curiously, the ^1H NMR spectrum of this $1 + 1$ cluster was reported to consist of a single multiplet at 4.71 ppm (i.e., very close to the water resonance). As the citrate ligands are magnetically-inequivalent, a total of six quartets arising from four magnetically-inequivalent protons per citrate might have been expected. Desferrioxamine is known to bind Al^{3+} more strongly than citrate or transferrin, and is used in the clinic for decreasing plasma aluminium levels after exposure to toxic levels.[33]

These ^1H NMR data suggest that Al^{3+} added to heparinized blood plasma (or plasma ultrafiltrate) in vitro initially binds to citrate. Citrate, which has three ionized carboxylate groups at neutral pH (pK values = 2.87, 4.35 and 5.69),[34] is known to be a strong ligand for Al^{3+},[11] and probably plays a role in promoting the absorption of aluminium from food into the blood stream. Here much of the Al^{3+} at the lowest dose studied (50 µmol l^{-1}) could have been transferred to transferrin, which is normally present at a concentration of 30–40 µmol l^{-1} in plasma and usually has only about one third of the Fe^{3+} sites (two per protein molecule) occupied.[14] This would leave about 40–53 µmol l^{-1} of vacant sites available for binding Al^{3+}. Perhaps citrate to transferrin transfer is very slow under the conditions used. There is good evidence that transferrin is the ultimate binding agent for Al^{3+} in vivo,[5,8] and Al^{3+} is known to bind strongly to transferrin in vitro.[6,7] An alternative, and less likely, explanation for our results is that Al^{3+} binding to transferrin (or another protein) induces a conformational change that in turn leads to citrate binding to the protein and broadening of resonances because of slow tumbling. This is difficult to rule out at the moment but might be clarified when experiments on Al^{3+} binding to transferrin in the presence of citrate are studied by NMR spectroscopy. So far our own attempts,[35] and those of others,[36] to detect Al^{3+} binding to transferrin by ^{27}Al NMR have not been successful, presumably due to quadrupolar broadening. The ^1H NMR methods such as those described here should be useful for investigating the effectiveness of potential therapeutic chelating agents designed to remove aluminium from blood plasma.

References

1 Aluminum in Chemistry, Biology and Medicine, eds. Nicolini, M., Zatta, P. F., and Corain, B., Cortina International, Verona, 1991.

2 Aluminium in Biology and Medicine, eds. Chadwick, D., and Whelan, J., CIBA Foundation Symposium 169, Wiley, New York, 1992.

3 Daydé, S., Filella, M., and Berthon, G., J. Inorg. Biochem., 1991, 38, 241.

4 Candy, J. M., Oakley, A. E., Klinowski, J., Carpenter, T. A., Perry, R. H., Atack, J. R., Perry, E. K., Blessed, G., Fairbairn, A., and Edwardson, J. A., Lancet, 1986, i, 354.

5 Martin, R. B., Clin. Chem. (Winston-Salem N.C.), 1986, 32, 1797.

6 Harris, W. R., and Sheldon, J., Inorg. Chem., 1990, 29, 119.

7 Fatemi, S. J. A., Kadir, F. H. A., and Moore, G. R., Biochem. J., 1991, 280, 527.

8 Day, J. P., Barker, J., Evans, I. J. A., Perks, J., Seabright, P. J., Ackrill, P., Lilley, J. S., Drumm, P. V., and Newton, G. W. A., Lancet, 1991, 337, 1345.

9 Venturini, M., and Berthon, G., J. Inorg. Biochem., 1989, 37, 69.

10 Fatemi, S. J. A., Williamson, D. J., and Moore, G. R., J. Inorg. Biochem., 1992, 46, 35.

11 Martin, R. B., in Aluminum in Chemistry, Biology and Medicine, eds. Nicolini, M., Zatta, P. F., and Corain, B., Cortina International, Verona, 1991, pp. 3–20.

12 Bell, J. D., Brown, J. C. C., and Sadler, P. J., Chem. Br., 1988, 24, 1021.

13 Peters, T., Jr., Adv. Protein Chem., 1985, 37, 161.

14 Crichton, R. R., Inorganic Biochemistry of Iron Metabolism, Ellis Horwood, Chichester, 1991.

15 Nicholson, J. K., Buckingham, M. J., and Sadler, P. J., Biochem. J., 1983, 211, 605.

16 Bell, J. D., Brown, J. C. C., and Sadler, P. J., NMR Biomed., 1989, 2, 246.

17 Bell, J. D., Brown, J. C. C., Nicholson, J. K., and Sadler, P. J., FEBS Lett., 1987, 215, 311.

18 Bell, J. D., Sadler, P. J., Macleod, A. F., Turner, P. R., and LaVille, A., FEBS Lett., 1987, 219, 239.

19 Nicholson, K. K., O'Flynn, M. P., Sadler, P. J., Macleod, A. F., Juul, S. M., and Sönksen, P. H., Biochem. J., 1984, 217, 365.

20 Bligh, S. W. A., Boyle, H. A., McEwen, A. B., Sadler, P. J., and Woodham, R. H., Biochem. Pharm., 1992, 43, 137.

21 Hahn, E. L., Phys. Rev., 1950, 80, 580.

22 Brown, F. F., and Campbell, I. D., Proc. R. Soc. London Ser. B, 1980, 289, 395.

23 Rabenstein, D. L., and Nakashima, T. T., Anal. Chem., 1979, 51, 1465.

24 Lindon, J. C., and Ferrige, A. G., Prog. NMR Spectrosc., 1981, 14, 27.

25 Sanders, J. K. M., and Hunter, B. K., Modern NMR-Spectroscopy. A Guide for Chemists, Oxford University Press, Oxford, 1987.

26 De Marco, A., and Wüthrich, K., J. Magn. Reson., 1976, 24, 201.

27 Guéron, M., J. Magn. Reson., 1978, 30, 515.

28 Kubal, G., Sadler, P. J., and Evans, R., J. Am. Chem. Soc., 1992, 114, 1117.

29 Kubal, G., Mason, A. B., Sadler, P. J., Tucker, A., and Woodworth, R. C., Biochem. J., 1992, 285, 711.

30 Sadler, P. J., and Tucker, A., Eur. J. Biochem., 1992, 205, 631.

31 Fatemi, S. J. A., Kadir, F. H. A., Williamson, D. J., and Moore, G. R., Adv. Inorg. Chem., 1991, 35, 409.

32 Freng, T. L., Gurian, P. L., Healy, D., and Barron, R., Inorg. Chem., 1990, 29, 408.

33 Leung, F. Y., Hodsman, A. B., Muirhead, N., and Henderson, A. R., Clin. Chem. (Winston-Salem N.C.), 1985, 31, 20.

34 Martell, A. E., and Smith, R. M., Critical Stability Constants, Plenum, New York, 1977, vol. 3, p. 161.

35 Kubal, G., Kiang, W., and Sadler, P. J., unpublished work.

36 Fatemi, S. J. A., Williamson, D. J., and Moore, G. R., J. Inorg. Biochem., 1992, 46, 35.

Determination of Total Phosphate in Waste Waters by On-line Microwave Digestion Incorporating Colorimetric Detection

Kathleen E. Williams and Stephen J. Haswell*
School of Chemistry, University of Hull, Hull, UK HU6 7RX

David A. Barclay
CEM Microwave Technology Ltd., 2 Middle Slade, Buckingham Industrial Park, Buckingham, UK MK18 1WA

Gaynor Preston
Severn Trent Laboratories, 156–170 Newhall Street, Birmingham, UK B3 1SE

A flow injection (FI) system for on-line microwave digestion of waste water samples with determination of total phosphate by means of colorimetric detection is described. Acidified samples are introduced into a water carrier stream and digested under continuous-flow conditions in thin-bore tubing. Following digestion, the samples are cooled on-line and then combined with further reagent streams for subsequent colorimetric detection based on the reduction of heteromolybdophosphoric acid to Molybdenum Blue as an FI peak at 690 nm. Signals from the flow-through detector are recorded as peak height on a chart recorder. Optimization of parameters such as digestion tube length, digestion tube diameter and reagent concentrations is discussed. Calibration was found to be linear up to 20 ppm of phosphate with a limit of detection of 0.10 ppm. Samples of waste water can be analysed at a rate of approximately 2 min per sample with typical sample relative standard deviations of <5% being achieved. Results for a range of samples were found to agree with those obtained by a conventional 'block' digestion autoanalyser method. The pre-treatment of samples with pyrophosphate phosphohydrolase ensured that the determination of total phosphate as orthophosphate could be achieved for samples containing pyrophosphate species.

Keywords: *Microwave digestion; on-line digestion; colorimetric detection; waste water; phosphate determination*

Waste water samples, which often contain high levels of suspended organic solids, are routinely analysed by the water industry for phosphate concentration.[1] This form of routine analysis requires rapid, simple and robust methodology in order to handle the large numbers and varying concentrations of phosphate species found in such samples. Most procedures for the determination of trace elements require the digestion of sample prior to instrumental analysis.[2] Commonly, this preliminary step proves to be both laborious and time consuming, particularly when using traditional digestion methods such as wet and dry ashing.[3] However, the development of microwave sample dissolution has proved to be of great advantage in that it dramatically reduces digestion time, and reduces both volatile analyte loss and sample contamination from the atmosphere.[4] The development of an on-line microwave digestion method would offer a more attractive approach to sample preparation over the discrete open or bomb digestion of samples. There have been a limited number of reports in the literature of systems for flow injection (FI) based methodologies[5] that will accommodate on-line sample preparation.[6-11] This paper describes the development of an FI system with on-line microwave digestion and subsequent colorimetric detection of phosphate in waste water samples.

Experimental

Reagents

All chemicals were of analytical-reagent grade, and distilled, de-ionized water was used throughout.

Ammonium heptamolybdate (0.005 mol l^{-1}) (*BDH, Poole, Dorset, UK*) *in* 0.4 mol l^{-1} *nitric acid* (*Fisons, Loughborough, Leicestershire, UK*).

Ascorbic acid (2% m/v) (*Aldrich, Gillingham, Dorset, UK*) *in* 1 l *distilled water with* 10 ml *of glycerol* [*May & Baker (now Rhone-Poulenc*), Dagenham, Essex, UK].

A few drops of Triton X-100 (Sigma, Poole, Dorset, UK) were added to each of the above reagents.

Phosphate stock standard solution, 100 ppm. Prepared from potassium dihydrogen orthophosphate (KH_2PO_4) (BDH) in 5% v/v nitric acid.

Nitric acid (5% v/v) *in distilled water.*

Stock solution of sodium tetrametaphosphate [(Na-PO_2)$_4$·$4H_2O$] (100 ppm) (*Albright & Wilson, London, UK*).

Stock solution of anhydrous trisodium trimetaphosphate [($NaPO_3$)$_3$] (100 ppm) (*Sigma*).

Inorganic enzyme pyrophosphatase (*pyrophosphate phosphohydrolase*; *EC* 3.6.1.1.) (*Sigma*).

Apparatus

The on-line system is illustrated in Fig. 1 and consisted of the following: a water carrier stream in 0.5 mm i.d. poly-(tetrafluoroethylene) (PTFE) tubing; an Ismatec MV-Z pump (Glattbrugg, Zurich, Switzerland); a Rheodyne injection valve (Model 5020 Anachem, Luton, Bedfordshire, UK) with a 1 ml sample loop; a Model MDS81 microwave oven (CEM, Buckingham, UK) containing 7.2 m of 0.5 mm i.d. PTFE tubing wrapped around a PTFE box; a 7 m cooling loop in an anti-freeze bath cooled by Peltier devices (MI1069T-03AC, Marlow Industries, Tadworth, Surrey, UK); a Rheodyne injection valve (Anachem 5020) with an on-line back-flush filter (made in-house) fitted instead of a sample loop; a CEM pressure sensor; a 516.75 kPa (75 psi) back-pressure regulator (Anachem P736); and a de-bubbler fitted to the outlet from the back-pressure regulator.

The outlet from the back-pressure regulator was coupled to a colorimetric detection system consisting of: two colorimetric reagent streams for molybdate and ascorbic acid reagents; two Gilson Minipuls 2 peristaltic pumps (Anachem); a 100 cm mixing coil; a 4 m reaction coil in a thermostatically controlled
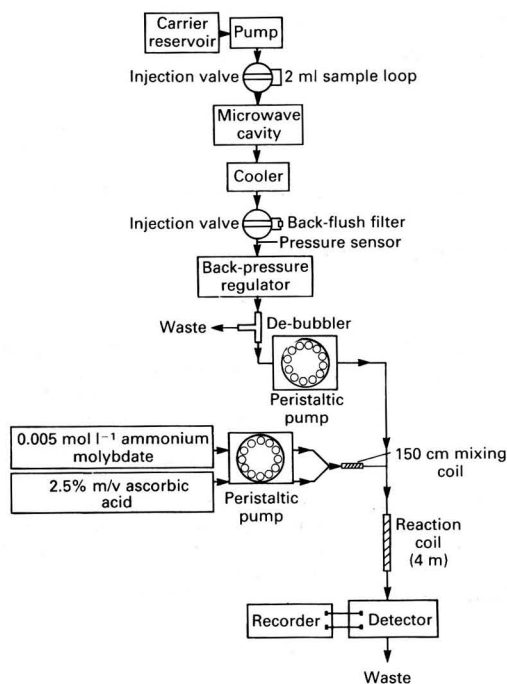
Fig. 1   Schematic diagram of the on-line digestion FI system

Fig. 2   Effect of carrier flow rate through the FI system on signal response

Fig. 3   Effect of sample injection volume on signal response

water-bath; a Cecil spectrophotometer (S & M Products, Didsbury, Greater Manchester, UK); and a Kipp & Zonen (Delft, Holland) BD112 flat-bed chart recorder.

Poly(tetrafluoroethylene) tubing of 0.5 mm i.d. was used throughout the whole system.

Procedure

Standards covering the range 0–20 ppm were prepared by taking appropriate dilutions of the stock standard phosphate solution and making up to volume in 5% v/v nitric acid. A 0.5 ml aliquot of concentrated nitric acid was added to 10 ml of waste water sample, resulting in a 5% v/v acidic solution. Standards and samples were analysed by injecting 2 ml aliquots into the system. Absorbance signals were recorded on a chart recorder and peak height measurements taken. Total analysis time for each sample was approximately 2 min. Replicate measurements were performed for each standard and sample.

Study on phosphate species present in samples

Samples and standards were prepared as described in the above procedure but without acidification. Sufficient units of enzyme activity were added to ensure hydrolysis of all pyrophosphate present in the standards and samples to orthophosphate. [Note: 1 U of enzyme activity will liberate 0.1 ppm min^{-1} of orthophosphate at pH 7.5 and 25 °C.] For example, 100 U of enzyme activity (500–700 U mg^{-1}) were added to 10 ml of a 10 ppm standard and the solution was left to stand at room temperature for 1 min before being acidified and analysed as detailed above.

Results and Discussion

Optimization of Digestion Conditions

It has been previously determined that the optimum microwave power and acid strength for sample digestion are 90 and 5% v/v, respectively.[2] The remaining variables controlling the
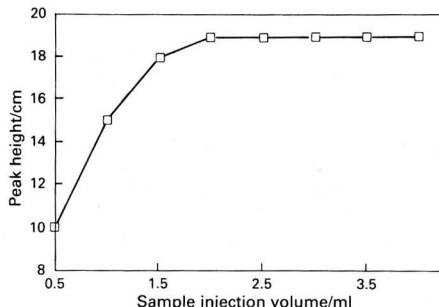
rate of digestion of sample in the microwave cavity are, therefore, flow rate, sample volume tube length and internal tube diameter. Signal sensitivity was evaluated by comparing the absorbance response for a standard 5 ppm phosphate solution in 5% v/v nitric acid. Having already selected a tube length of 7.2 m and an internal tube diameter of 0.5 mm,[10] the effect of flow rate on signal response was investigated.

The colorimetric reagent flow rate was kept constant throughout this experiment. Fig. 2 shows a plot of absorbance (measured as peak height) as a function of carrier flow rate through the FI system. At lower flow rates, dispersion will tend to increase with the sample slug being observed as a broad peak. However, as the carrier flow rate increases, the peaks become narrower while maintaining the same peak area; hence an increase in peak height is observed. It can be observed from the graph that an optimum signal response occurs when the carrier flow rate is set at 4.5 ml min^{-1}, indicating that on reaching the colorimetric reagents, an optimum reaction time and hence colour development has been achieved. At the higher flow rates (4.5–6 ml min^{-1}) there is insufficient reaction time to achieve optimum colour development and so the peak response rapidly begins to tail off.

Fig. 3 illustrates the effect of sample injection volume on signal response and clearly indicates that an optimum peak height for absorbance is achieved when a sample injection volume of 2 ml or more is used. Hence an optimum carrier flow rate of 4.5 ml min^{-1} and an injection volume of 2 ml were used.

Optimization of Phosphate Detection by FI

In order to obtain optimum signal sensitivity in the detection system it was necessary to minimize the dispersion of the sample slug as it passed through the detector. The degree of dispersion of the sample slug as it passed through the detector
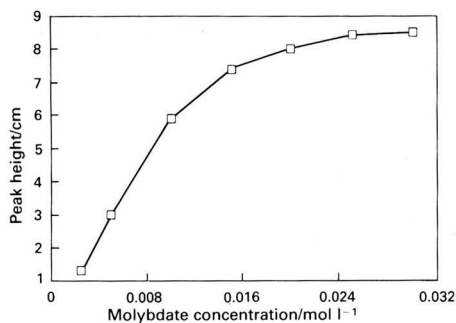
Fig. 4   Effect of molybdate concentration on signal response
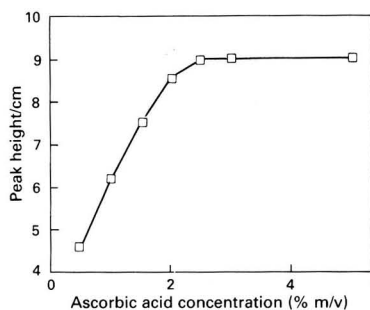
Fig. 5   Effect of ascorbic acid concentration on signal response
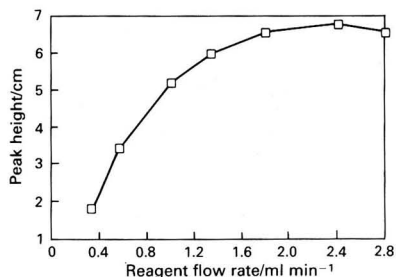
Fig. 6   Effect of reagent flow rate on signal response
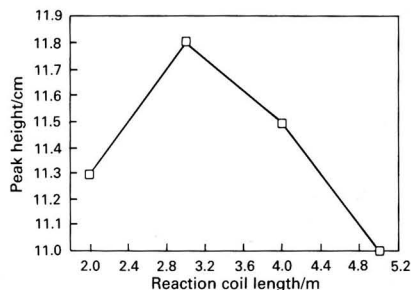
Fig. 7   Effect of changing reaction coil length for colour development on signal response

was controlled in effect by the flow rate, and the intensity of colour produced was found to be dependent on reagent concentration. Therefore, the two variables that most affect the signal sensivity were flow rate and reagent concentration. Signal sensitivity was evaluated by observing the absorbance response as peak height while holding the sample carrier flow rate constant at the pre-determined optimum. Figs. 4 and 5 show the effect of molybdate concentration and ascorbic acid concentration on signal response, respectively. Although the graph in Fig. 4 shows an optimum molybdate concentration being approached at 0.03 mol l^{-1}, it was found to be more practical to operate at a concentration of 0.015 mol l^{-1} molybdate, as solutions above this concentration were found to be unstable and began to change colour and re-precipitate after several hours. Fig. 5 simply shows that an optimum signal response is achieved at an ascorbic acid concentration of 2.5% m/v.

Hence the optimum reagent concentrations were chosen as 0.015 mol l^{-1} molybdate and 2.5% m/v ascorbic acid.

A study of the effect of reagent flow rate on peak height was carried out and the results are summarized in Fig. 6. As the flow rate increases, an increase in peak height is observed owing to a reduction in dispersion while maintaining sufficient reaction time for colour development to occur. At high flow rates, a reduction in peak response is attributed to inadequate time for reaction and colour development to occur. Hence an optimum peak response is observed at a flow rate of 2.4 ml min^{-1}.

The graph shown in Fig. 7 illustrates the effect of changing the reaction coil length for colour development on signal response. As the coil length increases, the time allowed for colour development increases and reaches an optimum at approximately 3 m, at which point the peak response begins to decrease owing to an increase of dispersion in the longer coils.

Hence it can be concluded that at reagent concentrations of 0.015 mol l^{-1} (molybdate) and 2.5% m/v (ascorbic acid), a flow rate of 2.4 ml min^{-1} and a coil length of 3 m, an optimum

signal response was obtained in the FI detection system for a given fixed carrier flow rate of 4.5 ml min^{-1}.

Calibration

Calibration using standards over the range 0–20 ppm phosphate in 5% v/v nitric acid was carried out and proved to be linear up to 20 ppm with relative standard deviations (RSDs) <5% ($n = 10$). The equation for the linear calibration graph was: $y = 1854x - 0.152$ ($r = 0.9983$). A limit of detection of 0.1 ppm was obtained with a sample throughput time of 30 h^{-1}.

Analysis of Samples

Table 1 shows a comparison of results for the determination of total phosphate in waste waters by a conventional 'block' batch digestion method with those obtained by the proposed FI methodology. The results, in general, were in good agreement with those obtained with the standard 'block' method and analysis was completed much more rapidly. The FI method was found to have a precision (RSD) of 1.4% ($n = 10$) at the 5 ppm level and a sampling rate of 25 h^{-1} (including sample preparation). No precision data (RSDs) were available for the batch method but they were expected from performance data to be in the range 1–5%. No particulates were observed in the flow system on leaving the microwave, indicating that complete digestion of suspended solids in the sample had taken place. The above results indicate that the proposed FI method represents a rapid and effective analytical methodology comparable in total phosphate recoveries to the traditional batch technique.

Phosphate Species Study

Previous studies have shown that only three classes of phosphate are stable to any extent in aqueous solution:[12] (i) orthophosphate (monophosphate); (ii) straight-chain polyphosphates (including pyro- and tripolyphosphate); and (iii) ring metaphosphates.

Table 1 Analysis of waste water samples by batch and FI methods for the determination of total phosphate

Sample number	Total phosphate by batch method (ppm)	Total phosphate by on-line FI method (ppm)	Precision (RSD) (%) ($n = 10$)
1	10.7	10.5	1.4
2	14.9	14.4	1.9
3	17.0	16.0	4.8
4	11.1	11.8	1.4
5	2.2	2.4	1.6
6	4.2	4.4	1.8
7	5.8	6.3	2.9
8	20.9	21.1	2.3
9	14.3	15.6	3.1
10	6.4	6.0	2.6
11	31.7	30.5	1.4
Total analysis time:	3 h	25 min	

Table 2 Percentage recovery of samples and standards for the determination of phosphate using the proposed FI method

Sample	Recovery (as orthophosphate) (%)	RSD (%)
Orthophosphate (10 ppm standard)	100	3.4
Trimetaphosphate (10 ppm standard)	101	2.4
Tetrametaphosphate (10 ppm standard)	99.3	3.1
Tetrapyrophosphate (10 ppm standard)	66.4	4.6
Pyrophosphate (10 ppm standard) + enzyme	99.1	2.7
Waste water sample + pyrophosphate spike (2 ppm)	68.1	3.1
Waste water sample + 2 ppm pyrophosphate spike + enzyme	99.5	2.8

Several studies have also shown that after complete hydrolysis, all of the ring and chain phosphates are converted into orthophosphate.[13]

It was considered important to determine whether or not all forms of phosphates present in waste water samples are converted into orthophosphate prior to detection and hence the total phosphate content is determined. Hence, several inorganic phosphates were chosen to be analysed and their percentage recoveries determined as orthophosphate. The phosphates analysed were as follows: tetrasodium pyrophosphate ($Na_4P_4O_7 \cdot 10H_2O$); sodium tetrametaphosphate [(Na-$PO_2)_4 \cdot 4H_2O$]; and trisodium trimetaphosphate [$(NaPO_3)_4$] (anhydrous).

By using the system and methodology described previously the results showed that good recoveries were obtained for the tetra- (101%) and trimetaphosphate (99%) but a fairly poor recovery was observed for the pyrophosphate (67%). This low percentage recovery is attributed to the rate of hydrolysis of pyrophosphate to orthophosphate. The three main factors affecting the rate of hydrolytic degradation of ring and chain phosphates in aqueous solution are temperature, pH and enzymes.[14] As the system was already operating at optimum temperature and pH (strong acid), it was necessary to examine the effects of enzymes on the rate of hydrolysis of pyrophosphate.

The inorganic enzyme pyrophosphatase (pyrophosphate phosphohydrolase; EC 3.6.1.1) was considered to be a suitable enzyme for this experiment.

Standard solutions were analysed using the methodology described and the results are reported in Table 2. Good recoveries were observed for ortho-, trimeta- and tetrametaphosphate, but a reduction of signal was found for the pyrophosphate standard. However, after treatment of the standard with the inorganic enzyme pyrophosphate phosphohydrolase, a recovery of 99.1% was achieved. On analysing waste water samples, the same reduction in signal was observed as before; however, the addition of enzyme enhanced the signal to give a spiked recovery of 99%. It can, therefore, be concluded that pre-treatment of samples with enzyme prior to acidification and analysis results in good percentage recoveries of total phosphate in samples where pyrophosphate might be present. Although pyrophosphates were not thought be be present in the waste water samples analysed, the proposed method is recommended where the form of phosphate in a sample is not known.

Conclusion

The proposed on-line sample digestion method with colorimetric detection was found to have a limit of detection of 0.1 ppm, a precision (RSD) of <5% ($n = 10$) and a sample throughput rate of 25 h^{-1} (including sample enzyme preparation). No particulates were observed in the flow system on leaving the microwave, indicating that complete digestion of suspended solids in the samples had taken place. Results for a range of waste water samples agreed with those obtained by a conventional 'block' digestion autoanalyser method. The pre-treatment of samples with the inorganic enzyme pyrophosphatase ensured that the determination of total phosphate as orthophosphate could be achieved for samples containing pyrophosphate species.

References

1 *Total Nitrogen and Total Phosphorus in Sewage Sludge. Section C. Methods for the Examination of Waters and Associated Materials*, HM Stationery Office, London, 1985.
2 Matusiewicz, H., and Sturgeon, R. E., *Prog. Anal. At. Spectrosc.*, 1989, **12**, 21.
3 Minczewski, J., Chwastowska, J., and Dybezynski, R., *Separation and Preconcentration Methods in Inorganic Trace Analysis*, Halsted Press, Chichester, 1983.
4 Gorsuch, T. T., *The Destruction of Organic Matter*, Pergamon Press, Oxford, 1970.
5 Růžička, J., and Hansen, E. H., *Flow Injection Analysis*, Wiley, New York, 2nd edn., 1988.
6 Burguera, M., Burguera, J. L., and Alarcon, O. M., *Anal. Chim. Acta*, 1986, **179**, 351.
7 Petersen, C., *New Sci.*, 1989, September, 44.
8 Burguera, J. L., de la Guardia, M., and Salvador, A., *J. Flow Inject. Anal.*, 1988, **5**, 121.
9 Haswell, S. J., and Barclay, D., *Analyst*, 1992, **117**, 117.
10 Williams, K. E., M.Sc. Thesis, University of Hull, 1991.
11 Hinkamp, S., and Schwedt, G., *Anal. Chim. Acta*, 1990, **236**, 345.
12 van Wazer, J. R., in *Encyclopedia of Chemical Technology*, eds. Kirk, R. C., and Othmer, D. F., Interscience, New York, 1953, vol. X, pp. 403–510.
13 van Wazer, J. R., *Anal. Chem.*, 1954, **26**, 1755.
14 van Wazer, J. R., *Phosphorus and its Compounds. Volume 1. Chemistry*, Wiley-Interscience, New York, 1958.

Isomeric Characterization of Polychlorinated Biphenyls Using Gas Chromatography–Fourier Transform Infrared/Gas Chromatography–Mass Spectrometry

Doyle M. Hembree, Jr.,* Norman R. Smyrl,* Willard E. Davis and David M. Williams
Plant Laboratory, Oak Ridge Y-12 Plant,† Martin Marietta Energy Systems, Inc., Oak Ridge, TN 37831-8189, USA

A new technique combining both mass spectrometry and infrared spectroscopy to analyse simultaneously the components from a single gas chromatographic injection has been applied to the quantitative and qualitative characterization (including distinguishing positional isomers) of polychlorinated biphenyl (PCB) mixtures. The sensitivity of vibrational spectroscopy to subtle differences in structure was shown to be highly complementary to gas chromatography–mass spectrometry (GC–MS) for qualitative identification of individual PCB isomers and congeners. A key feature of the infrared apparatus is the provision for low-temperature trapping (approximately 77 K) of the GC effluent for subsequent analysis. This technique produces infrared spectra that resemble normal room-temperature condensed-phase spectra (as opposed to the gas-phase spectra produced by light-pipe gas chromatography–Fourier transform infrared spectroscopy) and leads to lower detection limits (500 pg for 3,3′,4,5-tetrachlorobiphenyl). The GC–MS portion of the instrument provides superior quantitative capabilities with sub-picogram detection limits possible using selective ion monitoring.

Keywords: *Polychlorinated biphenyl; gas chromatography–mass spectrometry; gas chromatography–Fourier transform infrared spectroscopy; isomer identification*

In the past, mixtures of polychlorinated biphenyls (PCBs) have been widely used in many industrial applications because of their many desirable chemical and physical properties. However, the discovery that some members of this relatively large class of compounds (209 isomers and congeners are possible) are toxic to both humans and other forms of life has led to the virtual elimination of their use.[1] Efforts to dispose of these environmentally persistent compounds, often using improper disposal methods, have resulted in extensive contamination of many of the world's ecosystems including the North Atlantic, which may contain up to 79% of the total environmental inventory of USA-derived PCBs.[1] In order to assess properly the impact of the environmental burden of PCBs, it is essential that analytical procedures exhibiting adequate sensitivity and capable of making accurate qualitative as well as quantitative determinations be developed. In particular, it has been suggested that studies should be undertaken to assess the environmental fate and toxic effects of individual PCB congeners.[2,3]

Complex mixtures of PCBs such as those isolated from typical environmental samples are usually analysed by gas chromatography–mass spectrometry (GC–MS) or GC with an electron-capture detector. Many studies have been performed with capillary column GC to identify and quantify, at least tentatively, PCBs based on relative retention times and response factors.[2–7] However, isomer-specific identification of individual PCB compounds using GC–MS or GC is extremely difficult in practice and in most routine analyses results are simply reported as total PCBs, with no attempt made to identify individual compounds. The difficulty in distinguishing between similar chemical species becomes important for classes of compounds, such as PCBs, in which only a few members possess a property of interest, such as biological activity (polycyclic aromatic hydrocarbons and nitrogen heterocycles are further examples of important classes of compounds where isomer-specific identification is desirable).

Vibrational spectroscopy is an extremely sensitive probe of molecular structure and many attempts have been made to exploit this fact for analytical purposes.[8,9] The use of Fourier transform infrared (FTIR) spectroscopy to detect the effluent from a capillary column gas chromatograph using a gold-coated light-pipe has proved powerful (high picogram detec-
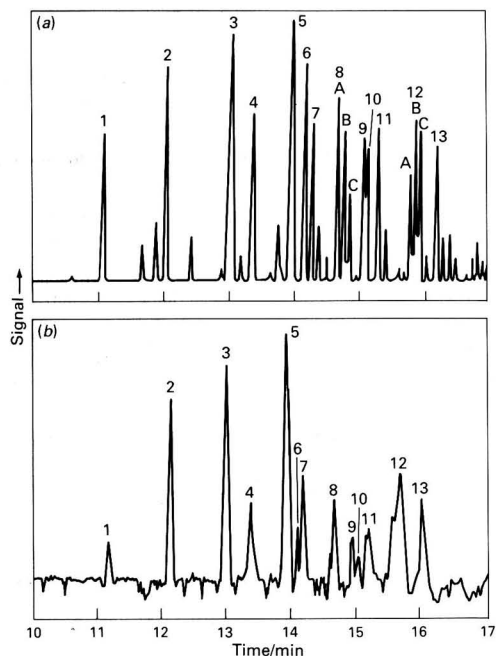

Fig. 1 Chromatograms of Aroclor 1242. (*a*) GC–MS total ion chromatogram. (*b*) IR functional group chromatogram (1400–1650 cm⁻¹ region) of Aroclor 1242 from the same GC injection as in (*a*)

* Authors to whom correspondence should be addressed.
† Operated for the US Department of Energy by Martin Marietta Energy Systems, Inc., under contract DE-AC05-84OR21400.

tion limits for strong infrared absorbers), but the technique is several orders of magnitude less sensitive than GC–MS, and produces gas-phase spectra that are difficult to use with the large, commercial condensed-phase libraries. The recent introduction of low-temperature trapping to capture the effluent from a capillary GC column,[10] combined with the use of a highly sensitive HgCdTe (MCT) IR detector, has reduced FTIR detection limits to the range of GC–MS (low picogram levels for strong infrared absorbers) and gives rise to condensed-phase spectra resembling those obtained at room temperature using conventional sampling methods. In this study, an instrument combining the capabilities of both FTIR and MS[11-13] to analyse simultaneously the various components in PCB mixtures as separated by capillary-column GC will be discussed. When isomer-specific identification is required GC–FTIR is shown to be highly complementary to conventional GC–MS.

Experimental

Apparatus

The common sample introduction point for the GC–FTIR/GC–MS instrument was a gas chromatograph (Model 5890A, Hewlett-Packard, Palo Alto, CA, USA) equipped with two matched 25 m methyl silicone gum capillary columns (Hewlett-Packard Model HP-1) connected to a single injector. The matched columns gave a 50:50 split ratio (*i.e.*, 50% of the injection was routed to the MS system and 50% to the FTIR system). The FTIR system was a Digilab FTS-45 spectrometer (Biorad, Digilab Division, Cambridge, MA, USA) equipped with an accessory (Digilab Tracer) for capturing the GC effluent on a ZnSe plate held at low temperature (approximately 77 K). Mass spectrometric data were collected with a Hewlett-Packard Model 5970B mass selective detector (MSD). Further details of the experimental arrangement are presented elsewhere.[11]

Table 1 Identification of the chromatographic peaks in Fig. 1

Peak number	Retention time/min*	IR identification	MS identification [hit index]
1	11.05	2,2'-Dichlorobiphenyl	2,4'-; **2,2'-**3,3'-; 4,4'-; 2,6-; 3,4- [98]
2	12.01	2,4'-Dichlorobiphenyl	4,4'-; 3,3'- [99] **2,4'-**; 2,3- [98]
3	12.95	2,2',5-Trichlorobiphenyl	2,3,4-; 2,4',5-; **2,2',5-** [99]
4	13.31	2,2',3-Trichlorobiphenyl and another trichloroisomer	2,4,6-; 2,4',5-; 2,4,5-; 2,2',5- [99]
5	13.88 13.91	2,4',5-Trichlorobiphenyl + 2,4,4'-Trichlorobiphenyl	2,3,4-; 2,3',5-; **2,4',5-;** **2,4,4'-**; 2,4,5- [99]
6	14.10	2',3,4-Trichlorobiphenyl	2,3',5-; 2,3,4-; 2,4,6-; 2,4',5-; 2,4,4'- [98]
7	14.21	2,3,4'-Trichlorobiphenyl	2,4,6-; 2,3',5- [99]
8A	14.63	2,2',5,5'-Tetrachlorobiphenyl	2,2',5,6'-; 2,2',4,5'-; **2,2',5,5'-;** 2,2',3,4-; 2,3,4',6-; 2,3,3',5'-; 2,2',3,4'-; 2,2',6,6'- [99]
8B	14.74	2,2',4,5'-Tetrachlorobiphenyl	2,3,4',6-; 2,3,3',5'-; 2,3',4',6-; 2,3,3',4-; **2,2',4,5'-;** 2,2',5,5'-; 3,3',5,5'-; 2,2',3,4-; 3,3'4,5'- [99]
8C	14.83	2,2',4,5-Tetrachlorobiphenyl	2,2',3,4-; 2,3,3',5'-; 2,3',4',6-; 2,3,3',4'-; 2,2',4,5'-; 2,2'5,5'-; 3,3',5,5'-; 2,3,4',6-; 2,2',6,6'- [99]
9	15.04	2,2',3,5'-Tetrachlorobiphenyl	2,2',3,4-; 2,3,4',6-; 2,3,3',5'-; 2,3',4',6-; 2,3,3',4'-; 2,2',5,6'-; 2,2',3,4'-; 2,2',6,6'- [99]
10	15.06	3,4,4'-Trichlorobiphenyl and a tetrachlorobiphenyl (no library spectrum)	2,2',3,4-; 2,2',3,4- [97]†
11	—	A tetrachlorobiphenyl (no library spectrum)	2,3,4',6-; 2,3,3',5'-; 3,3',4,5'-; 2,3',4',6-; 2,3,3',4'-; 3,3',5,5'-; 2,2',6,6'-; 2,2',3,4-; 2,3',4',5- [99]
12A	15.74	2,4,4',5-Tetrachlorobiphenyl	3,3',4,5'-; 2,3,3',4'-; 2,3,4,5-; 3,3',5,5'-; 2,4,4',6-; 2,3',4',5-; 2,3',4,4'-; 2,2',6,6'-; 2,3',5,5'- [99]
12B	15.81	2,3',4',5-Tetrachlorobiphenyl	3,3',4,4'-; 2,3',4,4'-; 2,2'6,6'-; 2,2',4,4'-; 2,2',3,4-; 2,3,4',6-; 3,3',5,5'- [99]
12C	15.85	2,3',4,4'-Tetrachlorobiphenyl	2,3,4',6-; 3,3',4,5'-; 2,3,4,5-; 3,3',4,4'-; 2,3',4',5-; **2,3',4,4'-;** 2,2',6,6'-; 2,2',3,4-; 2,3,3',5'- [99]
13	—	A tetrachlorobiphenyl (no library spectrum)	2,3,4',6-; 2,3,3',5'-; 3,3'4,5'-; 2,3,3',4'-; 2,3',5,5'-; 2,3',4',5-; 2,3',4,4'-; 2,2',6',6'-; 2,2',3,4- [99]

* Retention time of the standard of the PCB identified by IR analysis [under the same chromatographic conditions as Fig. 1(*b*)].
† Mass spectrum contains both a 258 and 292 mass fragment. The 258 mass (parent ion of trichlorobiphenyls) is about twice the intensity of the 292 mass.

Reagents

One hundred and thirty PCB standards (100 µg ml^{-1} in hexane) were analysed as received from Ultra Scientific (North Kingstown, RI, USA) in order to build GC–FTIR/GC–MS spectral libraries. Standard IR and mass spectra were obtained for 50 ng samples (100 ng injection). Aroclor 1242 (Ultra Scientific), a common PCB mixture containing 42% m/m chlorine, was used to test the capabilities of the instrument for analysing complex mixtures of PCBs.

Procedure

The gas chromatograph was operated in the splitless mode at a measured flow rate of 0.4 ml min^{-1} at 250 °C. High-purity helium treated to remove water was used as the carrier gas. All of the work described in this study was performed with a temperature programme consisting of a 2 min hold at 80 °C followed by a ramp to 250 °C at 10 °C min^{-1}. The MSD was operated in the scanning mode from 50 to 550 u. Infrared 'functional group' chromatograms were generated by monitoring the total IR intensity in the 1400–1650 cm^{-1} region, where most PCBs have relatively intense absorption bands due to C–C skeletal stretching. Individual PCBs were identified using computer searches of the National Institute of Standards and Technology mass spectrometry library (≈41 000 compounds) and the IR library generated from PCB standards (using the Digilab spectral library search routine).

Results and Discussion

The GC–MS total ion chromatogram and the IR functional group chromatogram for a 1 µl injection of Aroclor 1242 (1 µg ml^{-1} in hexane) are shown in Fig. 1(a) and (b), respectively. Identifications of the various chromatographic peaks are given in Table 1. The MS compound identifications
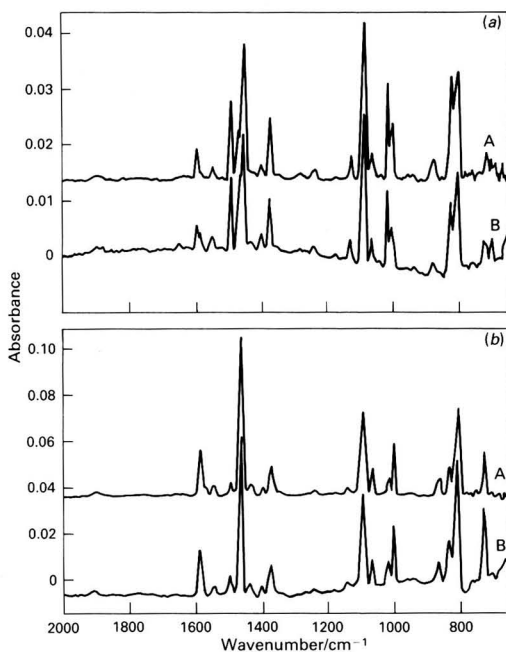
are followed by a 'hit' index, with a value of 100 representing a perfect match between the unknown and the standard spectrum (only the compounds with the highest hit index or indexes are given in Table 1). In most cases, multiple compounds had identical indexes, and the order in which the compounds are listed is not significant; MS identifications that agree with the IR results are listed in bold typeface. Examination of the mass spectrometric results clearly illustrates the difficulties associated with distinguishing positional isomers. In many cases, the correct isomer, identified by both the IR spectrum and retention time of the standard PCB, is not among the compounds with the highest MS hit index (chromatographic peaks 4, 6, 7, 8C, 9, 10, 12A and 12B).

In contrast to the MS results, when complete chromatographic separation was achieved, the IR spectral search provided unequivocal identification of the unknown PCB, except in cases where a standard spectrum was not available. The IR spectra obtained near the centre of chromatographic peaks containing co-eluting compounds are a superposition of the spectra of all of the compounds giving rise to the peak. Under such conditions, a spectral search usually provides no compound identification. However, by taking spectra from the leading and trailing edges of the peak, relatively 'clean' spectra of the first and last components comprising the peak can be obtained. As an example, the initial IR results for peak 5 in Fig. 1 gave no plausible identification of the compound(s) giving rise to the peak, while MS analysis indicated that five trichlorobiphenyl isomers were equally likely (i.e., these
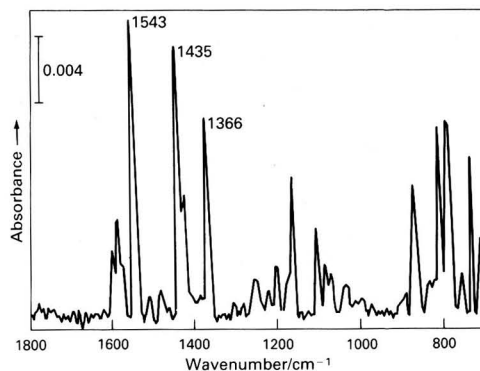
Fig. 3 IR spectrum of 25 ng of 3,3',4,5-tetrachlorobiphenyl obtained with the GC–FTIR Tracer unit (1800–700 cm^{-1})

Fig. 2 IR spectra of two PCB isomers isolated from Aroclor 1242. (a) A, Standard spectrum of 2,4',5-trichlorobiphenyl; and B, spectrum from leading edge of peak 5 in Fig. 1(b) (13.85 min). (b) A, Standard spectrum of 2,4,4'-trichlorobiphenyl; and B, spectrum from trailing edge of peak 5 in Fig. 1(b) (13.99 min)

Fig. 4 Signal-to-noise enhancement from FTIR signal averaging. A, IR spectrum of 1 ng of 3,3',4,5-tetrachlorobiphenyl (200 scans at 8 cm^{-1} resolution); and B, IR spectrum of the same 3,3',4,5-tetrachlorobiphenyl sample as in A obtained 'on-the-fly' (4 scans at 8 cm^{-1} resolution)

isomers have essentially identical mass spectra). The IR spectra obtained from the leading and trailing edges of peak 5 are shown in Fig. 2, and are compared with standard spectra of the identified compounds. Even though HP-1 methyl silicone gum GC stationary phase was used in this study, the elution order of the 2,4′,5- and 2,4,4′-trichlorobiphenyl isomers is consistent with relative retention times reported for SE-54.[2]

The quantitative response of the GC–FTIR/GC–MS instrument was investigated using 3,3′,4,5-tetrachlorobiphenyl as a model compound. The IR spectrum of this compound (25 ng) is shown in Fig. 3. The ability to enhance the signal-to-noise (S/N) ratio of smaller amounts of compounds obtained with the Tracer GC–FTIR unit is demonstrated in Fig. 4. The bottom spectrum was obtained 'on-the-fly' (4 scans at 8 cm^{-1} resolution) for 1 ng of 3,3′,4,5-tetrachlorobiphenyl. After completion of the GC run, the deposition plate was returned to the spot where the bottom curve was obtained. Two hundred scans at 8 cm^{-1} resolution were signal averaged to obtain the top spectrum in Fig. 4. Three spectral features at 1543, 1435 and 1366 cm^{-1} are easily observed in the top spectrum but are not discernible in the bottom spectrum.

Straight line regression calibrations for both instruments were computed for 3,3′,4,5-tetrachlorobiphenyl from 1 to 50 ng. The response for both instruments is linear over most of the range. The coefficients of determination (R^2) were 0.987 for the GC–MS data and 0.975 for the GC–FTIR calibration (three measurements were averaged for each point on the calibration lines). The detection limit for GC–MS was significantly lower than for FTIR because PCBs are relatively weak IR absorbers, in general, and this tetrachloroisomer is weaker than most other PCBs [a (absorptivity) = 1138 cm^{-1} measured experimentally for the 1543 cm^{-1} band]. Based on an S/N of 2, the detection limit for GC–MS was 200 pg using the total ion peak height and 2 pg using selective ion monitoring of the 292 mass fragment, while a detection limit of 500 pg was obtained using the peak height of the 1543 cm^{-1} band in the FTIR spectrum.

Conclusions

The 'double-hyphenated' technique of GC–FTIR/GC–MS provides, for the first time, a convenient means of obtaining condensed-phase IR spectra (at high sensitivity and similar to conventional spectra obtained at room temperature) simultaneously with the corresponding mass spectrum. Because the frequencies of the normal modes of vibration of very similar molecules, even positional isomers, are usually different, IR spectroscopy using low-temperature trapping is a powerful qualitative complement to conventional mass spectrometric detection of the effluent from a capillary column gas chromatograph.

References

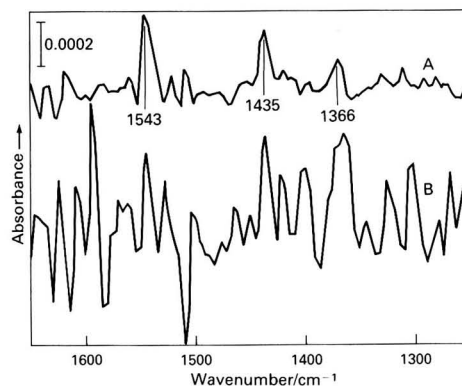1   The National Research Council, Committee on the Assessment of PCBs in the Environment, *Polychlorinated Biphenyls*, National Academy of Sciences, Washington, DC, 1979.
2   Mullin, M. D., Pochini, C. M., McCrindle, S., Romkes, M., Safe, S. H., and Safe, L. M., *Environ. Sci. Technol.*, 1984, **18**, 468.
3   Capel, P. D., Rapaport, R. A., Eisenreich, S. J., and Looney, B. B., *Chemosphere*, 1985, **14**, 439.
4   Cooper, S. D., Moseley, M. A., and Pellizzari, E. D., *Anal. Chem.*, 1985, **57**, 2469.
5   Steichen, R. J., Tucker, R. G., and Mechon, E., *J. Chromatogr.*, 1982, **236**, 113.
6   Bush, B., Murphy, M. J., Connor, S., Snow, J., and Barnard, E., *J. Chromatogr. Sci.*, 1985, **23**, 509.
7   Hasan, M. N., and Jurs, P. C., *Anal. Chem.*, 1988, **60**, 978.
8   Schneider, J. F., Reedy, G. T., and Ettinger, D. G., *J. Chromatogr. Sci.*, 1985, **23**, 49.
9   Hembree, D. M., Garrison, A. A., Crocombe, R. A., Yokley, R. A., Wehry, E. L., and Mamantov, G., *Anal. Chem.*, 1981, **53**, 1783.
10 Bourne, S., Haefner, A. M., Norton, K. L., and Griffiths, P. R., *Anal. Chem.*, 1990, **62**, 2448.
11 Smyrl, N. R., Hembree, D. M., Jr., Davis, W. E., Williams, D. M., and Vance, J. C., *Appl. Spectrosc.*, 1992, **46**, 277.
12 Wilkins, C. L., *Science*, 1983, **222**, 291.
13 Cooper, J. R., Bowater, I. C., and Wilkins, C. L., *Anal. Chem.*, 1986, **58**, 2791.

253

Addition and Measurement of Water in Carbon Dioxide Mobile Phase for Supercritical Fluid Chromatography

Dongjin Pyo and Doweon Ju
Department of Chemistry, Kangweon National University, Kangweon-do, Korea

A method for the addition of water to supercritical CO_2 is described. Carbon dioxide, the most widely used mobile phase in supercritical fluid chromatography, is a relatively non-polar fluid, and hence the addition of small amounts of polar modifiers could be necessary to migrate polar solutes. In this work, supercritical CO_2 is delivered from the pump to a μ-Porasil column that is saturated with water. After passing through the μ-Porasil column, supercritical CO_2 is changed to a new mobile phase with different polarity, and it is possible to separate polar samples by using this new mobile phase. The amount of water dissolved in supercritical CO_2 is measured by an amperometric microsensor, which is prepared from a thin film of perfluorosulfonate ionomer.

Keywords: *Supercritical carbon dioxide fluid; modifier; water; mobile phase*

Many developments have been reported since the first use of supercritical fluids as chromatographic mobile phases in 1962.[1] Especially in the last few years, supercritical fluid chromatography (SFC) has progressed from a laboratory curiosity to a viable analytical technique for solving many otherwise intractable problems. However, the most commonly used mobile phases in SFC are all relatively non-polar fluids. Carbon dioxide, the most widely used fluid, is no more polar than hexane[2,3] even at high densities. Solute polarity should be between that of the stationary phase and the mobile phase in order to effect a straightforward separation. Few real-world samples contain only non-polar solutes, so a major objective of research into SFC has been directed towards increasing the range of solute polarity that can be handled by the technique. To bring the SFC technique into routine use, mobile phases that are more polar than the commonly used CO_2 are necessary.

The solvent strength of supercritical CO_2, even at high density, is not sufficient for the elution of polar solutes. Polar mobile phases such as NH_3 exhibit useful properties,[4] but a more practical way to extend the range of compounds separable by SFC is the use of mixed mobile phases. The addition of modifiers (generally organic solvents) to supercritical CO_2 changes the polarity of the mobile phase and also leads to a de-activation of the column packing material.[5] In capillary SFC, most separations are carried out with pure CO_2 because of its compatibility with a flame-ionization detector (FID); indeed, except for formic acid and water the addition of any common modifier precludes the use of an FID.[6] Modifiers are essential in packed-column SFC for the elution of polar compounds[7] and are extensively used. Several papers have reported the influence of modifiers on peak shape, selectivity and retention time in capillary and packed column SFC.[5,7,8] In this work, a new mobile phase with enhanced polarity was prepared by passing supercritical CO_2 fluid through a μ-Porasil column saturated with water. It is shown that some polar samples can be separated with this new mobile phase in packed-column SFC.

Experimental

A CCS (Computer Chemical Systems, Avondale, PA, USA) Model 5000 supercritical fluid chromatograph was used with a 100×2 mm packed column (Nucleosil diol). This system was equipped with a C14W loop injector (Valco Instruments, Houston, TX, USA) and an FID. Supercritical fluid chromatography grade CO_2 (Scott Specialty Gases, Plumsteadville, PA, USA) was used as a basic mobile phase. Experimental conditions for SFC separations were as follows: supercritical

CO_2 at 150 °C, pressure programmed from 27.56 to 34.45 MPa (4000–5000 lb in^{-2}) at 0.28 MPa (40 lb in^{-2}) min^{-1}, FID detection at 300 °C, 10 cm^3 min^{-1} restrictor flow at 10.34 MPa (1500 lb in^{-2}). For the addition of water to supercritical CO_2, a μ-Porasil column, which is manufactured for normal-phase high-performance liquid chromatography by Waters (Milford, MA, USA), was used, its functional group being a hydroxy group (–OH). The μ-Porasil column was saturated with water by means of a Model 5560 reciprocating pump (Varian, Palo Alto, CA, USA) and placed between the pump and the injector. In order to measure the amount of water dissolved in the supercritical fluid, an amperometric microsensor was used, which was prepared from perfluorosulfonate (PFSI) polymer.[9] A constant-current power supply (0.1 μA, Sungun, Seoul, Korea) was used to measure the voltage drop across the sensor. The sensor output was recorded on a strip-chart recorder (Knauer, Berlin, Germany).

Results and Discussion

When dealing with the use of modifiers, it should be mentioned that some problems always arise. First, a binary mixture of eluents can contaminate the instrument. In particular, modifiers remaining in a pump can cause corrosion of the pump and be slowly eluted during the next run. This can affect the time required to achieve chemical equilibrium for the subsequent separations. Second, many modifiers can diffuse in the laboratory and contaminate the laboratory air. To overcome these problems, we designed the system that is shown in Fig. 1. A polar modifier (water) is added to the pressurized carbon dioxide fluid after the pump, and hence no modifier remains in the pump. Supercritical CO_2 is delivered from the pump to the μ-Porasil column, which is saturated with water. When supercritical CO_2 passes through the
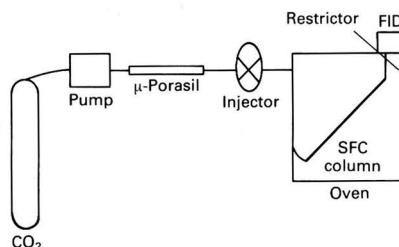

Fig. 1 Schematic diagram of the apparatus used for adding a polar modifier to the supercritical fluid mobile phase

μ-Porasil column, H$_2$O, retained on the –OH groups of μ-Porasil by hydrogen bonding, can dissolve in the pressurized supercritical fluids. With this method, non-polar supercritical CO$_2$ can have the characteristics of a polar mobile phase because it can absorb polar solvent (H$_2$O). Therefore, after passing through the μ-Porasil column, supercritical CO$_2$ is changed to a new mobile phase with different polarity, and it is possible to separate polar samples using this new mobile phase.

An experiment to separate some polar samples (insecticides and fungicides) with this new mobile phase was performed. Figs. 2 and 3 are chromatograms for mixtures of insecticides and fungicides obtained using a mixed mobile phase (supercritical CO$_2$–water). In contrast to the experiment in which only CO$_2$ was used as mobile phase, excellent separations were obtained. When only CO$_2$ was used for these samples, unseparated and very broad peaks were observed in about 25 min. The addition of a small amount of water to supercritical CO$_2$ reduced the retention and improved the peak shapes. The phenomena are in accord with the results reported by Blilie and Greibrokk.[5] The structure of each peak is shown in Table 1.

To measure the amount of water dissolved in supercritical CO$_2$, a polymer film[9] (i.e., a film of PFSI ionomer), which has a high affinity for water, was used. When the PFSI film was in contact with two electrodes and a constant current flowed through the film, the water that partitioned into the film from the surrounding environment was electrolytically decomposed. The change of voltage across two electrodes was used as a measure of the water content of the environment surrounding the sensor.

Fig. 4 shows a cross-section of the modifier (water) sensor used in this work. A platinum wire was wrapped with PFSI

thin film and another platinum wire was wound in a coil over the assembly. The sensor constructed in this way was placed in a plastic tube, and the entire modifier-measuring device was assembled together as shown in Fig. 5. A constant-current (d.c.) source was used to supply a current of about 0.1 μA to the sensor. The resistance of the PFSI film was changed according to the water content of the supercritical CO$_2$ fluid,
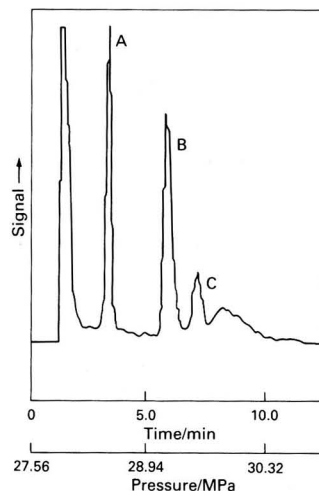
Fig. 2 Chromatogram of a mixture of insecticides and fungicides. A, Thiolix; B, kitazine; and C, captan

Table 1 Structures of peaks in the chromatograms

| Chromatogram	Peak	Commercial name	Chemical name	Structure
Fig. 2	A	Thiolix (insecticide)	1,4,5,6,7,7-Hexachloronorborn-5-ene-2,3-dimethanol sulfite	
	B	Kitazine (fungicide)	S-Benzyl-O,O-diisopropyl phosphorothioate	
	C	Captan (fungicide)	N-(Trichloromethylthio)cyclohex-4-ene-1,2-dicarboximide	
Fig. 3	A	Hinosan (fungicide)	O-Ethyl-S,S-diphenyl dithiophosphate	
	B	Parathion (insecticide)	O,O-Diethyl-O-4-nitrophenyl phosphorothioate	
	C	DDVP (insecticide)	2,2-Dichlorovinyl dimethylphosphate	
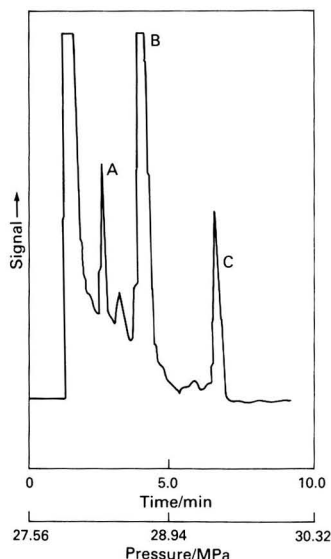
Fig. 3 Chromatogram of a mixture of insecticides and fungicides. A, Hinosan; B, parathion; and C, DDVP
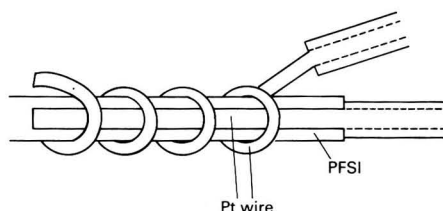
Fig. 4 Cross-section of the modifier sensor
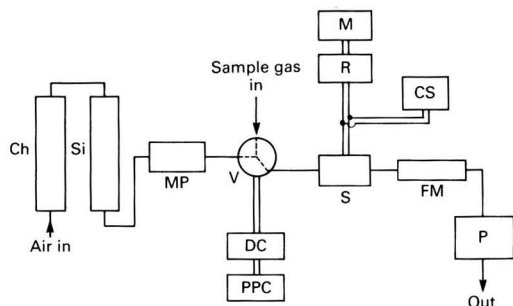
Fig. 5 Schematic diagram of the device used to measure water content: P, pump; V, solenoid valve; S, sensor; FM, flow meter; MP, magnesium perchlorate; R, recorder; M, multimeter; DC, 12 V power supply; PPC, programmable process controller; Ch, Si, charcoal, silica gel; and CS, current source

and the voltage difference between the two platinum wires was recorded and measured.

Fig. 6 shows chromatograms for the injection of (a) air saturated with water, and (b) supercritical CO_2 fluid saturated with water, through a μ-Porasil column at different time intervals. Air saturated with water was generated by passing air, with bubbling, through water contained in two sequential bottles, and was injected directly into the sensor through a three-way solenoid valve (Radio Shack, Fort Worth, TX, USA). The determination of water in CO_2 after passage through the μ-Porasil column was performed on-line, *i.e.*, supercritical CO_2 fluid was injected through a C14W loop-injector, and the sensor was placed directly after the μ-Porasil column.
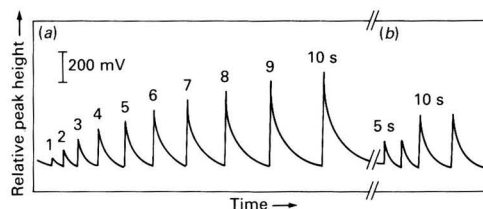
Fig. 6 Relative peak height at different time intervals (flow rate: 0.5 dm³ min⁻¹, temperature: 20 °C). (a) For air saturated with water and (b) for carbon dioxide fluid saturated with water
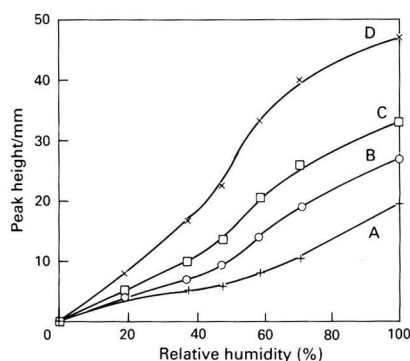
Fig. 7 Sensor response for various relative humidity levels (18.8, 37.1, 47.2, 58.3, 70.4 and 100% relative humidity). A, 10; B, 15; C, 20; and D, 25 °C

By using the data (Fig. 7) on the correlation of peak height with percentage relative humidity (RH) at different temperatures, the water content of supercritical CO_2 fluid, after passage through the water-saturated μ-Porasil column, could be determined. From the data in Fig. 6(b), the amount of water dissolved in supercritical CO_2 was measured as 54% RH or 3.00×10^{-3} g dm⁻³ at a pressure of 25.33 MPa (250 atm). The amount of water in the mobile phase remained constant for about 1 h, but after that decreased exponentially. Therefore, after three or four runs the column must be refilled with water for practical use. Sulfuric acid solutions of known compositions[10] were used to generate the standard RH streams.

References

1 Klesper, E., Corwin, A. H., and Turner, D. A., *J. Org. Chem.*, 1962, **27**, 700.
2 Hyatt, J. A., *J. Org. Chem.*, 1984, **49**, 5097.
3 Yonker, C. R., Frye, S. L., Lalkwarf, D. R., and Smith, R. D., *J. Phys. Chem.*, 1986, **90**, 3022.
4 Kuei, J. C., Markides, K. E., and Lee, M. L., *J. High Resolut. Chromatogr.*, 1987, **10**, 257.
5 Blilie, A. L., and Greibrokk, T., *Anal. Chem.*, 1985, **57**, 2239.
6 Wright, B. W., and Smith, R. D., *J. Chromatogr.*, 1986, **355**, 367.
7 Schmidt, S., Blomberg, L. G., and Campbell, E. R., *Chromatographia*, 1988, **25**, 775.
8 Yonker, C. R., and Smith, R. D., *J. Chromatogr.*, 1986, **361**, 25.
9 Huang, H., and Dasgupta, P. K., *Anal. Chem.*, 1990, **62**, 1935.
10 *CRC Handbook of Chemistry and Physics*, ed. Weast, R. C., CRC Press, Boca Raton, FL, 70th edn., 1989, pp. E-43 s.

Oxazole-based Tagging Reagents for Analysis of Secondary Amines and Thiols by Liquid Chromatography With Fluorescence Detection

Toshimasa Toyo'oka, Hitesh P. Chokshi, Robert G. Carlson, Richard S. Givens and Susan M. Lunte*
Center for Bioanalytical Research, University of Kansas, 2095 Constant Avenue, Lawrence, KS 66047, USA

The reactions of three fluorescent tagging reagents, 2-chloro-4,5-diphenyloxazole (DICLOX), 2-fluoro-4,5-diphenyloxazole (DIFOX) and 2-chloro-4,5-bis(p-N,N-dimethylaminosulfonylphenyl)oxazole (SAOX-Cl), with thiols and amines are reported. Emission maxima for the diphenyloxazole (DIOX) and SAOX derivatives of amines were 420 nm (λ_{ex} 320 nm) and 485 nm (λ_{ex} 360 nm), respectively. The emission wavelengths for the DIOX- and SAOX-thiols were 390 nm (λ_{ex} 310 nm) and 425 nm (λ_{ex} 330 nm), respectively. In all cases, the derivatives exhibited strong fluorescence whereas the reagents themselves exhibited only weak fluorescence. The labelled derivatives are very stable, less than 5% decomposition occurs after heating at 60 °C for 2 h. Fluorescence intensities of the amine derivatives were higher in neutral and alkaline than in acidic solutions and were virtually independent of solvent polarity. The thiol derivatives exhibited fluorescence intensities that were relatively constant under all conditions studied. The relative reaction rate toward both thiols and amines was DIFOX > SAOX-Cl > DICLOX. The reaction of proline with DIFOX was complete after 60 min at room temperature at pH 9.3. However, the yield with SAOX-Cl was only 70% at 60 °C after 3 h, and only a small amount of proline could be derivatized with DICLOX (less than 3%). Thiols, on the other hand, reacted relatively rapidly with SAOX-Cl. Therefore, SAOX-Cl was used for the determination of thiols and DIFOX was employed for amines in all subsequent studies. Detection limits (signal-to-noise ratio = 2) for authentic DIOX-amines ranged from 3.7 to 28.4 fmol, and SAOX-thiols ranged from 1.2 to 1.9 fmol.

Keywords: *Derivatizing reagents; secondary amine; liquid chromatography; fluorescence; amino acid*

Thiols and amines are important constituents of most living organisms. Several fluorogenic reagents have been employed for the determination of secondary amines, the most common being 5-dimethylaminonaphthalene-1-sulfonyl chloride (dansyl-Cl), 9-fluorenylmethylchloroformate (FMOC), and 3-chloro-7-nitrobenzofurazan (NBD-Cl) and its fluoro analogue (NBD-F).[1–8] Likewise, a number of different types of fluorescent tagging reagents, including N-(iodoacetylaminoethyl)-5-naphthylamine-1-sulfonic acid,[9,10] N-dansylaziridine,[11] N-substituted maleimide,[12–14] bimanes[15–18] and halogeno-benzoxadiazoles,[19–24] have been designed for thiols and are used as pre- and/or post-column derivatization reagents. Many of these reagents suffer from incomplete reactions, highly fluorescent hydrolysis products, solvent dependency of fluorescence or reagent toxicity.

In this paper, a series of halogeno-diaryloxazoles that function as fluorescent labelling reagents for secondary amines and thiols is reported. The reaction of the reagents 2-fluoro-4,5-diphenyloxazole (DIFOX), 2-chloro-4,5-diphenyloxazole (DICLOX) and 2-chloro-4,5-bis(p-N,N-dimethylaminosulfonylphenyl)oxazole (SAOX-Cl) (Fig. 1) with these analytes is described. The spectroscopic characteristics, stability and chromatographic behaviour of the labelled compounds are also given.

Experimental

Materials

L-Alanine, L-proline, *trans*-4-hydroxy-L-proline, L-prolyl-L-leucine, L-prolyl-glycyl-glycine, L-prolyl-L-leucyl-glycine amide, reduced glutathione (GSH), N-acetylcysteine and 2-mercaptopropionylglycine (MPG) were purchased from Sigma (St. Louis, MO, USA). Sodium tetraborate decahydrate was obtained from Fluka (Ronkonkoma, NY, USA). Disodium dihydrogen ethylenediaminetetraacetate (Na₂EDTA), sodium phosphate dibasic heptahydrate, sodium phosphate monobasic monohydrate, sodium carbonate and hydrochloric acid (35%) obtained from Fisher (Fair

Lawn, NJ, USA) were also used. Orthophosphoric acid (85%) and acetonitrile were of HPLC (high-performance liquid chromatography) grade (Fisher). Water used was purified by a NANOpure II system (Sybron/Barnstead, Boston, MA, USA). All other chemicals were of analytical-reagent grade and were used without further purification. 4,5-Diphenyl-2-3H-oxazolone (DIFOX-OH) and DICLOX were prepared by the method of Gompper and Herlinger.[25]

Apparatus

Two LC-6A pumps (Shimadzu, Columbia, MD, USA) were employed. Gradient elution was controlled by an SCL-6A system controller (Shimadzu) and the data were collected and analysed by a C-R3A Chromatopac (Shimadzu). All samples for chromatographic analysis were injected onto the column with a SIL-6A Auto Injector (Shimadzu). The column used in these studies was a 5 µm Supelco LC-8 column (250 × 4.6 mm i.d.; Supelco, Bellefonte, PA, USA). A Shimadzu SPD-6AV ultraviolet/visible (UV/VIS) detector and a Shimadzu RF-535 fluorescence detector were used in tandem to monitor the column eluent. All mobile phase solutions were sonicated for 15 min prior to use to remove air bubbles. The flow rate was 1.0 ml min⁻¹.
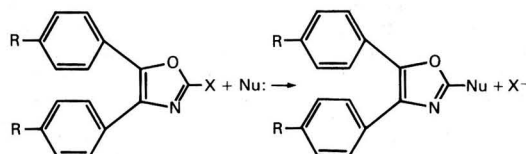
DICLOX: R = H, X = Cl
DIFOX: R = H, X = F
SAOX: R = SO₂N(CH₃)₂, X = Cl
Nu: RSH, RNH₂, R₂NH

Fig. 1 Structures of 2-fluoro-4,5-diphenyloxazole (DIFOX) and 2-chloro-4,5-bis(p-N,N-dimethylaminosulfonylphenyl)oxazole (SAOX-Cl) and their reactions with thiols and secondary amines

---

* To whom correspondence should be addressed.

Melting-points (m.p.s.) were determined on a Thomas-Hoover capillary melting-point apparatus and are uncorrected. Infrared (IR) spectra were determined on a Beckman (Fullerton, CA, USA) Acculab 3 grating spectrophotometer or an IBM IR/32 Fourier transform infrared (FTIR) spectrometer. Proton nuclear magnetic resonance (^{1}H NMR; δ_H) and ^{13}C NMR (δ_C) spectra were recorded on a Varian (Sunnyvale, CA, USA) XL300 or Bruker (Billerica, MA, USA) AM-500 spectrometer. Chemical shifts are reported in ppm (δ) relative to Me$_4$Si (δ = 0.00) as an internal standard. The multiplicity of ^{13}C NMR signals were determined by single frequency off-resonance decoupling experiments or distortionless enhancement by polarization transfer. The ^{19}F NMR (δ_F) spectra were recorded on the Varian XL300 and the chemical shifts are reported in ppm (δ) relative to α,α,α-trifluorotoluene (C$_6$H$_5$CF$_3$; δ = 63.7 ppm) as an internal standard. The UV/VIS absorption spectra were recorded on a Hewlett-Packard (Palo Alto, CA, USA) 8450A diode array spectrophotometer. Fluorescence emission spectra were obtained on an Aminco-Bowman spectrofluorimeter using the IP 28 photomultiplier with a 1 cm quartz cell. Wavelengths are reported in nanometres and are uncorrected. Widths at half-height ($W_{1/2}$) in the fluorescence emission spectra are reported in cm^{-1}. Mass spectra were acquired on a Ribermag quadrupole R-10-10, a Varian MAT CH-5 or a VG-ZAB (VG, Danvers, MA, USA) high-resolution mass spectrometer. The thin-layer chromatography analyses were carried out on Analtech silica gel plates (250 μm thickness) with a fluorescence indicator.

Synthesis of DIFOX

An 18-crown-6–acetonitrile complex was prepared using the method of Goekl and Cram.[26] To a solution of DICLOX (1.62 g, 6.35 mmol) in acetonitrile (60 ml), anhydrous KF (3.0 g) and the 18-crown-6–acetonitrile complex (1.5 g) were added. The resultant mixture was heated under reflux for 24 h. The reaction mixture was cooled and filtered, the filtrate was concentrated, and hexane (2 × 50 ml) added to the residue obtained. The resultant mixture was stirred for 10 min and then filtered rapidly. Upon concentration, the hexane filtrate gave a yellow oil, which was distilled (b.p. 130 °C at 0.02 mmHg) to afford 0.85 g (56%) of product. δ_H (CDCl$_3$) 7.63 (m, ArH), 6.55 (m, ArH), 7.37 (m, ArH); δ_F (CDCl$_3$) −98.2; m/z (%) 239 (M$^+$, 100), 192 (18), 165 (64), 105 (4), 89 (28), 77 (28) (Calc. for C$_{15}$H$_{10}$FNO: M$^+$, 239.0746. Found M, 239.0748).

Synthesis of SAOX-Cl

To a suspension of the oxazolone in POCl$_3$ (30 ml, 323 mmol) at 0 °C triethylamine (0.61 ml, 4.44 mmol) was added dropwise. The reaction mixture was then heated at 100 °C for 7 h, and the excess POCl$_3$ removed on a rotary evaporator. The residue obtained was dissolved in methylene chloride, and the organic layer washed with cold saturated sodium hydrogen carbonate. The methylene chloride layer was separated, dried (over MgSO$_4$) and concentrated to give a yellow solid (1.92 g, 92%), which was chromatographed on silica gel (100 g). Elution with methylene chloride and 10% EtOAc afforded SAOX-Cl as a white solid (1.45 g, 70%); m.p. 222–224 °C; δ_H (CDCl$_3$) 7.82 (6 H), 7.74 (2 H), 2.77 (6 H, s), 2.76 (6 H s); δ_C (CDCl$_3$) 147.6, 147.3, 137.2, 136.8, 136.4, 134.9, 131.1, 128.4, 128.4, 126.3, 126.9, 37.92, 37.90; IR(CHCl$_3$) 3020, 2970, 2820, 1600, 1510, 1455, 1400, 1350, 1160, 1090, 1050, 955, 840 cm^{-1}; m/z (%) 469 (M$^+$, 30), 362 (39), 313 (19), 253 (21), 190 (27), 163 (27), 92 (20) (Calc. for C$_{19}$H$_{20}$N$_3$O$_5$S$_2$Cl: M$^+$, 469.0532. Found: M, 469.0537).

Synthesis of 4,5-Bis(p-N,N-dimethylaminosulfonylphenyl)-oxazolone (SAOX-OH)

Chlorosulfonic acid (60 ml) was carefully added to DIFOX-OH (7.3 g, 0.03 mmol) at 0 °C. The reaction mixture was heated at 55–60 °C for 4 h, then cooled and added dropwise to ice–water (500 g). The pale-yellow solid was filtered, washed with water (4 l) and 2.0 g (2.22 mmol) of the crude mixture were added to dry benzene (100 ml) and concentrated to dryness to remove traces of water in the sample. δ_H ([^{2}H$_6$]-Me$_2$SO) 7.87 (1 H, d), 7.82 (1 H, d), 7.74 (1 H, d), 7.61 (1 H, d), 3.70 (1 H, dd, S–CH–H), 3.65 (1 H, dd, S–CH–H), 1.82 (3 H, s, CH$_3$); δ_C ([^{2}H$_6$]-Me$_2$SO) 153.9, 135.7, 133.9, 133.0, 131.8, 131.5, 129.0, 128.3 (two carbons), 125.4, 123.5, 37.6, 37.5; IR (KBr) 1725, 1590, 1550, 1320 cm^{-1}; m/z (%) 451 (M$^+$, 26), 344 (5), 235 (7), 211 (6), 185 (7), 164 (10), 104 (21), 103 (24), 76 (25), 44 (100) (Calc. for C$_{19}$H$_{21}$N$_3$O$_6$S$_2$: M$^+$, 451.0870. Found: M, 451.0873).

Synthesis of Diphenyloxazole (DIOX) Derivatives of Proline

To a mixture of proline (40 mg, 0.348 mmol) and triethylamine (90.6 ml) in benzene (25 ml) was added DIFOX (70 mg, 0.293 mmol) in hexane (1 ml). The reaction mixture was stirred at room temperature for 16 h, diluted with water (50 ml), and extracted with benzene (100 ml) and then with methylene chloride (100 ml). The aqueous layer was made acidic with concentrated hydrochloric acid and extracted with diethyl ether (200 ml). The ether layer was dried over MgSO$_4$ and concentrated to afford the adduct product as a white solid (48 mg, 49%). δ_H (CDCl$_3$) 7.62 (2 H, m, ArH), 7.45 (2 H, m, ArH), 7.30 (6 H, m, ArH), 4.58 (1 H, dd, N–CH–CO); 3.71 (2 H, m, N–CH$_2$), 1.9–2.5 (4 H, m); δ_C (CDCl$_3$) 172.5, 158.7, 139.8, 133.4, 131.4, 128.7, 128.6, 128.5, 128.4, 128.3, 127.7, 125.5, 61.3, 48.1, 29.6, 24.2; IR (CHCl$_3$) 3400–2300, 3000, 2900, 1740, 1625, 1510, 1490, 1455, 1420, 1250, 1225, 1030, 700 cm^{-1}; m/z (%) 334 (M$^+$, 27), 290 (70), 289 (22), 288 (34), 262 (35), 247 (23), 235 (13), 178 (16), 165 (40), 158 (25), 131 (21), 106 (6), 105 (65), 104 (40), 103 (25), 77 (100), 70 (70), 44 (79) (Calc. for C$_{20}$H$_{18}$N$_2$O$_3$: M$^+$, 334.1316. Found: M, 334.1305).

Synthesis of SAOX Derivatives of Proline

To a solution of proline (115 mg, 1 mmol) in 0.1 mol l^{-1} sodium carbonate (100 ml) was added SAOX (96 mg, 0.2 mmol) in acetonitrile (100 ml). The reaction mixture was stirred at room temperature for 3 h, concentrated to remove acetonitrile, and the aqueous solution extracted with ethyl acetate (3 × 50 ml). The aqueous solution was made acidic with 1 mol l^{-1} HCl and extracted with ethyl acetate (3 × 50 ml). The ethyl acetate layers obtained from extraction with aqueous HCl were combined, washed with water, dried (over MgSO$_4$) and concentrated to afford SAOX-proline as a yellow solid (60 mg, 60%); m.p. 241–243 °C. δ_H ([^{2}H$_6$]-Me$_2$SO) 7.82 (4 H, br s), 7.70 (4 H, dd), 4.49 (1 H, br d, N–CH–COOH), 3.67 (2 H, m, N–CH$_2$), 2.65 (6 H, s), 2.62 (6 H, s), 1.9–2.45 (4 H, m); δ_C ([^{2}H$_6$]-Me$_2$SO) 173.3, 158.5, 138.2, 136.7, 136.5, 134.3, 132.4, 132.4, 128.4, 128.3, 128.0, 124.8, 59.8, 47.7, 37.5, 30.2, 23.7; IR (KBr) 3420, 2980–2880, 1725, 1640, 1590, 1455, 1400, 1340, 1160, 950, 840, 750, 700 cm^{-1}; m/z (%) 548 (M$^+$, 1) 504 (4), 476 (1), 461 (1), 396 (1), 342 (1), 288 (2), 212 (7), 190 (3), 165 (3) (Calc. for C$_{24}$H$_{28}$N$_4$O$_7$S$_2$: M$^+$, 548.1399. Found: M, 548.1393). Both DIOX-alanine and SAOX-alanine were also synthesized and fully characterized.

Synthesis of DIOX-N-acetylcysteine

To a solution of N-acetylcysteine (163 mg, 1 mmol) in 0.1 mol l^{-1} sodium carbonate (100 ml) was added DIFOX (152 mg, 0.64 mmol) in acetonitrile (100 ml) and the mixture stirred at room temperature for 2 h. The reaction mixture was

concentrated to remove acetonitrile and the remaining aqueous solution extracted with ethyl acetate (3×50 ml). The aqueous layer was then made acidic with 1 mol l^{-1} HCl and extracted with ethyl acetate (3×50 ml). The ethyl acetate layers obtained from extraction with aqueous HCl were combined, washed with water, dried (over MgSO$_4$) and concentrated to afford DIOX-N-acetylcysteine as a white solid (170 mg, 70%); m.p. 131–133 °C; δ_H ([^{2}H$_6$]-MeSO$_4$) 8.46 (1 H, d, NH), 7.56 (4 H, m, ArH), 7.43 (m, 6H), 4.66 (1 H, m, CH), 3.70 (1 H, dd, S–CH–H), 3.65 (1 H, dd, S–CH–H), 1.82 (3 H, s, CH$_3$); δ_C ([^{2}H$_6$]-MeSO$_4$) 171.5, 169.4, 158.1, 146.7, 135.7, 131.4, 129.0 (two carbons), 128.7, 128.5, 127.8, 127.4, 126.2, 51.7, 33.3, 22.3; IR (KBr) 3400–2600, 1725, 1650, 1500, 1445, 1205, 765, 695 cm^{-1}; UV/VIS (acetonitrile) λ_{max} (log ε) 298 (4.18); fluorescence emission (acetonitrile) λ_{max} ($W_{1/2}$) 385 (3900); m/z (%) 382 (M$^+$, 1), 278 (5), 266 (1), 253 (30), 236 (31), 165 (20), 147 (11), 130 (15), 121 (15), 106 (6), 105 (63), 104 (45), 103 (19), 77 (51) (Calc. for C$_{17}$H$_{13}$NO$_3$S: M$^+$, 328.0987. Found: M, 382.0999).

Synthesis of SAOX-N-acetylcysteine

To a solution of N-acetylcysteine (163 mg, 1 mmol) in 0.1 mol l^{-1} sodium carbonate (100 ml) was added SAOX-Cl (96 mg, 0.02 mmol) in acetonitrile (100 ml). The reaction mixture was stirred at room temperature for 2 h, then concentrated to remove acetonitrile, and the aqueous solution extracted with ethyl acetate (3×50 ml). The aqueous solution was made acidic with 1 mol l^{-1} HCl and extracted with ethyl acetate (3×50 ml). The ethyl acetate layers obtained from extraction with aqueous HCl were combined, washed with water, dried (over MgSO$_4$) and concentrated to afford a yellow solid (101 mg, 85%); m.p. 179–181 °C; δ_H ([^{2}H$_6$]-MeSO$_4$) 8.46 (1 H, d, NH), 7.86 (4 H, m, ArH), 7.82 (4 H, m), 4.68 (1 H, ddd, CH), 3.79 (1 H, dd, S–CH–H), 3.50 (1 H, dd, S–CH–H), 2.65 (3 H, s, CH$_3$), 2.64 (3 H, d, CH$_3$), 1.82 (3 H, s, CH$_3$); δ_C ([^{2}H$_6$]-MeSO$_4$) 171.3, 169.4, 159.9, 146.2, 136.2, 135.2, 134.8, 134.7, 131.3, 128.29, 128.26, 128.12, 126.7, 51.4, 37.5, 33.3, 22.2; IR (KBr) 3400, 3070, 2600, 1730, 1650, 1600, 1500, 1335, 1155, 1045, 950, 840, 760, 750, 640 cm^{-1}; UV/VIS (acetonitrile) λ_{max} (log ε) 327 (4.25); fluorescence emission (acetonitrile) λ_{max} ($W_{1/2}$) 385 (3900); m/z (%) 467 (M$^+$, 16), 253 (3), 212 (3), 165 (3), 149 (1), 87 (21), 43 (100) (Calc. for C$_{19}$H$_{21}$NO$_5$S$_3$: M$^+$, 467.0642. Found: M, 467.0633).

Stock Solutions

Borate buffer (0.1 mol l^{-1}; pH 9.3) was prepared by dissolving 19.07 g of sodium tetraborate decahydrate in 1 l of water containing 2 mmol l^{-1} Na$_2$EDTA. Both DIOX (–N-acetyl-cysteine, alanine, proline and –OH) and SAOX derivatives (–N-acetylcysteine, –alanine, –proline and –OH) were dissolved in CH$_3$CN (1 mmol l^{-1} each). Stock solutions (1 mmol l^{-1}) of thiols or amines were prepared in water containing 1 mmol l^{-1} Na$_2$EDTA. All stock solutions, except the borate buffer, were stored in a refrigerator at 4 °C.

Effect of Solvent Polarity and pH on the Fluorescence Intensity of the Authentic Derivatives

Authentic DIOX or SAOX derivatives (5 μmol l^{-1}) were dissolved in solutions with pH varying from 2 to 12 (0.05 mol l^{-1} Britton–Robinson buffer). The Britton–Robinson buffer was prepared by mixing proportional amounts of Solutions A and B to achieve the desired pH; where Solution A consists of 4.5 g of 85% H$_3$PO$_4$, 2.4 g of acetic acid (AcOH) and 2.47 g of boric acid (H$_3$BO$_3$) diluted to 1 l, and Solution B is 0.2 mol l^{-1} NaOH (8.0 g l^{-1}). The fluorescence emission spectra were recorded in a 1 cm quartz cell on an Aminco-Bowman spectrofluorimeter (Model SPF 4-8940 SP) equipped with an IP 28 photomultiplier tube. The emission spectra were

recorded with an excitation wavelength of 313 nm. Fluorescence efficiencies were obtained by comparison with 2,4-diphenyloxazole (Aldrich, Milwaukee, WI, USA) as standard ($\phi_{fl} = 1.0$). The ϕ_{fl} value for a given derivative was calculated according to the equation

$$\phi_{fl}/\phi_{fl'} = I_{fl}(1 - 10^{-A'})/I_{fl'}(1 - 10^{-A})$$

where ϕ_{fl} and $\phi_{fl'}$ are the fluorescence quantum efficiencies for the given oxazole derivative and the standard, A and A' are the absorbances of the derivative and the standard solutions, and I_{fl} and $I_{fl'}$ are the areas under the emission curves of the derivative and the standard, respectively. Before the fluorescence emission spectra were recorded, the UV/VIS spectra of the samples were obtained using a diode array spectrophotometer. For fluorescence efficiency measurements, the concentrations of the solutions were adjusted so that the absorbances were less than 0.1, in order to minimize the error due to inner filter effects. Quantum efficiencies were measured in 100% acetonitrile and in a mixture of 50% acetonitrile and 50% 0.05 mol l^{-1} phosphate buffer, pH 7.

Determination of Reaction Rate Constants for Thiols and Amines

Several 1.5 ml vials containing 0.25 ml of 1 mmol l^{-1} DIFOX, DICLOX or SAOX-Cl in CH$_3$CN mixed with an equal volume of 10 μmol l^{-1} analyte in 0.05 mol l^{-1} sodium tetraborate (pH 9.3) containing 1 mmol l^{-1} Na$_2$EDTA were prepared. The reaction solutions of DIFOX and DICLOX were kept at room temperature (20–25 °C); SAOX-Cl was heated at 60 °C. All solutions were protected from light. At fixed time intervals, a vial was removed from the water-bath and cooled in ice-water, an equal volume of 1 mol l^{-1} HCl–CH$_3$CN (1 + 1) was added to quench the reaction and the aliquot monitored by HPLC with both UV (at 210 nm) and fluorescence detection to determine the progress of the reaction. A reagent blank without analyte was treated in a similar manner. The yield of the derivatization reaction at each point in time was calculated by comparing the peak areas with those of known amounts of the authentic derivative. The pseudo-first-order rate constants were calculated from these data.

Stability of DIOX and SAOX Derivatives

Several vials of each derivative (5 μmol l^{-1}) in 0.1 mol l^{-1} sodium tetraborate (pH 9.3) containing 2 mmol l^{-1} Na$_2$EDTA were heated in a water-bath at 60 °C for 2 h. After fixed time intervals, a vial was removed and an aliquot of the solution injected onto the column. The extent of decomposition was determined from the ratio of the peak areas for the derivative before and after heating.

HPLC Separation and Detection of Authentic Derivatives

Stock solutions of DIOX and SAOX derivatives were diluted to suitable concentrations (0.01–1.0 μmol l^{-1}). An aliquot of the respective stock solutions was separated by HPLC. Detection limits [signal-to-noise ratio (S/N) of 2] of these derivatives at suitable wavelengths were calculated from the difference between peak height of the derivative and noise level.

HPLC With Fluorescence Detection of Secondary Amino Acids and N-Terminal-proline Peptides Derivatized with DIFOX

A 0.25 ml volume of DIFOX (1 mmol l^{-1}) in CH$_3$CN and 0.25 ml of a solution of a mixture of secondary amino acids and proline-containing peptides (10 μmol l^{-1} each of L-proline, hydroxy-L-proline, L-prolyl-glycyl-glycine and L-prolyl-L-leucine) in 0.05 mol l^{-1} sodium tetraborate (pH 9.3) containing 1 mmol l^{-1} Na$_2$EDTA was added to a vial (1.5 ml volume). The

vial was capped and kept at room temperature protected from light for 1 h. Then 0.5 ml of 1 mol l^{-1} HCl–CH$_3$CN (1 + 1) was added to the solution to quench the reaction. The acidic solution was diluted to the desired concentration with H$_2$O–CH$_3$CN (1 + 1), and an aliquot injected onto the column. The DIFOX derivatives were separated under isocratic conditions using an eluent of 0.05 mol l^{-1} phosphate (pH 7)–CH$_3$CN (7 + 3).

Results and Discussion

Reaction Rate of Amines With DIFOX, DICLOX or SAOX-Cl

The reactions of DIFOX, DICLOX and SAOX-Cl with proline were compared. The time course for the formation of the labelled derivative was determined by HPLC with fluorescence detection. The production of the labelled proline by reaction with DIFOX at room temperature (RT) in 0.05 mol l^{-1} sodium tetraborate (pH 9.3)–CH$_3$CN (1 + 1) reached a maximum after 60 min and remained constant for 2 h. In contrast, DICLOX reacted with less than 3% of the proline even after 3 h under the same reaction conditions. The reaction of proline with SAOX-Cl at RT was extremely slow, with a yield of only about 5% after 4 h. However, when the latter reaction was carried out at 60 °C for 3 h the yield was increased to 70%.

Pseudo-first-order rate constants of 2.26 × 10^{-1} and 5.63 × 10^{-2} min^{-1}, respectively, were determined from reactions of 0.5 mmol l^{-1} of the reagent (DIFOX at RT or SAOX-Cl at 60 °C) and 5 µmol l^{-1} proline at pH 9.3. The reaction of alanine with DIFOX at RT was slower, 1.14 × 10^{-2} min^{-1}, and was not complete even after 5 h. When the reaction was carried out in 0.1 mol l^{-1} Na$_2$CO$_3$ (pH 11.5), the yield of DIOX-alanine was even lower. This low yield is due in part to the competing hydrolysis of DIFOX. The use of elevated temperatures was not suitable for the derivatization reaction with DIFOX, as both the number and amount of side products increase with rising temperature. Therefore, the recommended reaction conditions for DIFOX are RT at pH 9.3 in a solution containing 1 mmol l^{-1} Na$_2$EDTA. No side products other than the hydrolysis product were detected in the reaction of alanine with SAOX-Cl at 60 °C over a 5 h reaction time.

The reactivity of halogeno-diaryloxazoles toward nucleophiles is affected by the electron-withdrawing substituent on the aromatic ring (Fig. 1), as has been shown for halogenobenzoxadiazoles.[7–10] 2-Chloro-4,5-bis(p-nitrophenyloxazole), a dinitro derivative of DICLOX, reacts instantly with proline at RT. However, the derivative exhibits no fluorescence in polar solvents such as acetonitrile or methanol. Based on results with proline, the reactivity of p-substituted diaryloxazoles follows the order: NO$_2$ > SO$_2$NMe$_2$ > H. Furthermore, DIFOX is more reactive than its chloro analogue based on a comparison of DIFOX with DICLOX.

Reaction of Thiols With DIFOX or SAOX-Cl

The reactivity of DIFOX and SAOX-Cl toward N-acetyl-cysteine, which was selected as a representative of biological thiols, was also investigated in aqueous media (pH 9.3). The yields with SAOX-Cl increased with the reaction time and reached a maximum at 60 °C after 90 min. The time–yield profile of DIFOX at RT was almost superimposable with that of SAOX-Cl at 60 °C. The pseudo-first-order rate constants were measured by reacting 0.5 mmol l^{-1} reagent (DIFOX or SAOX-Cl) and 5 µmol l^{-1} of N-acetylcysteine at pH 9.3. The rate constants for N-acetylcysteine with both reagents were comparable: 7.90 × 10^{-2} min^{-1} (DIFOX at RT) and 1.04 × 10^{-1} min^{-1} (SAOX-Cl at 60 °C). Therefore, either reagent can be used for thiol analysis by HPLC. As the reaction of SAOX-Cl with amines is slower than that with DIFOX under the same derivatization conditions, SAOX-Cl appears to provide better selectivity for the determination of thiols.

Effect of Solvent Polarity and pH on the Fluorescence Characteristics of DIOX and SAOX Derivatives of Amines

In contrast to NBD and dansyl derivatives, oxazole derivatives show little change in fluorescence quantum efficiencies with increasing solvent polarity (Table 1 shows the ϕ_{fl} values obtained under aqueous conditions and Table 2 gives these values under non-aqueous conditions). The ϕ_{fl} value for proline changes from 0.39 to 0.51 in going from 100% acetonitrile to 50% acetonitrile. The ϕ_{fl} value for the SAOX derivatives decreases slightly in fluorescence as the solvent becomes more polar (0.45–0.37). This is in contrast to NBD-hydroxyproline, which exhibits a 45-fold decrease in ϕ_{fl}. Likewise, dansyl derivatives exhibit low values for ϕ_{fl} under aqueous conditions (Table 1).

To obtain the optimum pH and suitable detection wavelengths for the determination of amines, the correlation between pH and fluorescence intensity was investigated with authentic derivatives. As shown in Fig. 2, DIFOX derivatives of proline exhibited higher fluorescence emission intensity than alanine derivatives at all pH values tested. For all DIOX-amino acid derivatives, the fluorescence emission intensities were higher in neutral and alkaline solution (pH 5–10) than in acidic solution. Protonation of the nitrogen in amino acid derivatives (DIOX-amino acids) might be occurring at pH values lower than 3, leading to a decrease in the fluorescence intensity, as indicated in Fig. 2. The fluorescence emission intensities of SAOX-amino acids were about twice as high as those of DIOX-amino acids. The fluorescence intensities of DIOX-OH and SAOX-OH were relatively low at all pH values when compared with the amino acid derivatives. The emission intensity of DIOX-OH was slightly higher, whereas that of SAOX-OH was slightly lower in alkaline solution (pH 10 and 12).

Table 1 Fluorescence properties of oxazole derivatives under aqueous conditions

Derivative	λ_{max}/nm (log ε)	λ_{max}/nm ($W_{1/2}$/cm^{-1})	ϕ_{fl}	Ref.
DIOX-proline*	320 (4.22)	420 (4300)	0.51	—
DIOX-Cl*	286 (4.20)	365 (4500)	0.07	—
DIOX-OH*	301 (4.19)	410 (4200)	0.05	—
SAOX-proline†	361 (4.33)	475 (3500)	0.37	—
SAOX-OH†	334 (4.35)	440 (4100)	0.05	—
NBD-hydroxy-L-proline‡	500 (3.10)	536	0.010	6
DNS-glycine†	355 (0.73)	430	0.06	10

* In acetonitrile–phosphate buffer (1 + 1) (0.05 mol l^{-1}, pH 7.0). Relative to $\phi_{fl} = 1.0$ for 2,4-diphenyloxazole in cyclohexane at $\lambda_{ex} = 313$ nm.
† In H$_2$O, pH 9. Relative to $\phi_{fl} = 0.55$ for quinine hydrogen sulfate (in H$_2$SO$_4$) at $\lambda_{ex} = 366$ nm.
‡ In 0.01 mol l^{-1} Tris–Cl$^-$ buffer, pH 7. Relative to $\phi_{fl} = 0.93$ for fluorescein in 0.01 mol l^{-1} NaOH.

Table 2 Fluorescence properties of oxazole derivatives under non-aqueous conditions

Derivative	λ_{max}/nm (log ε)	λ_{max}/nm ($W_{1/2}$/cm^{-1})	ϕ_{fl}	Ref.
DIFOX-proline*	320 (4.22)	420 (4300)	0.39	—
NBD-hydroxy-L-proline†	470 (2.2) 336 (0.77)	526	0.24	6
SAOX-proline*	361 (4.33)	475 (3500)	0.45	—
DNS-tryptophan‡	335	533	0.37	10

* In acetonitrile. Relative to $\phi_{fl} = 1.0$ for 2,4-diphenyloxazole.
† In methanol–HCl. Relative to $\phi_{fl} = 0.55$ for quinine hydrogen sulfate.
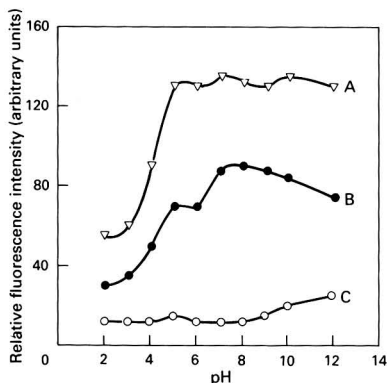‡ In methanol. Relative to $\phi_{fl} = 0.93$ for fluorescein.

Fig. 2 Effect of pH on the fluorescence intensities of authentic DIOX derivatives: A, DIOX-proline; B, DIOX-alanine; and C, DIOX-OH. Authentic derivative (5 μmol l^{-1} each) was dissolved in 0.05 mol l^{-1} Britton–Robinson buffer (pH 2–12). The fluorescence intensities were measured at the maximum wavelength

Fig. 3 Effect of pH on the fluorescence intensities of authentic derivatives: A, DIOX-N-acetylcysteine; B, SAOX-N-acetylcysteine; C, DIOX-OH; and D, SAOX-OH. Authentic derivative (5 μmol l^{-1} each) was dissolved in 0.05 mol l^{-1} Britton–Robinson buffer (pH 2–12). The fluorescence intensities were measured at the maximum wavelength
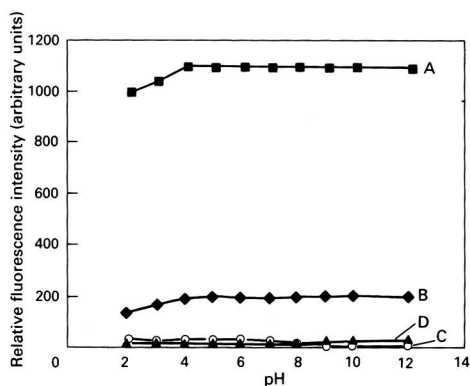

Fig. 4 HPLC separation of authentic DIOX derivatives. (a) Eluent, 0.1 mol l^{-1} H$_3$PO$_4$–CH$_3$CN (1 + 1); and (b) eluent, 0.05 mol l^{-1} phosphate (pH 7.0)–CH$_3$CN (7 + 3). Peak 1, DIOX-OH (0.21 pmol); peak 2, DIOX-alanine (0.16 pmol); and peak 3, DIOX-proline (0.19 pmol). Fluorescence detection, 420 nm (λ_{ex} 320 nm). Other HPLC conditions are given in the Experimental section

The wavelengths for the emission maxima of DIOX-proline (420–433 nm), DIOX-alanine (422–427 nm), SAOX-proline (483–493 nm) and SAOX-alanine (485–490 nm) were not greatly affected by increasing the pH above 7 (less than a 13 nm bathochromic shift). However, a 20 nm red shift for the excitation wavelength was observed in going from pH 2 to 7. In contrast, the emission maxima of the hydrolysis products DIOX-OH and SAOX-OH showed a much greater dependence on pH and exhibited a bathochromic shift (45–80 nm) with increasing pH.

Effect of pH on the Fluorescence Characteristics of Thiol Derivatives

The fluorescence emission intensities of DIOX-N-acetylcysteine and SAOX-N-acetylcysteine remain constant over a wide pH range. The intensities of SAOX-N-acetylcysteine were about 5 times higher than those of DIOX-N-acetylcysteine at all pH values tested (Fig. 3). The shift in the maximum wavelength of the thiol derivatives was negligible at all pH values (Table 1). Thiol determination with these reagents is possible over a wide pH range, as the derivatives show a higher fluorescence intensity and negligible shift of the excitation and emission wavelengths at all pH values. The relatively low fluorescence intensities of the hydrolysis pro-

ducts, DIOX-OH and SAOX-OH, over the entire pH range is an advantage of these reagents because of the low interference of the side products from derivatization.

Stability of DIOX and SAOX Derivatives

The stability of DIOX-proline, SAOX-proline, DIOX-N-acetylcysteine and SAOX-N-acetylcysteine was examined under various conditions. The derivatives exhibited less than 5% decomposition over a period of 2 h in 0.1 mol l^{-1} sodium tetraborate (pH 9.3) containing 2 mmol l^{-1} Na$_2$EDTA at 60 °C. Comparable results were observed in 100% acetonitrile solution at 60 °C. No decomposition was seen at pH 1 and RT for any sample tested. The oxazole derivatives have been found to be insensitive to visible (room) light, but will decompose after prolonged exposure to UV radiation.[27]

HPLC Separation and Detection of Authentic Derivatives

The HPLC separation of a mixture of authentic amine derivatives was carried out using a reversed-phase octyl-silica gel column (Supelco LC-8). At acidic pH, the hydrolysis products SAOX-OH or DIOX-OH elute before the amino acids [Fig. 4(a)]. The elution order at pH 7.0 was opposite to that in acidic solution [Fig. 4(b)] with DIFOX-OH eluting at approximately 33 and 66 min, respectively.

Table 3 Retention times (t_R) and detection limits of authentic DIOX and SAOX derivatives

Derivative	Eluent*	t_R/min	Detection limit (S/N = 2)/fmol
DIOX-proline†	1	8.6	5.8
	3	11.5	8.7
DIOX-alanine†	1	11.6	10.9
	3	10.1	14.6
DIOX-OH†	1	56.6	313
	3	8.6	77.9
SAOX-proline‡	1	8.8	5.3
	2	16.9	5.3
SAOX-alanine‡	1	10.4	9.0
	2	13.8	7.3
SAOX-OH‡	1	32.7	531
	2	11.9	126

* Eluent composition: 1, 0.05 mol l^{-1} phosphate (pH 7.0)–CH$_3$CN (7 + 3); 2, 0.1 mol l^{-1} H$_3$PO$_4$–CH$_3$CN (6 + 4); and 3, 0.1 mol l^{-1} H$_3$PO$_4$–CH$_3$CN (1 + 1).
† λ_{ex} = 320; λ_{em} = 420 nm.
‡ λ_{ex} = 360; λ_{em} = 485 nm.
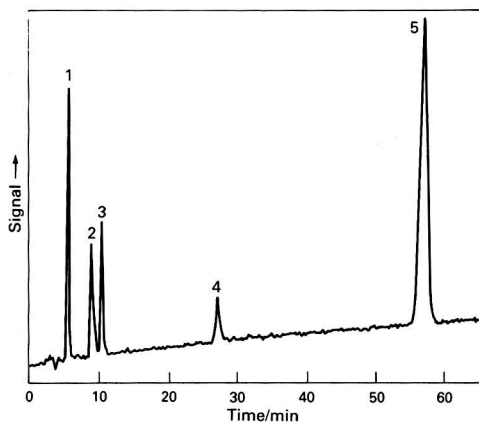

Fig. 5 HPLC separation of proline-containing peptides derivatized with DIFOX. Peak 1, hydroxy-L-proline (99 fmol); peak 2, L-proline (130 fmol); peak 3, L-prolyl-glycyl-glycine (110 fmol); peak 4, L-prolyl-L-leucine (96 fmol); and peak 5, DIOX-OH. Chromatographic conditions: 0.05 mol l^{-1} phosphate (pH 7.0)–CH$_3$CN (7 + 3)

Fig. 6 HPLC separation of thiols derivatized with SAOX-Cl. (a) Eluent, 0.1 mol l^{-1} H$_3$PO$_4$–CH$_3$CN (65 + 35); and (b) eluent, 0.05 mol l^{-1} phosphate (pH 7.0)–CH$_3$CN (7 + 3). Peak 1, GSH (50 fmol); peak 2, N-acetylcysteine (50 fmol); peak 3, MPG (59 fmol); and peak 4, SAOX-OH. Column, LC-8 (250 × 4.6 mm i.d., 5 µm) at RT; fluorescence detection, 425 nm (λ_{ex} 330 nm); and flow rate, 1.0 ml min^{-1}

The detection limits (S/N = 2) calculated from peak heights are listed in Table 3. The detection limits for authentic DIOX-alanine and DIOX-proline were 5.8–14.6 fmol; those for SAOX-alanine and SAOX-proline were 5.3–9.0 fmol. In contrast, the detection limits of the hydrolysis products were extremely high (DIOX-OH, 77.9–313 fmol; SAOX-OH, 126–531 fmol) compared with amino acid derivatives. The low yield (70%) under derivatization conditions with SAOX-Cl makes DIFOX the more useful reagent for the determination of secondary amines. Detection limits under typical derivatization conditions for proline were 100 fmol at an S/N of 2.[28]

The HPLC separation of authentic N-acetylcysteine derivatives and hydrolysis products was carried out using a reversed-phase octyl-silica gel column (Supelco LC-8). The hydrolysis products in acidic eluents (18.4 as against 17.2 min and 22.1 as against 19.6 min) overlapped the peaks of the N-acetylcysteine derivatives. In contrast, the complete separation was accomplished at a neutral pH [0.05 mol l^{-1} phosphate (pH 7.0)–CH$_3$CN].

The detection limits for authentic SAOX-N-acetylcysteine and DIOX-N-acetylcysteine in a neutral eluent were 1.2 and 3.6 fmol, respectively. Those in acidic eluent were 1.5 fmol

(SAOX-N-acetylcysteine) and 6.2 fmol (DIOX-N-acetylcysteine) (Table 2). The detection limits of SAOX-N-acetylcysteine were about 3 times lower than those of DIOX-N-acetylcysteine in both eluents. The detection limits using conventional fluorescence detection are lower than for other derivatization methods for thiols described previously.[5] Based on reaction speed, selectivity of the reagents toward thiols, and the detection limits of thiol derivatives, SAOX-Cl is a more effective tagging reagent than DIFOX for the determination of thiols.

HPLC Separation of Proline Peptides Derivatized With DIFOX

The separation of a mixture of secondary amino acids (L-proline and hydroxy-L-proline) and a mixture of short-chain peptides (L-prolyl-L-leucine, L-prolyl-glycyl-glycine and L-prolyl-L-leucyl-glycine amide) was studied by isocratic elution using a reversed-phase HPLC column (LC-8). Acetonitrile–phosphate buffer (pH 7.0) was selected as the eluent, as the compounds give a higher fluorescence intensity in neutral solution (pH 7.0) than in acidic solution. Furthermore, the capacity factor of the hydrolysis compound (DIOX-OH) of DIFOX is larger in neutral solution than in acidic solution

and its fluorescence intensity at pH 7.0 is lower. Under these conditions, the DIOX-OH would not be expected to interfere in the separation of the target amines.

The HPLC separation of DIOX-hydroxy-L-proline, DIOX-L-proline and DIOX-peptides by isocratic elution with 0.05 mol l^{-1} phosphate buffer (pH 7.0)–CH$_3$CN (7 + 3) is shown in Fig. 5. The elution order of the DIOX derivatives was hydroxy-L-proline, L-proline, L-prolyl-glycyl-glycine and L-prolyl-L-leucine. The detection limits (S/N = 2) were 3.7, 12.6, 7.4 and 28.4 fmol, respectively. With UV detection at 210 nm using the same effluent, DIOX-OH eluted at 58 min (Fig. 5).

HPLC Separation of Thiols Derivatized With SAOX-Cl

The separation of some thiol compounds labelled with SAOX-Cl was investigated by isocratic elution using a reversed-phase column (LC-8). As shown in Fig. 6, complete separation of three biological thiols was obtained in acidic [0.1 mol l^{-1} H$_3$PO$_4$–CH$_3$CN (65 + 35)] and neutral [0.05 mol l^{-1} phosphate (pH 7.0)–CH$_3$CN (7 + 3)]; SAOX-OH in neutral and acidic eluents was eluted at 32 and 19 min, respectively. In acidic eluent, SAOX-OH interfered with the separation of the derivatives of cysteine and homocysteine. The peak areas are almost the same for each thiol derivative. The SAOX-Cl itself did not elute under these isocratic conditions. The detection limits (S/N = 2) for GSH, N-acetylcysteine and MPG in neutral eluents were 1.4, 1.3 and 1.4 fmol, respectively. In acidic eluent, the extrapolated detection limits (S/N = 2) were 1.2 (GSH), 1.5 (N-acetylcysteine) and 1.9 fmol (MPG).

Conclusions

The purpose of this paper is to report the use of DICLOX, DIFOX and SAOX-Cl for the determination of secondary amines and thiols. DIFOX was found to be the most useful reagent of the three tested for detection of secondary amines. The reaction rate with primary amines is an order of magnitude slower than that with secondary amines, leading to increased selectivity. In addition, the excitation maxima for the secondary amino acid derivatives (320 nm) are well suited to He–Cd laser excitation using the 325 nm line. Owing to its excellent sensitivity and its selectivity for thiols, SAOX is ideal for the determination of thiols. Examples of the use of these reagents for the analysis of biological samples will be reported elsewhere.

References

1 Imai, K., and Toyo'oka, T., in *Design and Choice of Suitable Labelling Reagents for Liquid Chromatography*, eds. Frei, R. W., and Zeck, K., *J. Chromatogr. Lib.*, 1988, vol. 39A, Elsevier, Amsterdam, pp. 209.
2 Chen, R. F., *Arch. Biochem. Biophys.*, 1967, **120**, 609.
3 Einarsson, S., Josefson, B., and Lagerkvist, S., *J. Chromatogr.*, 1983, **282**, 609.
4 Ghosh, P. B., and Whitehouse, M. W., *Biochem. J.*, 1968, **108**, 155.
5 Imai, K., and Watanabe, Y., *Anal. Chim. Acta*, 1981, **130**, 377.
6 Ahnoff, M., Grundevik, I., Arfwidsson, A., Fonselius, J., and Persson, B.-A., *Anal. Chem.*, 1981, **53**, 485.
7 Watanabe, Y., and Imai, K., *J. Chromatogr.*, 1982, **239**, 723.
8 Andrew, J. L., Ghosh, P., Ternai, B., and Whitehouse, M. W., *Arch. Biochem. Biophys.*, 1982, **214**, 386.
9 Wu, C. W., and Stryer, L., *Proc. Natl. Acad. Sci. USA*, 1972, **69**, 1104.
10 Friedman, F. K., Chang, M. Y., and Beychok, S., *J. Biol. Chem.*, 1978, **253**, 2368.
11 Johnson, J. D., and Schwartz, A., *J. Biol. Chem.*, 1978, **253**, 5243.
12 Kanaoka, Y., *Yakugaku Zasshi*, 1980, **100**, 973.
13 Weltman, J. K., Szaro, R. P., Frackelton, A. R., Bunting, J. R., and Cathou, R. E., *J. Biol. Chem.*, 1973, **248**, 3173.
14 Kagedal, B., and Kallberg, M., *J. Chromatogr.*, 1982, **229**, 409.
15 Kosower, N. S., Kosower, E. M., Newton, G. L., and Ranney, H. M., *Proc. Natl. Acad. Sci. USA*, 1979, **76**, 3382.
16 Kosower, N. S., Newton, G. L., Kosower, E. M., and Ranney, H. M., *Biochim. Biophys. Acta*, 1980, **622**, 201.
17 Newton, G. L., Dorian, R., and Fahey, R. C., *Anal. Biochem.*, 1981, **114**, 383.
18 Toyo'oka, T., and Imai, K., *Analyst*, 1984, **109**, 1003.
19 Toyo'oka, T., and Imai, K., *J. Chromatogr.*, 1983, **282**, 495.
20 Imai, K., and Toyo'oka, T., *Methods Enzymol.*, 1987, **143**, 67.
21 Toyo'oka, T., and Imai, K., *Anal. Chem.*, 1984, **56**, 2461.
22 Toyo'oka, T., and Imai, K., *Anal. Chem.*, 1985, **57**, 1931.
23 Toyo'oka, T., Suzuki, T., Saito, Y., Uzu, S., and Imai, K., *Analyst*, 1989, **114**, 413.
24 Carlson, R. G., Chokshi, H. P., Givens, R. S., and Toyo'oka, T., *J. Org. Chem.*, submitted for publication.
25 Gompper, R., and Herlinger, H., *Chem. Ber.*, 1956, **89**, 2816.
26 Goekl, G. W., and Cram, D. J., *J. Org. Chem.*, 1974, **39**, 2445.
27 Carlson, R. G., unpublished data.
28 Lunte, S. M., and Wilson, M., unpublished data.

Low Level Determination of Formaldehyde in Water by High-performance Liquid Chromatography

Evangelo Cotsaris and Brenton C. Nicholson
Australian Centre for Water Quality Research, Private Mail Bag, Salisbury, South Australia, 5108

Low levels of formaldehyde in water were determined by derivatization with 2,4-dinitrophenylhydrazine at an optimized pH (1.5–2.5), solid-phase extraction with C_{18} adsorption cartridges and analysis by reversed-phase high-performance liquid chromatography with ultraviolet detection. A novel procedure for the removal of formaldehyde present as an impurity in blank water was responsible for lowering the detection limit to 0.1 µg l^{-1} for a 200 ml sample. A strong anion-exchange resin, in the hydrogen sulfite form, was used to adsorb formaldehyde and any other aldehyde impurities present in blank water. The use of C_{18} adsorption cartridges also minimized background effects. The recovery of C_1–C_3 aldehydes spiked into purified blank water was 83–93% with a relative standard deviation of 1.4–6.4%.

Keywords: *Formaldehyde; aldehydes; solid-phase extraction; high-performance liquid chromatography; 2,4-dinitrophenylhydrazine*

Formaldehyde is an increasingly important environmental pollutant, with evidence of its adverse effects on health becoming more apparent.[1-3] Formaldehyde enters the water environment mainly as a result of human activities, major sources being the discharge of trade waste effluents into waterways and the ozonation of water and waste waters.

Existing methods for the determination of formaldehyde in water usually involve derivatization with 2,4-dinitrophenylhydrazine (2,4-DNPH) followed by solvent extraction and analysis by high-performance liquid chromatography (HPLC).[4-6] These procedures are relatively easy to carry out and give reasonable sensitivity using ultraviolet (UV) detection. However, there are very few reliable techniques reported for the determination of the low concentrations of formaldehyde usually found in natural waters. Most analytical methods for the determination of formaldehyde are limited in their sensitivity as a result of high blank responses. Troublesome background peaks are difficult to eliminate because reagents and solvents contain trace amounts of formaldehyde as impurities. Some workers have attempted to decrease blank responses and hence lower detection limits by replacing solvent extraction with solid-phase extraction techniques.[7,8] Ogawa and Fritz[7] found that small columns packed with zeolite ZSM-5 were able to concentrate most low molecular mass aldehydes and ketones except for formaldehyde where recoveries were poor (1%). Takami *et al.*[8] demonstrated that moderately sulfonated cation-exchange resins could indeed concentrate formaldehyde present at microgram per litre levels from drinking water. However, these techniques are not particularly convenient as the solid-phase extraction cartridges require tedious preparation with custom-made packings. Furthermore, substantial background peaks are still observed at trace levels and attempts to reproduce the performance of some of these solid-phase packings by other workers have been unsuccessful.[9]

Formaldehyde present as an impurity in blank water may also contribute to high blank responses. Some workers have overcome the high blank formaldehyde response by utilizing unchlorinated bore water for the preparation of blank water.[6] However, the widespread occurrence of formaldehyde in the environment makes it virtually impossible to determine trace concentrations. To date, no attempt has been made to lower the detection limit by removing formaldehyde contamination from water that is used for the preparation of blank solutions.

In this study, a novel procedure for the removal of formaldehyde present as an impurity in blank water was used to lower the detection limits and to improve sensitivity. The method is based on the formation of the 2,4-DNPH derivative of formaldehyde at an optimized pH (1.5), solid-phase extraction with C_{18} adsorption cartridges, and analysis by reversed-phase HPLC with UV detection at 365 nm.

Experimental

Reagents

Aldehydes and ketones were obtained from commercial sources. Apart from formaldehyde, all carbonyl compounds were distilled under nitrogen prior to use. Owing to trimer formation the purification of the aldehydes is essential if reliable results are to be obtained. Formaldehyde solution, about 38% m/v, was assayed by the sulfide–iodimetric method[10] and was used without further purification. Hexane and dichloromethane were obtained from Mallinckrodt (nanograde) and further purified by extraction with 40% m/v sodium hydrogen sulfite solution.

Acetonitrile

High-performance liquid chromatography grade acetonitrile (Ajax Chemicals, Australia) was used.

Blank water

Blank water was prepared by the purification of distilled water to remove any traces of aldehyde impurities. A glass column (25 × 1 cm) was packed with a strongly basic anion-exchange Dianion PA 318 resin (Mitsubishi Chemical Industries, Japan). The column was pre-treated by eluting with 250 ml of 1 mol l^{-1} hydrochloric acid, 250 ml of distilled water, 250 ml of saturated sodium hydrogen sulfite solution and rinsed with a furhter 200 ml of distilled water. Blank water was prepared by passing distilled water through the pre-treated column at a rate of 2 bed volumes per hour. At least 10 l of distilled water with a total contaminant aldehyde concentration of up to 10 µg l^{-1} can be purified before any significant breakthrough occurs.

2,4-Dinitrophenylhydrazine

Aldehyde impurities were removed from 2,4-DNPH by a procedure adopted from van Hoof *et al.*[5] The 2,4-DNPH (100 mg), previously extracted five times with hexane–dichloromethane (70 + 30) and recrystallized twice from acetonitrile, was dissolved in 10 ml of 10 mol l^{-1} hydrochloric acid and 90 ml of blank water. The resultant solution was extracted three times with hexane (50 ml) to remove trace impurities and stored under the same solvent. The purified reagent solution is stable for at least one week, but should be re-extracted with

fresh hexane prior to use if the lowest detection limit is required.

2,4-Dinitrophenylhydrazone standards

Carbonyl hydrazone derivatives were prepared by standard procedures[11] and purified by recrystallization from ethanol. Stock solutions (1 g l^{-1}) of each derivative were prepared in acetonitrile. A mixed standard solution (1 mg l^{-1}) was prepared from the stock solutions in 50% v/v acetonitrile–water. The mixed standard should be freshly prepared prior to use.

Derivatization

A 4.0 ml aliquot of 2 mol l^{-1} 2,4-DNPH was added to a 200 ml water sample in a calibrated glass flask and the contents shaken for approximately 0.5 min to ensure good mixing. The pH is controlled using the 2 mol l^{-1} 2,4-DNPH solution so that addition of the reagent to the sample results in a pH of 1.5–2.5. Water samples with very high alkalinities should be checked for pH and adjusted accordingly to pH 1.5–2.5 with 1 mol l^{-1} HCl. After allowing 1 h for derivatization to proceed to completion, the derivative was extracted to prevent decomposition and further reaction.

Extraction Procedure

The 2,4-DNPH derivatives were extracted using a 3 ml C_{18} (100 mg) Bond-Elut cartridge (Varian) preconditioned with 20 ml of acetonitrile followed by 40 ml of blank water. The derivatives were eluted with 1 ml of acetonitrile followed by 1 ml of blank water, the eluates were combined in a 2 ml calibrated flask and made up to the mark with water. Typically, 100 µl injection volumes were employed for HPLC determination.

Apparatus

The HPLC determinations were performed with a Waters Associates liquid chromatograph equipped with two Model 501 solvent delivery systems, Model 680 automated solvent gradient controller, Model 444 UV detector set at a wavelength of 365 nm and a Model U6K injector. The column was a C_{18} reversed-phase Brownlee (Spheri-5 RP18), 5 µm particle size, 25 cm × 7 mm semi-preparative column.

Chromatographic Conditions

The mobile phase used was an acetonitrile–water mixture (65 + 35) at a flow rate of 1.5 ml min^{-1}.

Results and Discussion

Optimization of pH for Maximum Recoveries

The yields of 2,4-DNPH derivatives as a function of pH for a constant reaction time are shown in Fig. 1. Maximum recoveries of the C_1–C_3 aldehyde derivatives were obtained in the pH range 1.5–2.5. The acid concentration of the reagent was chosen to produce a pH at the lower end of the range in distilled water (pH 1.5), to allow for slight increases in pH that may occur with water samples that have a high alkalinity. For example, when 2 mol l^{-1} of 2,4-DNPH were added to a water sample with a high alkalinity of 450 mg l^{-1}, the resultant pH was 1.95 and still within the pH range for maximum recoveries.

Recoveries of aldehyde derivatives are dependent on two factors: (a) the extraction efficiency of the hydrazone derivatives on C_{18} adsorption cartridges; and (b) the reaction between 2,4-DNPH and the aldehyde. Both factors are known to be pH dependent. At low pH (<1.5) it was postulated that a proportion of the aldehyde derivatives were in the ionic form
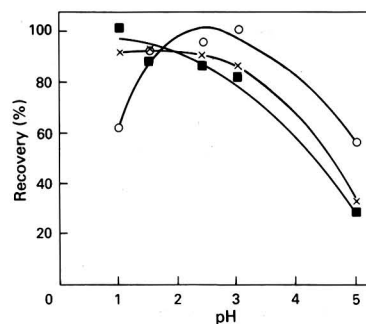

Fig. 1 Effect of reaction pH on the percentage yield of formaldehyde, acetaldehyde and propionaldehyde 2,4-DNPH derivatives. Reaction time, 1 h. ○, Formaldehyde; ×, acetaldehyde; and ■, propionaldehyde

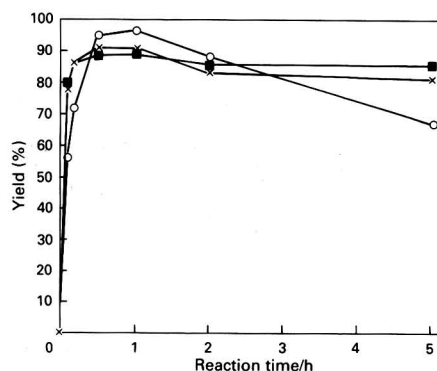**Fig. 2** Rate of derivatization of C_1–C_3 aldehydes with 2,4-DNPH at pH 1.5 *versus* time. ○, Formaldehyde; ×, acetaldehyde; and ■, propionaldehyde

and were not adsorbed onto C_{18} cartridges. At higher pH (>2.5) the derivatives should be in the molecular form and would be expected to adsorb onto the C_{18} cartridges *via* a hydrophobic interaction. However, there must be another mechanism in operation because the yields decreased with an increase in pH. This is presumably due to a decrease in the rate of the reaction. The reaction proceeds by a multi-step mechanism where the rate-limiting step involves the addition of 2,4-DNPH reagent to the protonated carbonyl moiety. At varying pH there are competing effects between the availability of the 2,4-DNPH reagent and the reactivity of the carbonyl group, hence the rate passes through a maximum which is characteristic of the basicity of 2,4-DNPH.[12] Bicking et al.[13] observed similar results when investigating the effect of pH on the reaction of 2,4-DNPH with formaldehyde and acetaldehyde. Consequently, there are two mechanisms operating that are dependent on pH, the adsorption of hydrazone derivative onto the C_{18} adsorption cartridge and the reaction between 2,4-DNPH and the aldehyde. We were unable to determine the mechanism that was the most critical.

The mild acidic reaction conditions (pH 1.5–2.5) are preferred to the more common highly acidic conditions (pH 0.5) employed in conventional derivatization.[4–6] Under highly acidic conditions a false positive formaldehyde result may be obtained, as numerous environmentally occurring compounds have been shown to generate formaldehyde under a variety of conditions.[14] In addition, the recovery of the aldehyde 2,4-DNPH derivatives by solid-phase extraction at pH 0.5 is poorer in comparison with that at pH 1.5–2.5.

Optimization of Reaction Time

The derivatization reaction for C_1–C_3 aldehydes was studied as a function of time at the optimum pH and found to reach equilibrium after 0.5 h as shown in Fig. 2. Reaction times longer than 1 h resulted in decreased yields; in particular the formaldehyde derivative did not appear to be stable for long periods.

Blank Responses and Detection Limit

A strong anion-exchange resin in the hydrogen sulfite form was used for the adsorption of trace concentrations of aldehydes present in blank water. Aldehydes and methyl ketones react with the hydrogen sulfite ions to form ionic α-hydroxyalkanesulfonates at the exchange site. Several workers have reported that aldehydes and methyl ketones are retained by an anion-exchange column in the hydrogen sulfite form.[15–17] Although no investigation was undertaken to determine the most suitable resin, the work by Williams and Strauss[17] demonstrated that a porous-type resin instead of a gel-type anion exchanger was the most appropriate. The resin (Dianion PA 318) evaluated was found to produce very low blank responses when used under conditions described in the experiment.

The detection limit, defined as twice the size of the background peaks for formaldehyde, was 0.1 µg l^{-1} for a 200 ml water sample. The blank is an order of magnitude lower than for most other published methods. Fig. 3 shows a typical liquid chromatogram of the 2,4-DNPH derivatives of some low molecular mass carbonyl compounds and the blank test with 200 ml of water.

The low detection limit is attributable to the removal of formaldehyde present in the reagents and blank water. Commercially available 2,4-DNPH contains substantial amounts of aldehydes that produce interferences in trace analysis. These impurities can by eliminated by purifying the reagent by extraction and recrystallization as described. However, formaldehyde is also introduced as a contaminant in the blank water. Without purification of the blank water by resin adsorption, a detection limit of below 1 µg l^{-1} is not attainable.

Another factor contributing to the low blank responses was the use of commercially available C_{18} adsorption cartridges for solid-phase extraction to replace the conventional liquid–liquid extraction techniques and other solid-phase packings. Solid-phase extraction with C_{18} cartridges minimizes the use of solvents and accordingly reduces the level of aldehyde contamination from this source.

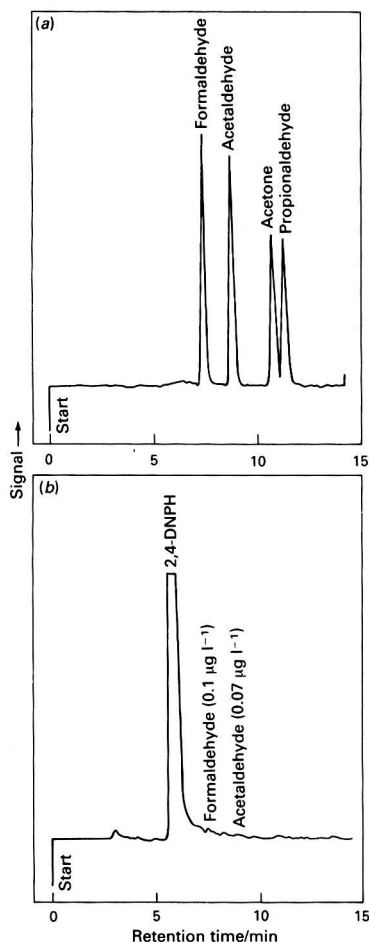Fig. 3 (a) HPLC trace of 2,4-DNPH derivatives of carbonyl standards, formaldehyde, acetaldehyde, acetone and propionaldehyde, equivalent to 10 µg l^{-1} concentration each. (b) Chromatogram of blank water. Scale: ×0.06 a.u.f.s. in both instances
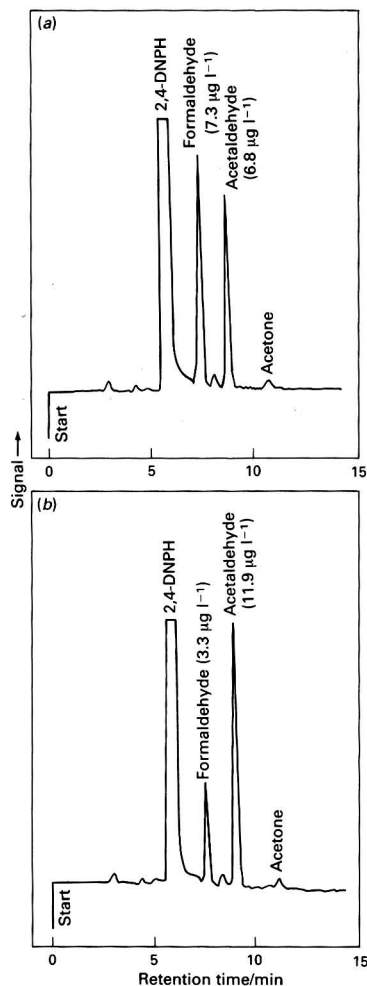

Fig. 4 Typical chromatograms of some low level aldehyde analyses. (a) Distilled water and (b) Milli-Q water. Scale: × 0.06 a.u.f.s. in both instances

Table 1 Recovery of aldehydes from spiked blank water*

Compound	Amount spiked/µg	Amount found/µg	Recovery† (%)	SD‡ (%)
Formaldehyde	50	46.0	92.0	6.4
Acetaldehyde	50	46.5	93.0	2.3
Propionaldehyde	50	44.2	88.4	1.4

* A 200 ml volume of blank water was used for recovery tests.
† Average of three runs.
‡ Standard deviation.

Table 2 Aldehyde concentrations of various samples

Sample	Formaldehyde/ $\mu g \, l^{-1}$	Acetaldehyde/ $\mu g \, l^{-1}$	Propion- aldehyde/$\mu g \, l^{-1}$
Distilled water*	7.3	6.8	ND†
Milli-Q water‡	3.3	11.9	ND
Rainwater	0.7	0.1	ND
Borewater	0.6	0.2	ND

* Prior to distillation, water was obtained from reverse osmosis plant in which formaldehyde was used as a membrane preservative.
† No peak detected.
‡ Water purified through a Milli-Q system.

Recoveries

The recovery of C_1–C_3 aldehydes was determined by repeated spikes on 200 ml of purified blank water at the 50 µg l^{-1} level. The results shown in Table 1 indicate that recoveries of derivatives were 88–93% with a 1.4–6.4% relative standard deviation.

Application

The method was found to be suitable for the determination of trace concentrations of aldehydes in a variety of waters. Results for the trace analysis of a number of samples are reported in Table 2. Typical chromatograms are shown in Fig. 4. The application of this improved method to a range of waters has demonstrated the widespread occurrence of formaldehyde and to a lesser extent other simple aldehydes and ketones. Accurate determination of trace concentrations of aldehydes in water is now possible.

The proposed method has advantages over conventional methods in terms of rapid and simple extraction procedures, mild derivatization conditions, high analytical sensitivity and low background effects.

References

1 Hileman, B., *Environ. Sci. Technol.*, 1982, **16**, 543.
2 U.S. Federal Panel On Formaldehyde, *Environ. Health Perspect.*, 1982, **44**, 139.
3 Hileman, B., *Environ. Sci. Technol.*, 1984, **18**, 218.
4 Fung, K., and Grosjean, D., *Anal. Chem.*, 1981, **53**, 168.
5 van Hoof, F., Wittocx, A., van Buggenhout, E., and Janssens, J., *Anal. Chim. Acta*, 1985, **169**, 419.
6 Whittle, P. J., and Rennie, P. J., *Analyst*, 1988, **113**, 665.
7 Ogawa, I., and Fritz, J. S., *J. Chromatogr.*, 1985, **329**, 81.
8 Takami, K., Kuwata, K., Sugimae, A., and Nakamoto, M., *Anal. Chem.*, 1985, **57**, 243.
9 Tomkins, B. A., McMahon, J. M., Caldwell, W. M., and Wilson, D. L., *J. Assoc. Off. Anal. Chem.*, 1989, **72**, 835.
10 American Public Health Association, *Standard Methods for the Examination of Water and Wastewater*, American Public Health Association, American Water Works Association, Water Pollution Control Federation, Washington, DC, 16th edn., 1985, pp. 479–480.
11 Shriner, R. L., Fuson, R. C., and Curtin, D. Y., *The Systematic Identification of Organic Compounds*, Wiley, New York, 5th edn., 1965.
12 Hine, J., *Physical Organic Chemistry*, McGraw-Hill, New York, 1956, ch. 8 and 11.
13 Bicking, M. K. L., Cooke, W. M., Kawahara, F. K., and Longbottom, L. E., *J. Chromatogr.*, 1988, **455**, 310.
14 Sawicki, E., and Sawicki, C. R., *Aldehydes—Photometric Analysis*, Academic Press, London, 1975, vol. 1.
15 Samuelson, O., *Ion Exchangers in Analytical Chemistry*, Wiley, New York, 1953, ch. 16.
16 DuVal, D. L., Rogers, M., and Fritz, J. S., *Anal. Chem.*, 1985, **57**, 1583.
17 Williams, P. J., and Strauss, C. R., *J. Sci. Food Agric.*, 1978, **29**, 527.

High-performance Liquid Chromatographic Detection of Trace N-Nitrosoamines by Pre-column Derivatization With 4-(2-Phthalimidyl)benzoyl Chloride*

Minghui Zheng
Department of Chemical Engineering, Tangshan University, Tangshan, Hebei, People's Republic of China
Chengguang Fu† and Hongda Xu
Research Centre of Physical and Chemical Analysis, Hebei University, Baoding, Hebei, People's Republic of China

A simple and sensitive method for the detection of N-nitrosoamines is described. N-Nitrosoamines in dichloromethane solution can be denitrosated to secondary amines with a hydrogen bromide–acetic acid mixture, the amines formed then react rapidly with 4-(2-phthalimidyl)benzoyl chloride to give fluorescent amides, which can be separated on an octadecylsilane column with aqueous acetonitrile as eluent. N-Nitrosodimethylamine, N-nitrosodiethylamine, N-nitrosodipropylamine, N-nitrosodibutylamine, N-nitrosopyrrolidine and N-nitrosopiperidine were used as model compounds to optimize the derivatization and chromatographic conditions. The realtive standard deviations ($n = 7$) at an analyte concentration of 8×10^{-6} mol l^{-1} were less than 5%. The detection limits were in the range 0.4–1. 6 pmol per injection.

Keywords: N-Nitrosoamine; 4-(2-phthalimidyl)benzoyl chloride; fluorescence derivatization; high-performance liquid chromatography

The carcinogenicity of N-nitrosodimethylamine was first discovered in 1956 by Magee and Barnes.[1] Since then, about 300 N-nitroso compounds have been discovered, approximately 90% of which are known to be potent carcinogens in animals.[2] N-Nitrosoamines are formed in air, water, soil and even in the human body when the appropriate amines and nitrite precursors are present.

High-performance liquid chromatographic separations of N-nitrosoamines have been reported.[3–5] Pre-column derivatization[6,7] or post-column derivatization[8,9] in high-performance liquid chromatography are used in order to allow the sensitive and selective detection of N-nitrosoamines.

4-(2-Phthalimidyl)benzoyl chloride (PlB–Cl) was used as a fluorescent derivatization reagent for compounds with amino groups.[10] However, no systematic studies of derivatization conditions of PlB–Cl with amines have been reported and there has been no study of amine derivatives of PlB–Cl using liquid chromatography.

In this paper, we develop a simple and sensitive method for the detection of trace N-nitrosoamines. The technique involves the use of high-performance liquid chromatography with fluorescence detection after pre-column reaction. N-Nitrosoamines were denitrosated to secondary amines with denitrosating reagent, the amines formed then react rapidly with PlB–Cl to give fluorescent amides, which can be separated on an octadecylsilane column. The derivatization and chromatographic conditions were optimized on the basis of experiments.
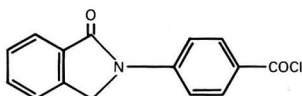
Experimental

Apparatus

A Perkin-Elmer series 3 liquid chromatograph equipped with an MPF-44B fluorescence detector, a 5 μm Nucleosil C$_{18}$

column (125 × 4.6 mm i.d.) and a Rheodyne Model 7105 injection valve with a 20 μl sample loop.

Reagents

All chemicals used were of analytical-reagent grade unless stated otherwise. Doubly distilled water was used throughout.

The N-nitrosoamines were synthesized by reaction of secondary amines with nitrites in an acidic medium,[2,10] and their structures were confirmed by mass spectrometry. These compounds were dissolved in dichloromethane and the stock solution (2 × 10^{-4} mol dm^{-3}) was diluted before use.

The PlB–Cl was prepared as described previously[11] and was dissolved in acetonitrile to give a 5 × 10^{-3} mol l^{-1} reagent solution.

The denitrosation reagent was prepared by diluting 5 ml of 47% m/m aqueous hydrobromic acid (guaranteed-reagent grade) to give a final volume of 26 ml with acetic anhydride.
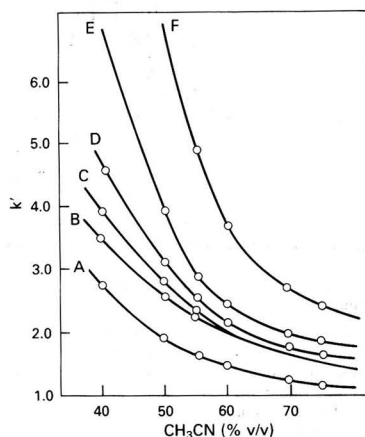

Fig. 1 Plot of capacity factor (k') as a function of acetonitrile percentage composition. Curves: A, N-nitrosodimethylamine; B, N-nitrosopyrrolidine; C, N-nitrosodiethylamine; D, N-nitrosopiperidine; E, N-nitrosodipropylamine; F, N-nitrosodibutylamine

---

Procedure

A 70 µl aliquot of denitrosation reagent was added to 100 µl of test solution (64 pmol–20 nmol per 100 µl) in a test-tube and heated for 5 min in a water-bath at 40 °C. After removal of the solvent under a flow of nitrogen, 100 µl of 0.4 mol l⁻¹ sodium hydrogen carbonate solution and 100 µl of PlB–Cl solution were added. The mixture was allowed to stand at room temperature for about 1 min. A 10 µl aliquot of the final mixture was injected into the high-performance liquid chromatograph.

Results and Discussion

Optimization of Conditions for Denitrosation Reaction

The *N*-nitrosoamines are known to undergo cleavage at the N–NO bond in the presence of a hydrogen bromide–acetic

Fig. 2 Chromatogram of PlB–Cl derivatives. Mobile phase, acetonitrile–water (48 + 52 v/v); flow rate, 0.8 ml min⁻¹; detector wavelength, λ_{ex} = 299 nm, λ_{em} = 426 nm; injection volume, 10 µl. Peak assignment is same as in Fig. 1. Each lettered peak corresponds to 20 pmol of *N*-nitrosoamine

acid mixture, resulting in the formation of the corresponding secondary amines and the liberation of nitric oxide.[2,7,10]

According to Drescher and Frank,[12] the denitrosation of *N*-nitroso compounds in dilute dichloromethane solution occurs readily at ambient temperature and the yield of denitrosation products is essentially independent of hydrogen bromide concentration provided that a minimum excess of approximately 10³ mol of hydrogen bromide per mol of *N*-nitroso compound is maintained. On the basis of our experiments, we found this to be true except for *N*-nitrosopyrrolidine. The denitrosation of *N*-nitrosopyrrolidine was completed in 90 min under the above conditions.

A systematic study of temperature and reaction time was performed with the temperature being varied between 20 and 40 °C and the reaction time between 1 and 90 min. The study indicated the optimum conditions to be 5 min at 40 °C.

Fluorescence Derivatization

The method of Tsuruta and Kobashi[11] was modified to the extent that the fluorescence derivatization was facilitated with sodium hydrogen carbonate rather than sodium hydroxide and reaction time was 1 min rather than 30 min. The optimum concentrations of sodium hydrogen carbonate and PlB–Cl for maximum reaction yield have been investigated. The maximum yield was achieved if the mole ratios of PlB–Cl to *N*-nitrosoamine was >3 and the sodium hydrogen carbonate to *N*-nitrosoamine was >120.

The derivatization of PlB–Cl with the secondary amines, produced by denitrosation, proceeded rapidly and was independent of temperature (0–80 °C), the reaction was complete within 1 min even at 0 °C. Therefore, the mixture was allowed to stand for 1 min at room temperature.

Fluorescence Properties of the Derivatives

The fluorescence spectra were measured in aqueous acetonitrile by stop–flow scanning. The wavelength maxima of fluorescence excitation and emission of the derivatives are 299 and 426 nm, respectively.

Chromatographic Conditions

The separation of PlB–Cl derivatives was studied on a reversed-phase column with aqueous acetonitrile. The dependence of retention time on the acetonitrile concentration in the eluent is shown in Fig. 1. The optimum separation was obtained with 48% v/v aqueous acetonitrile. Fig. 2 shows a typical chromatogram obtained with a mixture of six *N*-nitrosoamines.

Performance of Fluorescence Detection

Several characteristic of the method are given in Table 1.

Interferences

Aromatic amines gave no fluorescent products under the proposed derivatization conditions. Alcohols did not interfere
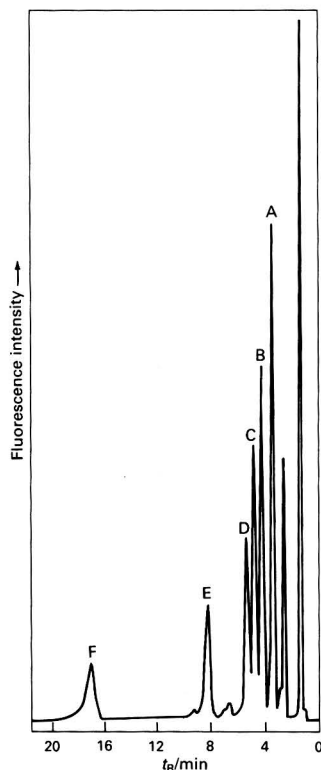
Table 1 Regression analysis of calibration graphs and other quantitative data for the *N*-nitrosoamines

Compound	Linear range/ nmol ml⁻¹	Calibration equation*	Correlation coefficient	RSD† (%)	Detection limit‡/pmol
N-Nitrosodimethylamine	0.32–200	$y = -0.311 + 0.175x$	0.999	2.8	0.6
N-Nitrosopyrrolidine	0.16–200	$y = 0.381 + 0.124x$	0.999	3.9	0.4
N-Nitrosodiethylamine	0.32–200	$y = -0.140 + 0.256x$	0.999	4.1	0.8
N-Nitrosopiperidine	0.32–200	$y = 0.393 + 0.240x$	0.999	3.7	0.4
N-Nitrosodipropylamine	0.64–200	$y = -0.840 + 0.397x$	0.999	4.9	1.6
N-Nitrosodibutylmine	0.64–200	$y = -0.269 + 0.782x$	0.999	3.9	1.6

* y in cm, x in nmol ml⁻¹.
† Relative standard deviation ($n = 7$). [*N*-nitrosoamine] = 8×10^{-6} mol l⁻¹.
‡ Signal-to-noise = 3.

with the determination of *N*-nitrosoamines when present at least up to 0.5 mol l⁻¹. Aliphatic amines could react with PIB–Cl under the above conditions. In order to identify *N*-nitrosoamines in the sample, a portion of the sample was reacted directly with PIB–Cl in a weak alkaline medium (pH = 8–10) and the amount of aliphatic amines in the sample was determined. Another portion of the sample was treated as mentioned in the text, and the total amount of *N*-nitrosoamines and aliphatic amines were examined. The concentration of the *N*-nitrosoamines could then be calculated.

Conclusion

The method described retains simplicity of technique and can be applied to determination of *N*-nitrosoamines in the environment. In combination with a solid-phase extraction technique[13] most of the *N*-nitrosoamines in aqueous samples can be detected down to required levels.

References

1 Magee, P. N., and Barnes, J., *J. Cancer*, 1956, **10**, 114.
2 Xu, H. X., N-*Nitroso Compounds in the Environment*, Science Press, Beijing, 1988.
3 Issaq, H. J., McConnell, J. H., and Weiss, D. E., *J. Liq. Chromatogr.*, 1986, **9**, 1783.
4 Issaq, H. J., Glennon, M., Weiss, D. E., Chmany, C. N., and Saavedra, J. E., *J. Liq. Chromatogr.*, 1986, **9**, 2763.
5 Issaq, H. J., Atamna, I. Z., Schultg, N. M., Muschik, G. M., and Saavedra, J. E., *J. Liq. Chromatogr.*, 1989, **12**, 771.
6 Wan, Q. H., and Fu, C. G., *Cepu*, 1986, **4**, 238.
7 Wang, Z., Fu, C. G., and Xu, H. D., *J. Chromatogr.*, 1992, **589**, 349.
8 Lee, S. H., and Field, L. R., *J. Chromatogr.*, 1987, **386**, 137.
9 Righezza, M., Murello, M. H., and Siouffi, A. M., *J. Chromatogr.*, 1987, **410**, 145.
10 Hu, R. M., and Ma, L. S., *Analysis of* N-*Nitroso Compounds*, Science Press, Beijing, 1980.
11 Tsuruta, Y., and Kobashi, K., *Anal. Chim. Acta*, 1987, **193**, 309.
12 Drescher, G. S., and Frank, C. W., *Anal. Chem.*, 1978, **50**, 2118.
13 Fu, C. G., and Wan, Q. H., *Fenxi Huaxue*, 1985, **13**, 595.

Ion-exclusion Chromatographic Determination of Hydrogen Carbonate in Natural Waters Using Unmodified Silica Gel and Conductimetric Detection

Michio Zenki, Tomiko Nabekura and Atsushi Kobayashi
Department of Chemistry, Faculty of Science, Okayama University of Science, Ridai-cho, Okayama 700, Japan

Tadashi Iwachido
College of Liberal Arts, Okayama University, Tsushima, Okayama 700, Japan

Yasuaki Shimoishi
School of Health Sciences, Okayama University, Shikata, Okayama 700, Japan

A simple and rapid ion-exclusion chromatographic method for the determination of hydrogen carbonate has been developed. Unmodified silica gel was used for the separation column instead of H+-form cation-exchange resin. By elution with water and monitoring with a conductimetric detector, excellent separation can be achieved. The chromatographic conditions for the separation of hydrogen carbonate, pore and particle sizes of packings and the separation mechanism are discussed. For the determination of hydrogen carbonate, borate buffer solution (pH 7.3) was added in order to keep the pH of the sample solution constant. The calibration graph was found to be linear in the range 2–20 µg ml⁻¹ of hydrogen carbonate. Common anions and cations such as chloride, nitrate, sulfate, sodium and calcium do not interfere. The method has been applied to the determination of hydrogen carbonate in river and lake waters.

Keywords: *Ion-exclusion chromatography; hydrogen carbonate; unmodified silica gel; conductimetric detection*

The simple and accurate determination of inorganic carbon species (*e.g.*, carbon dioxide, hydrogen carbonate and carbonate) is an important requirement in water purification, environmental and biological research.

Ion chromatography (IC)[1] with conductimetric detection is a useful tool for the determination of common anions, such as fluoride, chloride, bromide, nitrate, nitrite, phosphate and sulfate. The combination of a low-capacity ion-exchange column and low-conductivity eluents allows the determination of such ions at sub-ppm levels. However, the detection of hydrogen carbonate at trace levels is difficult, because it is a very weak acid ($pK_{a1} = 6.34$) and exists ordinarily as anions in basic solution. In addition, the resolution of hydrogen carbonate seems to be incomplete, and the peak for hydrogen carbonate overlaps sometimes with peaks for other compounds. Also, sodium hydrogen carbonate is used frequently as a component of the eluent for the separation of several anions.[2,3]

Detection of hydrogen carbonate using a spectrophotometric detector is also difficult because of its weak absorption above 210 nm. Indirect ultraviolet (UV) detection[4–6] was therefore carried out, using organic acids as eluents. However, hydrogen carbonate is similar in its retention behaviour to that of other common anions, *e.g.*, chloride.

On the other hand, ion-exclusion chromatography (IEC), developed by Wheaton and Bauman,[7] is a convenient method for the separation of non-ionic species from ionic species. Kreling and DeZwaan[8] and Tanaka and Fritz[9] reported the determination of hydrogen carbonate by IEC using a cation-exchange resin (H+-form, sulfonated polystyrene–divinylbenzene copolymer) and water as the eluent. This is the only reliable method that has been confirmed.

Silica gel is known to act as an ion exchanger.[10,11] Smith and Pietrzyk[12] have revealed that many inorganic cations can be separated on an unmodified silica gel column by IC. We have also reported some results regarding the chromatographic separations of alkali and alkaline-earth metal cations on unmodified silica gel.[13,14] The pK_a value of the silanol group is reported to be 7.1[15] and it is assumed that the silanol group of

the hydrated silica gel surface dissociates to a certain extent in slightly acidic or neutral solutions. Therefore, ion exclusion can be expected to take place in a similar manner to that occurring on a sulfonated cation-exchange resin. To date, no studies on the separation and determination of hydrogen carbonate with unmodified silica gel have been reported.

The purpose of this work was to demonstrate the use of an unmodified silica gel column for the separation of hydrogen carbonate by IEC. The method has been applied to the determination of hydrogen carbonate in natural waters.

Experimental

Apparatus

The high-performance liquid chromatographic system consisted of an LC-6A pump, a CDD-6A conductivity detector, a CT0-6AS column oven (all from Shimadzu, Kyoto, Japan) and a Rheodyne 7125 loop injector (Cotati, CA, USA). A Shimadzu Model C-R6A printer–plotter integrator was used to record the signal response. A 250×4 mm i.d. stainless-steel column filled with Develosil 30-5 (Nomura Kagaku, Seto, Japan) was used. A packed column of TSK SCX (150×4 mm i.d.) was purchased from Tosoh (Tokyo, Japan) and used for comparative purposes. The column temperature was maintained at 35 °C. The flow rate of the mobile phase was fixed at 0.8 ml min⁻¹, and the injected sample size was 100 µl.

Reagents

All the reagents used were of analytical-reagent grade. Water was obtained from a Millipore (Milford, MA, USA) Milli-Q water purification system (18 MΩ).

Stock standard solution (1000 µg ml⁻¹). Prepared by dissolving 1.377 ± 0.005 g of sodium hydrogen carbonate (Wako Pure Chemicals, Osaka, Japan) in 1 l of water.

Buffer solution (pH = 7.3). Prepared by dissolving 3.81 ± 0.01 g of sodium tetraborate in approximately 400 ml of water. The pH was adjusted to 7.3 ± 0.05 with boric acid, and the solution was diluted to 500 ml with water.

Sample Preparation

All the samples were passed through a 0.45 μm Millipore filter, and the filtrates were mixed with equal volumes of borate buffer solution and injected onto the column.

Results and Discussion

Chromatograms

A typical chromatogram, obtained with a silica-gel column (Develosil 30-5), distilled water as the mobile phase and conductimetric detection, is shown in Fig. 1(a). Under the same conditions, some different types of packing, such as cation- and anion-exchange resins and octadecylsilane, were tested. Fig. 1(b) depicts a chromatogram obtained with a TSK SCX column, which was used by Tanaka and Fritz.[9] It is interesting that both chromatograms are very similar, even though the properties and characteristics of the column packings are different from each other. The SCX column is a sulfonated polystyrene–divinylbenzene copolymer with a high cation-exchange capacity (4.2 mequiv^{-1} g), while Develosil 30-5 is a porous, spherical silica gel (pore size 3 nm; particle size 5 μm; surface area 650 m^2 g^{-1}). The surfaces of silica gels and their ion-exchange properties have been discussed extensively by Unger.[10] Chromatograms obtained with the silica gel columns are explained by assuming that the ion exclusion by the silanol group takes place in a manner similar to that of the sulfonic acid group. With other columns tested (LiCrosorb RP-18, Develosil ODS-5 and TSKgel IC Anion PW), the separation and resolution of hydrogen carbonate were incomplete.

Pore and Particle Size

The effects of the pore and particle size of the silica gels on the separation of hydrogen carbonate have been investigated. Nine packings, having pore and particle sizes of 3, 5 and 10 nm and 5, 7 and 10 μm, respectively, were packed into the stainless-steel column (250 × 4 mm i.d.). With decreasing pore and particle size of silica gels, the surface area increases, *i.e.*, the number of ion-exchange sites increases and hence the separation and resolution by the ion-exchange reaction can be affected significantly. In fact, the expected results were obtained for the separation and resolution of analytes in previous papers.[13,14] In this work, however, it was found that the retention behaviour (capacity factor) of hydrogen carbon-
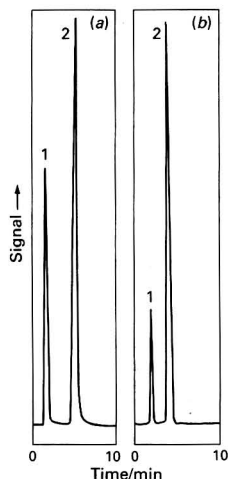
ate was almost independent of the pore and particle sizes of the packings. Only the shapes of the peaks were sharper with decreasing particle size. Fig. 2 shows the relationship between the particle size of the packings and the theoretical plate numbers (*n*). Silica gels with a smaller pore size (3 nm) and a smaller particle size (5 μm) are suitable for obtaining well-resolved, sharper peaks.

Column Length and Enhancement Column

The dependence of the separation of hydrogen carbonate on the column length was investigated. Three types of column, 50, 150 and 250 mm long (each 4 mm i.d.), were used and compared. In IEC a considerable amount of the resin is essential to achieve a reasonable separation.[9] Good resolution was obtained in about 5.2 min on the 250 × 4 mm i.d. column. The effect of ion-exchange enhancement[9] was investigated by inserting a second column of silica gel after the separation column. No enhancement was observed, which shows that the mechanism of enhancement differs between the silica gel and the sulfonated polystyrene–divinylbenzene copolymer. More careful consideration is necessary.

Mobile Phase

In order to determine the effect of pH on retention, mobile phases buffered at pH 4.0, 5.0, 6.0, 7.0 and 8.0 with HCl and NaOH were prepared and investigated. Higher pH values (above pH 8) were not tested as solutions of such pH damage the column. The peak resolution became poorer as the pH of the mobile phase decreased, and below pH 4 the peak for hydrogen carbonate disappeared. This was because of the lack of sensitivity, *i.e.*, no dissociation of hydrogen carbonate. Throughout the experiments, the signal due to carbon dioxide was not observed because of its neutrality. Mobile phases of higher pH (pH > 6.5) were found to produce a large baseline drift because of the increase in background conductivity. Therefore, distilled water was adopted for this work.

pH of the Sample Solution

The calibration graph was established from injection of different concentrations of the standard hydrogen carbonate solutions onto the column. The signal responses as a function of hydrogen carbonate concentrations up to 20 μg ml^{-1} are shown in Fig. 3(a). As expected, the plots are curved because of the difference in the degree of dissociation as a function of

Fig. 1 Chromatograms of hydrogen carbonate. (a) Develosil 30-5 (250 × 4 mm i.d.). (b) TSK SCX (150 × 6 mm i.d.). Peak 1, dip peak; and peak 2, HCO$_3^-$ (20 μg ml^{-1})
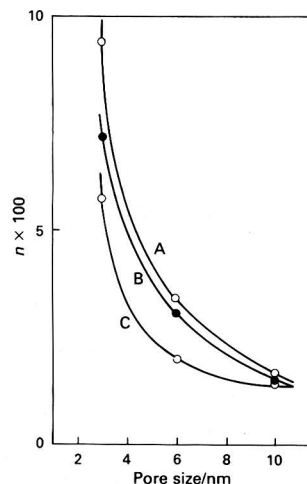

Fig. 2 Theoretical plate number *versus* pore size of packings. Particle size: A, 5; B, 7; and C, 10 μm
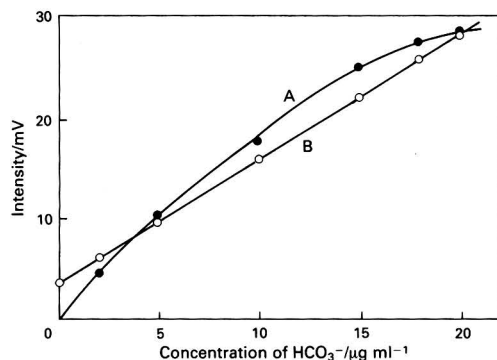
Fig. 3 Calibration graph. (a) Without buffer solution; and (b) with buffer solution (pH 7.3)
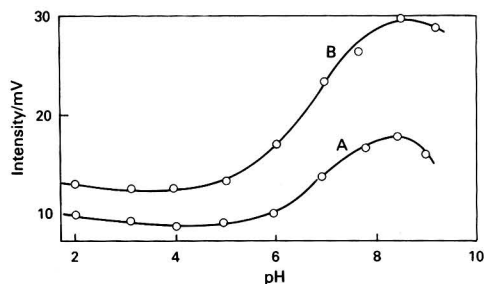

Fig. 4 Signal response *versus* pH of sample solution. Concentration of HCO_3^-: A, 10; and B, 20 µg ml^{-1}

Fig. 5 Chromatograms obtained with borate buffer solution. (a) Standard solution (HCO_3^-, 20 µg ml^{-1}). (b) River water (Takahashi). Peak 1, dip peak; peak 2, $H_2BO_3^-$; and peak 3, HCO_3^-

hydrogen carbonate concentration.[9] In order to improve the linearity of the calibration graph, samples were adjusted to constant pH by addition of a buffer solution prior to injection onto the column. Fig. 4 shows the relationship between pH of the sample solutions and signal response (peak height). The peak increased with increasing pH of the sample solution up to 8.5. This is a result of the increase of dissociation of carbonic acid, *i.e.*, hydrogen carbonate is predominant. In fact the molar fraction of hydrogen carbonate, calculated from the pK_a values of carbonic acid ($pK_{a1} = 6.34$, $pK_{a2} = 10.36$), reaches a maximum at pH 8.5. Unfortunately, it is known that the dissolution of silica gel becomes more serious above pH 8. As a pH between 7.0 and 7.5 was satisfactory for a quantitative determination, pH 7.3 was adopted.

Several types of buffer solution, such as acetate, ammonium, borate, phosphate and Good's buffer, were tested. Sodium tetraborate–boric acid buffer was selected because a suitable chromatogram was obtained, which is shown in Fig. 5(a). Boric acid ($pK_a = 9.24$) is as weak an acid as is hydrogen carbonate and is also expected to be eluted by IEC. It is known that the order of elution depends on the acid-dissociation constant, but the peak of borate appears between the dip peak and the hydrogen carbonate peak (retention time = 3.1 min). Even though the concentration of borate is high (1.0×10^{-2} mol l^{-1}), the strength of the borate signal is weak and therefore adequate.

Column Temperature

The effects of temperature on columns were investigated. Though the sensitivity (peak height) increased with increasing column temperature, the capacity factor for hydrogen carbonate decreased gradually. Therefore, the temperature of the column oven was maintained at 35 °C.
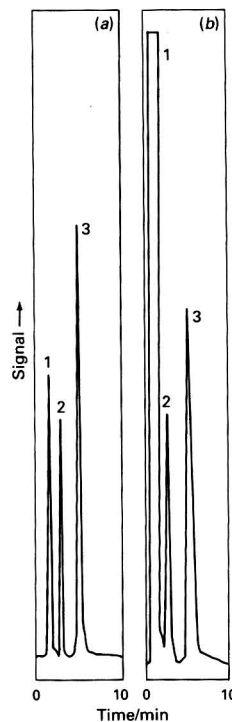
Interferences

Possible sources of interference in natural waters, such as chloride, nitrate, sulfate, silicate, phosphate, ammonium, sodium, potassium, magnesium, calcium, aluminium and iron, were investigated at concentrations of up to ten times that of hydrogen carbonate. All the ions tested were eluted faster than the borate peak, and caused no interference even at a ratio of interfering species to hydrogen carbonate of 10 : 1. In the analysis of some actual samples by IEC, sometimes the dip peak grew larger and the species that eluted after the dip peak were overlapped or disappeared. In this case, either removal of the matrix or dilution of the sample solution was necessary. However, in the proposed method, the borate peak was affected to some extent by the dip peak, but not by the hydrogen carbonate peak [Fig. 5(b)]. Therefore, there is no interference in the determination of hydrogen carbonate.

Calibration

The calibration graph was linear over the range 2–20 µg ml^{-1} for hydrogen carbonate. As shown in Fig. 3(b), the calibration plot does not pass through the origin because of the residual carbonate concentration in the borate buffer solution. The correlation coefficient for the calibration graph was 0.9999. When 10 and 20 µg ml^{-1} standard hydrogen carbonate solutions were injected consecutively the relative standard deviations measured for ten runs were 0.89 and 1.9%, respectively.

Application to Natural Waters

The method has been applied to the determination of hydrogen carbonate in some environmental waters. River and lake water samples were collected in Okayama Prefecture,

Table 1 Determination of hydrogen carbonate in natural waters

Sample* (dilution)	Amount/μg ml⁻¹			Recovery (%)	Other method‡
	Initial†	Added	Found†		
River—					
Asahi	22.7 ± 0.3	4.0	26.0 ± 0.4	97.4	24–29
		10.0	33.8 ± 0.4	103	—
Takahashi	45.0 ± 0.6	4.0	50.6 ± 0.5	103	45–61
(1 + 2)		10.0	47.6 ± 0.6	97.1	—
Yoshii	23.5 ± 0.4	4.0	27.8 ± 0.3	101	24
		10.0	34.6 ± 0.5	103	—
Lake—					
Ikenouchi	72.6 ± 0.5	10.0	82.6 ± 0.5	100	—
(1 + 5)					
Miyashita	120 ± 0.6	10.0	128 ± 0.6	98.5	—
(1 + 10)					
Hikoki	158 ± 0.9	10.0	170 ± 1.1	101	—
(1 + 10)					

* Samples were collected on January 28, 1992.
† Average of five determinations ± standard deviations.
‡ Indirect UV detection[6] and gas-diffusion flow injection.[16]

Japan. These samples were passed through a membrane filter (pore size 0.45 μm; Millipore) and submitted to chromatography as soon as possible. The recovery test was carried out by adding, with a microsyringe, 10 μl of the standard hydrogen carbonate solution to 10 ml of the filtered sample solutions. The results obtained for recovery tests are summarized in Table 1. A chromatogram of river water samples is shown in Fig. 5(*b*). A large dip peak due to large amounts of common anions (such as chloride, nitrate and sulfate) was observed. However, the resolution between the dip peak, borate peak and hydrogen carbonate peak was satisfactory. The results of the recovery tests also show that the proposed method could be utilized for practical applications.

References

1 Small, H., in *Ion Chromatography*, ed. Hercules, D., Plenum Press, New York, 1989, p. 149.
2 Hanaoka, Y., Murayama, T., Muramoto, S., Matsuura, T., and Nanba, A., *J. Chromatogr.*, 1982, **239**, 537.
3 Saigne, C., Kirchner, S., and Legrand, M., *Anal. Chim. Acta*, 1987, **203**, 11.
4 Brandt, G., and Kettrup, A., *Fresenius' Z. Anal. Chem.*, 1985, **320**, 485.
5 Brandt, G., Matuschek, G., and Kettrup, A., *Fresenius' Z. Anal. Chem.*, 1985, **321**, 653.
6 Hironaka, T., Oshima, M., and Motomizu, S., *Bunseki Kagaku*, 1987, **36**, 503.
7 Wheaton, R. M., and Bauman, W. C., *Ind. Eng. Chem.*, 1953, **45**, 228.
8 Kreling, J. R., and DeZwaan, J., *Anal. Chem.*, 1986, **58**, 3028.
9 Tanaka, K., and Fritz, J. S., *Anal. Chem.*, 1987, **59**, 708.
10 Unger, K. K., *J. Chromatogr. Libr.*, 1979, **16**, 130.
11 Dugger, D. L., Stanton, J. H., Irby, B. N., McConnell, B. L., Cummings, W. W., and Maatman, R. W., *J. Phys. Chem.*, 1964, **68**, 757.
12 Smith, R. L., and Pietrzyk, D. J., *Anal. Chem.*, 1984, **56**, 610.
13 Iwachido, T., Shinomiya, M., and Zenki, M., *Anal. Sci.*, 1990, **6**, 277.
14 Iwachido, T., Ikeda, T., and Zenki, M., *Anal. Sci.*, 1990, **6**, 593.
15 Hair, M. L., and Hertl, W., *J. Phys. Chem.*, 1970, **74**, 91.
16 Kuwaki, T., Tôei, K., Akiba, M., Oshima, M., and Motomizu, S., *Bunseki Kagaku*, 1987, **36**, T132.

Organic-phase Biosensors for Monitoring Phenol and Hydrogen Peroxide in Pharmaceutical Antibacterial Products

Joseph Wang, Yuehe Lin and Liang Chen
Department of Chemistry, New Mexico State University, Las Cruces, NM 88003, USA

Organic-phase biosensors open new opportunities for assays of challenging pharmaceutical products. Such opportunities are illustrated for the rapid determination of phenol and peroxide antiseptics in different anti-infective formulations. The tyrosinase and peroxidase enzyme electrodes offer reliable quantification of these antibacterial agents following sample dissolution in the organic solvent. The dynamic properties of these enzyme electrodes are exploited for rapid and reproducible flow-injection assays of the pharmaceutical products (relative standard deviation = 1.6–1.9%). Such developments should facilitate rapid quality control testing in the pharmaceutical industry and should be applicable to other therapeutic agents and products. Applicability to cosmetic products containing hydrogen peroxide is also demonstrated.

Keywords: *Organic-phase biosensor; phenol; pharmaceutical analysis; enzyme electrode*

The remarkable finding that enzymes can maintain their biocatalytic activity in non-aqueous environments[1] has led to the development of organic-phase biosensors.[2] The operation of enzyme electrodes in organic solvents offers several important advantages, including measurements of additional (hydrophobic) substrates, assays of new environments, extended sensor stability or simplified immobilization schemes. The ability to analyse previously inaccessible sample matrices can greatly expand the possibilities for biosensors. For example, recent studies have illustrated the utility of cholesterol oxidase and tyrosinase electrodes for direct amperometric assays of butter[3] and olive oils,[4] respectively. Numerous other potential applications of organic-phase enzyme electrodes are expected to be explored in the near future.

This paper describes the utility of organic-phase biosensors for challenging pharmaceutical products. Many pharmaceutical formulations are not readily dissolved in aqueous media. Hence, their bioassays (using traditional enzyme electrodes) usually require time-consuming sample manipulations, *e.g.*, solvent extraction. The introduction of organic-phase enzyme electrodes obviates the need for such sample pre-treatment and facilitates rapid assays of pharmaceutical products. Such opportunities are illustrated here for the monitoring of phenolic and peroxide antiseptics in anti-infective pharmaceutical formulations. The antibacterial activity of phenols and hydrogen peroxide[5,6] has led to their extensive therapeutic use. Tyrosinase- and peroxidase-based biosensors, known for their effective operation in non-aqueous environments,[4,7–9] are shown here to be highly suitable for the rapid determination of their corresponding substrates in pharmaceutical products. The reported coupling of these sensors with fast flow-injection operation should be particularly attractive for quality-control and process-monitoring applications in the pharmaceutical industry.

Experimental

Apparatus

Amperometric measurements were performed with a CV-27 voltammograph [Bioanalytical Systems (BAS)], in connection with an *x–y–t* recorder (BAS). The 10 ml cell (Model CV-2, BAS) was joined to the enzyme electrode, reference electrode [Ag–AgCl (3 mol l^{-1} NaCl), Model RE-1, BAS] and platinum-wire auxiliary electrode through holes in its Teflon cover. A magnetic stirrer and stirring bar facilitated the transport of the substrates. The flow-injection system consisted of a 50 ml syringe/carrier reservoir, held by the syringe pump (Model 341B, Sage), a Rainin Model 5041 sample

injection valve (20 µl), interconnecting Teflon tubing and the thin-layer electrochemical detector.

Modification of the glassy carbon electrode (Model MF 2012, BAS) was achieved by covering the surface with a 10 µl drop of the mixed enzyme–Eastman-AQ polymer solution. The coating was then allowed to dry with an air gun. The mixed enzyme–Eastman-AQ solutions were prepared by dissolving 2 mg of tyrosinase or 6 mg of horseradish peroxidase in 200 µl of the 1.4% polymer solution.

Reagents

Tyrosinase (EC 1.14.18.1, 2400 U mg^{-1}) (1 U = 16.67 nkat) and horseradish peroxidase (HRP, EC 1.11.1.7, 90 U mg^{-1}) were received from Sigma. Phenol (Fisher), hydrogen peroxide, tetraethylammonium *p*-toluenesulfonate (TEATS), acetonitrile (HPLC grade) and ferrocene (Aldrich) were used as received. The poly(ester-sulfonic acid) polymer (Eastman AQ 55D, 28% dispersion) was received from Eastman Chemical Products; prior to mixing with the enzyme it was diluted 20-fold with de-ionized water. 'Unguentine Plus' (Mentholatum), 'Campho-Phenique' (Sterling Drug), 'Stat-One, Hydrogen Peroxide Gel' (Continental Consumer Products) and 'Creme Hair Bleach' (Del Lab) were purchased from a local drugstore. Samples were dissolved in the following manner: 'Campho-Phenique' products, 0.10 g in 5 ml of propan-1-ol; 'Unguentine Plus', 0.47 g in 10 ml of propan-1-ol; 'Hydrogen Peroxide Gel', 0.113 g in 10 ml of acetonitrile, and 'Creme Hair Bleach', 0.20 g in 5 ml of propan-1-ol.

Procedure

Experiments were performed (at 25 ± 1 °C) in acetonitrile solutions (containing 4% v/v water and 0.05 mol l^{-1} TEATS) by holding the working electrode at the desired potential and allowing the transient current to decay. Potentials of 0.0 and −0.25 V were used for the quantification of hydrogen peroxide and phenol, respectively. Measurements of hydrogen peroxide were carried out in the presence of 5 × 10^{-3} mol l^{-1} ferrocene.

Results and Discussion

Several organic-phase electrodes, based on the activity of tyrosinase and peroxidase in non-aqueous media, have been developed in recent years.[4,7–10] One promising fabrication method involves the entrapment of these enzymes within

Eastman-AQ surface coatings (which are stable in various organic media).[10] Fig. 1 displays amperometric responses of the tyrosinase–Eastman-AQ coated electrode (in acetonitrile) to the addition of various dissolved pharmaceutical products (A) and to subsequent additions of a phenol standard solution (B–E). The tyrosinase electrode responds very rapidly to these additions, producing steady-state currents within 10–12 s. Note also the high sensitivity to these micromolar changes in the substrate concentration compared with the absence of response without the enzyme (broken line). The well-defined response of the organic-phase enzyme electrode offers convenient determinations of the phenol antiseptics based on the standard additions method. The resulting standard additions plots for these pharmaceutical formulations are displayed in Fig. 2. All plots exhibit a linear dependence (correlation coefficients, 0.999) that permits reliable quantification (following correction for the dilution factor). Phenol levels of 4.5% (a), 0.5% (b) and 4.5% (c) were thus calculated for these samples. Such values are in very good agreement with the labelled values [4.7% (a), 0.50% (b) and 4.7% (c)]. It should be pointed out that the antiseptic products used in Figs. 1 and 2 are insoluble in water, but can be readily dissolved in propan-1-ol.

Owing to its strong oxidizing power, hydrogen peroxide is commonly used as an antiseptic in anti-infective formulations, or as a bleaching agent in cosmetic products. The peroxidase–Eastman-AQ organic-phase biosensor can facilitate the quantification of hydrogen peroxide in such challenging products. Fig. 3 shows current–time recordings obtained at the peroxidase electrode for additions of dissolved 'Hydrogen Peroxide Gel' pharmaceutical (a) and 'Creme Hair Bleach' cosmetic (b) products, and for successive 1×10^{-5} mol l^{-1} additions of

hydrogen peroxide (B–E). In a similar way to its tyrosinase counterpart, the peroxidase electrode exhibits a fast ($\approx$20 s) and sensitive response to changes in the substrate concentration, which permits convenient quantification. Note also the absence of response without the enzyme (broken lines). The resulting standard additions plots (not shown) were highly linear (correlation coefficients, 0.999) and yielded hydrogen peroxide values of 3.3% (a) and 8.9% (b). [The labelled value for product (a) is 3.0%, while no value is given for product (b)]. Other commonly used peroxide species (e.g., benzoyl peroxide) can be measured in a similar fashion, based on the reported response of peroxidase electrodes towards organic peroxides.[11]

The fast response of the tyrosinase and peroxidase organic-phase electrodes can be exploited for high-speed flow-injection assays, as desired for quality control applications. Such flow analysis is simplified by the organic-phase operation, as the need for on-line sample pre-treatment (e.g., solvent extraction) is eliminated. We have recently reported on the adaptation of organic-phase biosensors for monitoring flowing streams.[10,12] Fig. 4 displays the amperometric response to phenol in the 'Campho-Phenique Cold Sore Gel' (F) and 'Campho-Phenique Pain Relieving Antiseptic' (G) products, together with peaks for phenol standard solutions of increasing concentration [5×10^{-5}–25×10^{-5} mol l^{-1} (A–E)]. The tyrosinase detector responds very rapidly to dynamic changes in the concentration, characteristic of flow-injection systems. Phenol levels of 4.4% (F) and 4.5% (G) can therefore be calculated, which are in good agreement with the labelled value (4.7%).

Various experimental variables affecting the flow-injection/organic-phase biosensing response were evaluated. Fig. 5, A shows the effect of the flow rate on the phenol peak. A nearly exponential decrease of the response is observed on increasing the flow rate from 0.4 to 3.4 ml min^{-1}. Apparently, the enzymic reaction requires slower passage of the sample plug to

Fig. 1 Amperometric response to additions of dissolved pharmaceutical products (A), followed by that to successive additions of 1×10^{-5} mol l^{-1} phenol (B–E). Samples, 'Campho-Phenique Cold Sore Gel' (a), 'Unguentine Plus Pain Relieving Cream' (b), and 'Campho-Phenique Pain Relieving Antiseptic' (c). Sample dilutions (in cell) of 1000- [(a) and (c)] and 200-fold (b). Operating potential, −0.25 V; medium, acetronitrile–water (96 + 4% v/v) containing 0.05 mol l^{-1} TEATS. The corresponding response without the enzyme is shown by the broken line

Fig. 2 Standard additions plots for phenol quantification in various pharmaceutical products: 'Campho-Phenique Cold Sore Gel' (a), 'Unguentine Plus Pain Relieving Cream' (b) and 'Campho-Phenique Pain Relieving Antiseptic' (c). Conditions as in Fig. 1
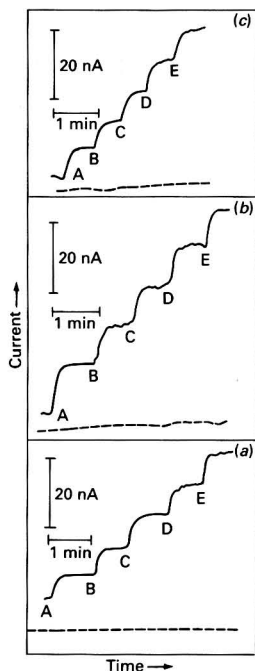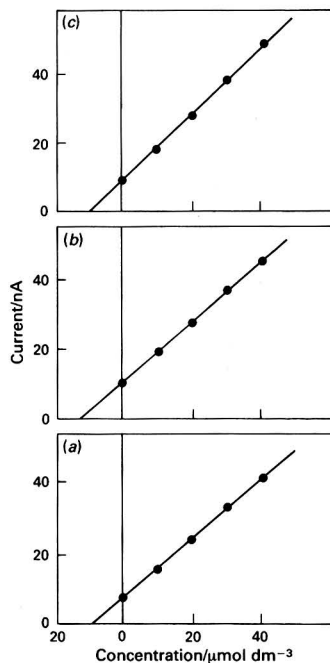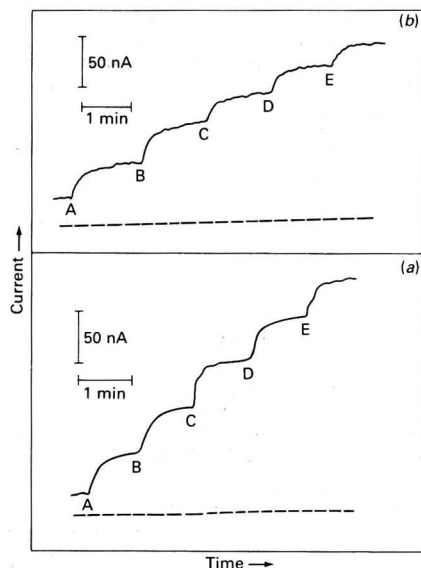
Fig. 3 Amperometric response to additions of dissolved products (A), followed by that to successive additions of 1×10^{-5} mol l^{-1} hydrogen peroxide (B–E). Samples, 'Hydrogen Peroxide Gel' (*a*) and 'Creme Hair Bleach' (*b*) (dilution factor, 1000 and 10000, respectively). Operating potential 0.0 V; medium, acetonitrile–water (96 + 4% v/v) containing 0.05 mol l^{-1} TEATS and 5×10^{-3} mol l^{-1} ferrocene. The corresponding response without the enzyme is shown by the broken line
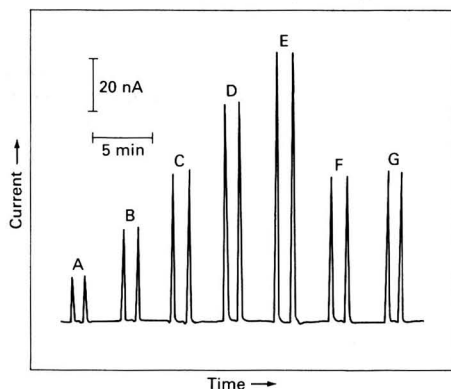

Fig. 4 Flow-injection peaks for phenol solutions of increasing concentration [5×10^{-5}–25×10^{-5} mol l^{-1} (A–E)] and for injections of dissolved 'Campho-Phenique Cold Sore Gel' (F) and 'Campho-Phenique Pain Relieving Antiseptic' (G) products. Dissolved samples were diluted 66.6-fold in the carrier solution prior to injection. Flow rate, 0.50 ml min^{-1}; carrier + electrolyte, acetonitrile –water (96 + 4% v/v), containing 0.05 mol l^{-1} TEATS; operating potential, -0.25 V

Fig. 5 Effect of flow rate (A) and operating potential (B) on the flow-injection response to a 2×10^{-4} mol l^{-1} phenol solution. Operating potential (A), -0.25 V; flow rate (B), 0.50 ml min^{-1}. Conditions as in Fig. 4
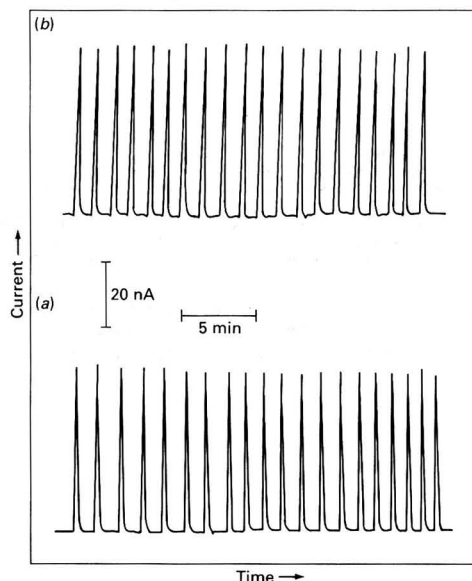
Fig. 6 Detection peaks for repetitive injections of dissolved 'Campho-Phenique Pain Relieving Antiseptic' (*a*) and 'Campho-Phenique Cold Sore Gel' (*b*) products. Other conditions as in Fig. 4

produce appreciable currents. The effect of the operating potential is shown in Fig. 5, B. A well-defined sigmoidal hydrodynamic voltammogram (HDV), with a rapid current increase between -0.05 and -0.25 V, is observed. Such an HDV, expected for the detection of the enzymically produced quinone species, indicates that ohmic drop effects are not substantial in the organic media (provided sufficient electrolyte is present).

The flow-injection response to phenol in pharmaceutical products is also highly reproducible. Detection peaks for a series of 20 repetitive assays of the 'Campho-Phenique Pain Relieving Antiseptic' (*a*) and 'Campho-Phenique Cold Sore Gel' (*b*) samples are displayed in Fig. 6. These prolonged

series yielded relative standard deviations (RSDs) of 1.7% (*a*) and 1.6% (*b*). Note again the fast response and rapid return to the baseline, as expected for Eastman-QA based organic-phase biosensors.[10]

Flow-injection measurements of hydrogen peroxide in the 'Hydrogen Peroxide Gel' and the 'Creme Hair Bleach' samples are displayed in Fig. 7. Also shown are peaks for hydrogen peroxide solutions of increasing concentration [1×10^{-4}–4×10^{-4} mol l^{-1} (A–D)] (*a*). The HRP–organic-phase electrode offers a fast, linear and stable flow-injection response [correlation coefficient (*a*), 0.999; RSDs (*n* = 20) of 1.9% (*b*) and 1.6% (*c*)]. Hydrogen peroxide levels of 6.9% (*b*) and 2.8% (*c*) have thus been calculated.

In conclusion, organic-phase biosensors offer unique opportunities for the pharmaceutical industry. Although such opportunities are illustrated here for measurements of phenolic and peroxide antiseptics, they could easily be extended to bioassays of other therapeutic agents and products. The
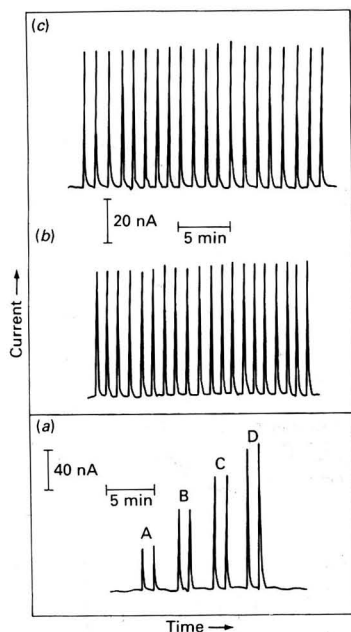
Fig. 7 Flow-injection peaks for hydrogen peroxide solutions of increasing concentration [1×10^{-4}–4×10^{-4} mol l^{-1} (A–D)] (a) and for repetitive injections of dissolved 'Creme Hair Bleach (b) and 'Hydrogen Peroxide Gel' (c) products. Dissolved samples were diluted 500- (b) and 50-fold (c) in carrier solution prior to injection. Operating potential, 0.0 V; carrier + electrolyte (96 + 4% v/v) containing 0.05 mol l^{-1} TEATS and 5×10^{-3} mol l^{-1} ferrocene; flow rate, 0.5 ml min^{-1}

the organic-phase biosensors should be suitable for *in situ* process monitoring during the production of drugs. The fast-responding flow-injection systems should be particularly attractive for the tasks of quality control and process monitoring in the pharmaceutical industry. Similar improvements and opportunities are anticipated for previously inaccessible and challenging sample matrices from other industries.

speed and simplicity that accrue from the organic-phase biosensing operation should greatly facilitate quality-control testing of pharmaceutical and cosmetic products. In addition,

References

1 Zaks, A., and Klibanov, A. M., *J. Biol. Chem.*, 1988, **263**, 3194.
2 Saini, S., Hall, G. F., Downs, M. E., and Turner, A. P. F., *Anal. Chim. Acta*, 1991, **249**, 1.
3 Hall, G. F., and Turner, A. P. F., *Anal. Lett.*, 1991, **24**, 1375.
4 Wang, J., Reviejo, A. J., and Mannino, S., *Anal. Lett.*, 1992, **25**, 1399.
5 *Merck Manual of Diagnosis and Therapy*, ed. Berkow, R., Merck, Rahway, NJ, 14th edn., 1982, p. 2300.
6 Jenkins, G., and Hartung, W., *The Chemistry of Organic Medicinal Products*, Wiley, New York, 1950, p. 100.
7 Hall, G. F., Best, D. J., and Turner, A. P. F., *Anal. Chim. Acta*, 1988, **213**, 113.
8 Schubert, F., Saini, S., and Turner, A. P. F., *Anal. Chim. Acta*, 1992, **245**, 133.
9 Wang, J., Wu, L. H., and Angnes, L., *Anal. Chem.*, 1991, **63**, 2993.
10 Wang, J., Lin, Y., and Chen, Q., *Electroanalysis*, 1993, **5**, 23.
11 Wang, J., Freiha, B., Naser, N., Romero, E. G., Wollenberger, U., Özsoz, M., and Evans, O., *Anal. Chim. Acta*, 1991, **254**, 81.
12 Wang, J., and Lin, Y., *Anal. Chim. Acta*, 1993, **271**, 53.

Agarose Gel Electrophoresis System for the Separation of Antibiotics used in Animal Agriculture

Michael J. Salvatore and Ilya Feygin
Merck & Co., Inc. P.O. Box 2000, Rahway, NJ 07065, USA

Stanley E. Katz
Department of Biochemistry and Microbiology, Cook College/NJAES, Rutgers—the State University of New Jersey, New Brunswick, NJ 08903-0231, USA

A novel electrophoresis system using agarose gel has been developed for the separation and as an aid in the classification of antibiotics. This system utilizes Nunc cell factory disposable tissue culture dishes, which serve as bioassay dish and cooling chamber for agarose gel, in a custom designed electrophoresis unit. Tris(hydroxymethyl) methylamine–succinate buffer at pH 6.0 and 8.0 are employed as the electrolyte for electrophoresis. Bioautography was used as the indicator of mobility. Any agar diffusion assay can be modified to use this system. A suggested name for this system is Nunc cell factory agarose gel electrophoresis (NUAGE). Selected antibiotics, representative of the aminoglycoside, β-lactam, macrolide, moenocinol, peptide, polyene, polyether, quinone and tetracycline classes, were separated with this system.

Keywords: *Agarose gel electrophoresis; animal agriculture; bioautography; separation of antibiotics; classification of antibiotics*

The current official, Association of Official Analytical Chemists (AOAC), methods of analysis rely primarily upon agar diffusion assays for the quantification of antibiotic levels in feeds.[1] These methods assume that the declared antibiotic is solely responsible for the biological response. These assays also assume a prior knowledge of the constituents of the feed. For example, an assay for erythromycin would be used to analyse feeds assumed to contain erythromycin. The key to error in these assays is the 'assumption' of the identity of the antibiotic prior to its analysis. There is no provision to identify the antibiotic in this type of assay because the results are demonstrated only by zones of inhibition.

The AOAC methods do not address the analysis of antibiotics occurring in mixtures. They cannot, *per se*, detect, separate or differentiate between individual, classes or mixtures of antibiotics. The design of these assays can completely mask the presence of other antibiotics. This is also true for combinations of antibiotics that act in synergy or as antagonists with each other; all of which can lead to erroneous and misleading results.

It is, therefore, important to develop an antibiotic identification and classification system. Such a system should provide rapid detection with the simplicity of an agar diffusion assay and a means of detecting separating and identifying individual classes and mixtures of antibiotics. A separation system designed to differentiate between antibiotics can be achieved by various means, some of which include: (*i*) exploitation of some chemical or physical property of the antibiotic molecule (*i.e.*, charge, size); (*ii*) selective destruction or inhibition of the activity of the antibiotic (*i.e.*, pH change, chemical inactivation); (*iii*) selective indication of individual antibiotics (*i.e.*, colour reaction, spectra); and (*iv*) selectivity by indirect means (*i.e.*, resistant microorganisms). To date, only separation by chemical or physical property has shown any merit.

There have been many classification systems based on chemical and/or physical properties described for the detection, separation and identification of antibiotics. These systems have been described for paper chromatography,[2–10] thin-layer chromatography,[11–18] paper electrophoresis[19–25] and gel electrophoresis.[26–35] All of these systems utilize differential solubility and/or mobility to detect, separate and identify antibiotics.

Paper and thin-layer chromatography systems take advantage of the antibiotic solubility and differential mobility in a solvent for classification. These systems use multiple transfer steps, solvents and support matrices to separate and characterize antibiotics into discernible groups. Low levels of antibiotics have to be concentrated prior to testing. If bioautography is used to indicate mobility and biological activity there is also a drying and antibiotic diffusion step.

In addition, complex mixtures can contain constituents (salts, fatty acids, *etc.*) that interefere usually by causing streaking or yield R_F (retardation factor) values that are not reproducible.[2–18] These types of systems are tedious and time consuming, ineffective for all antibiotics, insensitive and can expose the antibiotic to harsh conditions.

The aforementioned chromatography systems are very useful for organic-soluble antibiotics. Aqueous-soluble antibiotics, such as tetracyclines, aminoglycosides, *etc.*, are very difficult to characterize due to their lack of mobility.

Paper and gel electrophoresis utilize charge, shape and size to separate and characterize antibiotic molecules. Differential mobilities of antibiotic molecules in an electric field can be used for characterization. Systems have been described that utilize organic solvents, such as chloroform,[36] with paper electrophoresis and aqueous solvents, such as phosphate buffer, with agarose gel electrophoresis.[6,16–20,22,24–30]

Paper electrophoresis is more suitable for antibiotic residue analysis than it is for chromatography. It is a simpler and more direct method of analysis. It can handle organic- as well as aqueous-soluble antibiotics for characterization. However, this type of system contains the same insensitivity, overloading, streaking, drying and antibiotic diffusion problems as chromatography. In addition, electroendoosmosis can further affect the accuracy of the characterization.

Gel electrophoresis is, by far, the best of the separation systems. Overloading, and thus sensitivity can be minimized by using thicker support layers without increasing electroendoosmosis. Streaking can be minimized by decreasing the amount of gel comprising the matrix. Finally, drying and antibiotic diffusion problems are eliminated by overlaying the gel with a biological indicator contained in a similar type of matrix.

The gel electrophoresis system presented herein detects,

separates, classifies and identifies 17 antibiotics currently used in animal agriculture when used in conjunction with the solvent separation system of Salvatore and Katz.[23]

Experimental

Reagents

The reagent ingredients were dissolved in de-ioinized water, the pH was adjusted and the total volume made up 1 l.

Tris–succinate buffer, pH 6.0. Tris(hydroxymethyl)methylamine (Tris; 1.82 g) and 0.95 g succinic acid.

Tris–succinate buffer, pH 8.0. Tris(hydroxymethyl)methylamine (3.03 g) and 0.85 g succinic acid.

Sterile isotonic saline solution. Sodium chloride (9.0 g). Sterilize for 20 min at 121 °C.

1% Agarose–Tris–succinate, pH 6.0. Agarose (10.0 g) and 1.0 l of Tris–succinate buffer pH 6.0. Sterilize for 20 min at 121 °C. After sterilization agarose–Tris–succinate was kept at 48 °C until use.

1% Agarose–Tris–succinate, pH 8.0. Agarose (10.0 g) and 1.0 l of Tris–succinate buffer pH 8.0. Sterilize for 20 min at 121 °C. After sterilization agarose–Tris–succinate was kept at 48 °C until use.

Culture Media

The media described below were re-hydrated in 1 l of distilled water, adjusted to the appropriate pH and autoclaved at 121 °C for 20 min. Media containing agar were kept in a water-bath at 48 °C until use.

Medium A. Antibiotic medium 3 (53.0 g) and 0.1 g manganese(ous) sulfate H_2O (Fisher Scientific, Springfield, NJ, USA), pH 6.95–7.05.

Medium B. Nutrient broth (8.0 g) and 2.0 g yeast extract, pH 6.95–7.05.

Medium C. Medium B and 15.0 g Bacto-Agar, pH 6.95–7.05.

Medium D. Yeast extract (10.0 g) and 10.0 g anhydrous dextrose (Fisher Scientific), pH 6.55–6.65.

Medium E. Medium D and 15.0 g Bacto-Agar, pH 6.55–6.65.

All biological media were purchased from Difco Laboratories, Detroit, MI, USA).

Antibiotics

Antibiotics were chosen because of their use in animal agriculture in the USA. Their preparation is outlined in the AOAC manual.[1] Fosfomycin and L-proline (no antibiotic activity) were used as indicators of mobility. Fosfomycin was prepared by following the same procedure as that for streptomycin. The following antibiotics were used in these studies: bacitracin, zinc salt; bambermycin; chlortetracycline hydrochloride; erythromycin; fosfomycin, disodium; hygromycin; lincomycin hydrochloride; monensin, sodium salt; neomycin sulfate; novobiocin, sodium salt; nystatin; oleandomycin, phosphate salt; oxytetracycline dihydrate; penicillin G, sodium salt; spectinomycin dihydrochloride; streptomycin sulfate; tylosin tartrate; virginiamycin. All antibiotics except bambermycin, fosfomycin and virginiamycin were purchased from Sigma, St. Louis, MO, USA. Bambermycin was obtained from Hoechst Pharmaceuticals, Somerville, NJ, USA, virginiamycin was obtained from Smith Kline and Beckman, Paoli, PA, USA. Fosfomycin was obtained from Merck, P.O. Box 2000, Rahway, NJ, USA.

Culture Maintenance and Preparation

Bacillus subtilis

Bacillus subtilis [American Type Culture Collection (ATCC) 6633] was prepared according to the procedures outlined in

the AOAC manual.[1] Spore suspensions were sub-divided into 2 ml aliquots ($\approx 6 \times 10^8$ viable spores per ml) and stored at 4 °C. Overlays were prepared by dilution of 0.5 ml of spore suspension with 4.5 ml of medium B. Five ml of diluted spore suspension were added per 100 ml of molten medium C.

Saccharomyces cerevisiae

Saccharomyces cerevisiae (ATCC 9763) was prepared according to the procedures outlined in the AOAC manual.[1] A fresh culture was used each day to prepare overlays. For the overlays, a fresh broth culture was diluted with medium D to 70% transmission at 660 nm in a Spectronic 20 spectrophotometer (Fisher Scientific). Four millilitres of this culture was added per 100 ml of molten medium E.

Electrophoretic Gels

Two hundred ml of agarose–Tris–succinate buffer at either pH 6.0 or 8.0 (see Reagents section) was dispensed onto the top support shelf of a Nunc cell factory [Laboratory Disposable Products (Springfield, NJ, USA); Fig 1]. Air bubbles were removed by flaming with a bunsen burner and the agarose was allowed to solidify on a levelling table. After solidifying, 950 ml of a 30% solution of antifreeze, coolant and water was dispensed into the bottom chamber of the cell factory. The gel was cooled to 4 °C in a refrigerator and stored until use.

Electrophoresis

Equivalent volumes (about 750 ml) of a solution of Tris–succinate buffer at 4 °C was dispensed into each buffer trough
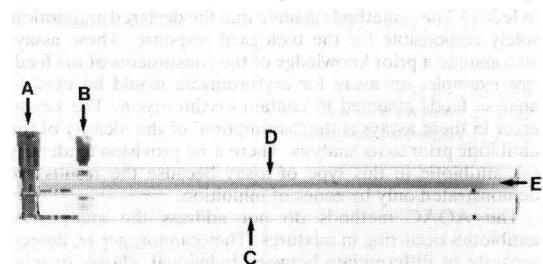
Fig. 1 Side view of a Nunc cell factory containing an agarose gel layer. A, Coolant outlet; B, coolant inlet; C, cooling chamber; D, agarose layer; and E, support shelf
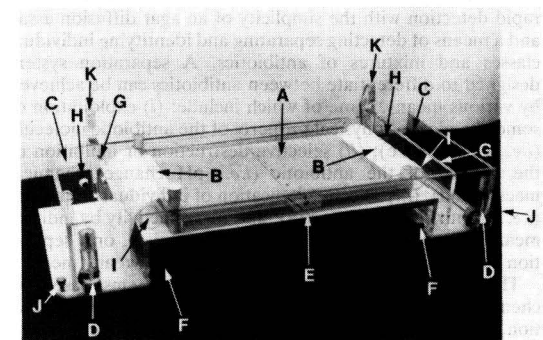
Fig. 2 Corner view of electrophoretic chamber (base) containing Nunc cell factory, paper wicks and wick supports. A, Nunc cell factory; B, paper wicks; C, buffer troughs; D, electrodes; E, cell factory support; F, trough connector; G, trough baffle; H, trough outlet (to pump); I, wick support; J, levelling screw; and K, cover support
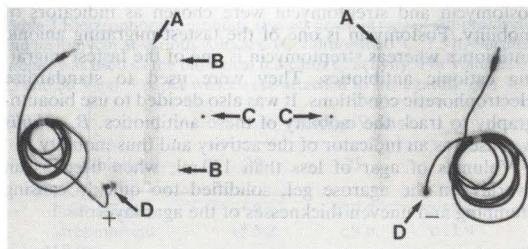
Fig. 3 Top view of cover for electrophoretic chamber with electrode wire leads. A, Vacuum ports; B, inlet and outlet ports; C, air vent controls; and D, electrode wire leads
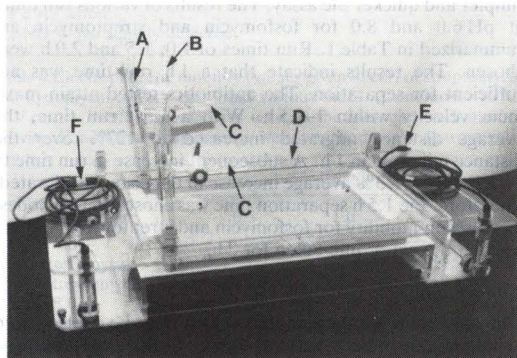
Fig. 4 Corner view of electrophoretic chamber with cover and cooling connector valves. A, Inlet connector valve; B, outlet connector valve; C, purge valve; D, chamber cover; E, cathode wire lead; and F, anode wire lead

in the electrophoresis chamber (Fig. 2). A circulating pump [Master Flex variable speed pump, Cole Parmer (Chicago, IL, USA)] connected to both buffer troughs was used to recirculate electrolyte (about 10 rev min⁻¹). A cell factory containing agarose–Tris–succinate gel at the appropriate pH was placed on the gel support between the two buffer troughs. Two glass wick supports, one at each end of the cell factory, were also placed on the gel support. Four mm wells were then punched into the centre of the gel about 2.5 cm apart with a gel punch [Bio-Rad Laboratories (Richmond, CA, USA)]. Twenty microlitres of sample to be assayed was pipetted into each well. To track the migration from the origin and current flow an indicator dye (Bromocresol Green, 10% solution) was pipetted into the centre well for each determination. Paper wicks [15.25 × 14 cm (6 × 5½ in) Whatman filter paper No. 3] were soaked in buffer and placed about 1 cm from each end of the gel, on top of the wick support and into the buffer trough.

The chamber cover (Fig. 3) was placed on top of the electrophoretic chamber that connected the buffer troughs to a computer controlled power supply (Bio-Rad Laboratories). To remove excess condensate, the cover was also connected to a vacuum line *via* rubber tubing and a liquid trap.

The cooling chamber of the cell factory was connected to a refrigerated water circulator (Bio-Rad Laboratories) *via* an inlet and outlet valve (Fig. 4). The circulator was brought to the appropriate temperature, the air purged from the coolant lines and the feed and return valves opened. The coolant was allowed to circulate until the appropriate gel temperature was achieved. The chamber was connected to the power supply and a constant voltage applied to the gel for the specified time.

Bioautography

After electrophoresis, the cell factories were removed from the electrophoresis chamber, the coolant was poured out of the bottom chamber and water at 50 °C was dispensed into the bottom chamber. The gel was allowed to reach 48 °C. The cell factory was then placed on a level table and 150 ml of the appropriate inoculated medium (see Culture Maintenance and Preparation Section) was poured over the top of the agarose layer and allowed to solidify. The water in the bottom layer was poured out of the bottom chamber, the plate was covered and incubated at the appropriate temperature for 18 h (or overnight).

Mobility was demonstrated by measuring the location of the zones of inhibition. The distance from the origin to the beginning of the zone, plus one half the diameter, along with the position of the zone was recorded.

Electroendoosmosis

Twenty microlitres of a 5 mg ml⁻¹ aqueous solution of L-proline was pipetted into each well of a cell factory and assayed electrophoretically under the appropriate conditions. A methanol solution of 1% ninhydrin was then pipetted into each well and along each lane of the gel. These gels were warmed for 1 h by filling the bottom chamber of the cell factory with 48 °C water. A yellow colour appeared where there was a presence of L-proline. L-Proline was assayed in each position five times and the results were averaged.

Results and Discussion

Design of Electrophoretic Equipment

Gel matrix and support

Many types of gel matrices have been described for use in electrophoresis; some of which are better suited than others for specific applications. Polyacrylamide and starch gels are more suitable for protein separations whereas agar and agarose are typically used for the separation of smaller molecules. Therefore, it is imperative to use a gel that has a consistent composition (batch-to-batch) and lacks interfering components.

The amount of agarose typically used in these types of gels ranges from 1 to 2%.[6,16–20,24–30,32–35] However, a 1% concentration was chosen in this system to minimize any residual electroendoosmotic effects and allow easier spreading. Concentrations of greater than 1% led to stiffer gels that had a tendency to clump and solidify before a uniform layer could be spread. Concentrations of less than 1% led to softer gels that accumulated water during electrophoresis and the results were not reproducible. The amount of prepared agarose used per plate was 200 ml, which gave a gel 4 mm in thickness. Volumes less than this generally led to clumping and uneven gels.

Cooling is one of the major problems in electrophoresis. Uneven cooling can lead to poor separations. Therefore, a means to consistently cool gel layers during electrophoresis is of primary importance. Nunc cell factories, which are usually used for the proliferation of tissue/cell cultures, were selected as cooling chambers. A side view of a cell factory loaded with agarose gel prior to electrophoresis is shown in Fig. 1. It consists of a sealed chamber with inlet (A) and outlet (B) valves and a 1 cm lip on top of the chamber. The top part of the chamber and the top lip can be used as a dish to support the gel layer. It is also level from one end to the other to allow pouring of a gel layer that is flat and of uniform thickness. The chamber normally used for growing tissue culture can be filled with antifreeze and the inlet and outlet valves connected to a chiller/recirculator, which will circulate coolant, at constant temperature, to the chamber and ultimately cool the gel layer.

Electrophoretic chamber

It was necessary to design a chamber in which the electrophoresis could be performed. This chamber is shown in Fig. 2. It consists of: a shelf (E), which will support the cell factory/agarose gel; and two buffer troughs (C); which contain

baffles (G) and platinum wire electrodes (D). These troughs were situated at either end of the shelf with enough space to allow the placement of wick supports (I). To eliminate suction effects, a tube (F) was placed between the troughs connecting them and levelling screws (J) were placed on the base. Electrolyte gradients were also eliminated by connecting trough outlets (H) with tygon tubing to a pump circulating electrolyte between troughs. The height of the support shelf and the outside of the electrophoretic chamber were adjusted to accommodate the connection of the troughs and the agarose gel with paper wicks (B). Finally, supports (K) for the cover were placed opposite the electrodes preventing motion.

bThe cover for the chamber is seen in Fig. 3. It is designed to cover the distance between the buffer troughs completely. It has two ports (B) that fit over the inlet and outlet that connect the cell factory to the chiller/recirculator. It also has two vacuum ports (A) for the removal of moisture and any gas generated during electrophoresis. These vacuum ports are connected to a vacuum trap *via* rubber tubing. To control air flow into and ultimately out of the chamber, two air vent controls (C) are placed in the centre of the cover. Finally, two wire leads (D) with female to male connectors were attached to the lid, the female connectors mated exactly with the male connectors on the chamber. Connection to a power pack is made *via* these leads. Orientation of the poles can be in either direction.

It was also necessary to develop a valve system to connect the cell factory to the chiller/recirculator. This was accomplished by a loop of tygon tubing with branch points. Each branch point carried coolant to and from the electrophoretic chamber. This tubing was connected (Fig. 4) to an inlet connector valve (A), which had a bypass valve (C) to purge any air before it could enter the coolant chamber of the cell factory. The outlet connector valve (B) was connected to tubing that returned the coolant to the chiller/recirculator. It also has a purge valve (C) to remove unwanted air from the system.

Electrophoretic Conditions

In order to obtain consistent results from each electrophoretic separation, it was necessary to standardize the system. Each parameter had to be examined to maximize resolution and maintain consistency.

Before such parameters were examined, it was necessary to determine the type of electrolyte to be used. This electrolyte would be used in the aqueous as well as the solid phase of the system and would be selected such that any background interference would be minimized. For this reason citrate (divalent cation chelator) and phosphate (cation chelator and antibiotic uptake inhibitor) buffers were eliminated as electrolyes.[37,38] Smither and Vaughan[35] developed a system that utilized Tris–succinate at pH 6.0 and 8.0 to separate antibiotics in agar and agarose gel and which had no background interference. Therefore, Tris–succinate was the electrolyte of choice. It is also important to determine mobility as related to pH as Smither and Vaughan[35] have demonstrated. The pH values chosen, 6.0 and 8.0, were sufficiently spread to allow differentiation between the antibiotics and still lie in the range of biological activity.

The best means of applying the sample to the gel had to be determined. It was apparent that a well should be used as a reservoir for the sample. This would minimize spreading and the diffusion of the antibiotic into the gel. The well size should be sufficiently small not to affect migration but large enough to hold a concentration of antibiotic that could be detected. A well size of 4 mm was chosen. Sensitivity and reproducibility problems were seen with smaller well sizes. Well sizes of larger than 4 mm resulted in migration and reproducibility problems.

Finally, it was necessary to select a marker that could be used to determine maximum migration. The antibiotics

fosfomycin and streptomycin were chosen as indicators of mobility. Fosfomycin is one of the fastest migrating anionic antibiotics whereas streptomycin is one of the fastest migrating cationic antibiotics. They were used to standardize electrophoretic conditions. It was also decided to use bioautography to track the mobility of these anitibiotics. *B. subtilis* was used as an indicator of the activity and thus mobility.

Volumes of agar of less than 150 ml, when used as an overlay on the agarose gel, solidified too quickly causing clumping and uneven thicknesses of the agar layer.

Time

Run time was studied under the premise that this system should be simple and rapid. Thus, the faster the run time the simpler and quicker the assay. The results of various run times at pH 6.0 and 8.0 for fosfomycin and streptomycin are summarized in Table 1. Run times of 1.0, 1.5 and 2.0 h were chosen. The results indicate that a 1 h run time was not sufficient for separation. The antibiotics tested attain maximum velocity within 1–1.5 h. With a 1.5 h run time, the average distance migrated increased to 127% over the distance migrated in 1 h. A subsequent increase in run time to 2 h led only to a 3% average increase in the distance migrated. Therefore, the 1.5 h separation time was chosen as the modest increases in mobility for fosfomycin and streptomycin did not warrant the extra time taken for 2 h.

Temperature

Temperature is another parameter that must be controlled to maintain consistency and accuracy. Other workers have indicated that a temperature range of 10 to 20 °C should be maintained during electrophoresis.[26–35] With modern temperature controllers, it is easier to regulate the system temperature. Therefore, a narrower range of temperature can be maintained, resulting in increased accuracy and reproducibility.

The results of electrophoresis performed on fosfomycin and streptomycin at 10, 15 and 20 °C are summarized in Table 2. Overall a 1 °C increase in temperature resulted in an increase

Table 1 Electrophoretic mobility (values given in cm) of streptomycin and fosfomycin at various times. (Conditions: 20 V cm^{-1}, 10 °C. *Bacillus subtilis* was used as the biological indicator of activity)

	Time/h		
Antibiotic	1.0	1.5	2.0
pH 6.0—			
Fosfomycin	a* 3.2	a 7.1	a 73
Streptomycin	c‡ 2.7	c 5.2	c 5.6
pH 8.0—			
Fosfomycin	a 4.5	a 10.4	a 10.6
Streptomycin	c 3.3	c 5.8	c 6.0

* a = Anion.
‡ c = Cation.

Table 2 Electrophoretic mobility (values given in cm) of streptomycin and fosfomycin at various temperatures. (Conditions: 20 V cm^{-1}, 1.5 h *Bacillus subtilis* was used as the biological indicator of activity)

	Temperature/°C		
Antibiotic	10	15	20
pH 6.0—			
Fosfomycin	a* 7.1	a 7.9	a 8.6
Streptomycin	c† 5.2	c 5.7	c 6.3
pH 8.0—			
Fosfomycin	a 10.4	a 11.1	a 12.3
Streptomycin	c 5.8	c 6.5	c 7.2

* a = Anion.
† c = Cation.

Table 3 Electrophoretic mobility (values given in cm) of streptomycin and fosfomycin at various voltages. (Conditions: 10 °C, 1.5 h. *Bacillus subtilis* was used as the biological indicator of activity. For voltages of 25 and 30 V cm⁻¹ paper wicks were attached to the agarose gel)

	Voltage/V cm⁻¹		
Antibiotic	20	25	30
pH 6.0—			
Fosfomycin	a* 7.1	a 10.2	a 13.6
Streptomycin	c† 5.2	c 9.6	c 13.9
pH 8.0—			
Fosfomycin	a 10.4	ND‡	ND
Streptomycin	c 5.8	c 11.0	ND

* a = Anion.
† c = Cation.
‡ ND = No activity detected.

Table 4 Electrophoretic mobility (values given in cm) of streptomycin and fosfomycin at 25 V cm⁻¹ and various times. (Conditions: 10 °C, 25 V cm⁻¹. *Bacillus subtilis* was used as the biological indicator of activity. For all times paper wicks were attached to the agarose gel)

	Time/h		
Antibiotic	0.5	1.0	1.5
pH 6.0—			
Fosfomycin	a* 5.0	a 7.5	a 10.2
Streptomycin	c† 4.8	c 7.2	c 9.6
pH 8.0—			
Forfomycin	a 7.5	a 11.1	ND‡
Streptomycin	c 5.0	c 7.6	c 11.0

* a = Anion.
† c = Cation.
‡ ND = No activity detected.

in mobility of 2.1% at pH 6.0 and 1.8% at pH 8.0 for fosfomycin. With streptomycin, a 2.1% increase was seen at pH 6.0. At pH 8.0 there was a 2.4% increase in mobility. However, for streptomycin at both pH 6.0 and 8.0, tailing was observed with increases in temperature. At 15 °C a 1.0 cm tail and at 20 °C a 2.5 cm tail was observed. The results indicate that although there is enhanced separation at increased temperatures tailing also increases. Therefore, it would be best to run separations at 10 °C.

Voltage

The voltage used per centimetre of gel (the driving force) is another parameter that will affect the mobility and accuracy of the system. It is very important to use a power source that can provide constant current. Lightbown and de Rossi[32] and Smither and Vaughan[35] suggested votlages of between 20 and 30 V cm⁻¹.

The results of electrophoresis performed on fosfomycin and streptomycin at 20, 25 and 30 V cm⁻¹ are summarized in Table 3 and the results of electrophoresis of fosfomycin and streptomycin at 25 V cm⁻¹ at 0.5, 1.0 and 1.5 h are shown in Table 4. The data indicated that 20 V cm⁻¹ was the maximum voltage that should be used with this system. At voltages of 25 and 30 V cm⁻¹ the paper wicks adhered to the agarose gel making them difficult to remove. It must also be kept in mind that any increase in voltage will result in a quadratic increase in the heat generated. Thus, the lower the voltage the easier it is to regulate cooling.

Electroendoosmosis

When designing any electrophoretic separation system, it is important to consider the effects that electroendoosmosis will have on the migration of an ion. Typically, electroendoosmosis will cause a shift in migration towards the cathode; the

Table 5 Electrophoretic mobility of selected antibiotics. (Conditions: 1.5 h, 20 V cm⁻¹, 10 °C. *Bacillus subtilis* was used as the biological indicator for all antibiotics except nystatin; *Saccharomyces cerevisiae* was the biological indicator for nystatin. Mobility of each antibiotic was adjusted for electroendoosmotic drift)

		Mobility/cm	
Antibiotic	Class	pH 6.0	pH 8.0
Erythromycin	Macrolide	c* 2.5	c 3.1
Oleandomycin	Macrolide	c 2.5	c 3.0
Tylosin	Macrolide	c 1.2	c 1.3
Hygromycin b	Aminoglycoside	c 5.2	c 5.0
Neomycin	Aminoglycoside	c 5.5	c 5.5
Streptomycin	Aminoglycoside	c 5.2	c 5.8
Lincomycin	Aminoglycoside-like	c 3.0	c 2.6
Spectinomycin	Aminoglycoside-like	c 6.0	c 5.0
Chlortetracycline	Tetracycline	c 1.6	a† 1.5
Oxytetracycline	Tetracycline	c 1.3	a 1.3
Bacitracin	Peptide	c 1.6	a 0.5
Virginiamycins	Peptide-like	c 1.3	a 2.3/a 0.8
Bambermycins	Moenocinol	a 3.8/a 2.4	a 2.3/a 1.6
Monensin	Polyether	a 1.4	a 1.3
Novobiocin	Quinone	a 1.4	a 2.4
Nystatin	Polyene	c 0.6	c 0.6
Penicillin G	β-Lactam	a 2.7	a 3.8

* c = Cation.
† a = Anion.

extent of which is a property of the support matrix. Electroendoosmosis was monitored at both pH 6.0 and 8.0 utilizing L-proline as the migrating ion and ninhydrin as the indicator of mobility. These results indicate slight migration (0.2 cm) toward the cathode at both pH 6.0 and 8.0. Electroendoosmotic effects were the same at both pHs. Although this migration is negligible, 0.2 cm should be used as a correction factor, when determining the exact mobilities of antibiotics. Correction factors should be determined using the individual apparatus.

Electrophoretic Mobility of Antibiotics

The results of the electrophoretic mobilities of the 17 antibiotics tested are given in Table 5. The macrolide antibiotics (erythromycin, oleandomycin and tylosin) migrated as cations. Erythromycin and oleandomycin migrated the furthest and showed similar mobilities at both pH 6.0 and 8.0. These two antibiotics also demonstrated an increase in mobility with an increase in pH.

The aminoglycoside class of antibiotics (hygromycin B, neomycin and streptomycin) migrated as cations and have similar mobilities. At pH 6.0, neomycin migrated the furthest of these antibiotics, to 5.5 cm. At pH 8.0, however, streptomycin migrated the furthest with an increase in mobility to 5.8 cm, followed by neomycin, which had no enhancement of mobility, and hygromycin B, which showed a decrease of mobility to 5.0 cm.

The aminoglycoside-like class of antibiotics (lincomycin and spectinomycin) also migrated as cations with lincomycin migrating 3.0 cm and spectinomycin 6.0 cm, at pH 6.0. Both antibiotics demonstrated a decrease in mobility with increasing pH.

The tetracycline class of antibiotics (chlortetracycline and oxytetracycline) migrated as cations at pH 6.0, with chlortetracycline being the fastest of the two antibiotics. At pH 8.0, however, these two antibiotics reversed direction and migrated as anions with chlortetracycline being the faster of the two antibiotics.

The peptide and peptide-like antibiotics (bacitracin and virginiamycin) migrated toward the cathode at pH 6.0; bacitracin migrated the furthest. With a change in pH, both of
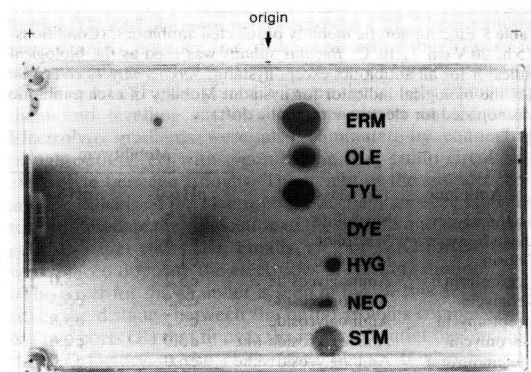
Fig. 5 Top view of a pH 6.0 agarose gel containing an indicator dye and various antibiotics after electrophoresis and bioautography. ERM, Erythromycin; OLE, oleandomycin; TYL, tylosin; HYG, hygromycin B; NEO, neomycin; and STM, streptomycin. *Bacillus subtilis* was used as the biological indicator

Fig. 6 Top view of a pH 8.0 agarose gel containing an indicator dye and various antibiotics after electrophoresis and bioautography. ERM, Erythromycin; OLE, oleandomycin; TYL, tylosin; HYG, hygromycin B; NEO, neomycin; and STM, streptomycin. *Bacillus subtilis* was used as the biological indicator
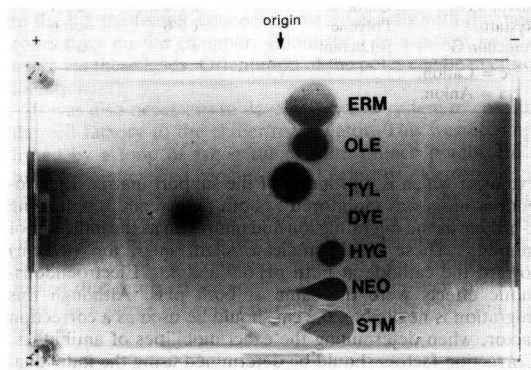
Table 6 Selected electrophoretic conditions for the separation of antibiotics. (Conditions were selected that will maximize separation while maintaining efficiency)

Parameter	Condition
Time	1.5 h
Temperature	10 °C
Voltage	20 V cm^{-1}
Electrolyte	Tris–succinate; pH 6.0 and 8.0
Matrix	Agarose; 1.0%
Matrix thickness	4 mm; 200 ml per dish
Sample volume	40 µl
Sample receptable	Well; 4 mm
Overlay thickness	3 mm; 150 ml per dish

Figs. 5 and 6, respectively. Also demonstrated are the enhancements in zone size with increasing pH.

Conclusion

The conditions that maximize separation of antibiotics while maintaining efficiency are summarized in Table 6. This system represents an efficient and easy to perform method for the separation and identification of classes of antibiotics and, in some cases, individual antibiotics of the same class.

This system eliminates the insensitivity, overloading, streaking and antibiotic diffusion problems associated with chromatography and paper electrophoresis. It has the ability to separate and characterize antibiotics that are usually affected by harsh conditions (drying, solvent exposure, *etc.*). Agar diffusion assays currently in use for antibiotic testing can be adapted to this system. This system has been used for the quantitative and qualitative analysis of 17 antibiotics used in animal feeds.[39] Finally, elements of this system are disposable, Nunc cell factories make gel handling very easy and assay plates can be disposed of like any other disposable bioassay dish.

these antibiotics acted as anions with virginiamycins migrating the furthest. Virginiamycins at this pH also separates into two components, both of which migrated further than bacitracin.

The peptide-like antibiotics (bacitracin and virginiamycins) migrated toward the cathode at pH 6.0; bacitracin migrated the furthest. With a change in pH, both of these antibiotics acted as anions with virginiamycins migrating the furthest. Virginiamycins at this pH also separates into two components, both of which migrated further than bacitracin.

Also summarized in Table 5 are the electrophoretic mobilities of the miscellaneous class of antibiotics. Bambermycin demonstrated two components at both pH 6.0 and 8.0. Both components migrated toward the anode and demonstrated a decrease in mobility with an increase in pH. Monensin acted as an anion and migrated toward the anode. The distance migrated decreased slightly with an increase in pH. Novobiocin also acted as an anion by migrating to the anode. Unlike monensin, it demonstrated an increase in mobility when the pH was raised to 8.0. Nystatin exhibited some slight cationic activity and did not demonstrate any difference in migration from one pH to another. Penicillin G migrated towards the anode at both pH 6.0 and 8.0. It displayed an increase in mobility with an increase in pH.

Examples of the typical biological responses seen after electrophoresis and bioautography for the macrolide and aminoglycoside antibiotics at pH 6.0 and 8.0 are shown in

References

1 *Official Methods of Analysis of the Association of Official Analytical Chemists*, ed. William, S., 15th edn., Association of Official Analytical Chemists, Arlington, VA, 1990, sect. 957.23-975.61.
2 Betina, V., *Nature (London)*, 1958, **182**, 796.
3 Betina, V., *J. Chromatogr.*, 1964, **15**, 379.
4 Betina, V., in *Methods in Enzymology*, ed. Hash, J. H., Academic, New York, 1975, vol. 43, pp. 101–172.
5 Betina, V., and Nemec, P., *Nature (London)*, 1960, **187**, 1111.
6 Goodall, R. R., and Levi, A. A., *Nature (London)*, 1946, **158**, 675.
7 Macek, K., in *Chromatography: A Laboratory Handbook of Chromatographic and Electrophoretic Methods*, ed. Heftmann, E., 3rd edn., Van Nostrand Reinhold, New York, 1975, pp. 139–163.
8 Wagman, G. H., and Bailey, J. V., *J. Chromatogr.*, 1969, **41**, 263.
9 Wagman, G. H., and Weinstein, M. J., *Chromatography of Antibiotics*, Elsevier, New York, 1973, pp. 23–405.
10 Wagman, G. H., and Weinstein, M. J., *Chromatography of Antibiotics*, 2nd edn., Elsevier, New York, 1984, pp. 23–504.
11 Aszalos, A., Davis, S., and Frost, D., *J. Chromatogr.*, 1968, **37**, 487.
12 Aszalos, A., and Frost, D., in *Methods in Enzymology*, ed. Hash, J. H., Academic, New York, 1968, vol. 18, 172–213.
13 Betina, V., *J. Antibiot. Ser. A*, 1964, **17**, 127.
14 Ikekawa, T., Iwami, F., Akita, E., and Umezawa, H., *J. Antibiot. Ser. A*, 1963, **16**, 56.
15 Ito, Y., Namba, M., Nagahama, N., Yamaguchi, T., and Okuda, T., *J. Antibiot., Ser. A*, 1964, **17**, 218.

16 Stahl, E., in *Chromatography: A Laboratory Handbook of Chromatographic and Electrophoretic Methods*, ed. Heftmann, E., 3rd edn., Van Nostrand Reinhold, New York, 1975, pp. 164–188.

17 Synder, L. R., in *Chromatography: A Laboratory Handbook of Chromatographic and Electrophoretic Methods*, ed. Heftmann, E., 3rd edn., Van Nostrand Reinhold, New York, 1975, pp. 46–76.

18 Salisbury, C. D. C., Rigby, C. E., and Chan, W., *J. Agric. Food Chem.*, 1989, **37**, 105.

19 Audubert, R., and de Mende, S., *The Principles of Electrophoresis*, Hutchinson, London, 1959, pp. 1–120.

20 Lederer, M., *An Introduction to Paper Electrophoresis and Related Methods*, Elsevier, New York, 1957, pp. 1–193.

21 Maede, K., Yagi, A., Naganawa, H., Kondo, S., and Umezawa, H., *J. Antibiot.*, 1969, **22**, 635.

22 Michl, H., in *Chromatography: A Laboratory Handbook of Chromatographic and Electrophoresis Methods*, ed. Heftmann, E., 3rd edn., Van Nostrand Reinhold, New York, 1975, pp. 282–311.

23 Salvatore, M. J., Jr., and Katz, S. E., *J. Assoc. Off. Anal. Chem.*, 1988, **71**, 1101.

24 Umezawa, H., and Kondo, S., in *Methods in Enzymology*, ed. Hash, J. H., Academic, New York, 1975, vol. 43, pp. 279–291.

25 Vondracek, M., in *Chromatography: A Laboratory Handbook of Chromatographic and Electrophoretic Methods*, ed. Heftmann, E., 3rd edn., Van Nostrand Reinhold, New York, 1975, pp. 815–840.

26 Freidlin, P. J., *Avian Dis.*, 1988, **32**, 370.

27 Giddings, J. C., in *Chromatography A Laboratory Handbook of Chromatographic and Electrophoretic Methods*, ed. Heftmann, E., 3rd edn., Van Nostrand Reinhold, New York, 1975, pp. 27–45.

28 Grynne, B., *Acta Pathol. Microbiol. Scand., Sect. B: Microbiol.*, 1973, **8**, 583.

29 Horng, H., and Ko, H., *Proc. Natl. Sci. Counc., Repub. China, Part 2*, 1977, **10**, 321.

30 Horng, C., Hsieh, J., Ko, H., Jan, R., and Li, J., *Proc. Natl. Sci. Counc., Repub. China*, 1979, **3**, 382.

31 Jorgenson, J. W., *Anal. Chem.*, 1986, **58**, 743A.

32 Lightbown, J. W., and de Rossi, P., *Analyst*, 1965, **90**, 89.

33 Lott, A. F., and Vaughan, D. R., *Soc. Appl. Bacteriol. Tech. Ser.*, 1983, **18**, 331.

34 Lott, A. F., Smither, R., and Vaughan, D. R., *J. Assoc. Off. Anal. Chem.*, 1985, **68**, 1018.

35 Smither, R., and Vaughan, D. R., *J. Appl. Bacteriol.*, 1978, **44**, 421.

36 Whitaker, J. R. in *Paper Chromatography and Electrophoresis*, ed. Zweig, G., and Whitaker, J. R., Academic, New York, 1967, vol. I, pp. 1–356.

37 Cassidy, P. J., 1990, personal communication.

38 Zimmerman, S. B., 1990, personal communication.

39 Salvatore, M. J., and Katz, S. E., *J. Assoc. Off. Anal. Chem.*, in the press.

Optical Characteristics of a Ruthenium(II) Complex Immobilized in a Silicone Rubber Film for Oxygen Measurement

Xiang-Ming Li, Fu-Chang Ruan and Kwok-Yin Wong
Department of Applied Biology and Chemical Technology, Hong Kong Polytechnic, Hong Kong

The optical characteristics of tris(4,7-diphenyl-1,10-phenanthroline)ruthenium(II) perchlorate immobilized in a silicone rubber film were studied for its application to the measurement of oxygen. The luminescence intensity and the degree of quenching of the ruthenium complex by oxygen were shown to be affected by the concentration of the complex in the silicone rubber film. The optimum concentration was found to be about 0.2 mmol dm^{-3}. At this concentration, the silicone rubber film containing the immobilized ruthenium complex emits the highest luminescence intensity and is able to undergo a high degree of quenching of the luminescence by oxygen. The quenching curves for 20 samples containing various concentrations of the ruthenium complex were correlated with high accuracy by using a modified form of the Stern–Volmer equation. The film preparation procedure and the solvent used were found to be critical for performance. The effect of the film thickness on the luminescence intensity and the dynamic response was also studied.

Keywords: *Optical sensing; oxygen; ruthenium complex; silicone rubber*

Oxygen concentration is one of the most frequently measured parameters in chemical, biological and biomedical systems. The Winkler titration has been adopted for the measurement of oxygen for many years and is considered, to some extent, to be the standard method.[1] However, the time-consuming and cumbersome nature of the titration has hindered its application to process monitoring. The Clark electrode[2] was considered to be a breakthrough as regards techniques for the measurement of oxygen. However, it is based on the reduction of oxygen at the cathode and the diffusion-limited passage of oxygen through the membrane. Any factor that can change the diffusion resistance, such as fouling of the membrane or a change in flow conditions in the testing fluid, could cause measurement error.[3,4] The development of new techniques for the measurement of oxygen has been a continuous process over the last decade. Techniques for optical sensing of oxygen, based on the quenching by oxygen of the luminescence of various chemicals, such as organic dyes,[5] polycyclic aromatic hydrocarbons[6–9] and transition metal complexes,[10–14] have been developed. Of the compounds studied, the transition metal complexes have the distinct advantages of a long excited-state lifetime and strong absorption in the visible region. Recent developments in optical oxygen sensors have been reviewed.[15] One of the advantages of using luminescent chemicals for optical sensing of oxygen is that the mechanism does not consume oxygen. Such a feature makes the technique immune to the interferences caused by changes in resistance during diffusion of oxygen into the probe. Another advantage of the optical sensing technique is that it can be miniaturized, as a consequence of the development of miniaturized optical fibre techniques, for *in vivo* measurement. The optical sensing technique also provides a means for application to the remote sensing of oxygen. The luminescent chemical can be placed at the location where the monitoring of oxygen is required, and the light source and light sensor can be placed in the visible range without physical contact with the luminescent chemical. A pressure-sensitive paint using platinum–porphyrin developed by Kavandi *et al.*[16] is one example of remote sensing. This paint can be used for continuous mapping of the surface pressure on aircraft or other aerodynamic surfaces. The underlying principle of the paint is that the change in pressure results in a change in oxygen level in the paint and also in the luminescence intensity of the platinum–porphyrin dissolved in a silicone resin.

In order to prevent the possibility of a reaction occurring between the luminescent chemical and the species in the measuring environment, the luminescent chemical should usually be immobilized in a matrix. Various studies[14,17] have shown that silicone rubber is a suitable matrix for the immobilization of luminescent transition metal complexes. The luminescence of the complex in the silicone rubber can be quenched by oxygen to a greater extent than in many other polymers. The successful development of optical sensors for in-contact or remote measurement of oxygen depends on an understanding of the optical characteristics of the luminescent chemicals immobilized in a suitable matrix. Demas and co-workers[11,13] have studied tris(4,7-diphenyl-1,10-phenanthroline)ruthenium(II) perchlorate as a sensing dye for oxygen sensors. They prepared the sensing film by soaking a silicone rubber film in a dichloromethane solution of the ruthenium complex.[11] In our study of the same complex as a sensing material it was found that the performance of the film is highly dependent on the method of preparation and on the concentration of the ruthenium complex in the polymer. This paper describes a detailed study of the optical characteristics of the tris(4,7-diphenyl-1,10-phenanthroline)ruthenium(II) complex immobilized in a silicone rubber film, which should provide useful information for the development of a sensing material for an optical oxygen sensor. In addition, a modified form of the Stern–Volmer equation proposed previously[14] was used to fit all the oxygen quenching data obtained in this work. The results showed that this three-parameter equation could be used to correlate the oxygen quenching data obtained for a transition metal complex immobilized in a silicone rubber film as the oxygen sensing material.

Experimental

Materials

The [Ru(Ph$_2$phen)$_3$](ClO$_4$)$_2$ (Ph$_2$phen = 4,7-diphenyl-1,10 phenanthroline) was synthesized and purified as described by Lin *et al.*[18] Potassium aquapentachlororuthenate(III) was obtained from Johnson Matthey. The ligand Ph$_2$phen was purchased from Aldrich. Silicon rubber (RTV 732) was purchased from VersoChem; it was a clear silicone rubber without a filler such as silica. All other chemicals were of analytical-reagent grade and were used without further purification. Oxygen and nitrogen (99.9%) were purchased from Hong Kong Oxygen.

Preparation of the Oxygen Sensing Films

The oxygen sensing film was made by immobilizing the ruthenium complex in the silicone rubber. Two solvents, ethanol and 1,2-dichloroethane, were used to prepare a

solution of the ruthenium complex in order to study the effect of the solvents on the optical characteristics of the films. The ruthenium complex concentrations were 0.05 mmol dm^{-3} in ethanol and 0.062 mmol dm^{-3} in 1,2-dichloroethane. The oxygen sensing films containing various concentrations of the ruthenium complex were made by mixing various amounts of the solutions with pre-polymerized silicone rubber. The number of moles of the ruthenium complex added was calculated by using the molar concentration of the solution, the mass of the solution added and the density of the solution. The mixture of solution and silicone rubber was cast into moulds to make films with various thicknesses coated on glass slides. The preparation method was similar to that described previously.[14] In order to control the film thickness, metal sheets of different thicknesses (0.1–0.5 mm) with central holes were placed on the top of the glass slides to form moulds. A small droplet of the paste-like mixture of solution and pre-polymer was placed in the central hole of the mould. The volume of the mixture added should be kept smaller than the void volume of the mould. Another piece of glass slide [with a poly(tetrafluoroethylene) (PTFE) film coating on its surface to prevent sticking] was placed on the top of the mould and pressed so that the paste became a uniform film in the mould. The final sensing film formed in the mould had the same thickness as the metal sheet without noticeable shrinking or expansion. The volume of the sensing film was calculated by dividing the mass of the film by its density, which was measured separately using a block of the same polymer. The concentration of the ruthenium complex in the sensing film was calculated by dividing the number of moles of the ruthenium complex added to make the film by the volume of the sensing film. As the solvent is removed after the silicone rubber is solidified, the final concentration of ruthenium complex in the film can be higher than that in the solution. The polymerization of the silicone rubber was retarded by preventing moisture from penetrating into the polymer film, because moisture served as the catalyst for the polymerization of the RTV silicone rubber. Keeping the duration of the polymerization process to about 48 h resulted in a satisfactory uniform distribution of the ruthenium complex in the polymer film, which was critical for obtaining consistent results. The film was evacuated under vacuum for 48 h to remove all solvent residues before use.

Instrumentation

The luminescence intensity measurements were conducted on a Perkin-Elmer LS-5 luminescence spectrometer coupled with a microcomputer. Two gas flow meters, individually calibrated by using a volumetric method, were utilized to measure the relative flow rates of oxygen and nitrogen.

Luminescence Intensity Measurement

Oxygen and nitrogen gases were mixed in a 1 m long tube and then fed into a flow cell in which the oxygen sensing film with the immobilized ruthenium complex was exposed to the mixed gas stream, and the glass slide was facing the excitation light in the spectrometer. By varying the relative flow rates of oxygen and nitrogen, a steady environment with various concentrations of oxygen could be maintained in the flow cell. The oxygen concentration (%) was calculated by dividing the oxygen flow rate by the sum of the oxygen and nitrogen flow rates. The luminescence intensities of the oxygen sensing films were measured using the spectrometer. All the samples were excited at 467 nm, which was the excited wavelength producing maximum emission intensity at 608 nm. All the emission intensities were measured at 608 nm and all the measurements were made at room temperature (25 ± 2 °C) and 101.325 kPa (1 atm).

Response Times of the Sensing Films

Response times of the sensing films were measured by switching the gas stream alternately between oxygen and nitrogen. The luminescence intensity over the whole time course of measurement was recorded by the computer. These data were processed subsequently and the response time was defined as the time taken for the luminescence intensity to change to 95% of the whole range of the change in the luminescence intensity when the sensing film was changed from a pure oxygen to a pure nitrogen environment.

Results and Discussion

An ideal oxygen sensing film based on the quenching of luminescence by oxygen should have the highest luminescence intensity in an environment without oxygen and have the lowest luminescence intensity in an environment of 100% oxygen. Such a feature of the sensing film would result in a high signal-to-noise ratio, which is critical for fabricating an oxygen sensor with high sensitivity and high accuracy, and at low cost. The luminescence intensities of the sensing films (thickness 0.2 mm) in an environment without oxygen, I_0, containing various concentrations of the ruthenium complex and prepared using different solvents are shown in Fig. 1. The solvent effect was significant. The films using ethanol showed a much higher luminescence intensity than those using 1,2-dichloroethane. There are two possible reasons for this 'solvent effect'. First, the solvent might affect the aggregation status of the counter ions of the ruthenium complex in the solvent because of the difference in solvent polarity. In a less polar environment, the complex would tend to form an ion pair with the counter ions, which might act as a quencher of the excited state of the metal complex. The aggregation status of the complex with its counter ions is fixed when the silicone rubber is solidified. The second reason for the 'solvent effect' might be that trace amounts of 1,2-dichloroethane are trapped in the polymer film during curing, which could cause heavy atom quenching of the fluorescence of the complex. The graph of luminescence intensity *versus* concentration of ruthenium complex showed a maximum at a concentration of about 0.2 mmol dm^{-3}. As the concentration increased beyond 0.25 mmol dm^{-3}, the luminescence intensity decreased, which suggested that self-quenching of the ruthenium complex might occur at high concentration levels. As the sensing films prepared using ethanol as solvent showed better performance than those using 1,2-dichloroethane, ethanol was selected as the solvent for the preparation of all the sensing films. All the results presented below are for those sensing films prepared using ethanol as solvent.

The ratio of the luminescence intensity, I_0/I_{100}, is plotted in Fig. 2 as a function of the concentration of the ruthenium complex in the silicone rubber film, where I_{100} denotes the
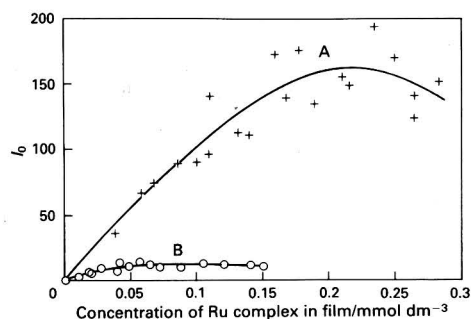

Fig. 1 Effects of solvent and ruthenium complex concentration on the apparent luminescence intensity of oxygen sensing films (film thickness: 0.2 mm). Solvents used: A, ethanol; and B, dichloroethane
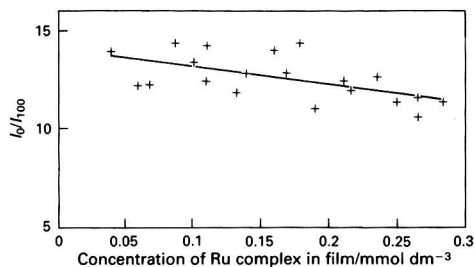
Fig. 2 Effects of ruthenium complex concentration on the oxygen quenching ratio (film thickness, 0.2 mm)

luminescence intensity in a 100% oxygen environment at 101.325 kPa (1 atm). This ratio represents the degree of quenching by oxygen of the luminescence of the ruthenium complex, which is directly related to the sensitivity of the sensing films to oxygen. As shown in Fig. 2, the ratio showed a moderate decrease as the concentration of the ruthenium complex increased. Considering both the intensity and the intensity ratio, the optimum concentration of the ruthenium complex in the silicone rubber film for oxygen sensing is about 0.2 mmol dm^{-3}.

It is well known that the Stern–Volmer plots of the oxygen quenching data for luminescent transition metal complexes in silicone rubber films are not linear.[11,14,17] In order to use the sensing films for the measurement of oxygen, a model should be utilized to correlate the luminescence intensity data with the oxygen concentration. A two-parameter model requires a minimum of two data points, which can only be used to correlate data having a linear relationship. A three-parameter model requires a minimum of three data points, which is the minimum requirement for a non-linear data set. In theory, any data curve can be fitted by using an equation with an infinite number of parameters. However, a good correlation using the minimum number of parameters could reduce the effort required to obtain the calibration data. A modified form of the Stern–Volmer equation, based on the kinetics of oxygen quenching and the solubility equation of oxygen in the polymer, has been proposed by Li and Wong[14] for correlating the luminescence intensity of a transition metal complex in a polymer with the oxygen concentration

$$I_0/I = 1 + Ap_{O_2} + Bp_{O_2}/(1 + bp_{O_2}) \quad (1)$$

where I_0 is the luminescence intensity of the sensing film in an environment without oxygen, I is the luminescence intensity of the sensing film exposed to an environment with an oxygen partial pressure of p_{O_2} (Pa) outside the polymer film, A and B are parameters combined with the kinetic constants of oxygen quenching and the parameters of the solubility equation, and b is a parameter in the solubility equation. Unlike the two-site model, it considers all the photoexcited molecules in the silicone-rubber film can be quenched by oxygen. Details of the theoretical analysis can be found elsewhere.[14] Twenty sets of oxygen quenching data for oxygen sensing films with various concentrations of ruthenium complex in silicone rubber were fitted by using the modified form of the Stern–Volmer equation, *i.e.*, eqn. (1). The standard deviations of the correlation are listed in Table 1. The maximum relative error, estimated by dividing the standard deviation by I_0/I_{100}, was 0.85%. Many of the relative errors were below 0.5%. Two of the quenching curves for the oxygen sensing films containing high and low ruthenium complex concentrations are shown in Fig. 3. The solid lines in Fig. 3 connecting the data points are the fitting curves obtained by using eqn. (1). The results demonstrate that eqn. (1) can be used for correlating the oxygen quenching data for a luminescent transition metal complex immobilized in a silicone rubber film and that this equation can serve as a calibration equation for oxygen

Table 1 Standard deviations of the correlation for oxygen sensing films

| No.	Concentration of ruthenium complex in films/ mmol dm^{-3}	I_0/I_{100}	Standard deviation
1	0.038	13.9	0.1182
2	0.058	12.2	0.0448
3	0.067	12.1	0.0493
4	0.086	14.3	0.0642
5	0.100	13.4	0.0357
6	0.109	12.4	0.0433
7	0.110	14.2	0.0537
8	0.131	11.8	0.0521
9	0.139	12.8	0.0391
10	0.158	14.0	0.0454
11	0.167	12.9	0.0611
12	0.177	14.4	0.0446
13	0.189	11.0	0.0376
14	0.210	12.4	0.0387
15	0.215	11.9	0.0364
16	0.234	12.6	0.0579
17	0.249	11.4	0.0362
18	0.264	11.5	0.0618
19	0.264	10.6	0.0263
20	0.283	11.4	0.0484
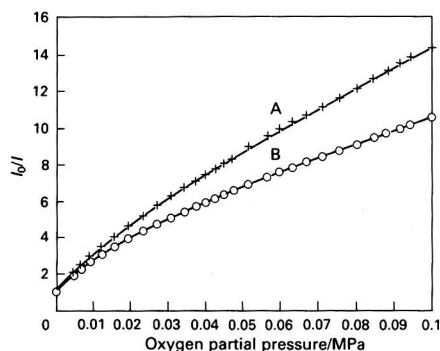
Fig. 3 Fitting of the oxygen quenching curves (film thickness: 0.2 mm). Concentration of complex in film: A, 0.086; and B, 0.264 mmol dm^{-3}
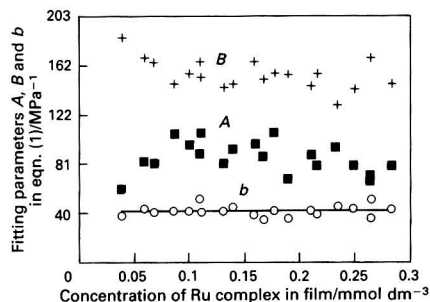

Fig. 4 Fitting parameters of the modified Stern–Volmer equation [eqn. (1)]. Mean values of $b = 4.17$

sensing devices using this type of sensing film. The parameters obtained by using a least-squares fitting algorithm for the fitting equations of all the samples are plotted in Fig. 4. The value for the parameter b in eqn. (1) is almost constant at 4.17, which is consistent with the theoretical analysis[14] that b is only affected by the solubility of oxygen in the silicone rubber film. The parameters A and B show a higher concentration dependence than parameter b. The concentration dependence of A and B is not explicitly included in the analysis, which
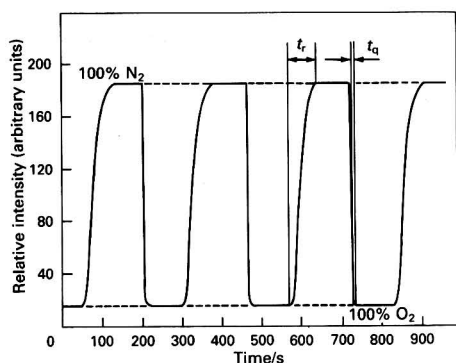
Fig. 5 Dynamic response of the luminescence intensity to a change in the oxygen concentration in the environment of an oxygen sensing film (film thickness: 0.2 mm; ruthenium complex concentration: 0.234 mmol dm^{-3})

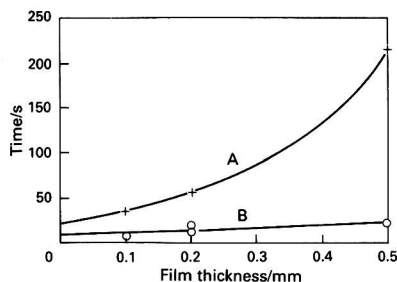**Fig. 6** Effect of the film thickness on the response time (ruthenium complex concentration: 0.149 mmol dm^{-3}). A, 95% recovery; and B, 95% quenching
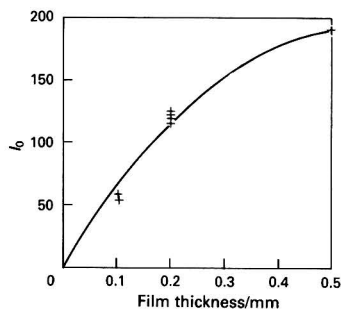

Fig. 7 Effect of the film thickness on the apparent luminescence intensity (ruthenium complex concentration: 0.149 mmol dm^{-3})

allows for further improvement of the theoretical model. However, such a shortcoming of the model does not hinder its application as an accurate calibration equation.

In addition to luminescence intensity and sensitivity, the dynamic response time is another important parameter for oxygen sensing. Different applications have different requirements for the response time. For example, the response time should be less than 1 s for pressure mapping. In contrast, a response time of the order of 1 min is satisfactory for the monitoring of aerobic cell cultures. In theory, a thinner film requires less time for the oxygen concentration inside the film to reach equilibrium with the environment outside the film. However, a thinner film would be expected to emit a lower

luminescence intensity when making comparative measurements at the same concentration level. The dynamic response of the luminescence intensity of an oxygen sensing film (thickness 0.2 mm) to a change in the oxygen concentration of the environment is shown in Fig. 5. The recovery time, t_r, is significantly longer than the quenching time, t_q, as shown in Fig. 5. This might be because the oxygen molecules are adsorbed in the silicone rubber matrix, and hence the adsorption process is faster than the desorption process. The effect of film thickness on the response time is shown in Fig. 6 and its effect on the apparent luminescence intensity is shown in Fig. 7. As the film thickness is increased, the apparent luminescence intensity is also increased; this can be explained by the fact that more of the luminescent complex is presented to the path of the light beam in a thicker film. However, the luminescence intensity is not directly proportional to the film thickness. As the film thickness is increased to 0.5 mm, the magnitude of the increase in the luminescence intensity decreases, as the silicone rubber is able to reflect and absorb part of the excitation and emission light. The selection of film thickness in a specific application should be a compromise between the luminescence intensity and the response time.

References

1   Skoog, D. A., West, D. M., and Holler, F. J., *Fundamentals of Analytical Chemistry*, Saunders, Philadelphia, 5th edn., 1988, p. 344.
2   Clark, L. C., *US Pat.*, 2 913 386, 1959.
3   Li, X. M., and Wang, H. Y., in *Transient D.O. Measurement Using a Computerized Membrane Electrode. Horizons of Biochemical Engineering*, ed. Aiba, S., University of Tokyo Press, Tokyo, 1987, p. 213.
4   Li, X. M., and Wang, H. Y., *US Pat.*, 4 921 582, 1990.
5   Gehrich, J. L., Lubbers, D. W., Opitz, N., Hansmann, D. R., Miller, W. W., Tusa, J. K., and Yafuso, M., *IEEE Trans. Biomed. Eng.*, 1986, **BME-33** (2), 117.
6   Grishaeva, T. I., and Zakharov, A. I., *Zh. Anal. Khim.*, 1990, **45**, 1333.
7   Peterson, J. I., Fitzgerald, R. V., and Buckhold, D. K., *Anal. Chem.*, 1984, **56**, 62.
8   Kroneis, H. W., and Marsoner, H. J., *Sens. Actuators*, 1983, **4**, 587.
9   Optiz, N., Graf, H. J., and Lubbers, D. W., *Sens. Actuators*, 1988, **13**, 159.
10 Wolfbeis, O. S., Leiner, M. J. P., and Posch, H. E., *Mikrochim. Acta, Part III*, 1986, 359.
11 Bacon, J. R., and Demas, J. N., *Anal. Chem.*, 1987, **59**, 2780.
12 Wolfbeis, O. S., Weis, L., Leiner, M. J. P., and Ziegler, W. E., *Anal. Chem.*, 1988, **60**, 2028.
13 Carraway, E. R., Demas, J. N., DeGraff, B. A., and Bacon, J. R., *Anal. Chem.*, 1991, **63**, 337.
14 Li, X. M., and Wong, K. Y., *Anal. Chim. Acta*, 1992, **262**, 27.
15 Surgi, M. R., in *Applied Biosensors*, ed. Wise, D. L., Butterworth, Guildford, 1989, ch. 9.
16 Kavandi, J., Callis, J., Gouterman, M., Khalil, G., Wright, D., Green, E., Burns, D., and McLachlan, B., *Rev. Sci. Instrum.*, 1990, **61**, 3340.
17 Carraway, E. R., Ph.D. Dissertation, Univesity of Virgina, 1989.
18 Lin, C. T., Böttcher, W., Chou, M., Creutz, C., and Sutin, N., *J. Am. Chem. Soc.*, 1976, **98**, 6536.

Adsorptive Differential-pulse Voltammetric Determination of Trace Amounts of Ruthenium

R. Palaniappan and T. Ashok Kumar
Applications Development Laboratory, Electrochemical and Spectral Division, Elico Pvt. Ltd., B-90, Sanath Nagar Industrial Estate, Hyderabad-500 018, India

An electrochemical technique for the convenient determination of trace amounts of ruthenium was developed, based on the adsorptive accumulation of Ru^{II}–salicylaldehyde thiosemicarbazone on the surface of a hanging mercury drop electrode, followed by the reduction of the adsorbed complex during the cathodic scan. The adsorptive differential-pulse voltammetric curve exhibited a well-defined cathodic peak at −0.750 V *versus* a saturated calomel electrode. Cyclic voltammetry was used to characterize the interfacial and redox behaviour. The optimum analytical conditions for the determination of ruthenium, for the working range 5–80 ng cm^{-3}, were etablished. A statistical evaluation of the experimental results is reported. The method was applied to the determination of ruthenium in synthetic solutions of various compositions as well as in catalysts.

Keywords: *Adsorptive differential-pulse voltammetry; ruthenium determination; adsorptive wave; salicylaldehyde thiosemicarbazone*

Adsorptive voltammetry involves the preliminary adsorptive concentration of an electroactive complex on the surface of a hanging mercury drop electrode (HMDE) at a fixed potential more positive than the reduction potential of the complex, and subsequent measurement of the reduction peak of the adsorbed complex during the cathodic scan. The principles as well as some analytical applications of this method have been described by various workers.[1–8]

Several polarographic methods have been reported for the determination of trace amounts of ruthenium,[9–14] but neither their sensitivity or selectivity is very satisfactory. Because of the importance of ruthenium, a sensitive method is required for its reliable determination. In particular, the quantification of ruthenium at trace levels is desired for geological surveys, catalytic applications and material sciences.

In previous electrochemical studies[15–19] the polarographic properties of the ruthenium complex with salicylaldehyde thiosemicarbazone (SAT) were examined and it was found that the complex is adsorbed on mercury electrodes, after undergoing single-electron reduction. This adsorptive property of the ruthenium–SAT complex can be successfully utilized for the highly sensitive determination of ruthenium by adsorptive differential-pulse voltammetry (ADPV). The aim of the present study was to establish the optimum conditions for this determination and its applicability to real/synthetic sample analysis.

Experimental

Apparatus

Pulse polarographic and absorptive voltammetric measurements were performed with an Elico (Hyderabad, India) Model CL-90 instrument equipped with a Polarecord *x–y* recorder. The three-electrode system consisted of a dropping mercury electrode (DME) or HMDE, a platinum auxiliary electrode and a saturated calomel reference electrode.

Cyclic voltammetric measurements were carried out by using an EG&G Princeton Applied Research (Princeton, NJ, USA) Model 174A polarographic analyser in conjunction with a Metrohm (Herisau, Switzerland) 663 VA stand, operated in the HMDE mode. The pH measurements were carried out using an Elico digital pH meter (Model LI-120).

Materials and Reagents

Analytical-reagent grade chemicals and doubly distilled water were used throughout. Mercury metal (Merck, Darmstadt, Germany) of 99.8% purity was washed successively with 5% nitric acid, conductivity water and doubly distilled water under vacuum. Sodium perchlorate solution (1.0 mol dm^{-3}) was used as the supporting electrolyte. Walpole acetate buffers with pH values from 2.0 to 6.0 were prepared by mixing 0.1 to 1.0 mol dm^{-3} hydrochloric acid and 0.1 to 1.0 mol dm^{-3} sodium acetate, depending on the requirement.

A stock solution of Ru^{III} was prepared by dissolving RuCl$_3$.3H$_2$O (Arora Metthey, Calcutta, India) in the minimum volume of 1 mol dm^{-3} hydrochloric acid (approximately 0.01 mol dm^{-3}) and standardized by spectrophotometry.[20] An aliquot of this solution was diluted as required.

For the interference studies, solutions of other noble metals such as Pd^{II}, Rh^{III}, Ir^{III} and Pt^{II} in 1 mol dm^{-3} hydrochloric were prepared fresh as stock solutions from the analytical-reagent grade salts PdCl$_2$, RhCl$_3$.3H$_2$O, IrCl$_3$·3H$_2$O and PtCl$_2$ (Arora-Metthey), respectively. The stock solution of Pd^{II} was standardized gravimetrically by precipitation with dimethylglyoxime.[21] The Rh^{III} solution was also standardized gravimetrically by precipitation as the sulfide, followed by ignition to the oxide and then reduction to the metal in the presence of hydrogen.[21] The Ir^{III} solution was standardized with 2-mercaptobenzothiazole, and the Pt^{II} solution as described by Ayres and McCrory.[20,21] Osmium tetroxide (Aldrich, Milwaukee, WI, USA) was weighed carefully in an ampoule and dissolved in 0.5 mol dm^{-3} sodium hydroxide, and the solution was neutralized with sulfuric acid and diluted to a known volume before being standardized by titrimetry.[20]

Salicylaldehyde thiosemicarbazone (m.p. 235 °C) was prepared by the method of Sah and Daniels.[22] A stock solution of SAT (0.01 mol dm^{-3}) was prepared in 96% ethanol.

General Procedure

To a 50 cm^3 calibrated flask, an appropriate volume of ruthenium solution to yield a final concentration of ruthenium between 5.0×10^{-8} and 8.0×10^{-7} mol dm^{-3} (5–80 ng cm^{-3}) was placed. The pH of the solution was adjusted to 4.5 with 10 cm^3 of 2.5 mol dm^{-3} acetate buffer, and 5 cm^3 of 0.01 mol dm^{-3} ethanolic SAT solution and 10 cm^3 of 1.0 mol dm^{-3} sodium perchlorate were added. The solution was made up to 50 cm^3 with water and placed in a voltammetric cell. After 10
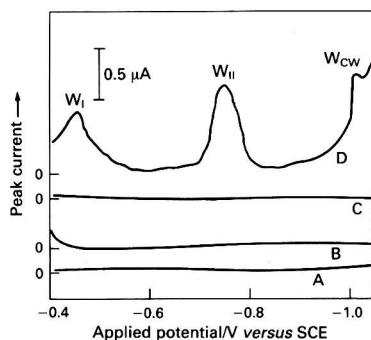
Fig. 1 Differential-pulse polarograms of the Ru^{III}–SAT system. A, 0.5 mol dm^{-3} acetate buffer and 0.2 mol dm^{-3} $NaClO_4$ at pH 4.5; B, A plus 5.0×10^{-5} mol dm^{-3} Ru^{III}; C, A plus 1.0×10^{-3} mol dm^{-3} SAT; and D; C plus 5.0×10^{-5} mol dm^{-3} Ru^{III} under the following conditions: drop time, 1 s; potential sweep rate, 6 mV s^{-1}; and pulse modulation amplitude, -50 mV. W_I and W_{II} are the first and second reduction waves, whereas W_{CW} is a catalytic wave

min de-aeration with no voltage applied, ruthenium was accumulated on the HMDE at -0.540 V for a period of 90 s from a stirred solution. The stirring was then stopped and after 15 s the ADPV curve was recorded over the potential range from -0.540 to -0.850 V under the following instrumental conditions: pulse amplitude, 50 mV; scan rate, 12 mV s^{-1}; and sensitivity, 0.1 μA V^{-1}. The peak for ruthenium was measured at about -0.750 V.

Procedure for the Analysis of Ruthenium Catalysts

Catalyst (0.1 ± 0.0001 g) was accurately weighed into a poly(tetrafluoroethylene) (PTFE) dish. Approximately 10 cm^3 of water, 2 cm^3 of conc. sulfuric acid and an excess of hydrofluoric acid (49%), to remove silicon if present, were added. The contents of the dish were evaporated to dryness on a hot-plate. On cooling, water and conc. hydrochloric acid were added to the residue in the dish so that the final solution would be 10% in hydrochloric acid. The contents of the dish were then heated until dissolution was complete; the solution was cooled, transferred into a 50 cm^3 calibrated flask and brought to volume with water. Diluted sample solutions were treated as described under the General Procedure.

Results and Discussion

Polarographic and Cyclic Voltammetric Study of the Complex

The DP polarograms for 5.0×10^{-5} mol dm^{-3} Ru^{III} with 1.0×10^{-3} mol dm^{-3} SAT in 0.5 mol dm^{-3} acetate buffer (pH 4.5) containing 0.2 mol dm^{-3} sodium perchlorate, under DME conditions, are shown in Fig. 1 (D). The polarogram of the solution, including either ruthenium (B) or SAT (C), was almost the same as that of the acetate buffer solution (A). Neither the reduction wave of Ru^{III} nor that of SAT was observed in the potential window studied here.

Two waves for the reduction of Ru^{III} appear at -0.450 V (W_I) and -0.750 V (W_{II}) apart from the catalytic wave (W_{CW}) around -1.050 V.[23] Under these conditions, it was found that the first wave (W_I) corresponds to the quasi-reversible one-electron reduction of Ru^{III} to Ru^{II}[17] and that the second wave (W_{II}) is caused by the two-electron reduction of the adsorbed Ru–SAT complex.[23] The second wave was chosen for this work because of its adsorptive character and its well-defined shape and sensitivity.

The repetitive cyclic voltammetry of the system was investigated with an HMDE to evaluate the interfacial and redox behaviour. Typical cyclic voltammetric curves are shown in Fig. 2 (A,C) preceded by accumulation at -0.540 V
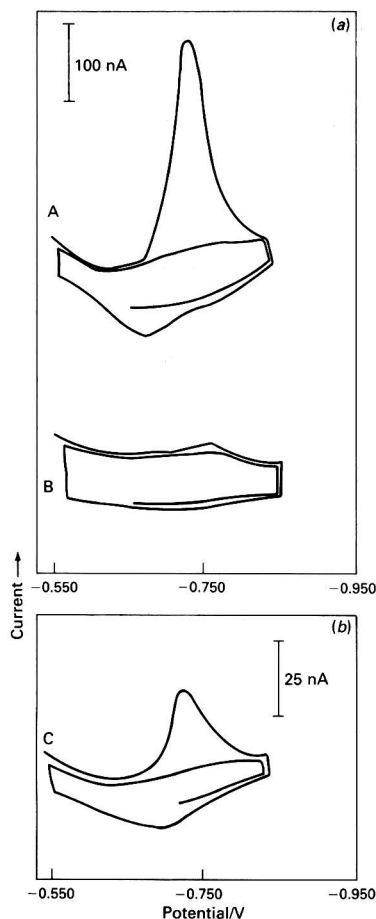

Fig. 2 Repetitive cyclic voltammograms for A, 5.0×10^{-7} mol dm^{-3} and C, 5.0×10^{-8} mol dm^{-3} Ru^{III} with 1.0×10^{-3} mol dm^{-3} SAT solution, A and C, with; and B, without a 90 s accumulation time at -0.540 V, with stirring at 400 rev min^{-1} and a scan rate of 100 mV s^{-1}. Electrolyte as in Fig. 1

for 90 s. In the absence of prior accumulation, only a very minute peak was observed at around -0.750 V [Fig. 2(B)]. The cathodic peak was found at almost the same potential as the DP polarographic peak, and the reduction peak in the first scan, after an accumulation time of 90 s, was much higher than that in the second scan. The peak current (i_p) was a linear function of the scan rate (v) in the range 10–100 mV s^{-1} for both 5.0×10^{-7} and 2.0×10^{-8} mol dm^{-3} Ru^{III}, and the peak potential became more negative with increasing scan rate, v, indicating an adsorption process.[24,25]

When the electrode was exposed to the solution at -0.540 V, the peak current gradually increased with exposure time, which indicates that the longer accumulation time leads to the adsorption of more of the metal complex on the electrode surface, thereby yielding a larger peak current. At very low concentrations (approximately 2.5×10^{-8} mol dm^{-3} of Ru^{III}), only the second wave (attributed to the reduction of the adsorbed complex) is observed, with an accumulation time of 90 s.

The redox processes associated with diffusion are not sensitive to surfactants, whereas the adsorption is known to be inhibited by the addition of surfactants. The effect of surfactants on the peak current of the DP polarographic curve was examined. The peak height was considerably reduced by

Table 1 Effect of pH on the peak current obtained for the ADPV of the Ru^{III}-SAT complex after accumulation at -0.540 V for 90 s. Ru^{III} = 5.0×10^{-7} mol dm^{-3}; [SAT] = 1.0×10^{-3} mol dm^{-3}

pH	Peak current at -0.750 V/nA
2.0	14
3.0	126
4.0	278
4.5	280
5.0	243
6.0	150

the addition of 0.05 or 0.1 cm^3 of solution (at the concentrations given in parentheses) of surfactants, such as sodium dodecyl sulfate (0.5 mg cm^3), gelatin (0.5 mg cm^3) and Triton X-100 (0.1 mg cm^3), to the medium used. The peak disappeared at gelatin concentrations greater than 0.02%. Ordinary diffusion waves were not affected by the addition of 0.02% of gelatin. Therefore, adsorption is responsible for the appearance of the peak.

Electrocapillary curves can yield some information about the adsorption of a particular species. An electrocapillary curve was obtained by measuring the drop times of the DME in acetate buffer solution containing 1.0×10^{-7} mol dm^{-3} Ru^{III} and 1.0×10^{-3} mol dm^{-3} SAT. A substantial change in drop time was observed in the potential region more positive than -0.750 V. This indicates that the adsorption of the Ru^{II}-SAT complex on the surface of the DME changes the surface tension of the mercury drop.

Optimum Analytical Conditions

To determine the optimum conditions for the adsorption preconcentration of the Ru^{III}-SAT complex at the HMDE, the effects of varying accumulation time, accumulation potential, SAT concentration and voltage scan rate, as well as the effects of other elements on the peak current, were investigated by ADPV.

The influence of the pH on the ADPV peak current of a 5.0×10^{-7} mol dm^{-3} solution of Ru^{III} in the presence of 1.0×10^{-3} mol dm^{-3} SAT is summarized in Table 1. At pH 2.0 (0.3 mol dm^{-3} acetate buffer) no significant adsorption of the complex at the electrode surface was observed. The current was at a maximum in the pH range 4.0–4.5 in acetate buffer solutions containing 0.1 mol dm^{-3} sodium perchlorate, 1.0×10^{-3} mol dm^{-3} SAT and 5.0×10^{-7} mol dm^{-3} Ru^{III}. As the concentration of the acetate buffer solution was increased from 0.1 to 0.3 mol dm^{-3} at the optimum ph (4.5) the peak current also increased. However, the peak current was independent of concentration in the buffer concentration range 0.3–0.8 mol dm^{-3}.

The effect of convection mass transport was also evaluated. Accumulation of the Ru^{III}-SAT complex from a stirred solution gave rise to an ADPV peak current 2.4 times as large as that obtained with the quiescent solution in the same accumulation period (90 s). In the example of a stirred solution the voltammetric curves were recorded after a 15 s rest period. The effect of accumulation time at an HMDE under 400 rev min^{-1} stirring was studied by ADPV in 0.5 mol dm^{-3} acetate buffer solution–0.1 mol dm^{-3} sodium perchlorate–1.0×10^{-7} mol dm^{-3} Ru^{III}–1.0×10^{-3} mol dm^{-3} SAT. It was found that the peak height increased with accumulation time and that the limiting current occurred within 60 s, corresponding to complete coverage of the electrode surface by the adsorbed species. If the process is diffusion controlled, with no adsorptive accumulation, the peak height will be independent of the accumulation time before scanning.[26,27] This also proves that the DP curve is an adsorption curve. All the ADPV curves were recorded with an accumulation time of 90 s.

Table 2 Results for the ADPV determination of Ru in synthetic mixtures

Sample	Composition of synthetic mixture/ ng cm^{-3}	Ruthenium found* ng cm^{-3}	Standard deviation/ ng cm^{-3}
1	Ru^{III} 10.5, Mo^{VI} 65.0 Pd^{II} 50.0, Rh^{III} 5.5	10.9	0.6
2	Ru^{III} 15.0, Rh^{III} 10.5 Os^{VIII} 110, Fe^{III} 1000	15.6	0.8
3	Ru^{III} 20.5, Ir^{III} 350 Ag^{I} 300, Rh^{III} 12.5 Os^{VIII} 150, Pd^{II} 50.5	21.3	1.1
4	Ru^{III} 25.5, Os^{VIII} 200 Ir^{III} 500 Au^{III} 150	26.1	0.7

* Average of five determinations.

Table 3 Results for the ADPV determination of Ru in various catalysts

Catalyst sample	Ru present* (%)	Ru found† (%)	Standard deviation/ ng cm^{-3}
Ruthenium–alumina	1.08	1.12	0.05
Ruthenium–silica–alumina	1.98	2.03	0.08
Ruthenium–platinum (1.08%)–alumina	0.46	0.49	0.03

* Certified value.
† Average of six determinations.

The SAT concentration had a pronounced effect on the DP adsorptive peak current. The ADPV curve peak current for 5.0×10^{-7} mol dm^{-3} ruthenium increased almost linearly with increasing SAT concentrations between 1.0×10^{-4} and 5.0×10^{-4} mol dm^{-3}, then remained constant in acetate buffer solution, with an accumulation potential, E_{acc}, at 0.540 V for 90 s in stirred solution.

The influence of the accumulation potential on the peak current for 1.0×10^{-7} mol dm^{-3} Ru^{III} in the presence of 1.0×10^{-3} mol dm^{-3} SAT was studied. At potentials more negative than -0.700 V, reduction of the complex began. The best accumulation potential was about -0.540 V, which was slightly negative relative to the first single-electron reduction peak. This implies that the adsorbed species is a SAT complex of Ru^{II}.

The ADPV current was almost unchanged with scan rates from 1 to 12 mV s^{-1}, so a scan rate of 12 mV s^{-1} was chosen. The peak current increased with the pulse amplitude, and the potential shifted to more positive values. The recommended pulse amplitude was 50 mV, which afforded reasonable sensitivity and peak shape.

The ADPV peak current (i_p)–concentration relationship was found to be linear for 5.0×10^{-8} to 8.0×10^{-7} mol dm^{-3} Ru^{III} under the optimized analytical conditions. Linear calibration graphs were obtained over two concentration ranges, viz., from 5.0×10^{-8} to 5.0×10^{-7} and from 5.0×10^{-7} to 8.0×10^{-7} mol dm^{-3}. The calibration plot started to deviate from linearity when the Ru^{III} concentration was further increased and a plateau was finally reached at above 8.0×10^{-7} mol dm^{-3} Ru^{III}, probably owing to saturation of the electrode surface by the adsorbed complex. The average sensitivities were 562.5 and 507.7 nA µmol^{-1} for 5.0×10^{-8}–5.0×10^{-7} and 5.0×10^{-7}–8.0×10^{-7} mol dm^{-3}, respectively. The limit of determination was 5.0×10^{-8} mol dm^{-3}. The precision of the method was calculated from nine successive measurements on 5.0×10^{-7} and 1.0×10^{-7} mol dm^{-3} Ru^{III} (90 s accumulation time); the mean peak currents were 283.0 and 57.4 nA, respectively (the relative standard deviations were 2.6 and 3.1%). Correlation coefficients of 0.9954 and 0.9928 were obtained for 5.0×10^{-8}–5.0×10^{-7} and 5.0×10^{-7}–8.0×10^{-7} mol dm^{-3} Ru^{III}, respectively.

In adsorptive voltammetry, interference can arise from competitive adsorption of ions or their complexes on the surface of the HMDE or from reduction peaks in the vicinity of the analyte peak. Of the various cations tested individually in the determination of 1.0×10^{-7} mol dm^{-3} Ru^{III}, no interference was observed in the presence of the following ions at the amount stated: Zn^{2+}, Ni^{2+}, Fe^{2+}, Fe^{3+}, Mn^{2+} and Mo^{6+} (100-fold excess); Cd^{2+}, Ag^+, Pb^{2+}, Ir^{3+}, Cr^{3+} and Sn^{2+} (50-fold excess); Au^{3+}, Co^{2+}, Os^{8+}, Cu^{2+} and As^{3+} (20-fold excess); Pd^{2+}, Pt^{2+} and V^{5+} (10-fold excess); and Rh^{3+} (equimolar amount). An additional peak was observed in the presence of 1.0×10^{-5} mol dm^{-3} cobalt, at 120 mV negative to the peak of interest, but this did not affect the determination of Ru^{III}. Tervalent Rh seriously interfered by increasing the peak current above the equimolar amount.

Analytical Applications of the Method

As the proposed method proved to be sensitive and free from most of the associated metal ions, it was applied to the determination of ruthenium in synthetic mixtures (Table 2) and a few catalysts (Table 3). The results obtained for the determination of ruthenium (Table 2 and 3) further confirmed the analytical usefulness of the proposed method. The method described provides a simple approach to the determination of trace levels of ruthenium. The interfacial accumulation results in a substantial enhancement of the voltammetric response, permitting convenient determination at the ng cm^{-3} level.

References

1   Kalvoda, R., *Ann. Chim. (Rome)*, 1983, **73**, 239.
2   Kalvoda, R., *Anal. Chim. Acta*, 1982, **138**, 11.
3   Vydra, F., Stulik, K., and Julakova, E., *Electrochemical Stripping Analysis*, Ellis Horwood, Chichester, 1979.
4   Nurnberg, H. W., *Instrumentelle Multielementanalyse*, VCH, Weinheim, 1985.
5   Pihlar, B., Valenta, P., and Nurnberg, H. W., *Z. Anal. Chem.*, 1981, **307**, 337.
6   Wang, J., *Am. Lab.*, 1985, **17**, 41.
7   van den Berg, C. M. G., *J. Electroanal. Chem., Interfacial Electrochem.*, 1986, **215**, 111.
8   Wang, J., Lin, M. S., and Villa, V., *Analyst*, 1987, **112**, 1303.
9   Love, D. L., and Greendale, A. E., *Anal. Chem.*, 1960, **32**, 780.
10 Wagnerova, M., *Collect. Czech. Chem. Commun.*, 1962, **27**, 1130.
11 Buckley, J. P., *Anal. Chim. Acta*, 1970, **52**, 379.
12 Hojman, J. Stefanovic, A., Stankovic, B., and Zuman, P., *J. Electroanal. Chem. Interfacial Electrochem.*, 1971, **30**, 469.
13 Medyantseva, E. P., Ulaklovich, N. A., Romanova, O. N., and Budnikov, G. K., *Zh. Anal. Khim.*, 1989, **44**, 695.
14 Medyantseva, E. P., Budnikov, G. K., Romanova, O. N., and Zhivolup, I. V., *Zh. Anal. Khim.*, 1987, **42**, 1846.
15 Palaniappan, R., *Analyst*, 1989, **114**, 1043.
16 Palaniappan, R., and Revathy, V., *Analyst*, 1989, **114**, 517.
17 Palaniappan, R., *J. Electrochem. Soc. India*, 1990, **39**, 21.
18 Palaniappan, R., and Paul, A., *Proc. Indian Acad. Sci. (Chem. Sci.)*, 1989, **101**, 115.
19 Palaniappan, R., *Bull. Electrochem.*, 1991, **7**, 367.
20 Beamish, F. E., and van Loon, J. C., *Recent Advances in Analytical Chemistry of Noble Metals*, Pergamon Press, London 1972, pp. 357, 358, 466.
21 Beamish, F. E., and van Loon, J. C., *Analysis of Noble Metals*, Academic Press, New York, 1977, pp. 131–135, 141, 142, 145, 146.
22 Sah, P. T., and Daniels, T. C., *Recl. Trav. Chim. Pays-Bas*, 1950, **69**, 1545.
23 Palaniappan, R., Ph.D. Thesis, Madras University, India, 1989.
24 Osteryoung, R. A., Lauer, G., and Anson, F. C., *Anal. Chem.*, 1962, **34**, 1833.
25 Li, Q., and Li, S., *Dianfenxi Huaxue*, 1989, **1**, 65.
26 Koryta, J., *Collect. Czech. Chem. Commun.*, 1953, **18**, 206.
27 Li, Q., and Li, S., *Fenxi Ceshi Tongbao*, 1989, **3**, 45.

Determination of Trace Concentrations of Arsenic in Nickel-base Alloys by Electrothermal Atomic Absorption Spectrometry

Suh-Jen Jane Tsai and Yea-Ling Bae
Department of Applied Chemistry, Providence University, Taichung Hsien, Taiwan

A procedure for the determination of trace concentrations of arsenic in nickel-base alloys was developed. Solid samples of nickel-base alloys were decomposed with a mixture of hydrochloric acid and nitric acid (4 + 1), the resulting solution was heated nearly to dryness and the residue was dissolved in about 2 ml of distilled, de-ionized water. Most of the excess of the acids was removed by repeating the heating and dissolution procedures. The final solutions were analysed by electrothermal atomic absorption spectrometry using a pyrolytic graphite platform in a pyrolytic graphite coated graphite tube at 193.7 nm. Various pre-treatment conditions, which included chemical modifiers, hydrazine and potassium iodide, were evaluated. Potassium iodide gave satisfactory results. The accuracy of the analytical results was checked using certified reference materials. The optimum conditions that gave the highest precision and accuracy of the results were established.

Keywords: *Arsenic determination; nickel-base alloy; electrothermal atomic absorption spectrometry*

Nickel-base superalloy is one of the most important materials in the aerospace industry. The presence of trace elements had deleterious effects on the mechanical and physical properties of high-temperature alloys.[1–3] The significance of close control of trace elements in nickel-base superalloys was reinforced in a detailed study by Ford in 1984.[4] Trace elements present in either the raw materials or the finished castings were extremely damaging to the creep life and creep ductility of cast nickel-base alloys. Among the six trace elements studied, *viz.*, Bi, Te, Se, Pb, Ag and Mg, Bi was the most detrimental in reducing the creep life. In contrast, Mg improved the castability of superalloys. Hence, accurate determinations of trace metals in superalloys have always been necessary. Lowe's report[5] also addressed the significance of the determination of trace elements in nickel-base alloys. A unique design of a high-temperature hollow-cathode source was proposed for the simultaneous determination of concomitant trace elements in nickel-base superalloys directly from drillings or small pieces. Trace amounts of As in solid samples have also been measured with a resistively heated furnace.[3] There are only a few reports on this subject owing to the complexity of the matrix of superalloys.

Matrix interferences in electrothermal atomic absorption spectrometry (ETAAS) were effectively reduced using an analytical system with a stabilized temperature platform furnace (STPF).[6,7] Therefore, it was considered worthwhile to develop an analytical procedure for the determination of trace elements in nickel-base superalloys with an STPF. Among the three popular atomization methods, namely flame, hydride generation and graphite furnace, the electrothermal method offers the highest sensitivity and lowest detection limits in most instances. The hydride generation technique coupled with AAS, inductively coupled plasma atomic emission spectrometry (ICP-AES), gas chromatography or molecular absorption spectrometry has been successfully applied to the determination of trace amounts of arsenic in both environmental and biological samples.[8–13] However, the coexistence of more than 20 elements in a solution of superalloys prevented the adaptation of hydride generation AAS or AES to determine trace contents of superalloys without tedious separations. When an alkaline solution of a reductant, often $NaBH_4$, was mixed with the acidic analyte solution, the sample solution solidified, which made the stripping of volatile metal hydrides almost impossible.

The main problem in determining trace amounts of arsenic by ETAAS is matrix interferences. These were often elimin-

ated by introducing effective chemical modifiers such as nickel compounds, palladium and magnesium nitrate.[14] Successful applications of modifiers have been reported in analyses of samples other than nickel-base superalloys[15–17] and the reaction mechanisms involved have been studied.[18,19] This paper describes a selective and sensitive method for the determination of arsenic by ETAAS. The accuracy of the proposed method was evaluated with a certified reference material (CRM) of nickel-base alloy.

Experimental

Apparatus

A Perkin-Elmer Model 1100B atomic absorption spectrometer fitted with an HGA-700 furnace and AS-70 autosampler was used. Integrated absorbances (peak area) values were used in measurements. Experimental parameters and peak profiles were recorded with an Epson EX-800 printer. An electrodeless discharge lamp (EDL) equipped with a Perkin-Elmer EDL power supply was used for the determination of arsenic. New pyrolytic graphite coated graphite tubes (part No. B010-9322) and pyrolytic graphite platforms (part No. B010-9324) were used. Maximum power heating was used for the atomization step. A Barnstead Nanopure II system was employed for water purification.

Reagents and Standards

Concentrated hydrochloric acid and nitric acid were singly distilled acids obtained from Eastar Chemicals. Standard solutions of arsenic (H_3AsO_4 in HNO_3, 0.5 mol l^{-1}) and titanium ($TiCl_4$ in HCl, 5 mol l^{-1}) were prepared from Titrisol solutions (Merck). Standard solutions of Ga, In, V (prepared in 2% HNO_3) Ge and Ta (prepared in H_2O–trace HF) were products of Inorganic Ventures. Niobium (atomic absorption standard solution, in water), Zr (atomic absorption standard solution, in 5% HCl) and hydrazine hydrate solution (24% m/v) were products of Aldrich. Working solutions were prepared from 1000 mg l^{-1} stock solutions by serial dilution. Distilled, de-ionized water (DDW) prepared with a Barnstead Nanopure II system was used in all experiments. The nickel-base alloy spectroscopic standard (SS) CRM 346A IN 100 Alloy was obtained from the Bureau of Analysed Samples. Purified grade argon (99.99%) was used as the purge gas during sample analysis.

Procedures

A 0.02000 g amount of sample was digested with a minimum volume of HCl–HNO$_3$ (4 + 1). After digestion, the sample solution was heated nearly to dryness and the residue was dissolved in a few millilitres of DDW. Most of the excess of the acids was removed by repeating the heating and dissolution procedures. The sample solutions were then treated with either of the following procedures: method A, the solution was diluted to 10 ml with 0.2% HNO$_3$; method B, 0.05 g of citric acid and 3.0 ml of hydrazine hydrate solution (15% m/v) were added and the sample solution was diluted to 10 ml with 0.2% HNO$_3$; method C, 1 ml of 5.0% m/v KI solution was added before dilution with 0.2% HNO$_3$. The corresponding blank solutions were also prepared.

Calibration solutions of 0.2–0.8 ng of arsenic were prepared by dilution of the working solutions with 0.2% HNO$_3$. These solutions were analysed by ETAAS.

The concentration of arsenic was determined by injecting 2, 3, 5 or 10 µl of the sample solution onto the platform in a pyrolytic graphite coated graphite tube. The optimum 'dry,' 'char' and 'atomize' HGA-700 programme developed in this laboratory was followed and the integrated areas of the absorption peaks were recorded. The recommended analytical conditions and the temperature programme are summarized in Table 1. Blanks were run regularly and their values were subtracted from the gross values to obtain the net values reported.

Results and Discussion

The optimum conditions for arsenic determinations are given in Table 1. Arsenic was determined by both the direct calibration method with standard arsenic solutions and the method of standard additions.

Temperature Programme/Heating Programme

The background interferences can be partly eliminated by careful control of the temperature programmes. Fig. 1 shows the effect of charring temperature on the signal intensities. The absorbances of SS CRM 346A IN 100 Alloy and the arsenic standard solutions were monitored at an atomization temperature of 2300 °C. The signal intensities decreased

gradually above 1300 °C. This was due to the atomization of arsenic at any temperature higher than 1300 °C. In order to minimize the volatilization losses of arsenic during the charring cycle, 1300 °C was chosen as the charring temperature.

Fig. 2 shows the absorbances of arsenic as a function of the atomization temperature. The signal intensity of the SS CRM 346A IN 100 Alloy reached a plateau when the temperature increased to 2300 °C, whereas the absorbances of standard arsenic solutions decreased rapidly above this temperature. This indicated that some of the arsenic atoms were expelled from the graphite tube at higher temperatures.

Interferences

Potential interfering ions, including gallium, germanium, indium, niobium, tantalum, vanadium, zirconium and titanium, were studied. In order to elucidate the effects of foreign ions on the determination of arsenic, several sample solutions spiked with different metal ions were analysed. The relative absorbances were monitored with various concentrations of foreign ions up to 800 ppm. The relative absorbance (rel. abs.) was defined by the following equation:

$$\text{rel. abs.} = \frac{\text{absorbance of } (500 \text{ pg As} + \text{foreign ions})}{\text{absorbance of } 500 \text{ pg As}}$$

Table 2 summarizes the effects of metal concentrations on the relative absorbances. Zirconium caused a large enhancement of the absorption signals. The relative absorbance increased dramatically from 1.21 to 4.55 as the concentration increased from 40 to 800 ppm. As the zirconium enhancement varied linearly with concentration, the interference of zirco-

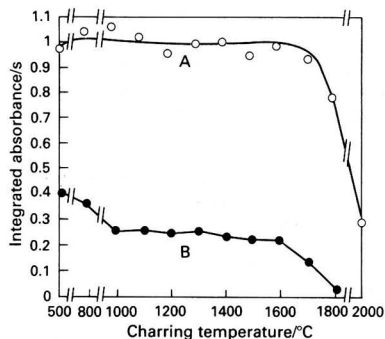**Table 1** Optimum analytical conditions for arsenic determinations

Light source	Electrodeless discharge lamp
Supply power	8 W
Background corrector	D$_2$ lamp
Lamp current	8 mA
Wavelength	193.7 nm
Slit	0.7 nm
Signal processing	Peak area
Integration time	5.0 s
Internal gas	High-purity Ar (99.99%)
Tube/site	Pyrolytic graphite coated graphite/platform
Characteristic mass*	15.9 pg

Furnace conditions—

Step No.	Furnace temperature/°C	Time/s Ramp	Time/s Hold	Gas flow rate/ ml min^{-1}	Read on
1	120	10	20	300	—
2	1300	10	10	300	—
3	20	5	10	300	—
4	2300	0	5	0.0	0.0
5	2650	1	5	300	—
6	20	5	5	300	—

* Mass of As giving a peak absorbance of 0.0044.

Fig. 1 Absorbances of arsenic as a function of charring temperature at an atomization temperature of 2300 °C. A, 38.0 µg of SS CRM 346A IN 100 Alloy and B, 680 pg of standard As
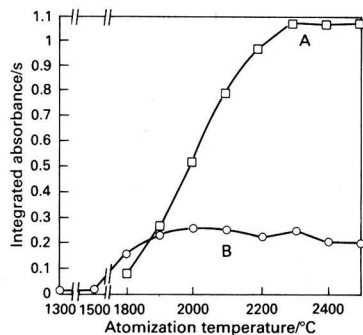

Fig. 2 Absorbances of arsenic as a function of the atomization temperature at a charring temperature of 1300 °C. A, 38.0 µg of SS CRM 346A IN 100 Alloy and B, 680 pg of standard As

nium could be corrected by keeping the same concentration of interfering ion in both the standard solutions and the sample solutions as the calibration graphs were established.

Tantalum, indium and vanadium gave a 30% enhancement of the absorption signals over the same concentration range. Therefore, the interferences from these three ions could be corrected similarly. The enhancement of the arsenic signals might be due to the stabilization of arsenic through the formation of less volatile compounds during the charring step, the non-specific absorption of the concomitant materials, e.g., the molecular absorption of metal chlorides, oxides and other salts which formed within the range 300–800 °C,[18] or the formation of thermostable intermetallic compounds and/or solid solutions.

Titanium and niobium caused less than a 10% deviation in the relative absorbances. This indicated that the tolerance limits of these ions were up to 800 ppm. The effects of gallium and germanium on the absorption signals of analyte were interesting. Arsenic, gallium and germanium are highly volatile elements. These elements formed monoxides which were thermally stable only up to 600 °C even in the presence of a chemical modifier, such as nickel nitrate.[18] The possible mechanisms involved in the atomization of arsenic in a graphite furnace were discussed by Styris et al.[19] The gaseous species, As_2O_3, was decomposed thermally into As_2, arsenic oxide, higher arsenic oxides and condensed-phase arsenic. Once the condensed-phase arsenic was formed it would polymerize into dimers, which would sublime, causing losses of analyte and resulting in low absorption signals of arsenic.

The vaporization of the gaseous oxides was another major contributor to arsenic losses. Sufficient atomization would occur if the dissociation adsorption of the AsO or As_2 and the desorption of the resulting arsenic proceeded successfully. In the presence of gallium there was less opportunity for arsenic to be polymerized as the latter was 'diluted' by gallium. Consequently, the relative absorbances were increased. The stabilization of arsenic could also be the result of the formation of thermostable intermetallic compounds similar to those, $[Pd_xAs_yO_m]$, which had been proposed by Styris et al.[19] The oxide Ga_2O_3 was first formed in a graphite tube and then reduced to Ga_2O, GaO and CO, which was released.[18,20] As the concentration of gallium increased (above 400 ppm), the dissociation adsorption of arsenic oxide became less effective and more AsO was carried out of the graphite tube by the argon. This resulted in a smaller enhancement of the arsenic signals.

Germanium when present in low concentrations (less than 160 ppm) had a negligible effect on the stabilization of arsenic atomization. As shown in Table 2, a slight depression of the relative absorbances was found. The formation of GeO was one of the reasons for the lower sensitivity in the determination of germanium by ETAAS.[21] The atomization of germanium was improved through the formation of thermally stable intermetallic compounds and germanates when chemical modifiers, $Ni(NO_3)_2$ and $Fe(NO_3)_3$, were employed. As

the ratio of the concentrations of analyte and interfering ion varied, different intermetallic compounds would be obtained.[22] The relative absorbance increased dramatically to 1.38 as the concentration of germanium increased to 240 ppm. Less enhancement was observed as the concentration of metal increased.

The formation of different intermetallic compounds could cause different degrees of improvement of the arsenic atomization. The erratic results with gallium and germanium could be mainly due to the high volatility of GaO and GeO and the formation of intermetallic compounds between arsenic and interfering ions.

In this work, the atomic absorption of arsenic was monitored at 193.7 nm. The predominant molecular absorption wavelengths are 244.5 and 265.94 nm for GaO and GeO, respectively.[20,21] Although the molecular absorption of metal oxides could also contribute to the signal enhancement of the analyte, the contribution of molecular oxides could be negligible. However, the gaseous reactions involved in a graphite tube are very complicated and diverse mechanisms have been suggested. Further investigations are required in order to verify the mechanisms involved.

Pre-treatment/Chemical Modifier

The nickel-base alloy SS CRM 346A IN 100 Alloy for trace analysis, contains over 50% Ni, with the composition (values in mg g^{-1}) C 1.5, Cr 100, Mo 30, Al 55, Co 150, Tl 50, V 10, Pb 0.022 and trace amounts of Bi, Ag, Se, Te, Tl, Sb, As, Cd, Ga, Sn, Zn, Mg, Ca and In. The certified arsenic content was 51 ± 2 ppm. As sulfate caused a large depression of the arsenic signals and enhanced the interferences from alkali metal ions,[15,23] sulfuric acid is not recommended for sample decomposition. After the solid sample had been decomposed completely with HCl–HNO_3 (4 + 1), sample solutions were prepared by the following pre-treatment procedures: in method A, the decomposed sample was diluted with 0.2% HNO_3 directly; in method B, 0.05 g of citric acid and 3.0 ml of hydrazine hydrate solution (15% m/v) were added before the solution was diluted; and in method C, 1 ml of potassium iodide solution (5.0% m/v) was added before dilution with 0.2% HNO_3.

Chemical modification techniques have been widely applied in trace analysis by ETAAS. The addition of chemical modifiers would result in either an increase in the volatility of unwanted elements or a decrease in the volatility of the atoms of interest. Nickel has often been employed as an effective chemical modifier and has been successfully applied to the determination of trace amounts of arsenic in environmental samples.[14] Nickel is known to form thermally stable complexes, $Ni(AsO_3)_2 \cdot NiO$, or other arsenides with arsenate ions.[24] The addition of nickel stabilized the As atoms up to 1300–1500 °C. Hence the As atoms would not be released until the atomization step. In work by Stein et al.,[15] trace concentrations of arsenic (about 10 µg l^{-1}) in potable, fresh and estuarine water were precisely and accurately determined by ETAAS with the addition of 0.05% of nickel.[15] The concentration of the chemical modifier was often 10^4 times higher than the analyte concentration. As there was over a 10^4-fold excess of nickel present in a sample of SS CRM 346A IN 100 Alloy, the sample solution was analysed directly after dilution with 0.2% HNO_3 as in method A. As listed in Table 3, the analytical results were 41.9 ± 6.1 and 35.2 ± 1.3 ppm for the calibration graph method and the method of standard additions, respectively.

Although the addition of nickel compounds prevented the charring losses of arsenic, serious interferences still existed. Different behaviours had been observed when trivalent and pentavalent arsenic were analysed by ETAAS.[23] Standard arsenic solutions prepared from As_2O_3 or Na_2HAsO_4 could be measured with a relative standard deviation of <5%, while

Table 2 Effect of metal concentration on relative absorbance. Relative absorbance = absorbance of (500 pg As + foreign ions)/absorbance of 500 pg As. Results given are the averages of five determinations

Element	Concentration (ppm)									
	40	80	160	240	320	400	480	600	680	800
Zr	1.21	1.63	2.14	2.65	2.63	3.12	3.57	3.96	4.31	4.55
Ta	1.14	1.27	1.33	1.13	1.21	1.26	1.27	1.20	1.17	1.20
In	1.31	1.36	1.37	1.37	1.36	1.34	1.37	1.37	1.33	1.38
V	0.98	1.31	1.28	1.23	1.33	1.32	1.34	1.36	1.32	1.28
Ti	1.02	1.03	1.06	0.96	0.95	1.06	1.03	0.97	0.91	0.91
Nb	1.09	1.07	1.12	1.12	1.19	1.07	0.97	0.97	0.91	1.04
Ga	1.18	1.25	1.22	1.15	1.09	1.95	1.55	1.46	1.27	1.40
Ge	0.86	0.89	0.97	1.38	1.34	1.16	1.15	1.24	1.29	1.43

those prepared from As_2O_5 resulted in a relative standard deviation of $\geq 20\%$. This implied that better analytical results would be obtained if trivalent arsenic was measured in a graphite tube. Based on this prediction, a volume of reductant was added before the sample solutions were analysed. After the nickel-base alloys had been decomposed completely, both trivalent and pentavalent arsenic were possibly present in the sample solutions. Hydrazine hydrate had been successfully employed as an effective reductant in the determination of trace amounts of As, Sb and Sn in high-purity selenium.[25] However, the addition of hydrazine did not improve the analytical results as given in Table 3. Potassium iodide also functions as an effective reductant to reduce As^V to As^{III} in the hydride generation step.[26] Therefore, the sample solution was treated with potassium iodide according to method C. A great improvement in the analytical results was found. Details are given in the following section.

Quantitative Results

Integrated absorbances are susceptible to the total number of atoms present in the light path and independent of the rate of atomization. Therefore, integrated absorbances were recorded instead of peak height absorbances. A calibration graph with a linear range from 0.2 to 0.8 ng was established [correlation coefficient $(R) = 0.9994$, $-$(intercept $\times K$) $(B) = -0.0100$, 1/slope $(K) = 4.1555$; see Table 3]. This work showed that the addition of potassium iodide resulted in more accurate and precise results for nickel-base alloys. The nickel-base alloy CRM was analysed to validate the accuracy of the proposed procedure. There was good agreement between the certified arsenic content and the results obtained with both the calibration graph method and the method of standard additions (Table 3). By adding various amounts of standard arsenic to sample solutions (0.40–0.60 ng), a recovery of $99 \pm 3\%$ was obtained. The detection limit was 0.30 ng g^{-1}.

Conclusions

Trace amounts of arsenic in relatively complex samples, nickel-base superalloys, were successfully determined. A solid

sample was decomposed with HCl–HNO$_3$ $(4 + 1)$ and after the removal of the excess of the acids, 1 ml of 5.0% m/v potassium iodide solution was added before dilution with 0.2% HNO$_3$. The resulting solutions were analysed by ETAAS. The addition of an effective reductant, potassium iodide, reduced As^V to As^{III} and gave reproducible results. The relatively high accuracy of the proposed methods was demonstrated by good agreement with the results obtained by the proposed method and with certified values.

References

1 Andrews, D. G., and Headridge, J. B., *Analyst*, 1977, **102**, 436.
2 Bäckman, S., and Karlsson, R. W., *Analyst*, 1979, **104**, 1017.
3 Headridge, J. B., and Nicholson, R. A., *Analyst*, 1982, **107**, 1200.
4 Ford, D. A., *Met. Technol.*, 1984, **11**, 438.
5 Lowe, D. S., *Analyst*, 1985, **110**, 583.
6 Sturgeon, R. E., *Fresenius' J. Anal. Chem.*, 1990, **337**, 538.
7 L'vov, B. V., *Anal. Chem.*, 1991, **63**, 924A.
8 Narsito, Agterdenbos, J., and Santosa, S. J., *Anal. Chim. Acta*, 1990, **237**, 189.
9 Van Elteren, J. T., Gruter, G. J. M., Das, H. A., and Brinkman, U. A. Th., *Int. J. Environ. Anal. Chem.*, 1990, **43**, 41.
10 Van Elteren, J. T., Haselager, N. G., Das, H. A., de Ligny, C. L., and Agterdenbos, J., *Anal. Chim. Acta*, 1991, **252**, 89.
11 Schramel, P., and Xu, L.-Q., *Fresenius' J. Anal. Chem.*, 1991, **340**, 41.
12 Cutter, L. S., Cutter, G. A., and San Diego-McGlone, M. L. C., *Anal. Chem.*, 1991, **63**, 1138.
13 Sanz, J., Gallarta, F., and Galban, J., *Anal. Chim. Acta*, 1991, **255**, 113.
14 Schlemmer, G., and Welz, B., *Spectrochim. Acta, Part B*, 1986, **41**, 1157.
15 Stein, V. B., Canelli, E., and Richards, A. H., *At. Spectrosc.*, 1980, **1**, 133.
16 Bettinelli, M., Pastorelli, N., and Baroni, U., *Anal. Chim. Acta*, 1986, **185**, 109.
17 Bozsai, G., Schlemmer, G., and Grobenski, Z., *Talanta*, 1990, **37**, 545.
18 Volynsky, A., Tikhomirov, S., and Elagin, A., *Analyst*, 1991, **116**, 145.
19 Styris, D. L., Prell, L. J., and Redfield, D. A., *Anal. Chem.*, 1991, **63**, 503.
20 Shan, X., Yuan, Z., and Ni, Z., *Anal. Chem.*, 1985, **57**, 857.
21 Kolb, A., Muller-Vogt, G., Wendl, W., and Stobel, W., *Spectrochim. Acta, Part B*, 1987, **42**, 951.
22 Xuan. W.-K., and Li, J.-G., *Spectrochim. Acta, Part B*, 1990, **45**, 669.
23 Chakraborti, D., De Jonghe, W. and Adams, F., *Anal. Chim. Acta*, 1980, **119**, 331.
24 Koreckova, J., Frech, W., Lundberg, E., Persson, J.-A., and Cedergren, A., *Anal. Chim. Acta*, 1981, **130**, 267.
25 Ivanova, E., Vracheva, N., Havezov, I., and Jordanov, N., *Fresenius' Z. Anal. Chem.*, 1988, **330**, 516.
26 Donaldson, E. M., and Leaver, M. E., *Talanta*, 1988, **35**, 297.

Table 3 Analytical parameters and results of As determinations. Mean results of five determinations $\pm$ standard deviation. The mass of standard arsenic added ranged from 0.4 to 0.6 ng.

Calibration graphs: concentration = $K \times$ absorbance + B

Linear range/ng	R^2	K	B
0.200–0.800	0.9994	4.1555	−0.0100

Analytical results—

	As in SS CRM 346A IN 100 Alloy (ppm)*		
	Method A	Method B	Method C
Direct measurement	41.9 ± 6.1	18.2 ± 9.3	51.4 ± 4.5
Standard additions method	35.2 ± 1.3	40.0 ± 6.3	51.0 ± 4.0
Recovery	—	—	$99 \pm 3\%$
Detection limit	—	—	0.30 ng g^{-1}

* Certified As content: $51 \pm 2\%$.

Flame Atomic Absorption Spectrometric Determination of Magnesium in Nickel-base Alloys

Suh-Jen Jane Tsai and Yea-Ling Bae
Department of Applied Chemistry, Providence University, Taichung Hsien, Taiwan

Flame atomic absorption spectrometry (FAAS) was employed for the determination of magnesium with wavelength 285.4 nm, slit-width 0.7 nm and air–acetylene flame (flow rates 2 and 15.5 l min^{-1}, respectively). A pre-treatment procedure for the determination of trace concentrations of magnesium in nickel-base alloys was developed. Matrix interferences could be effectively eliminated by the addition of both ethylenedi-aminetetraacetic acid and $SrCl_2$. The accuracy of the results was checked with certified reference materials of nickel-base alloys. For IN100 and Inconel alloy 718 with a certified magnesium content of 130 ± 9 and a reference value of 12 ± 5 ppm, the procedure gave values of 130 ± 3 and 7 ± 1 ppm, respectively. The detection limit was 0.50 ng g^{-1} and the recovery ranged from 97 ± 4 to 104 ± 2%.

Keywords: *Magnesium determination; nickel-base alloy; flame atomic absorption spectrometry*

The determination of trace amounts of magnesium in nickel-base superalloys[1] and environmental samples[2] has always been a challenge. Flame atomic absorption spectrometry (FAAS) gives low detection limits in the determination of a few elements. In fact, magnesium is one of the most sensitive elements that can be determined by FAAS.[3] However, it is subject to interferences from a number of anions, cations and detergents.[4–7] The interference of silicate was eliminated by the addition of releasing agents such as La,[8] and most of the interferences from cations can be eliminated by strontium chloride.[4] Among the various types of flames, the air–acetylene flame provided the most suitable atom reservoir for magnesium determinations, because there are less interferences from foreign ions.[9,10]

The merit of the method proposed here is that trace amounts of magnesium in a complex matrix can be determined without tedious solvent extractions. The accuracy of the method was evaluated with certified reference materials of nickel-base alloys, namely IN100 and Inconel alloy 718. The good accuracy and precision of the results showed the high reliability of this method when applied to the analysis of nickel-base alloys.

Experimental

Apparatus

A Perkin-Elmer Model 2380 atomic absorption spectrometer equipped with a flow spoiler and a hollow cathode lamp operated at 8 mA was used for magnesium determinations. The operating conditions were wavelength 285.4 nm, slit-width 0.7 nm, and air–acetylene flame (flow rates 2 and 15.5 l min^{-1}, respectively). A Barnstead Nanopure II system was employed for water purification.

Reagents and Standards

Concentrated hydrochloric acid and nitric acid were singly distilled acids from Eastar Chemical. A standard solution of magnesium (1.000 ± 0.002 g $MgCl_2$ in 6% HCl) was prepared from Titrisol solutions (Merck). Strontium chloride hexahydrate, $SrCl_2·6H_2O$, was obtained from Merck, sodium ethyl-enediaminetetraacetate (EDTA) from RDH and lanthanum chloride heptahydrate, $LaCl_3·7H_2O$ (99.9% ACS reagent), from Aldrich. Working solutions were prepared from 1000 mg l^{-1} stock solutions by serial dilution.

The certified reference materials of nickel-base alloys, IN100 (SS-CRM No. 346A) and Inconel alloy 718 (BS 718 A) were obtained from the Bureau of Analysed Samples and

Brammer Standard, respectively. Purified grade argon (99.99%) was used as the purge gas during sample analysis.

Procedures

A precisely weighed amount (about 0.01 g) of sample was digested with a minimum volume of HCl–HNO$_3$ (4 + 1). The solution was heated mildly until the decomposition process was completed. The sample solution was then treated according to one of the following procedures: method A, the sample solution was diluted to 10 ml with distilled, de-ionized water; method B, 1 ml of lanthanum solution (5.0% m/v) was added to the sample solution before dilution; method C, the sample solution was prepared similarly, but Sr solution (5.0% m/v) and EDTA solution (4.0% m/v) were added before dilution.

In order to ascertain the optimum concentration of Sr and EDTA, a series of sample solutions that contained different amounts of Sr (0.20, 0.30, 0.40, 0.50, 0.80, 1.0, 2.5 and 5.0% m/v) and EDTA (0.12, 0.24, 0.40, 0.80 and 2.4% m/v) were prepared. The corresponding blank solutions were also prepared.

Results and Discussion

Trace amounts of magnesium in nickel-base alloys were determined by FAAS using the given operating parameters and the results are given in Table 1. The certified reference materials IN100 and Inconel alloy 718 were employed for evaluating the accuracy of the proposed method. The compo-

**Table 1** Analytical parameters and results of Mg determinations

Calibration graphs:* concentration = K × absorbance + B

Linear range (ppm)	R^2	K	B
0.050–0.30	0.9986	1.5859	−0.0063

Analytical results†—

	Mg content (ppm)	Mg found (ppm)		
		Method A	Method B	Method C
IN100	130 ± 9	ND	80 ± 3	130 ± 3
Inconel alloy 718	12 ± 5	ND	—	7 ± 1
Detection limit	—	—	—	0.50 ng g^{-1}

* Light source, hollow cathode lamp; wavelength, 285.4 nm; slit-width, 0.7 nm; flame, air–acetylene, oxidizing (lean, blue); R^2 = correlation coefficient; K = 1/slope; B = −(intercept × K).

† Results of four determinations; ND = not detectable; detection limit = 3σ of blanks ($n = 7$).

sition of IN100 was (values in mg g^{-1}) C 1.5, Cr 100, Mo 30, Al 55, Co 150, Ti 50, V 10, Pb 0.022 and trace amounts of Bi, Ag, Se, Te, Tl, Sb, As, Cd, Ga, Sn, Zn, Ca and In. The certified magnesium content was 130 ± 9 ppm. The composition of Inconel alloy 718 was (values in mg g^{-1}; numbers in parentheses are not certified but are provided for information only) C 0.36, Si 1.2, Mo 30.6, Fe 192.1, Mn 0.8, Cu 0.6, Al 5.7, Ti 10.2, P 0.07, Ni 520, Co 3.2, Nb 51.9, S 0.01, Cr 181.9, B 0.046, V (0.3), Sn (0.04), W (0.8), V (0.3). A reference value of 12 ± 5 ppm Mg was not certified, but was for information.

After solid samples had been decomposed with $HCl–HNO_3$ (4 + 1), the sample solutions were prepared according to methods A, B and C above. It was not possible to detect any absorption signal of Mg atoms when sample solutions of nickel-base alloys were analysed directly after decomposition according to method A. This indicated that there were serious interferences from the matrix. Several cations, anions and detergents interfere in the determination of magnesium by FAAS.[4,6] For example, aluminium interfered through the reaction[6,11]

$$MgO + Al_2O_3 \rightarrow MgAl_2O_4$$
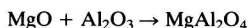
Once the thermally stable magnesium aluminate spinel $MgAl_2O_4$ has been formed, it would be extremely difficult for the atomization process to proceed. The addition of lanthanum would decrease the silicate interference.[8] Although the addition of 1 ml of lanthanum solution (5.0% m/v) as in method B altered the result from undetectable to 80 ± 3 ppm of magnesium, further improvement was still required. Strontium chloride eliminated most of the interferences from cations except those due to Fe^{III}, Cr^{III} and Ti^{IV}.[4] Strontium could function as a releasing agent through the reaction

$$Sr + MgO \rightarrow SrO + Mg$$
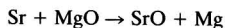
The reagent EDTA is known to chelate with many metal ions, including magnesium ions. The refractory compounds of magnesium would be greatly reduced through chelation. The experimental results showed that the addition of both strontium and EDTA solutions had considerable effects on the analysis. In fact, method C gave the most satisfactory results.

In order to ascertain the optimum conditions for the pre-treatment of nickel-base alloys, serial analyses were performed with different strontium concentrations (0.20–2.5%) and EDTA concentrations (0.12–2.4%). The best results for IN100 were obtained with 0.24% m/v EDTA and 0.30 m/v strontium. For Inconel alloy 718, the optimum concentrations of EDTA and Sr in the sample solutions were 0.4 and 0.5% m/v, respectively. For IN100 with a certified magnesium content of 130 ± 9 ppm the proposed method gave 130 ± 3 ppm and for Inconel alloy 718 with a reference value of 12 ± 5 ppm this method gave 7 ± 1 ppm. The proposed method gave a detection limit of 0.50 ng g^{-1} and the recovery ranged from 97 ± 4 to 104 ± 2% (seven determinations). This shows that trace amounts of magnesium in nickel-base alloys can be determined accurately and precisely with the proposed FAAS procedure.

References

1 Lowe, D. S., *Analyst*, 1985, **110**, 583.
2 Pal, T., Jana, N. R., and Das, P. K., *Analyst*, 1992, **117**, 791.
3 Gimeno Adelantado, J. V., Peris Martinez, V., Pastor Garcia, A., and Bosch Reig, F., *Talanta*, 1991, **38**, 959.
4 Ramakrishna, T. V., Robinson, J. W., and West, P. W., *Anal. Chim. Acta*, 1966, **36**, 57.
5 Firman, R. J., *Spectrochim. Acta*, 1965, **21**, 341.
6 Halls, D. J., and Townshend, A., *Anal. Chim. Acta*, 1966, **36**, 278.
7 Ramakrishna, T. V., West, P. W., and Robinson, J. W., *Anal. Chim. Acta*, 1968, **40**, 347.
8 Stojanovic, D. Dj., Vajgand, V. J., and Nikolic, S. D., *Spectrochim. Acta, Part B*, 1987, **42**, 915.
9 Andrew, T. R., and Nichols, P. N. R., *Analyst*, 1967, **92**, 156.
10 Shaw, F., and Ottaway, J. M., *Analyst*, 1975, **100**, 217.
11 Harrison, W. W., and Wadlin, W. H., *Anal. Chem.*, 1969, **41**, 374.

Determination of Trace Amounts of Aluminium in Natural Waters by Solid-phase Spectrofluorimetry

José Luis Vílchez, Alberto Navalón, Ramiro Avidad, Trinidad García-López and Luis Fermín Capitán-Vallvey*
Department of Analytical Chemistry, University of Granada, E-18071 Granada, Spain

A spectrofluorimetric method for the determination of trace amounts of aluminium was developed, based on solid-phase spectrofluorimetry. Aluminium reacted with salicylidene-o-aminophenol to form a fluorescent complex that was adsorbed on a dextran-type cation-exchange gel. The fluorescence of the gel, packed in a 1 mm silica cell, was measured directly with use of a solid-surface attachment. The applicable concentration range was from 0.20 to 14.00 μg l^{-1}, with a relative standard deviation of 1.0% and a detection limit of 0.02 μg l^{-1}. The method was applied to the determination of aluminium in natural waters. The method is more sensitive and selective than that based on salicylidene-o-aminophenol alone.

Keywords: *Salicylidene-o-aminophenol; aluminium determination; solid-phase spectrofluorimetry; natural water*

During the last decade, there has been an increased interest in the biological importance of aluminium because of evidence for the systemic toxicity of the element and the development of accurate analytical techniques.

Aluminium is used in building and vehicle construction, and in the manufacture of paint, electrical equipment, packaging containers and cooking utensils. It is used therapeutically as an antacid, in drinking-water purification and as an antiperspirant.

Aluminium toxicity has been linked to encephalopathy,[1–3] osteomalacia and osteodistrophy,[4,5] anaemia,[6,7] gastrointestinal symptoms[8] and possible cardiotoxicity[9] features.

Analyses for aluminium are mainly used to determine the blood and urine levels in individuals who work with aluminium and in patients subjected to haemodialysis[10] or receiving total parenteral nutrition.[11]

Monitoring of patients on haemodialysis is critical. Sequential determination of aluminium in serum is required and even the water used in dialysis must be checked to ensure that levels of aluminium remain low.[12]

Aluminium determination by fluorescence measurements has been widely studied, and numerous methods have been proposed.[13] One of the best known involves salicylidene-o-aminophenol as a reagent.[14–16] This method yields a sensitive and relatively selective procedure, although there are several disadvantages regarding practical applications.[15]

Solid-phase spectrofluorimetry (SPF) combines the measurement of solid-surface fluorescence with the use of a solid support (*e.g.*, an ion-exchange gel) to preconcentrate the analyte, which has been rendered fluorescent by the use of an appropriate reagent. This approach has been found to be useful for the analysis of very dilute solutions, such as water.[17–22]

In this paper, a method for the determination of trace amounts of aluminium by SPF is described, which was applied satisfactorily to the determination of aluminium in natural waters.

By using this methodology, a higher sensitivity, a lower detection limit and a lower interference level than in solution are obtained.

Experimental

Reagents

All the reagents used were of analytical-reagent grade unless stated otherwise.

* To whom correspondence should be addressed.

Sephadex CM C-25 cation-exchange gel (Pharmacia Fine Chemicals, Uppsala, Sweden) was used in the sodium form and without pre-treatment in order to avoid contamination.

Salicylidene-o-aminophenol (SOAPh). This was synthesized as described earlier[19] and used as a 1.0 × 10^{-3} mol l^{-1} solution in acetone, which was stable for at least 1 week. Solutions of lower concentrations were prepared fresh each day.

Standard aluminium(III) stock solution, 1.0 mg ml^{-1}. Prepared from Al(NO$_3$)$_3$·9H$_2$O (Merck, Darmstadt, Germany) in 0.1 mol l^{-1} nitric acid and standardized by titrimetry with ethylenediaminetetraacetic acid (EDTA) (Xylenol Orange as indicator). Working solutions were prepared by appropriate dilutions with doubly distilled water.

Buffer solutions. Solutions of the required pH were prepared from 1.0 mol l^{-1} sodium acetate (Merck) solution and 1.0 mol l^{-1} acetic acid (Merck).

Apparatus

All spectrofluorimetric measurements were performed with a Perkin-Elmer LS 5 luminescence spectrometer (Norwalk, CT, USA), equipped with a xenon discharge lamp (9.9 W) pulsed at line frequency, Monk–Gillieson F/3 monochromators, a Rhodamine 101 counter to correct the excitation spectra, a Hamamatsu R928 photomultiplier, a Houston Omnigraphic x–y recorder (Houston Instruments, Houston, TX, USA), a variable-angle solid-surface accessory, designed and constructed in-house (see Fig. 1),[23] and a Braun Melsungen Thermomix 1441 thermostat (B. Braun, Germany). In order to compare all the spectrofluorimetric measurements and ensure reproducible experimental conditions, the LS 5 spectrometer was checked daily with a sample of the fluorescent polymer standard *p*-terphenyl (1.0 × 10^{-7} mol l^{-1}) having a relative fluorescence intensity of 90% at λ_{em} = 340 nm, λ_{ex} = 295 nm; the slit-widths were 2.5 and 2.5 nm, and the sensitivity factor was 0.594.

The LS 5 spectrometer was interfaced with an IBM PS/2 30-286 microcomputer, with RS 232C connections for spectral acquisition and subsequent calculation of the excitation–emission matrices.[24] The contour plots in the excitation–emission plane were produced by linking points of equal fluorescence intensity. A Canon BJ-300 printer (Canon, Tokyo, Japan) was used for graphical representation.

A Crison 501 digital pH meter (Crison Instruments, Barcelona, Spain) with a combined glass–saturated calomel electrode and an Agitaser 2000 rotating agitator (Tecnotrans, Barcelona, Spain) were also used.
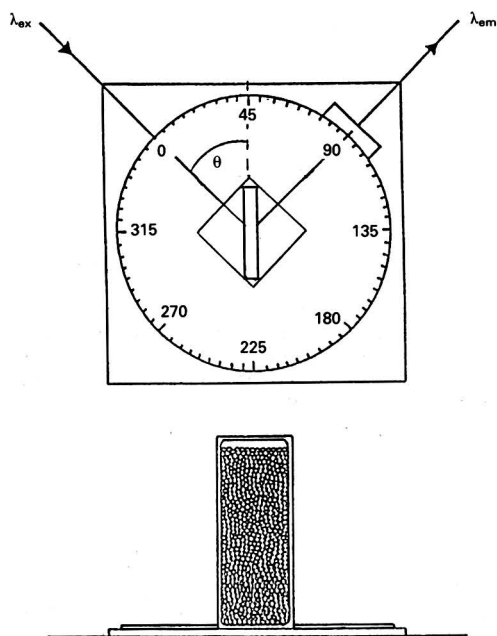
Fig. 1   Variable-angle solid-surface accessory

Fluorescence Measurements

The measured relative fluorescence intensity (RFI) of the gel beads, containing the fluorescence products and packed into a 1 mm silica cell, was the diffuse transmitted fluorescence emitted from the gel at the unirradiated face of the cell. The optimum angle between the cell plane and the excitation beam was 45° in all instances.[23]

Procedures

Basic procedure

A 500 ml water sample containing 0.20–14.00 μg l^{-1} of Al^{III} was transferred into a 1 l polyethylene bottle, and 2.5 ml of 1.0 mol l^{-1} acetic acid–acetate buffer (pH 5.80), 2.5 ml of 1.0 × 10^{-3} mol l^{-1} SOAPh and 100 mg of Sephadex CM C-25 gel were added. The mixture was shaken mechanically for 10 min. Afterwards, the gel beads were collected by filtration under suction and, with the aid of a pipette, were packed into a 1 mm cell, together with a small volume of the filtrate. A blank solution containing all the reagents except aluminium was prepared and treated in the same way as described for the sample. The fluorescence intensities (20.0 ± 0.5 °C) of the sample and blank were always measured 5 min after loading the samples at λ_{em} = 508 nm, with λ_{ex} = 410 nm. A calibration graph was established in the same way, with use of aluminium solutions of known concentration.

Procedure for natural waters

The above-mentioned reagents were added to a volume of natural water sample containing an adequate amount of Al^{III}, levelled off at 500 ml with doubly distilled water and placed in a 1 l polyethylene bottle. The subsequent steps were as in the basic procedure. The calibration graph method was used for calibration purposes.

Sample treatment

Natural waters (preserved by addition of 0.25 ml of concentrated nitric acid per litre of sample) were passed through a
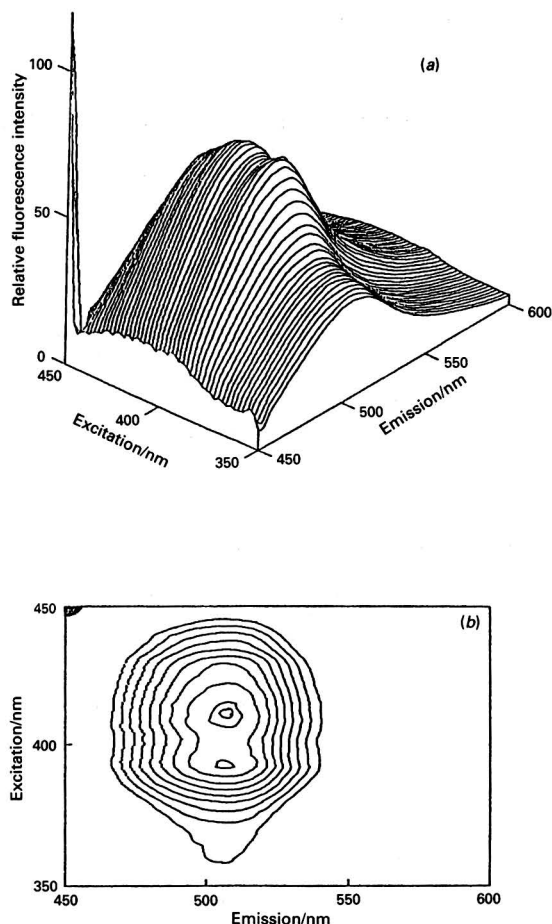
Fig. 2   (a) Projected three-dimensional spectrum of the aluminium–SOAPh complex fixed on Sephadex CM C-25 gel in an acetic acid–acetate buffer (pH 5.80). Increments in excitation wavelengths were 2 nm for each emission scan and scan speed was 240 nm min^{-1}. (b) Contour plot of the excitation–emission matrix of the aluminium–SOAPh complex fixed on Sephadex CM C-25 gel in an acetic acid–acetate buffer (pH 5.80). The contours join points showing the same relative fluorescence intensity

filter-paper with a pore size of 0.45 μm (Millipore, Milford, MA, USA) and the filtrates were collected in polyethylene containers that had been cleaned carefully with nitric acid. The samples were stored at 4 °C until analysis. Analyses were performed with the least possible delay. The usual precautions were taken to avoid contamination.[25]

Results and Discussion

Spectral Characteristics

The reagent SOAPh reacts with Al^{III}, originating in solution as a 1:1 fluorescent chelate at slightly acidic pH (approximately 6).[14-16] In the presence of Sephadex cation-exchange gel, the complex, probably cationic, is adsorbed on the gel, as the complex is not adsorbed on anion-exchange gels. A CM C-25 dextran-type gel was selected as it was found to have a lower background fluorescence.

In Fig. 2(a), the three-dimensional spectrum of the aluminium–SOAPh complex adsorbed on the gel (after the contribution of the blank has been subtracted) is represented as an

isometric projection, where the emission spectra at stepped increments of the excitation wavelength have been recorded and plotted. Computer software allows the spectrum to be examined from a high or low excitation wavelength.

In Fig. 2(b), the three-dimensional spectrum has been transformed into a contour plot in the excitation–emission plane, in order to ascertain both excitation and emission maxima.

The peak wavelengths in the excitation spectra of the SOAPh–Al^{III} system are identical for the immobilized and solvated systems (410 nm). The maxima of the emission spectra for the two systems differ, being located at 520 nm in solution and at 508 nm in the gel phase. The modification of the features of the fluorescence spectra was considered to be a result of the modification of the surrounding environment of the complex in the gel phase with respect to solution.

In addition, it was observed that a decrease in the excitation slit-width (Slit$_{ex}$) or an increase in the emission slit-width (Slit$_{em}$) increased the fluorescence signal. A similar effect has been reported by other workers.[26] For optimum excitation and emission, slit-widths of 2.5 nm were selected in both instances.

From a study of the half-life time of the excited state of the complex in the solid phase at different temperatures, it was concluded that the luminescence process was fluorescence ($\tau < 5 \times 10^{-6}$ s).

Optimization of Variables

pH dependence

First, a buffer solution from those proposed in the literature was chosen on this system in solution. The ammonium acetate–hydrochloric acid buffer[16] cannot be used, because it alters the gel. The sodium acetate–acetic acid buffer solution was found to afford the best results. The optimum pH value for the formation and fixation of the species falls in the narrow range 5.50–6.00. At pH <3.5 or >7.5 the complex is not formed and/or not fixed on the gel (Fig. 3).

The fluorescence is independent of ionic strength, adjusted with the buffer solution, NaCl or NaClO$_4$, up to 0.01 mol l^{-1}. For higher values, the fluorescence emission decreases according to the equation: RFI = 8.2 × $\mu^{-1/2}$ (RFI = relative fluorescence intensity; μ = ionic strength; r = 0.995). This effect can be attributed to the competition from other ions in the ion-exchange equilibrium.[27]

SOAPh concentration

The optimum SOAPh concentration for maximum fluorescence intensity was 5.0 × 10^{-6} mol l^{-1} for an SOAPh-to-aluminium ratio of about 11 : 1. At higher SOAPh concentrations, however, the quenching effect observed in solution appeared more pronounced in the gel phase, probably owing to the re-absorption effect of the solid matrix (SOAPh fixed on Sephadex).[28]
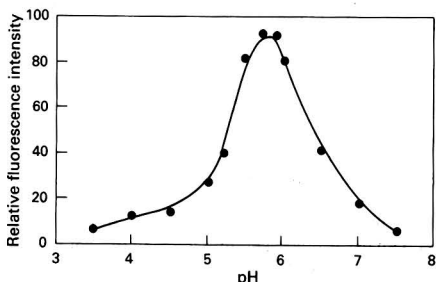
Fig. 3 Influence of pH on relative fluorescence intensity. [SOAPh], 2.0 × 10^{-5} mol l^{-1}; [Al^{III}], 1.85 × 10^{-6} mol l^{-1}; acetic acid–acetate buffer solution; Sephadex CM C-25, 100 mg; sample, 500 ml; stirring time, 10 min; λ_{ex}, 410 nm; λ_{em}, 508 nm; and T, 20.0 ± 0.5 °C

Influence of temperature

The effect of temperature on the ion-exchange process and hence, on the fluorescence emission, was studied. The ion-exchange process was independent of temperature in the range 0–40 °C, with measurement of RFI at 20.0 ± 0.5 °C. In the latter instance, the fixation of species was carried out at room temperature. On the other hand, RFI decreased when the temperature of the system increased, the effect being totally irreversible. The decrease of RFI was 0.4% at 10 °C, 0.8% at 20 °C, 12.2% at 30 °C, 43.1% at 40 °C and 78.5% at 50 °C. All RFI measurements reported here were performed at 20.0 ± 0.5 °C.

Other experimental conditions

The stirring times necessary for maximum RFI development were 10, 15, 20 and 25 min for 500, 1000, 1500 and 2000 ml samples, respectively. As the use of a large amount of the gel lowered the RFI, only the amount required to fill the cell and facilitate handling, i.e., 100 mg, was used in all the measurements. With regard to the stability of the fixed complex, the RFI, after an initial increase during 2 min of 10%, remained constant for at least 3 h. The order of addition of reagents did not affect the results obtained. The order used was aluminium, buffer, SOAPh and gel.

Effect of sample volume on sensitivity

In previous papers,[17–22] it was mentioned that one of the main advantages of SPF methods is the potential increase in sensitivity with increase in the sample volume taken for analysis. This effect can be assessed by measuring the RFI of Sephadex equilibrated with different volumes of solutions containing the same concentration of Al^{III} and proportional amounts of the other reagents.

Plots of RFI versus sample volume show an increase in fluorescence signal with sample volume, tending asymptotically to a constant RFI value above a certain volume. The shape of the graphs suggests a Langmuir-type isotherm, as is observed in some ion-exchange spectrophotometric studies.[29]

Stoichiometry of the Complex Fixed on the Gel

The stoichiometry of the SOAPh–Al^{III} complex fixed on Sephadex CM C-25 gel was studied by continuous-variation and molar-ratio methods. In both instances, the ligand-to-metal ratio found was 1 : 1. This species is identical with the complex reported by Dagnall et al.[15] and Morishige[16] in solution. The cationic nature of the complex could justify its fixation on the gel. In this study the tendency of the gel to sorb complexes with a large number of ligands was not observed. This occurrence has been described by several workers.[30–32]

Calibration and Precision

The calibration graphs for samples treated according to the procedure described above are linear for the concentration ranges 0.20–14.00 µg l^{-1} for 500 ml, 0.20–12.0 µg l^{-1} for 1000 ml and 0.10–10.0 µg l^{-1} for 1500 and 2000 ml sample volumes. The analytical parameters are summarized in Table 1.

The reproducibility of the proposed method and of the packing of the gel in the 1 mm cell was determined. The precision was measured for an aluminium concentration of 1.00 µg l^{-1} by performing ten independent determinations. The relative standard deviations (RSDs) ($p = 0.05$, $n = 10$) were 1.0, 0.9, 0.8 and 0.8% for 500, 1000, 1500 and 2000 ml samples, respectively. The precision (RSD) of the packing operation, calculated from ten measurements, was 0.9% for the aluminium–SOAPh complex fixed on the gel, 0.9% for the gel blank (gel with SOAPh and buffer) and 0.8% for the gel only. It appears, therefore, that one of the main factors

Table 1 Analytical parameters

	Sample volume/ml			
Parameter	500	1000	1500	2000
Intercept	0.1	0.3	0.2	0.2
Slope	4.68	6.65	8.56	10.34
Linear dynamic range/µg l^{-1}	0.20–14.00	0.20–12.00	0.10–10.00	0.10–10.00
Correlation coefficient	0.999	0.998	0.998	0.998
Detection limit/µg l^{-1}	0.022	0.016	0.014	0.012
Determination limit/µg l^{-1}	0.075	0.053	0.047	0.039
RSD* (%)	1.0	0.9	0.8	0.8

* RSD = relative standard deviation.

Table 2 Methods for the spectrofluorimetric determination of aluminium

Reagent	Detection limit*/ µg l^{-1}	Ref.
SOAPh	0.27	14
Morin	0.27	35
Salicylidene-2-amino-3-hydroxyfluorene	0.2	36
6-(4-Methylsalicylideneamino)-m-cresol	0.2	16
N-Salicylidene-2-hydroxy-4-carboxyaniline	0.2	37
Morin†	0.1	38
2,6-Bis[(o-hydroxy)phenyliminomethyl]-1-hydroxybenzene	0.1	39
2,4-Dihydroxybenzaldehyde semicarbazone	0.08	40
N-Salicylidene-2-hydroxy-5-sulfoaniline	0.08	37
Morin‡	0.02	18
SOAPh‡	0.02	This work

* Or minimum concentration used for calibration.
† Extraction procedure.
‡ Ion-exchange spectrofluorimetry.

Table 3 Effect of foreign ions on the determination of 1.00 µg l^{-1} of aluminium

Foreign ion or species	Tolerance level/µg l^{-1}
Li^I, Na^I, K^I, NH$_4$$^+$, Ca^{II}, Mg^{II}, Sr^{II}, Ba^{II}, Mn^{II}, Co^{II}, Ni^{II}, Cu^{II}, Zn^{II}, Cd^{II}, Hg^{II}, Pb^{II}, Sn^{II}, Fe^{II}, Pd^{II}, Fe^{III}, Cr^{III}, Ga^{III}, In^{III}, Tl^I, Tl^{III}, La^{III}, Y^{III}, As^{III}, Sb^{III}, Bi^{III}, Ce^{IV}, Se^{IV}, Mo^{VI}, W^{VI}, Cl$^-$, Br$^-$, I$^-$, ClO$_4$$^-$, NO$_3$$^-$, NO$_2$$^-$, SO$_4$$^{2-}$, SO$_3$$^{2-}$, SiO$_3$$^{2-}$	>10 000
F$^-$	100
Be^{II}	2

Table 4 Determination of aluminium in natural waters

Water	Amount found*/µg l^{-1}
Tap water (Granada City)	156 ± 2
Raw water (Genil River)	37.6 ± 0.3
Raw water (Quentar Dam)	19.0 ± 0.1
Raw water (Aguas Blancas River)	17.2 ± 0.2
Mineral water (Lanjarón)	5.12 ± 0.08
Mineral water (Ortigosa del Monte)	14.5 ± 0.2

* Average value ± standard deviation of three determinations.

Table 5 Recovery study of aluminium in natural waters

Water*	Amount added/ µg l^{-1}	Amount found†/ µg l^{-1}	Recovery (%)
Tap water (Granada City)/10 ml‡	—	3.12	—
	1.00	4.10	99.5
	2.00	5.20	101.6
	3.00	6.10	99.7
Raw water (Genil River)/50 ml‡	—	3.76	—
	1.00	4.74	99.6
	2.00	5.70	99.0
	3.00	6.68	98.8
Raw water (Quentar Dam)/100 ml‡	—	3.80	—
	1.00	4.90	102.1
	2.00	5.75	99.1
	3.00	6.92	101.8
Raw water (Aguas Blancas River)/ 100 ml‡	—	3.44	—
	1.00	4.48	100.9
	2.00	5.40	99.3
	3.00	6.50	100.9
Mineral water (Lanjarón)/250 ml‡	—	2.56	—
	1.00	3.52	98.9
	2.00	4.54	99.6
	3.00	5.60	100.7
Mineral water (Ortigosa del Monte)/ 100 ml‡	—	2.90	—
	1.00	3.96	101.5
	2.00	4.85	99.0
	3.00	5.80	98.3

* Final volume 500 ml in all instances.
† Data are the average values of three determinations.
‡ Initial sample volume in each instance.

affecting the reproducibility is the packing of the gel. Centrifugation of the gel when packed in the cell did not lead to improved precision.

Sensitivity and Detection Limit

The sensitivity in SPF methods can be enhanced by increasing the volume of the sample. In practice, this increase can be calculated from the slope of the calibration graphs. The calculated values of the sensitivity ratio (S) for the samples analysed in this study are: $S_{2000/500} = 2.21$, $S_{1500/500} = 1.83$ and $S_{1000/500} = 1.42$, where the subscripts represent the sample volumes (ml). The non-linear dependence of sensitivity *versus* sample volume can be attributed to the decrease in the distribution coefficient with analyte concentration, as is usual in a non-linear isotherm.

The increase in sensitivity obtained with the proposed method is substantial, particularly with respect to solution methods that involve use of SOAPh as a reagent. In order to compare this increase in sensitivity, the calibration graph for the determination of Al^{III} with SOAPh in solution, was established, *i.e.*, for the method of Dagnall *et al.*[14] Under our experimental conditions, the equation for the calibration graph was RFI = 0.16[Al^{III}] (r = 0.999), the ratio of the slopes being 29 : 1.

The IUPAC detection limits[33] and the limits of determination[34] were calculated for 500, 1000, 1500 and 2000 ml sample volumes. The results are reported in Table 1.

The proposed method was compared with methods described in the literature for the spectrofluorimetric determination of aluminium. For comparison purposes those methods

that were considered to be among the most sensitive reported to date were selected (Table 2).

Effect of Foreign Ions

A systematic study was carried out on the effect of foreign ions on the determination of Al^{III} at the 1.00 µg l^{-1} level. A 10 mg l^{-1} level of potentially interfering ions was tested first, and if interference occurred the ratio was reduced progressively until interference ceased. Higher ratios were not tested. Tolerance was defined as the amount of foreign ion that produced an error not exceeding ±5% in the determination of the analyte. The results are summarized in Table 3.

Interference levels were lower than those found in solution methods.[14–16] On the other hand, the proposed method is more selective than those involving methods based on morin.[18,35,38]

Determination of Aluminium in Natural Waters

The method was applied to the determination of aluminium in water samples. Tap water from Granada, which is treated with aluminium compounds for flocculation purposes, raw water from Granada supplies to the city reservoirs (Quentar Dam, Genil River and Aguas Blancas River), and mineral water from Lanjarón (Granada) and Ortigosa del Monte (Segovia) natural springs were selected. The volume of water used for the analysis depended on the aluminium content: 10 ml of tap water; 50 ml of raw Genil River water; 100 ml of raw Quentar Dam water, raw Aguas Blancas River water and Ortigosa del Monte spring water; and 250 ml of Lanjarón spring water. The analysis was carried out by the calibration graph method.

The average aluminium content (based on three determinations) in the samples studied is listed in Table 4.

The aluminium content found in tap water was higher than that in raw waters. This is related to the use of commercial aluminium salts in the water-treatment plant, as previously stated.

In order to check the accuracy of the proposed method a recovery study was carried out on the waters mentioned above. For this, various amounts of aluminium were added, and the percentage recovery was determined. Table 5 shows the results obtained for all the water samples.

References

1 Alfrey, A. C., Legendre, G. R., and Kaehny, W. D., *New Engl. J. Med.*, 1976, **294**, 184.
2 Dunea, G., and Mahurkan, S. D., *Ann. Intern. Med.*, 1978, **88**, 502.
3 Davism, A. M., Oli, H., and Walker, G. S., *Lancet*, 1982, **2**, 785.
4 Wills, H. R., *Clin. Chem. (Winston-Salem, N.C.)*, 1985, **31**, 5.
5 Gardiner, P. E., and Ottaway, J. M., *Anal. Chim. Acta*, 1981, **128**, 57.
6 Fernández Soto, I., Allende, M. T., and Díaz de Greñi, M. C., *Nefrología*, 1986, **6**, 71.
7 Drueke, T., Touam, M., and Lacour, B., *Nefrología*, 1986, **6**, 67.
8 Andreoti, S. P., Bergtein, J. M., and Sherrad, D. J., *New Engl. J. Med.*, 1984, **310**, 1079.
9 Siderman, S., and Marior, D., *Nephron*, 1982, **31**, 1.
10 Joffe, P., Olsen, F., Heaf, J. G., Gammelgaard, B., and Podenphant, J., *J. Clin. Nephrol.*, 1989, **32**, 133.
11 Vargas, J. H., Klein, G. L., Ament, M. E., Ott, S. M., Sherrad, D. J., Horst, R. L., Berquist, W. E., Alfrey, A. C., Slatopolsky, E., and Coburn, J. W., *Am. J. Clin. Nutr.*, 1988, **48**, 1070.
12 Woolfson, A. D., and Gracey, G. M., *J. Clin. Pharm. Ther.*, 1988, **13**, 243.
13 Fernández Gutierrez, A., and Muñoz de la Peña, A., in *Molecular Luminescence Spectroscopy: Methods and Applications, Part I*, ed. Schulman, S. G., Wiley, New York, 1985, ch. 4, pp. 372–546.
14 Dagnall, R. M., Smith, R., and West, T. S., *Chem. Ind. (London)*, 1965, **34**, 1499.
15 Dagnall, R. M., Smith, R., and West, T. S., *Talanta*, 1966, **13**, 609.
16 Morishige, K., *Anal. Chim. Acta*, 1980, **121**, 301.
17 Capitán, F., Manzano, E., Navalón, A., Vilchez, J. L., and Capitán-Vallvey, L. F., *Analyst*, 1989, **114**, 969.
18 Capitán, F., Manzano, E., Vilchez, J. L., and Capitán-Vallvey, L. F., *Anal. Sci.*, 1989, **5**, 549.
19 Capitán, F., Navalón, A., Vilchez, J. L., and Capitán-Vallvey, L. F., *Talanta*, 1990, **37**, 193.
20 Capitán, F., de Gracia, J. P., Navalón, A., Capitán-Vallvey, L. F., and Vilchez, J. L., *Analyst*, 1990, **115**, 849.
21 Capitán, F., Manzano, E., Navalón, A., Vilchez, J. L., and Capitán-Vallvey, L. F., *Talanta*, 1992, **39**, 21.
22 Capitán, F., Sánchez-Palencia, G., Navalón, A., Capitán-Vallvey, L. F., and Vilchez, J. L., *Anal. Chim. Acta*, 1992, **259**, 345.
23 Manzano, E., Ph.D. Thesis, University of Granada, Spain, 1989.
24 Oms, M. T., Cerdá, V., García-Sanchez, F., and Ramos, A. L., *Talanta*, 1988, **35**, 671.
25 American Public Health Association, American Water Works Association, Water Pollution Control Federation, *Métodos Normalizados para el Análisis de Aguas Potables y Residuales*, Díaz de Santos, Madrid, 1992, pp. 1.45–1.47.
26 García-Vior, L. O., and Possidoni de Albinati, J. F., *An. Quim., Ser. B*, 1987, **83**, 319.
27 Waki, H., Noda, S., and Yamashita, M., *React. Polym.*, 1988, **7**, 227.
28 Laserna, J. J., Ph.D. Thesis, University of Málaga, Spain, 1980.
29 Yoshimura, K., Ishii, N., and Tarutani, T., *Anal. Chem.*, 1986, **58**, 591.
30 Yoshimura, K., Waki, H., and Ohasi, S., *Talanta*, 1976, **23**, 449.
31 Toshimitsu, Y., Yoshimura, K., and Ohasi, S., *Talanta*, 1979, **26**, 273.
32 Capitán-Vallvey, L. F., Bosque-Sendra, J. M., and Valencia, M. C., *Analusis*, 1989, **17**, 601.
33 IUPAC, Nomenclature, Symbols, Units and Their Usage in Spectrochemical Analysis, *Pure Appl. Chem.*, 1976, **45**, 105.
34 Guidelines for Data Acquisition and Data Quality Evaluation in Environmental Chemistry, *Anal. Chem.*, 1980, **52**, 2242.
35 Will, F., *Anal. Chem.*, 1961, **33**, 1360.
36 White, C. E., McFarlane, H. C. E., Fogt, J., and Fuchs, R., *Anal. Chem.*, 1967, **39**, 367.
37 Morishige, K., *Anal. Chim. Acta*, 1974, **72**, 295.
38 Medina Escriche, J., and Hernández Hernández, F., *Analyst*, 1985, **110**, 287.
39 Capitán, F., Avidad, R., Navalón, A., and Capitán-Vallvey, L. F., *Mikrochim. Acta*, 1992, **107**, 65.
40 Morishige, K., *J. Inorg. Nucl. Chem.*, 1978, **40**, 843.

COMMUNICATION

Network Analysis: Acoustic Energy Transmission Detection of Polynucleotide Hybridization at the Sensor–Liquid Interface

Hongbo Su, Mengsu Yang, Krishna M. R. Kallury and Michael Thompson*
Department of Chemistry, University of Toronto, 80 St. George Street, Toronto, Ontario, Canada M5S 1A1

Palladium has been sputtered onto the surface of gold-plated thickness-shear mode acoustic wave sensors. Adsorption of polynucleotides onto the PdO surface is confirmed by X-ray photoelectron spectroscopy and by gas-phase sensor measurements. Hybridization of complementary strands of polynucleotide at the device–liquid interface results in series resonant frequency signals (network analysis) that are significantly higher than expected from mass-based responses. This observation is interpreted in terms of the perturbation of acoustic energy transmission by changes in interfacial properties on hybridization. Preliminary measurements of changes in motional resistance from network analysis are also presented.

Keywords: *Polynucleotide hybridization; acoustic wave sensor*

The ability of complementary deoxyribonucleic acid (cDNA) sequences to form double-stranded hybrids with high efficiency and specificity in the presence of a mixture of many non-complementary nucleic acids was first reported by Hall and Spiegelman.[1] Since this work, DNA probe technology has formed the basis of tests for genetic disease, detection of pathogenic organisms such as viruses, bacteria and parasites, establishment of personal identity in forensic cases, and assays for mutation, activation, amplification and expression of oncogenes.[2] For most of the applications, hybridization probes labelled with radioisotopes such as ^{32}P or ^{125}I are utilized because of their sensitivity and non-involvement of the label in the chemical reactivity of the probe molecule. However, owing to factors such as the time and effort involved in such radiolabelling procedures and the problem of fluctuations in specific activity, alternative transduction techniques have been explored. The two categories of hybridization detection in vogue consist of 'indirect systems' which utilize phenomena such as luminescence, and 'direct' analytical devices which are based on biosensor design.[3]

A recent addition to the strategy of direct detection of hybridization is the signal offered by the thickness-shear-mode (TSM) acoustic wave device.[4] Fawcett *et al.*[5] reported the immobilization of single strand nucleic acid on 9 MHz AT-cut piezoelectric crystals through covalent binding to a styrene–acrylic acid copolymer. Frequency measurements in air were observed following hybridization of polyadenylic acid(5') with polyuridylic acid(5'). In a similar procedure a single strand *Salmonella* DNA probe was bound to a device, but in this case the solution part of the complementary DNA was adsorbed onto particles in order to apply the gas-phase measurement.[6] The first *in situ* liquid-phase measurement involved attachment of single strand DNA to a self-assembled

monolayer of 11-mercaptoundecanoic acid bound to the gold electrode of a TSM device.[7] A subsequent experiment also demonstrated *in situ* detection of DNA hybridization (invoking a conventional mass-based response), although no evidence was presented to confirm the occurrence of hybridization at the sensor–liquid interface.[8]

The present work has been concerned with the role of interfacial properties such as surface viscosity and roughness on the TSM liquid-phase response,[9–11] and with complete characterization of the sensor by a network analysis method.[12] This technique provides the measurement of a large number of parameters in addition to the resonant frequency of the TSM crystal.[12,13] In spite of the fact that several metals and their complexes have been investigated for their interaction with DNA, very few reports have dealt with the role of metal-oxide surfaces. Therefore, a study has been undertaken to elucidate the immobilization of nucleic acids on PdO deposited onto Au-plated quartz TSM crystals with a view to the development of nucleic acid hybridization probes through acoustic transduction. The preliminary results of this work are presented here.

Experimental

Instrumentation

An HP 4195A Network/Spectrum Analyzer (Hewlett-Packard, Palo Alto, CA, USA) was used to characterize the TSM device. A 9 MHz AT-cut quartz crystal (ICM, Oklahoma City, OK, USA) with gold electrodes (diameter 0.51 cm) was coated with about 500 Å of Pd by sputtering a Pd target (99.95%, Pure Tech, Carmel, NY, USA) under Ar + O_2 using an Ultek 2400-8SA system (Perkin-Elmer, Palo Alto, CA, USA). X-ray photoelectron spectroscopy (XPS) of the polynucleotide-immobilized surfaces was performed with a Leybold Max 200 ESCA Instrument.

---

* To whom correspondence should be addressed.

Procedures

Polyadenylic acid(5') {poly[A], relative molecular mass (M_r) > 100 000} and polycytidylic acid(5') (poly[C], M_r 370 000–400 000) (Sigma, St. Louis, MO, USA) were immobilized by imposing 20 μl of nucleic acid solution (1 mg ml^{-1}) onto the Pd surface. The surface was rinsed with water and immersed in water and buffer solution (70 °C, pH 7.0 phosphate and 0.1 mol l^{-1} NaCl) for 20 min followed by drying in an oven (80 °C).

Polyuridylic acid(5') (poly[U], M_r 800 000–1 200 000) and polyguanidylic acid(5') (poly[G], M_r 170 000–300 000) (Sigma) solutions (0.2 mg ml^{-1}) were incubated to 60 °C and injected into the measurement cell which contained the poly[A] and poly[C]-coated devices, respectively. The polynucleotide-coated devices were stabilized in buffer solution at 60 °C prior to the injection and about 0.3 mg of polynucleotide was introduced upon each injection. The other, uncoated, side of the device was protected under nitrogen. Controlled experiments with non-complementary solutions were performed following the same procedure.

Results and Discussion

Characterization of the Palladium Oxide/Polynucleotide Surface by X-ray Photoelectron Spectroscopy

The XP spectra of the individual polynucleotide and the hybridized surfaces (Poly [C], Poly [U], Poly [A], Poly [G], Poly [A/U] and Poly [G/C]) were recorded without buffer treatment to avoid any contribution from these species. The C(1s) : N(1s) ratios and the N(1s) : P(2p) binding energy peak ratios computed from the low resolution elemental composition data are presented in Table 1. Also presented in the same table are the values of the ratio C(1s)$_{[C-N+C-O]}$: C(1s)$_{[C-O]}$ calculated for all six surfaces from high resolution experiments. From the data in Table 1, it can be observed that the C(1s) : N(1s) ratios are in good agreement with the calculated values.

The N(1s) : P(2p) binding energy peak ratios are a fraction higher than the theoretical values for the individual polynucleotide surfaces. This is probably due to the orientation of the molecules on the Pd surface which could result in the attenuation of the P(2p) peak. Similar attenuation was observed by Bain and Whitesides for the S(2p) peak of thiols on Au surfaces.[14] However, the hybridized surfaces do exhibit ratios close to the theoretical values, indicating that these surfaces are more uniform and possess a greater degree of orientation compared with the individual polynucleotide surfaces.

The immobilization of the polynucleotides on the PdO surface could also be verified from the high resolution C(1s) peak ratios. As these molecules only contain C–N/C–O and C=O carbons which appear around 286–287 eV and 288–289 eV, respectively, the ratio of these two peaks, in comparison with the corresponding theoretical values, also serves to confirm the deposition of the polynucleotides.

The exact nature of the binding of polynucleotides to the Pd surface is not yet clearly understood. The XPS technique

shows that the deposition of Pd under an Ar + O_2 environment produces a PdO layer, the Pd (3d) peak corresponding to the oxide appearing around 336.5 eV in contrast to Pd metal which displays its Pd (3d) peak around 335.5 eV. The interaction of Pt^{II} with nucleotides was demonstrated to involve the N-7 nitrogen of the purine ring of the guanine moieties.[15] Similarly, the complexation of cytosine with Ag^I was shown to occur through the endocyclic N-3 nitrogen of the former.[16] If these data are any indication, the present Pd^{II} surfaces can also be presumed to react with the N-3 and N-7 nitrogens of the pyrimidine and purine oligonucleotides. Further spectroscopic studies are underway to pinpoint the nature of interaction of Pd^{II} with these oligonucleotides. However, the most important feature of the immobilized polynucleotides is their stability under the hybridization conditions and their ability to interact with their complementary strands.

Detection of Polynucleotide Hybridization by Acoustic Energy Transmission

Frequency measurements recorded in air after the immobilization of the polynucleotide and subsequent drying at room temperature with nitrogen, show average decreases of about 1200 and 630 Hz for Poly [C] and Poly [A], respectively. Each of these two immobilized oligonucleotide surfaces was subjected to three sets of experimental conditions before network analysis. Thus, in experiment I, the Poly [C] surface was treated with Poly [A] and after analysis, the solution was drained off and the surface rinsed twice with buffer and then treated with Poly [G] solution. After liquid phase analysis, the surface was washed with hot buffer, dried with nitrogen and the frequency recorded in air. In experiment II, the Poly [A] used in experiment I was substituted with Poly [U], the rest of the procedure remaining the same. In experiment III, the Poly [C] surface was treated with Poly [G] alone. A similar three set (IV–VI) study was made with the Poly [A] surface, using (i) Poly [C], then Poly [U]; (ii) Poly [G], then Poly [U] and (iii) Poly [U] alone.

The frequency decreases registered, in air, with the immobilized Poly [C] surface for experiments I–III were about 150–220 Hz. Similarly, for the immobilized Poly [A] surface, the frequency shifts for experiments IV–VI were about 70–180 Hz. Interestingly the series resonance frequency exhibits significantly higher values in the solution phase upon hybridization (Table 2). For the same set of experiments, the frequency decreases in solution are about 3–7 times larger than those in air. The real-time measurements of the frequency response of the two polynucleotide-coated TSM devices upon exposure to complementary and/or non-complementary polynucleotide solutions are shown in Fig. 1. These results clearly demonstrate the occurrence of a sequence-specific hybridization process at the sensor–liquid interface when complementary nucleotides are used. The frequency shifts were negligible when the polynucleotide-coated surfaces were exposed to the non-complementary polynucleotide solution.

One of the parameters derived from the network analysis of

Table 1 XPS ratios from elemental composition and high resolution measurements on the C(1s) binding energy peaks

Oligonucleotide on the Pd^{II} surface	C(1s) : N(1s)		N(1s) : P(2p)		C(1s)$_{[C-N+C-O]}$: C(1s)$_{[C-O]}$	
	Found	Calculated	Found	Calculated	Found	Calculated
Poly [C]	3.3 : 1	3 : 1	3.5 : 1	3 : 1	6.2 : 1	7 : 1
Poly [U]	3.9 : 1	3 : 1	3 : 1	2 : 1	2.9 : 1	3 : 1
Poly [A]	2.3 : 1	2 : 1	5.6 : 1	5 : 1	No C=O carbons	
Poly [G]	3.1 : 1	2 : 1	5.7 : 1	5 : 1	8 : 1	9 : 1
Poly [A/U]	2.5 : 1	2.5 : 1	3.8 : 1	3.5 : 1	15 : 1	13 : 1
Poly [C/G]	2.5 : 1	2.5 : 1	3.8 : 1	4 : 1	6 : 1	8 : 1

Table 2 Series resonant frequency decreases of the polynucleotide-immobilized TSM devices upon hybridization

| Experiment | Immobilized polynucleotide | | Injection steps | | $\Delta f_{in\ air}$/Hz | $\Delta f_{in\ soln}$/Hz |
	Sample	$\Delta f_{in\ air}$/Hz	1	2		
I	poly[C]	1283	poly[A]	poly[G]	162	680
II	poly[C]	1156	poly[U]	poly[G]	218	544
III	poly[C]	1215	poly[G]		151	1169
IV	poly[A]	654	poly[C]	poly[U]	177	520
V	poly[A]	624	poly[G]	poly[U]	73	500
VI	poly[A]	624	poly[U]		102	570
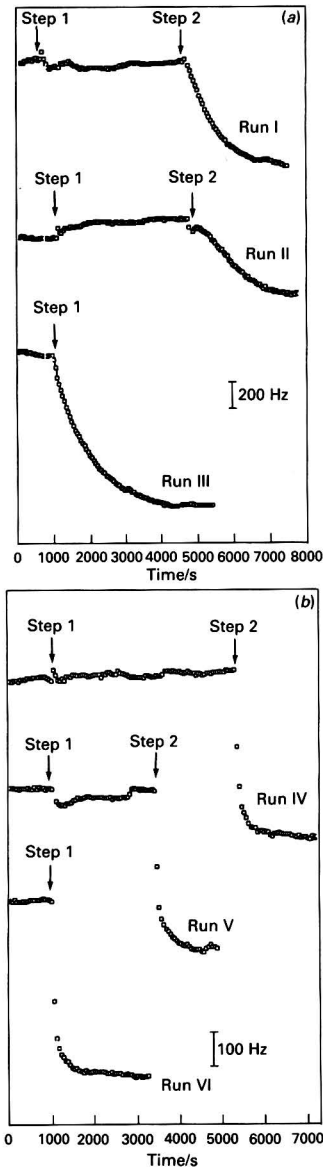
Fig. 1 Responses of the series resonant frequency of (a) the poly[C]- and (b) the poly[A]-coated TSM devices exposed to non-complementary (step 1) and complementary (step 2) polynucleotide solutions. Immobilized poly[C] treated with: poly[A] and then with poly[G] (run I); poly[U] and then poly[G] (run II); poly[G] only (run III). Immobilized poly[A] treated with: poly[C] and then poly[U] (run IV); poly[G] and then poly[U] (run V); poly[U] alone (run VI)
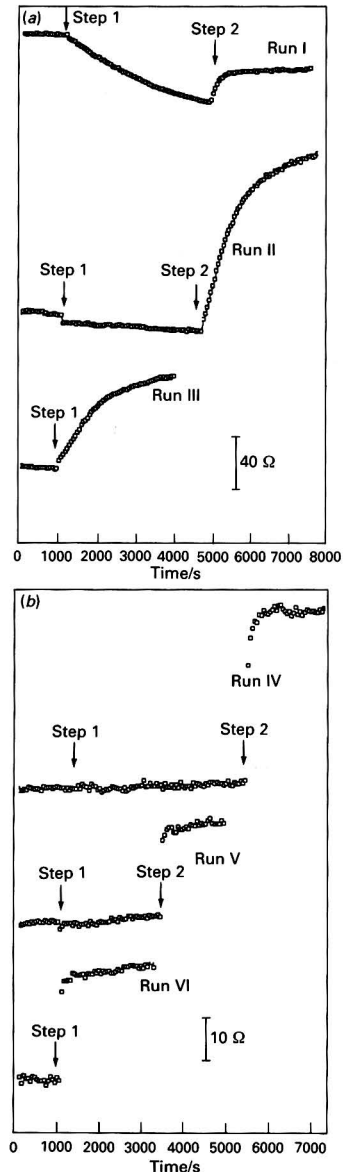
Fig. 2 Responses of the equivalent circuit resistance. For conditions see Fig. 1

the TSM device is the electric equivalent circuit resistance. The motional resistance, R_m, represents the dissipation of acoustic energy into the quartz and into the surroundings. The amount of acoustic energy transmitted to the liquid is mediated by the sensor–liquid interface and R_m changes with the structure of the interface. Rigid mass loading has a minimal effect on the resistance. The response of the resistance during the hybridization is depicted in Fig. 2. Our results indicate that R_m increases as hybridization occurs. However, a surprising unexpected difference in the behaviour of R_m can be observed that is dependent on the nature of the polynucleotide bound to the surface or based on the sequence of addition of the polynucleotide solutions in experiments I–VI. Thus, when immobilized Poly [C] is treated with the non-complementary Poly [A], a significant decrease in R_m occurs. On the other hand, when immobilized Poly [A] is reacted with a solution of Poly [C], no change in R_m is observed. Further, when immobilized Poly [C] is treated first with Poly [A] solution and then with Poly [G], only a marginal increase in R_m is observed, in comparison with the large shift in R_m recorded in experiment II (immobilized Poly [C] + Poly [U] and then Poly [G]). This increase in R_m is even larger than the example where immobilized Poly [C] is treated immediately with Poly [G] solution (experiment III). It is to be noted that the largest shift in R_m is associated with a minimal decrease in frequency (experiment II *versus* experiments I and III).

Similar variations in R_m are observed with the immobilized Poly [A] surface. The largest increase in R_m is noticed in experiment I where Poly [A] is first treated with a solution of Poly [C] and then with Poly [U]. The R_m value of the straight Poly [A]–Poly [U] hybridization (experiment VI) is intermediate between experiments IV and V.

The above observations concerning the R_m clearly indicate that although non-complementary polynucleotides do not bind to immobilized polynucleotide surfaces, they do cause a significant shift in the structure of the surface-bound molecules. As the most plausible reason for such changes with molecules such as the oligonucleotides is an orientational change at the interface, it is to be assumed that the non-complementary nucleotides bring about such alterations in the surface-anchored nucleotide molecules. Polynucleotides consist of polar sugar phosphate moieties and relatively less polar nucleobase moieties. As the binding of the polynucleotides to the PdO surface is presumed to be through the nitrogen atoms of their nucleobase, a flip-flop of these moieties will expose the sugar phosphate moieties to the liquid phase on top. The immobilized Poly [C] undergoes twice as large a shift in R_m upon treatment with Poly [U] and then Poly [G], in comparison with the immobilized Poly [A] which shows

maximum shift in R_m when treated with Poly [C] followed by Poly [U]. It appears that more sugar phosphate moieties are exposed to the medium in the former compared with the latter, which in turn indicates that pyrimidine systems undergo orientational changes more readily than purine bases at metallic surfaces.

This work demonstrates that the network analysis technique can be utilized not only for following nucleic acid hybridization but also for the study of orientational changes during the interaction between either complementary or non-complementary strands.

References

1 Hall, B. D., and Spiegelman, S., *Proc. Natl. Acad. Sci., U.S.A.*, 1961, **47**, 137.
2 Symons, R. H., *Nucleic Acid Probes*, CRC Press, Boca Raton, FL, 1989.
3 Downs, M. E. A., Kobayashi, S., and Karube, I., *Anal. Lett.*, 1987, **20**, 1897.
4 Thompson, M., Kipling, A. L., Duncan-Hewitt, W. C., Rajaković, Lj. V., and Čavić-Vlasak, B. A., *Analyst*, 1991, **116**, 881.
5 Fawcett, N. C., Evans, J. A., Chien, L.-C., and Flowers, N., *Anal. Lett.*, 1988, **21**, 1099.
6 Richards, J. C., and Bach, D. T., *Eur. Pat.*, 0 295 965, 1988.
7 Su, H., M.Sc. Thesis, University of Toronto, 1991.
8 Okahata, Y., Matsunobu, Y., Kuniharu, I., Masayuki, M., Murakami, A., and Makino, K., *J. Am. Chem. Soc.*, 1992, **114**, 8299.
9 Rajaković, Lj. V., Čavić-Vlasak, B. A., Ghaemmaghami, V., Kallury, K. M. R., Kipling, A. L., and Thompson, M., *Anal. Chem.*, 1991, **63**, 615.
10 Duncan-Hewitt, W. C., and Thompson, M., *Anal. Chem.*, 1992, **64**, 94.
11 Yang, M. Thompson, M., and Duncan-Hewitt, W. C., *Langmuir*, in the press.
12 Kipling, A. L., and Thompson, M., *Anal. Chem.*, 1990, **62**, 1514.
13 Martin, S. J., Granstaff, V. E., and Frye, G. L., *Anal. Chem.*, 1991, **63**, 2272.
14 Bain, C. D., and Whitesides, G. M., *J. Phys. Chem.*, 1989, **93**, 1670.
15 Hartwig, J. F., and Lippard, S. J., *J. Am. Chem. Soc.*, 1992, **114**, 5646.
16 Menzer, S., Sabat, M., and Lippert, B., *J. Am. Chem. Soc.*, 1992, **114**, 4644.

000526

Moving?

ADDRESS

TOWN   COUNTY/STATE

POSTAL CODE   COUNTRY

PLEASE PRINT YOUR NEW ADDRESS ABOVE AND RETURN
THIS COMPLETED SHEET INCLUDING ADDRESS LABEL TO:

THE DISTRIBUTION CENTRE
BLACKHORSE ROAD
LETCHWORTH
HERTS SG6 1HN ENGLAND

CUMULATIVE AUTHOR INDEX

JANUARY–MARCH 1993

Pre- and Post-Symposia and Short Courses XXVIII Colloquium Spectroscopicum Internationale

PRE-SYMPOSIUM

3rd Kingston Conference. Analytical Spectroscopy in the Earth Sciences
June 28–29, 1993   *Kingston University, Surrey*

SHORT COURSES

Introductory Chemometrics
June 29, 1993   *University of York*
Vapour Generation Techniques: Theory and Practice
June 29, 1993   *University of York*
Spectroscopic Data Handling
July 4–6, 1993   *University of York*

POST-SYMPOSIA

5th Surrey Conference on Plasma Source Mass Spectrometry
July 4–6, 1993   *Lumley Castle Hotel, Co. Durham*
Application of Glow Discharge in Optical and Mass Spectroscopy
July 4–7, 1993   *University of York*
Graphite Atomizer Techniques in Analytical Spectroscopy
July 4–7, 1993   *University of Durham*
Trace Elements in Clinical Biochemistry
July 7, 1993   *University of Durham*

For further information contact—
XXVIII COLLOQUIUM SPECTROSCOPICUM INTERNATIONALE
Department of Chemistry (CSI Secretariat)
Loughborough University of Technology, Loughborough, Leicestershire, UK LE11 3TU

Book Reviews

Voltammetric Determination of Molecules of Biological Significance
By W. Franklin Smyth. Pp. x + 133. Wiley. 1992. Price £35.00. ISBN 0-471-93345-7.

This small book covers the application of voltammetric techniques to the determination of biologically important compounds. Intended as a 'concise practical guide', the text is divided into eight chapters, in accordance to the nature of the electroactive functionality (following the order nitrogen-, sulfur-, and oxygen-containing molecules, hydrocarbons, halogen-containing and organophosphorus molecules, organometallics and inorganic molecules). The versatility and remarkable sensitivity of voltammetric techniques, particularly pulse voltammetry, adsorptive stripping voltammetry and amperometric detection for liquid chromatography, for trace measurements of such compounds are illustrated. Modern trends, including biosensors, modified electrodes and immunoassays are also discussed (but in a limited depth). Recent advances in *in vivo* voltammetry, ultramicroelectrodes or detection for capillary electrophoresis are not covered. Detailed theory is not given and the approach is primarily experimental. The book is clearly written, well organized and full of practical examples. It is illustrated with 50 figures, 33 tables and over 300 references (up to 1990!). Overall, the book represents a very good source of useful information, and is highly recommended for those using electrochemical techniques for measuring biological compounds.

Joseph Wang

Chemical Analysis in Complex Matrices
Edited by Malcolm R. Smyth. Pp. 295. *Analytical Chemistry Series*. Ellis Horwood. 1992. Price £50.00. ISBN 0-13-127671-9.

The 'complex matrices' given in the title encompass air (for monitoring quality), animal feeds, human foods, the types of components found in brewing, biological fluids (and analyses of these for drugs), adhesives and sealants.

The editor provides an interesting introduction to the chapters by other authors in which each stage (or 'unit process') of an analytical investigation is identified and some emphasis is placed upon defining objectives in advance, on evolving appropriate methods of sampling, and the preparation of the samples.

The subject of the most lengthy chapter is the analysis of drugs in biological fluids; it covers spectroscopic, immunoassay, chromatographic and voltammetric procedures of various kinds and includes 271 references.

As the editor and all of the contributors are at establishments in Ireland it could be expected that the chapter about brewing might emanate from a historic company with a harp as its trade mark, and it does. The chapter includes a review of the process and of applications for techniques such as atomic absorption and near infra-red spectroscopy, chromatography, *etc.*, together with the Servo Chem Automatic Beer Analyzer ('SCABA'), which is capable of analysing 20 samples of beer per hour for alcohol, gravity, colour and pH.

The chapter on sealants and adhesives reviews current types and their analysis, with emphasis mainly on nuclear magnetic resonance and chromatography but including differential-pulse anodic stripping voltammetry to obtain a profile of trace metals. In specific examples other techniques are mentioned, and still others, including thermal analysis, in the conclusion.

The chapter on analysis of air for quality and pollution includes discussion of different types of emissions, lists the procedures for sampling and methods of analysis for volatile components recommended by NIOSH, and the EPA recommendations for methods to determine toxic organic compounds in air. (In this connection it should be remembered that the exposure limits cited are not always the current ones for United Kingdom as given in Health and Safety Executive publication EH 40/92 'Occupational Exposure Limits 1992'.)

The final chapter covers chemical analysis of animal feeds and human foods and it is pleasing to note that once again the importance of sampling is stressed. There is mention of the routine procedures for protein, oil and fat, carbohydrate and fibre and nutritional analysis for amino acids *etc.*, is included. Systems are given for extraction of drugs, pesticides and growth-promoting agents from certain feedstuffs.

It is an interesting book and should prove helpful for practitioners in the fields mentioned. Parts of the text are more reviews of existing procedures rather than original matter but the volume contains enough that is original to make it of general interest; in many cases the details of extractions from the matrices should be most helpful.

I would recommend it for purchase by libraries and analysts in the fields concerned.

D. Simpson

Preparative and Process-Scale Liquid Chromatography
Edited by G. Subramanian. *Ellis Horwood Series in Chemical Engineering*. Pp. 286. Ellis Horwood. 1991. Price £55.00. ISBN 0-13-678327-9.

The book opens with a chapter that compares preparative with analytical liquid chromatography by considering operational and equipment differences and system operation. This is followed with a very practical chapter on design and control of process-scale systems discussing safety factors, selection of components (*e.g.* columns, pumps, valves and pipework), automation and validation. A further chapter on the technical structure of liquid chromatography separation plants details differences between those operating with organic solvents and those with aqueous solvents and also considers plant control systems.

The next chapter discusses column packings used in preparative chromatography. Although the discussion essentially considers only straight phase media it addresses questions concerning production routes to preparative silicas and design factors of the media (*e.g.*, particle size, pore volume and size, and particle shape). This is followed by chapters on column technologies, strategies for optimizing process chromatographic systems and determination of operating parameters in process systems. The latter chapter discusses selection of stationary and mobile phases, detectors, eluent and gradient elution regimes.

A chapter on ion-exchange processes considers selection of different grades of media, factors to consider during scale-up particularly for protein separations and media re-use. This is followed by a chapter on continuous moving bed systems that is far too long, occupying over 20% of the book, and is essentially an advertisement for a particular system.

A chapter on large scale purification of bacterial proteins discusses advantages and disadvantages of different packings and some aspects of process design. The following chapter on affinity chromatography argues in favour of this approach for protein separations to reduce the number of purification steps.

Finally there are two chapters on enantio-separations. The first describes chirality and reviews chiral packings (essentially those available for analytical applications). The second discusses optimization of preparative scale enantio-separations.

This book contains a lot of material that should be of interest to analytical chromatographers interested in preparative scale systems and to synthetic chemists considering process chromatography. However, it is this reviewer's opinion that it has been very poorly edited, contains numerous typographical errors, has poorly presented diagrams in many chapters (in one case half a blank page where a diagram has been omitted), there is too much repetition of topics between chapters and finally that excessive chapter on continuous moving bed systems. For the required price I do not recommend it.

G. P. R. Carr

Recent Developments in Ion Exchange 2
Edited by P. W. Williams and M. J. Hudson, Pp. x + 366. Elsevier Applied Science. 1990. Price £50.00; US$ 90.00. ISBN 1-85166-520-X.

The proceedings of a conference are never exciting reading material, unless the conference concerns a new field in science. Ion exchange is obviously not a new field, hence the collection of papers on recent developments will only appeal to a few readers. A newcomer to the field will not, however, receive a balanced picture of what is of concern now in ion exchange from this rather eclectic collection.

The various subjects discussed are covered by the headings: Biological Materials, Inorganic Ion Exchangers, Nuclear Industry, Theoretical Aspects and New Advances, New Materials, and Industrial Applications. However, under these headings are hidden several papers concerned with analytical applications (mainly of ion chromatography) with little or no relevance to the subject of the heading. These are the papers by Senior, Laeubli, Humphrey, and Ryder, for instance. Some of the introductory papers, such as those of Williams (on biological materials), and Bibler (on nuclear industry, where only 2 out of the 58 references are later than 1983), are more historical surveys than an exposition of recent developments. It is noteworthy that the physical chemistry of ion exchangers and the ion-exchange process appears to be a closed subject, as no new developments in this sub-field are reported (perhaps with the exception of the paper by Watson, that deals with viscous flow in the pores of macroreticular resins).

A seemingly novel method, electrochemical ion exchange, is described in the papers by Allen et al. and by Adams and Hudson. This is distinct from electrochemical methods applied to ion transport through or along ion-exchange membranes. The main features of the method have already been established prior to 1987, and its performance is not particularly impressive. Still, the concept of using electric current, as in coulometry, for the sorption and desorption of ions less noble than hydrogen is interesting. Also new and of interest are inorganic exchangers of the pillared or intercalated type, described in the papers by Dyer and Gallardo, Alberti et al., Ferragina et al., and Hudson et al. These exchangers permit larger ions or molecules to enter them, but do not change their dimensions by swelling excessively, and may have some enhanced selectivity. Pellicular ion exchangers are also relatively new materials, that combine the advantages of low swelling, very rapid kinetics and good selectivity as described in the papers by Cook and by Pohl.

The camera-ready format of the papers detracts considerably from the appearance of the book. In particular, the editorial modifications were printed in a different type (generally much smaller, sometimes in bold italics) than the main text, producing an unpleasant aspect. Most of the papers have abstracts, but some (those of Cook, Ferragina et al., and McGarvey and Gonzalez) have none. The editorial work on the whole appears not to have been very careful.

For the sake of those readers that might need access to the information included in some specific papers, the book should be on the shelves of some central libraries. Most libraries, and certainly individual practitioners of ion exchange, can do without it.

Y. Marcus

Immunochemical Assays and Biosensor Technology for the 1990s
Edited by Robert M. Nakamura, Yasushi Kasahara, Gary A. Rechnitz. Pp. ix + 411. American Society for Microbiology. 1992. Price US $43.00 (member): US $51.00 (non-member). ISBN 1-55581-040-3.

This book is broadly divided into three sections dealing with the concepts of immunochemical assays, the principles of different types of non-isotopic immunoassay and biosensors. The section on concepts is built around chapters dealing with general principles, the choice of labels and antibodies available, together with guidance on the validation of assays. Authors are faced with a major dilemma when preparing texts in the field of immunoassay because of the wealth of knowledge and attendant literature, and it is often difficult to do justice to the breadth of the subject whilst offering a critical viewpoint. Thus, the opening chapter on general principles whilst covering the topic does not focus sufficient attention on some of the important aspects, e.g. reaction kinetics and specificity. The following two chapters deal with labels with a considerable degree of overlap; some useful critical observations are made by Larry Kricka and will be of help to those readers who are new to the field wanting some help through the maze of labels that are available.

The chapter on design and production of antibodies is a valuable contribution. This is an area of considerable growth where art is giving way to science and the inherent benefit to the analyst; the authors explore some of the strategies that can be employed to produce antibodies to meet specific analytical goals. The evaluation of these products is then given a rigorous airing; the discussion should give confidence to clinicians who use the results.

The second section on non-isotopic assays explores the principles and design of several different immunoassay configurations. However, I was disappointed with the limited amount of consideration given to the principles of light scattering immunoassay. The chapter on homogeneous enzyme immunoassay was also disappointingly brief, particularly as there are so many exquisite variations on the theme of modulating catalytic activity. These are becoming 'black box' technologies and consequently there is a need to explore them thoroughly by the written word because the routine analyst has little opportunity to do so at the bench. One could make a similar observation about the limited treatment of homogeneous fluoroimmunoassay.

One of the major developments in this field is now in the integration of immunoassays into delivery systems. Unfortunately this does not receive sufficient coverage; again this is often technology where the literature is not in the public domain. It is important that analysts are aware of design strategies, limitations and potential applications although one accepts that patents can scare off all but the brave or rich.

My particular disappointment with this book was the section on biosensors because the title had led me to expect a review of immunoassay technology that would lead the reader logically into the expanding, and often 'difficult', literature on

immunosensors. Thus, whilst there was a good chapter on electrochemical detection in immunoassay, which should have appeared in the previous section, there was very little discussion of immunosensor technology (theory or application). Thus there was nothing on the surface plasmon, total internal reflection, piezoelectric *etc.* devices, where it is even more important to explain the basic principles to the reader.

Despite some rather negative comments I think that the book is nicely presented and offers some valuable contributions; however, it does not provide the link between immunochemistry and sensor technology expected from the title and it is not sufficiently comprehensive in reviewing all of the analytical principles that are going to have an impact in the next few years.

C. P. Price

Biosensor Principles and Applications
Edited by Loïc J. Blum and Pierre R. Coulet. Bioprocess Technology Series 15. Pp. x + 357. Marcel Dekker. 1992. Price US$ 125.00 (US and Canada); US$143.75 (all other countries). ISBN 0-8247-8546-0.

This is an excellent text containing a wealth of detailed information of interest not only to the specialist in biosensor research, but to those working in the many biosensor related areas such as fabrication technologies, clinical diagnostics, environmental monitoring, synthetic chemistry and data processing who are looking for ideas or applications.

The book consists of 14 chapters written by world leaders in biosensor research. It opens with a useful introduction to biosensors by Pierre Coulet that addresses the philosophy and definition of the term 'biosensor'. This is followed by three chapters dedicated to electrochemical biosensors covering amperometric enzyme electrodes, amperometric enzyme immunoassay biosensors and potentiometric enzyme electrodes. The often neglected area of thermally sensitive devices is covered in detail by Bengt Danielsson in a chapter on Enzyme Thermistors.

Other chapters cover the use of piezoelectric and field-effect-transistor (FET)-based biosensors, while three chapters address the rapidly growing area of the fibre-optic sensors. These contributions are divided into chemically mediated, fluorophore and chromophore, and bioluminescence- and chemiluminescence-based biosensors.

All the above chapters follow a similar format that includes details on the general principles of the biosensor type, fabrication techniques (with particular emphasis on the problem of immobilization of the bioactive component at the sensor tip), problems and limitations (re-usability is common to most of these, particularly with respect to antibody–antigen systems where the reactions are difficult to reverse without using extreme conditions that damage the sensitive bioactive components in the sensor membrane. The instrumentation required for obtaining and processing the sensor signal is also discussed as is the design of the biosensor itself. Examples of applications are also included.

Each chapter finishes with a useful section on research trends and potential developments. Problems and limitations are presented in a way that helps the reader to develop a realistic appraisal of biosensors, rather than to oversell their usefulness, a very laudable attitude given the exaggerated claims that have been all too common in the past.

In contrast to the contributions mentioned above, which deal with biosensors in terms of the transduction mechanism, the final four chapters approach the topic of biosensors from a different perspective. Chapters 11 and 12, entitled Immunosensors and Microbial Biosensors, respectively, approach the topic from the point of view of the biosensing element. While this does lead to a certain amount of overlap with the content of the previous chapters, it enables the reader to see how a particular approach, such as the use of microbes rather than enzymes or antibodies as the biosensitive component in the sensor, has been applied across the range of transducers (electrochemical, acoustic, thermal, optical) available. This is very useful as it collates and expands on information that is scattered over the previous chapters.

These contributions are followed by a chapter by Vadgama and Desai on *in vivo* biosensors. The development of inplantable devices for real-time monitoring of important clinical species remains a major challenge to all sensor researchers. The authors have reviewed the progress to date and highlight existing problems and the potential of *in vivo* biosensors. Interestingly, they adopt the broader definition of the biosensor that focuses on the application rather than the device itself (*i.e.* a sensor that is directly in contact with a biological matrix or surface but which does not necessarily incorporate a biological component itself). This enables the authors to include devices such as catheter ISEs and oxygen sensors, tissue and transcutaneous oxygen sensors, the Severinghaus CO_2 electrode, pH ISFETS and optrodes in their review as well as 'mainstream' biosensors such as the glucose, lactate and other enzyme-based sensors.

This broad view of the term 'biosensor' is in contrast to that adopted by the authors of the previous chapters who tend to insist of the presence of a biorecognition element in the sensor transduction cycle. However, these divergences of opinion are understandable as these authors are clinical users of sensors rather than inventors, and the problems involved with developing *in vivo* devices are common to all types of sensors.

The editors finish up with a chapter discussing the trends and prospects for biosensors. In this chapter, they highlight different areas of research that could make a significant impact on the performance of biosensors.

Each chapter is extensively referenced (100–200 references in most cases) with reasonably up-to-date citations (up to 1990), and the book is completed by a detailed index. The authors list includes Guilbault, Arnold, Bannister, Karube, Kaufmann, Kimura, Turner and Wolfbeis and other experts in biosensor research. All in all, this is an excellent addition to the growing literature on biosensors and I recommend it to anyone working or interested in the development or applications of biosensors.

Dermot Diamond

Gas Chromatographic Enantiomer Separation with Modified Cyclodextrins
By Wilfried A. König. *Chromatographic Methods.* Series Editors W. Bertsch, H. Frank, W. G. Jennings and P. Sandra. Pp. viii + 168. Hüthig. 1992. Price DM 138.00. ISBN 3-7785-2026-1.

The past decade has witnessed a remarkable increase in research on chiral separations for analysis, due partly to the greater demands of regulatory authorities for high quality characterization of drugs, pesticides and food additives, but also to an increasing interest in the problems of chiral discrimination *per se.* Many of these analytical methods have been based on the successful development of enantioselective stationary phases for HPLC. Thus the present book by Professor König is all the more welcome for bringing a well-balanced focus on recent developments in enantioselective GC, which until now has been something of a cinderella in the field. This monograph largely summarizes the contributions of the König group in developing practicable GC phases for enantioseparation based on substituted cyclodextrins (CDs), but does so with a helpful perspective on the valuable contributions of others in the field, including Schurig and Armstrong. The book consists of two principal sections, a

general introduction to the historical and synthetic development of modified CDs, and an extensive collection of applications based primarily (but not exclusively) on the well characterized phases developed by the König group. Two very short chapters give an initial treatment on the putative mechanism of host–guest interactions with modified CDs, together with a summary of some recent studies with high-field ¹H NMR.

A brief but valuable discussion of the historical development of enantioselective GC methods, based partly on an earlier monograph by the same author in 1987, concludes with the prophetic statement by Szejtli in 1987 predicting the 'successful utilization of derivatized CDs in capillary GC for the excellent chiral recognition and resolution of many racemates'. That this should have been so quickly demonstrated independently by Schurig (actually in 1987) and by König in 1988, leading to the renaissance of enantioselective GC, is in itself remarkable. The general introduction gives an authoritative account of the synthesis and fundamental properties of a range of derivatized CDs, limited necessarily to those developed by the author, or well known in the literature. Apart from some obvious typographical errors and a few inconsistencies in the author's own use of his valuable scheme of abbreviations for the CD derivatives [e.g., in Table 6 heptakis-(3-O-butyryl-2,6-di-O-pentyl)-cd is incorrectly described as the γ-CD derivative], this is a valuable introduction to the essential reactivity and chemistry of α-, β- and γ-CDs.

Although the detailed description of synthetic routes (all of them published) can be regarded as peripheral in a monograph on chromatographic methods, they do afford a useful insight into the difficulties involved and the care required to characterize the products adequately, illustrating the use of Gray's reductive depolymerization method, quantitative GC, GC–MS and NMR. The description of the author's so-called 'inversely substituted' derivatives is particularly valuable, whereby the secondary hydroxyl at C_2 and the much less reactive hydroxyl at C_3, located on the wider end of the CD torus, are substituted by pentyl groups, while the primary C_6 hydroxyl at the narrower end of the torus is selectively substituted by various alkyl groups, to give the 6-O-alkyl-2,3-O-pentyl CD derivative (by contrast with the more easily formed 2,6-O-pentyl-3-O-alkyl CDs previously described). This chapter also gives useful practical data on the preparation and testing of Pyrex glass and fused silica capillary columns.

This monograph has an excellent collection of applications, all the more remarkable for its diversity considering the relatively short time since the development of these new phases. The author has wisely chosen to group the applications for ease of reference by classes of compound, ranging from alkanes and cycloalkanes, through epoxy alcohols, carbohydrates, and ketones to amino acids. There is a particularly useful discussion on the problems of racemization of amino acids and some new techniques for the analysis of all amino acids involved in protein synthesis. Most of the major fields of application are covered in this extensive chapter, including the assignment of absolute configuration to natural compounds (pheromones, flavours, peptide antibiotics), determination of enantiomeric excess in asymmetric synthesis (with a nice discussion of the Sharpless asymmetric epoxidation procedure), in chiral synthons, auxiliaries and catalysts and in several pharmaceuticals. A small sub-chapter on the analysis of chiral drugs is the only section devoted to a specific application area, illustrated by reference to barbiturates and similar heterocyclic systems. It would have been helpful to have included a table cross-referencing the many other drugs described under the individual chemical classes, e.g., antibiotics, ibuprofen (non-steroidal anti-inflammatory), anaesthetics and CNS agents. However, this is a minor criticism, given the comprehensive index provided. Moreover, some advances in techniques are presented, including the use of two-dimensional GC, where the peak is 'heart-cut' from the first-column

for resolution on a chiral column. It would have been useful to have referred to recent applications in SFC, notably by Schurig in 1991.

The monograph concludes with brief reference to the putative mechanisms of supramolecular host–guest interactions, and some preliminary data on high-field ¹H NMR studies of model systems.

The book is strongly recommended as an introduction to the new field of chiral GC on modified CD phases, for which this monograph will serve as an excellent guide both to newcomers and experienced researchers alike. As a source book of applications the author has succeeded in condensing work from some 270 citations into a readable and useful format. This book should serve as a valuable stimulus to further research in the field and will be invaluable to those wishing to gain an informed insight into the present state-of-the-art of chiral GC based on modified CD phases.

Anthony F. Fell

Coal Quality and Combustion Performance. An International Perspective
Edited by J. F. Unsworth, D. J. Barratt and P. T. Roberts. *Coal Science and Technology 19*. Series Editor Larry L. Anderson. Pp. x + 638. Elsevier. 1992. Price US$223.00; Dfl435.00. ISBN 0-444-88703-2.

This book emphasizes the challenge the fuel technologist has in designing combustion and heat-exchange systems for a material so diverse in composition and physical characteristics as coal. I particularly like the efforts of the authors to validate the analytical methods by establishing international round-robin exercises for sampling and analysis of coal. They have then utilized their analytical and fuel oil combustion experience to produce a text giving help and a fundamental understanding of the qualities of international coals and their influences on combustion plant efficiency and related processes. I agree with the authors whole-heartedly in their suggestion that the volume will earn its rightful place alongside the works of other distinguished authors in the field. It certainly will sit on my own bookshelves alongside the works of Lowry.

The text of the book is easy to read and flows logically from chapter to chapter. The three main sections, described briefly later, are all prefaced, which I found particularly helpful in establishing the scene for the following chapters. Figures and illustrations are also clear and well thought out. However, the reproduction of the plates, particularly the scanning electron micrographs, is a little disappointing in relation to the other very high qualities of the book.

To give a flavour of this exceptional book, I will briefly comment on the contents of its chapters. The book sets the scene for the later chapters nicely by describing in the introduction the international scene in coal trade and the fundamental approach to research, i.e., coal constitution, laboratory assessment of combustion behaviour, burning trials in pilot scale plant and finally usage, as in power station combustion.

The first part of the book, Part A, Coal Characteristics, continues with descriptive chapters on coal quality and analysis, organic structure of coal with two very interesting sections on rank and maceral composition. Finally, in this section of the book the last chapter deals with specific inorganic heteroatom influences on coal combustion, i.e., sulfur and nitrogen and also the effect of other mineral matter.

Part B of the book details chapters on the influence of organic components on combustion performances. Particular emphasis is given to pulverization, pyrolysis, char-oxidation, with a very useful chapter on maceral influences on high temperature oxidation temperature. Carbon burn-out is

discussed in some detail with full scale validation of burn-out calculation models. Finally, in Part B, the development of a model for flame stability is discussed and the influence of rank demonstrated. The authors clearly state the assumptions made in their model predictions and the limitations in their calculations.

The final section, *Part C*, of the book deals with the influence of heteroatom and inorganic components on combustion performance.

Chapter 10, in this section, deals with coal quality effects on boiler operation and pollutant emissions and clearly demonstrates the inadequacy of the conventional, and much used, 'slagging and fouling indices', to predict boiler performance. The authors rightly conclude that such indices should not be taken as generally applicable to all coal-fired boiler systems. The atmospheric emission section of this chapter discusses particulates, oxides of nitrogen, sulfur and carbon, and trace elements, in the light of current international legislative limits. The final three chapters of the book deal with the prediction of ash deposition by combustion limits and suggested practical methods for prevention and removal, the evaluation of ultra-fine coal as an option for industrial fired boilers and finally the fates of fly ash, nitrogen and sulfur during combustion.

I consider I have been privileged to be asked to review a book of such high quality and fuel technologists world-wide, I am sure, will recognize its worth and add it to their own bookshelves.

W. C. Pearce

HPLC Methods on Drug Analysis
By Mantu K. Ghosh. Pp. xvi + 586. Springer-Verlag. 1992. Price DM198.00. ISBN 3-540-53824-0; 0-387-53824-0.

The book reviews HPLC methods of analysis for over 230 different drugs. Methods are presented for the analysis of drug substances, formulated products and for the measurement of drugs in biological matrices such as plasma and urine. Literature references from over 50 journals and publications are used, with the majority coming from the established chromatography and pharmaceutical publications such as *Journal of Chromatography* (including Biomedical applications), *Journal of Chromatographic Science, Journal of Pharmaceutical and Biomedical Analysis* and *Clinical Chemistry*.

Each drug entry is arranged alphabetically and contains information on the compound, such as the Chemical Abstracts Service number, chemical name, empirical formula, molecular mass, proprietary names, clinical use, solubility and light absorption. This is followed generally by several HPLC methods covering a variety of applications.

Within each method, details are given of type of sample, extraction procedures, equipment used, column, mobile phase, flow rate, internal standard, injection size, method of detection and recording, and the reference publication. A particularly valuable section in each entry includes data on retention times of related substances such as metabolites, degradation products and co-prescribed or similar drugs.

Other useful information contained in the book are tables of HPLC separation system characteristics, descriptive guides to sorbent selection and a solvent miscibility table. Of lesser value are tables of elemental atomic weights and unit conversion factors. A list of abbreviations and glossary of terms used in the text are also included.

Overall, the book contains a comprehensive survey of HPLC methods for the drugs listed and will be a valuable addition to the literature of any practising analytical chemist in the areas of pharmaceutical chemistry, dosage form analysis, bioanalysis and clinical chemistry.

Some important modern drugs are omitted from the book, presumably because of their omission from the general current literature. Chiral chromatography is mentioned for some drugs, but is not covered in specific detail.

The book will be a good practical guide to analysts wishing to set up methods, not only for those drugs listed, but also for compounds with similar structures and properties.

The author has clearly undertaken a painstaking and thorough review of the recent literature on HPLC methods for drug analysis, and his book can be recommended for general use by analysts in the pharmaceutical field.

I. E. Davidson

Mass Spectrometry in the Biological Sciences: A Tutorial
Edited by Michael L. Gross. Pp. xxi + 461. *NATO ASI Series. Series C: Mathematical and Physical Sciences. Volume 353.* Kluwer Academic. 1991. Price Dfl255.00; US$146.00; £87.00. ISBN 0-7923-1539-1.

The spectacular advances in the science of mass spectrometry since 1975 formed the subject for the NATO Advanced Study Institute on Mass Spectrometry in the Molecular Sciences held in Italy in June 1990. At that Institute, the senior lecturers decided, wisely, against publishing a series of short articles in mass spectrometry as a record of the meeting and instead came up with the idea of a tutorial-type review. Divided into three parts on instrumentation (140 pages), methods (180 pages), and applications to biomolecules (130 pages), the volume is designed to serve as a tutorial on the current status of biological mass spectrometry. It is said to be appropriate for newcomers and graduate chemists. There are 29 contributions from a group of 52 internationally respected authors.

The instrumental topics include the theory of electric and magnetic sectors, hybrid tandem mass spectrometry, triple quadrupole systems, ion traps, Fourier transform mass spectrometers, time-of-flight analysers and ion detectors. The section on methods covers the major in-vogue ionization techniques such as electrospray and matrix assisted laser desorption, as well as more established methods such as plasma desorption, continuous-flow fast atom bombardment, liquid chromatography–mass spectrometry, semi-empirical molecular orbital theory, and neutralization–reionization mass spectrometry. Reflecting current trends in the literature, the majority of the applications concern peptides, glycopeptides and proteins, but nucleic acid components and lipids are also covered to some extent. Each contribution is accompanied by a list of references, predominantly citing papers published from 1985 to 1990. The book ends with a subject index.

So, what makes this book different from other collections of reports? It is called a tutorial. Presumably this title implies a didactic approach, maybe even an interactive text with self-assessment questions, and writing that is somewhat less passive or formal than in a standard textbook. The reader may even expect practical hints that do not often appear in conventional reviews. Unfortunately, none of these expectations is realized. This reviewer could not distinguish the contributions from conventional reviews (apart from some of the chapters on applications which have much the same format as conventional papers). Hence, the book's sub-title is misleading.

Many of the reviews are clear and enjoyable expositions but are not gentle enough for newcomers to mass spectrometry. I would only recommend this book to those with a grasp of the basics and a background in the traditional aspects (electron ionization, gas chromatography–mass spectrometry, and so on). Such readers could use this 'tutorial' to update and extend their knowledge to modern methods.

One set of authors was brave enough to note that their field is developing so rapidly 'that this picture may well be out of date by the time this chapter is in print'. However, the book succeeds in reflecting the status of biological mass spectrometry in 1990. In fact, the volume covers a wider range of mass spectrometry than might be expected. Overall, there is a lot of useful information in this book but beware, the information is not as accessible as the title suggests.

M. E. Rose

Analytical Artifacts: GC, MS, HPLC, TLC and PC

By Brian S. Middleditch. *Journal of Chromatography Library. Volume 44.* Pp. xxiv + 1034. Elsevier. 1992. Price US$241.50. Dfl. 495.00. ISBN 0-444-97159-6.

How often as an analyst have you tried to fit the odd peak and perplexing mass spectrum to the problem in hand, only to discover that the compound in question was a contaminant? Indeed in these days when detection limits are going to much lower levels, whilst the range of analytes are becoming far more complex, the problem of the formation of artifacts and general contamination is a serious one.

This latest book from Brian Middleditch should be on every Analyst's shelf. Based on a format originally used with his earlier work on 'Priority Pollutants' this latest book has expanded on the mass spectra shown there and includes details of chromatography and other analytical procedures used. Each entry is headed by the common name, empirical formula and molecular mass based on the most abundant isotope (*e.g.*, Cl = 35, not 35.5). This is followed by the mass spectrum, all

EI at 70 eV. Next a structure, CAS number, Merck Index and synonyms.

The bulk of the entry is an abstract describing the reported appearance of the artifact complete with description of its origin, spectra of any derivatives formed and a reference.

To help with the interpretation there are 8-peak style tables laid out with details of the mass spectra. A comprehensive index of references and authors is also given.

This is the moment when the book becomes a real joy to read. When first opened I was intrigued by an entry 'Pink Beards and Black Spots'. The entry describes work by A. J. P. Martin in the early days of chromatography when purple spots due to amino acids appeared to grow a pink beard. Eventually the cause was traced to the fan used to dry the paper after the first direction which had a badly sparking commutator. This deposited black spots of copper on the paper and the pink beards were due to complexes of the amino acids with copper.

Well the book has many tales like that and the author addresses this in his preface. 'This book . . . is dedicated to the innumerable scientists who made mistakes, used impure chemicals and solvents, suffered the consequences of unanticipated side-reactions, and were otherwise exposed to mayhem yet were not too embarrassed to publish their findings. Contributions to a sequel will be gratefully received.'

Lest this review suggest that the book only comprises such tales it should be stressed that the bulk of the entries describe the artifacts most of us are familiar with such as plasticizers, TLC binders, decomposition products in stale blood, artifacts from stationary phases and more. These are listed as that, so there is a section on TLC artifacts with cross references to the individual entries where the artifact is described in detail.

In conclusion this is a book to be recommended for every laboratory carrying out analytical work using TLC, GC and mass spectrometry. I am looking forward to the sequel; indeed I may have an embarrassing tale or two of my own to tell.

N. J. Haskins

Conference Diary

Date	Conference	Location	Contact

March

30–1/4	12th Pharmaceutical Technology Conference	Elsinore, Denmark	**The 12th Pharmaceutical Technology Conference,** 24 Menlove Gardens North, Liverpool, UK L18 2EJ

April

3–4	VDI-Meeting on Progress in Thermic, Catalytic and Sorptive Exhaust Cleaning	Mannheim, Germany	**VDI,** Verein Deutscher Ingenieure (Kommission Reinhaltung der Luft), Graf Recke-Strasse 84, P.O. Box 1139, D-W-4000 Düsseldorf 1, Germany
4–8	XIIIth World Congress on Occupational Safety and Health	New Delhi, India	**National Safety Council,** P.O. Box 26754, Siom, Bombay 400022, India
5–7	3rd International Conference on Ion-Beam and Surface Specific Analysis Techniques	Namur, Belgium	**Professor G. Demortier,** Facultes Universitaires, N-D de la Paix, 22 rue Muzet, B-5000 Namur, Belgium
5–9	4th International Meeting on Trace Elements in Medicine and Biology	Chamonix, France	**A. Favier,** Laboratoire de Biochimie C., Hopital A. Michallon, B.P. 217X, F-38943 Grenoble Cedex 09, France **Tel:** +33 76 76 54 07. **Fax:** +33 76 42 66 44
5–8	Annual Chemical Congress, 'New Materials: New Toxicology'	Southampton, UK	**Mervyn Richardson,** BASIC, 6 Birch Drive, Maple Cross, Rickmansworth, Hertfordshire, UK WD3 2UL **Tel:** +44 923 774187. **Fax:** +44 494 714516
6–7	BTS Colloquium (of the British Toxicology Society) on Early Markers of Carcinogenesis	Canterbury, Kent, UK	**Dr. E. S. Harpur,** Sterling Winthrop Research Centre, Willowburn Avenue, Alnwick, North Cumberland, UK NE66 2JH
13–17	International Meeting on the Effects of War Activities in the Environment	Zadar, Croatia	**Mervyn Richardson,** BASIC, 6 Birch Drive, Maple Cross, Rickmansworth, Hertfordshire, UK WD3 2UL **Tel:** +44 923 774187. **Fax:** +44 494 714516
18–21	Fourth International Symposium on Pharmaceutical and Biomedical Analysis	Baltimore, MD, USA	**Shirley E. Schlessinger (Symposium Manager),** PBA '93, Suite 1015, 400 East Randolph Drive, Chicago, IL 60601, USA **Tel:** +1 312 527 2011.
19–21	ANAKON '93	Baden–Baden, Germany	**Gesellschaft Deutscher Chemiker,** Abteilung Tagungen, Varrentrappstrasse 40–42, Postfach 90 04 40, D-6000 Frankfurt am Main 90, Germany **Tel:** +49 69 79 17 366. **Fax:** +49 69 79 17 475
19–22	Annual Physics Congress: Spectroscopy, The Changing Face of Physics	Brighton, UK	**Spectroscopy, The Changing Face of Physics,** The Conference Department, The Institute of Physics, 47 Belgrave Square, London, UK SW1X 8QX **Tel:** +44 71 235 6111. **Fax:** +44 71 259 6002
19–23	Focus '93: The Association of Clinical Biochemists Annual National Scientific Meeting and Exhibition	Birmingham, UK	**Pat Nielsen,** Pipers, Main Street, Akeley, Buckingham, UK MK18 5HW
19–22	ECIO '93: European Conference on Integrated Optics	Neuchatel, Switzerland	**O. Parriaux,** Conference Chair, Centre Suisse D'Electronique et de Microtechnique, Maladiere 71, Case Postale 41, CH-2007, Neuchatel, Switzerland **Tel:** +41 38 205 111. **Fax:** +41 38 205 630
20–23	International Symposium on Electroanalysis in Biomedical, Environmental and Industrial Sciences	Loughborough, Leicestershire, UK	**Dr. Arnold Fogg,** Electroanalysis Conference, Chemistry Department, Loughborough University of Technology, Loughborough, Leicestershire, UK LE11 3TU
20–23	5th European Congress on Biopharmaceutics and Pharmacokinetics	Brussels, Belgium	**Mrs. F. Rey,** 3/17 Avenue de l'Observatoire, B-1180 Brussels, Belgium **Tel:** +31 2 375 1648. **Fax:** +31 2 375 3299
25–29	Eurolab 93, 12th SFBC National Meeting/10th IFCC European Congress of Clinical Chemistry	Nice, France	**Groupe SEPFI,** Technoexpo, 8 rue de la Michodière, 75002 Paris, France **Tel:** +33 1 47 42 92 56. **Fax:** +33 1 42 66 14 28

Date	Conference	Location	Contact
25–29	**84th AOCS Annual Meeting & Expo: A joint meeting with the Japan Oil Chemists' Society**	Anaheim, CA, USA	**American Oil Chemists' Society,** P.O. Box 3489, Champaign, IL 61826-3489, USA
26–1/5	**'Wasser', Berlin'93**	Berlin, Germany	**Cornelia Wolff,** v.d. Sahl, AMK Berlin, Ausstellungs-, Messe- und Kongress-GmbH, Postfach 19 17 40, D-1000 Berlin 19, Germany
27	**Validating Multicomponent Analysis**	London, UK	**Mr. T. Frost,** The Wellcome Foundation, Dartford, UK DA1 5AH

May

Date	Conference	Location	Contact
2–7	**CLEO/QELS '93, The Thirteenth Conference on Lasers and Electro-Optics concurrently with the Quantum Electronics and Laser Science Conference**	Baltimore, MD, USA	**Meetings Department,** Optical Society of America, 2010 Massachusetts Avenue, NW, Washington, DC 20036-1023, USA **Tel:** +1 202 223 9034. **Fax:** +1 202 416 6100
3–5	**EuroResidue II: Residues of Veterinary Drugs in Food**	Veldhoven, The Netherlands	**Dr. N. Haagsma,** Department of the Science of Food of Animal Origin, Faculty of Veterinary Medicine, University of Utrecht, P.O. Box 80.175, NL-3508 TD Utrecht, The Netherlands **Tel:** +31 30 535 365. **Fax:** +31 30 532 365
3–5	**Fifth Symposium on the Analysis of Steroids**	Szombathely, Hungary	**Professor S. Görög,** c/o Chemical Works of Gedeon Richter Ltd., P.O. Box 27, H-1475 Budapest, Hungary **Tel:** +36 1 157 4566. **Fax:** +36 1 157 1578
4	**Capillary Chromatography: the Spring Symposium and Annual General Meeting of the Chromatographic Society**	Greenford, Middlesex, UK	**The Executive Secretary,** The Chromatographic Society, Suite 4, Clarendon Chambers, 32 Clarendon Street, Nottingham, UK NG1 4BU **Tel:** +44 602 500596. **Fax:** +44 602 500614
4–5	**ASTM Symposium On Quality And Statistics: Total Quality Management**	Atlanta, GA, USA	**Scott Orthey,** ASTM, 1916 Race Street, Philadelphia, PA 19103, 215/299-5507, USA
4–6	**Deauville Conference and Symposium on Analytical Sciences—SAS 93**	Deauville, France	**Sabine Lauras,** Nicko & Cri Associés, 7 rue d'Argout, F-75002 Paris, France **Tel:** +33 1 42 33 47 66. **Fax:** +33 1 40 41 92 41
4–6	**9th Optical Fibre Sensors Conference**	Florence, Italy	**Annamaria Scheggi,** Instituto di Ricerce, Sulle Onde Elettromagnetiche, del Consiglio Nazionale delle Ricerche, Via Pancialichi, 64, Florence, Italy **Tel:** +39 55 43 78 512. **Fax:** +39 55 41 08 93
6–12	**Interpack'93 (Environmentally Justified Packaging)**	Düsseldorf, Germany	**Düsseldorfer Messegesellschaft mbH 'NOWEA',** P.O. Box 32 02 03, Stockumer Kirchstrasse 61, D-W-4000 Düsseldorf 30, Germany
9–14	**HPLC '93, 17th International Symposium on Column Liquid Chromatography**	Hamburg, Germany	**Gesellschaft Deutscher Chemiker,** Abteilung Tagungen, Varrentrappstrasse 40–42, Postfach 90 04 40, D-6000 Frankfurt am Main 90, Germany **Tel:** +49 69 79 17 360. **Fax:** +49 69 79 17 475
9–13	**EMAS '93—Modern Developments and Applications in Microbeam Analysis**	Rimini, Italy	**Abraham Boekestein,** Mansholtlaan 12, Postbus 356, D-6700 Wageningen, Germany
10–13	**International Environment '93 and Analysis '93**	London, UK	**Eileen Davies,** IE '93, 12 Alban Park, Hatfield Road, St Albans, Hertfordshire, UK AL4 0JJ **Tel:** +44 727 855574. **Fax:** +44 727 841694
11–15	**IV Encontro de Usuarios de RMN**	Rio de Janeiro, Brazil	**The Associacao de Usuarios de Ressonancia Magnetica Nuclear (Auremn),** A/C Sonia Maria Cabral de Menezes, Petrobras/Cempes/Diquim, Radial 2, Quadra 7, 21910.240 Cidade Universitaria, Ilha Do Fundao, Rio de Janeiro, RJ, Brazil
20–21	**4th International Meeting on Scnning Laser Ophthalmoscopy, Tomography and Microscopy**	Heidelberg, Germany	**Reinhard Burk or H. E. Volcker,** Augenklinik, Ruprecht-Karles-Universitat Heidelberg, Im Neunheimer Feld 400, 6900 Heidelberg, Germany **Tel:** +49 6221 56 66999. **Fax:** +49 6221 56 5422
23–28	**41st ASMS Conference on Mass Spectroscopy**	Las Vegas, NV, USA	**American Society for Mass Spectrometry,** P.O. Box 1508, East Lansing, MI 48826, USA **Tel:** +1 517 337 2548.
24–26	**11th Dechema Annual Meeting on Biotechnology**	Frankfurt, Germany	**Dechema,** P.O. Box 970146, D-W-6000 Frankfurt am Main 97, Germany

Date	Conference	Location	Contact
24–27	**15th International Symposium on Capillary Chromatography (ISCC)**	Riva del Garda, Italy	**Professor Dr. P. Sandra,** IOPMS, Kennedypark 20, B-8500 Kortrijk, Belgium **Tel:** +32 56 204960. **Fax:** +32 56 204859
24–29	**XV Mendeleev Congress on General and Applied Chemistry**	Minsk, Byelorussia	**Dr. V. N. Makatun,** Organizing Committee of the Mendeleev Congress, Presidium of Byelorussian Academy of Sciences, 66, F. Scorina Avenue, Minsk, Byelorussia
25–27	**Vth International Symposium on Quantitative Luminescence Spectrometry in Biomedical Sciences**	Ghent, Belgium	**Professor Dr. Willy R. G. Baeyens,** University of Ghent, Pharmaceutical Institute, Harelbekestraat 72, B-9000 Ghent, Belgium
25–27	**Control and Instrumentation Exhibition '93**	Birmingham, UK	**Stephen Ward,** Enterprise Public Relations, 165 Kensington High Street, London, UK W8 6SH
27–28	**2nd European Symposium on Analytical Supercritical Fluid Chromatography and Extraction (ESASF)**	Riva del Garda, Italy	**Professor Dr. P. Sandra,** IOPMS, Kennedypark 20, B-8500 Kortrijk, Belgium **Tel:** +32 56 204960. **Fax:** +32 56 204859
27–28	**European Conference on Environmental Pollution, Aquatic and Atmospheric Environment, Air/Water Quality, Hazardous Wastes and Hydrology**	Helsinki, Finland	**Dr. V. M. Bhatnagar,** Alena Chemicals of Canada, P.O. Box 1779, Cornwall, Ontario, Canada K6H 5V7 **Tel:** +1 613 932 7702.

June

Date	Conference	Location	Contact
2–4	**International Symposium on Analysis of Peptides**	Stockholm, Sweden	**The Swedish Academy of Pharmaceutical Sciences Symposium on 'Analysis of Peptides',** P.O. Box 1136, S-111 81 Stockholm, Sweden **Tel:** +46 8 24 50 85. **Fax:** +46 8 20 55 11
3	**NMR Symposium**	Turku, Finland	**Professor J. Mattinen,** Abo Akademi, Institution for Organisk Kemi, Akademig 1, SF-20500 Abo 50, Finland
3–4	**European Conference on Analytical Chemistry, Chromatography and Spectroscopy and Thermal Analysis**	Brno, Czechoslovakia	**Dr. V. M. Bhatnagar,** Alena Chemicals of Canada, P.O. Box 1779, Cornwall, Ontario, Canada K6H 5V7 **Tel:** +1 613 932 7702.
7–9	**ESIS '93: European Seminar on Infrared Spectroscopy**	Lyon, France	**G. Lachenal,** Laboratoire d'Etudes des Matériaux Plastiques et des Biomatériaux, Université Claude Bernard, Lyon 1, 43 Boulevard du 11 Novembre 1918, F-69622 Villeurbanne Cédex, France **Tel:** +33 72 43 12 11. **Fax:** +33 78 89 25 83
8–11	**The Seventh International LIMS Conference**	Egham, Surrey, UK	**The Conference Registrar,** 18 Portway Drive, West Wycombe, Buckinghamshire, UK HP12 4AU **Tel:** +44 494 448048. **Fax:** +44 494 448154
13–17	**6th European Congress on Biotechnology**	Firenze, Italy	**Congress Secretariat, c/o Professor Laura Frontali,** Department of Cell and Developmental Biology, University of Rome 'La Sapienze', P. le Aldo Moro 5, 00185 Rome, Italy **Tel:** +39 6 445 3950. **Fax:** +39 6 499 12351
13–17	**3rd Scandinavian Symposium on Chemometrics**	Arhus, Denmark	**SSC3 Secretariat,** Department of Chemical Technology, Danish Technological Institute, Teknologiparken, DK-8000 Arhus C, Denmark **Tel:** +45 86 14 24 00. **Fax:** +45 86 14 74 45
14–16	**PREP-93, 10th International Symposium on Preparative Chromatography**	Arlington, VA, USA	**Ms. Janet Cunningham,** Barr Enterprises, P.O. Box 279, Walkersville, MD 21793, USA **Tel:** +1 301 898 3772. **Fax:** +1 301 898 5596
14–20	**European Organization for Quality Control**	Helsinki, Suomi-Finland	**Mrs. Tarja Jalasto,** Finnish Society for Quality Control, Laaksolahdentie 41, P.O. Box 1, SF-02730 Espoo, Suomi-Finland
16	**Substances and Processes Dangerous to the Environment**	Preston, Lancashire, UK	**Dr. Paul Illing,** Health and Safety Executive, R425 Magdalen House, Stanley Precinct, Bootle, UK L20 3QZ **Tel:** +44 51 951 3420. **Fax:** +44 51 922 7918
17–18	**International Conference on Analytical Chemistry & Applied Chromatography/ Spectroscopy**	Toronto, Canada	**Dr. V. M. Bhatnagar,** Alena Chemicals of Canada, P.O. Box 1779, Cornwall, Ontario, Canada K6H 5V7 **Tel:** +1 613 932 7702.

Date	Conference	Location	Contact
27–1/7	Fullerenes '93, 1st International Interdisciplinary Colloquium on the Science and Technology of the Fullerenes	Santa Barbara, CA, USA	Gill Spear, Pergamon Seminars, c/o Elsevier Advanced Technology, Mayfield House, 256 Banbury Road, Oxford, UK OX2 7DH; Tel: +44 865 512242. Fax: +44 865 310981 or for North America, Kim Cavellero, Pergamon Seminars, 660 White Plains Rd., Tarrytown, NY 10591-5153, USA Tel: +44 865 512242. Fax: +44 865 310981
29–4/7	XXVIII Colloquium Spectroscopicum Internationale	York, UK	Dr. B. L. Sharp, Loughborough University of Technology, Department of Chemistry, Loughborough, Leicestershire, UK LE11 3TU

July

Date	Conference	Location	Contact
4–7	XXVIII CSI Post-Symposium: Graphite Atomizer Techniques in Analytical Spectroscopy	Durham, UK	XXVIII CSI Post-Symposium, Department of Chemistry, (CSI Secretariat), Loughborough University of Technology, Loughborough, Leicestershire, UK LE11 3TU Tel: +44 509 22575. Fax: +44 509 233163
4–8	6th International Conference on Indoor Air Quality and Climate, Indoor Air'93	Helsinki, Suomi-Finland	Professor Olli Seppänen, SF-02150 Espoo, Finland
4–9	22nd Meeting of the Federation of European Biochemical Societies	Stockholm, Sweden	Dr. Stefan Nordlund, FEBS '93, Department of Biochemistry, Arrhenius Laboratories, Stockholm University, S-10691 Stockholm, Sweden
11–14	International Symposium on Polymer Analysis and Characterization	Crete	Judith A. Sjoberg, Professional Association Management, 815 Don Gaspar, Sante Fe, NM, USA
11–15	Chemometrics III, 3rd Czechoslovak Chemometric Conference	Brno, Czechoslovakia	Dr. Josef Havel, Department of Analytical Chemistry, Masaryk University, Kotlarska 2, CS-61137 Brno, Czechoslovakia Tel: +42 5 712984. Fax: +42 5 740108
12–14	R & D Topics Meeting 1993	Bradford, W. Yorkshire, UK	Miss P. Hutchinson, Analytical Division, The Royal Society of Chemistry, Burlington House, Piccadilly, London, UK W1V 0BN Tel: +44 71 437 8656. Fax: +44 71 734 1227
19–21	6th Symposium on Handling of Environmental and Biological Samples in Chromatography	Guildford, Surrey, UK	M. Frei-Häusler, IAEAC Secretariat, Postfach 46, CH-4123 Allschwil 2, Switzerland Tel: +41 61 632789. Fax: +41 61 4820805
19–23	12th International Symposium on Nuclear Quadrupole Interactions	Zurich, Switzerland	Professor D. Brinkmann, Physik–Institut, University of Zurich, Schonberggasse 9, CH-8001 Zurich, Switzerland
25–29	107th AOAC Annual International Meeting and Exposition	Washington, DC, USA	Margaret Ridgell, AOAC, 2200 Wilson Boulevard, Suite 400, Arlington, VA 22201-3301, USA

August

Date	Conference	Location	Contact
9–11	3rd Soil and Sediment Residue Analysis Workshop	Winnipeg, Manitoba, Canada	Dr. G. R. Barrie Webster, Pesticide Research Laboratory, Department of Soil Science, University of Manitoba, Winnipeg, Manitoba, Canada R3T 2N2. Tel: +1 204 474 6039. Fax: +1 204 275 6019; or Professor Dr. Joseph Tarradellas, IGE, Federal Technical Institute EPF-L, CH-1015 Lausanne Ecublens, Switzerland
9–13	Asianalysis II: Second Asian Conference on Analytical Chemistry	Changchun, China	Professor Erkang Wang, Asianalysis II, Changchun Institute of Applied Chemistry, Chinese Academy of Sciences, P.O. Box 1022, Changchun, Jilin 130022, China Tel: +86 431 682 801 (ext. 562). Fax: +86 431 685 653
9–13	ILC '93: International Conference on Luminescence and Optical Spectroscopy on Condensed Matter	Storrs, CT, USA	Professor Douglas Hamilton, Physics Department, 2152 Hillside Road, University of Connecticut, Storrs, CT 06269-3046, USA

Entries in the above listing are at the discretion of the Editor and are free of charge. If you wish to publicize a forthcoming meeting please send full details to: *The Analyst* Editorial Office, Thomas Graham House, Science Park, Milton Road, Cambridge, UK CB4 4WF. Tel: +44 (0)223 420066. Fax: +44 (0)223 420247.

Conference Report

19th International Symposium on Chromatography: September 13–18, 1992, Aix-en-Provence, France

Although there are now a number of series of specialized conferences in various areas of separation science, the 19th meeting in the more wide-ranging series of 'International Symposia on Chromatography' attracted a large number of delegates. Analysts clearly perceive a need to keep informed of progress in a broadly based set of topics in chromatography and related areas. The lively and informative meeting lived up to expectations.

The Symposium began with the award of the Martin and Jubilee Medals of the Chromatographic Society to Professors J. Jorgenson (North Carolina) and K. Markides (Uppsala), respectively. Plenary Lectures were then presented describing the state-of-the-art in: chiral separation (D. W. Armstrong); field-flow fractionation (J. C. Giddings); capillary electrophoresis in bio-analysis (B. L. Karger); and isoelectric focusing (P. G. Rhighetti). These were followed by 62 oral presentations, some in parallel sessions, spread over five days. A necessarily subjective list of highlights includes: application of capillary GC with atomic emission detection (P. Sandra); narrow-bore capillary GC (V. Packova); analysis of polar substances by SFC (M. B. Evans and T. A. Berger); packed-bed hydrodynamic chromatography (J. C. Kraak); synthesis of functionalized polysiloxane stationary phases (H. Frank); chromatofocusing in protein analysis (C. Horvath); sample introduction in micellar electrokinetic chromatography (J. Vindevogel); biosensor and immunospecific detectors in liquid chromatography (G. Marko-Varga and F. E. Regnier); and coupled solid-phase extraction–GC–ECD in environmental analysis (R. A. Baumann). An increasing emphasis on microcolumn chromatography was evident from lectures by J. F. Chervet and O. I. Voroshilova.

Advances across the chromatographic range were described in over 300 posters. Here, applications dominated, especially in the analysis of environmental, biomedical, food and fuel samples; but practical and instrumental developments were also well to the fore, with new GC and HPLC phases, especially for chiral separations, detectors, coupled methods and chemometrics all strongly represented. Much attention was paid to sample preparation, particularly by supercritical fluid extraction. A poster by F. I. Onuska on microwave-assisted extraction attracted much interest.

The conference ended with a comprehensive Plenary Lecture by H. Mandery summarizing and contrasting the application areas of the various chromatographic techniques. Clearly chromatography continues to develop on several fronts and maintains its pre-eminent place in analytical laboratories.

The meeting was accompanied by a large exhibition of chromatographic instrumentation and accessories. Notable among these was the launch by Hewlett-Packard of a new instrument for supercritical fluid chromatography. This permits simultaneous programming of mobile phase composition, density and temperature. Operation in gas, liquid or supercritical mode is hence possible—the concept of 'borderless' chromatography.

The 20th International Symposium on Chromatography will be held in Bournemouth, UK, in September 1994.

K. D. Bartle
School of Chemistry,
University of Leeds,
Leeds, UK LS2 9JT

Chirality Medal

Nominations are invited for the Chirality Medal to be awarded in 1993 at the 4th International Symposium on Chiral Discrimination in Montreal, Quebec, Canada.

The Chirality Medal was instituted by the Italian Chemical Society in connection with the International Symposium on Chiral Discrimination in Rome in 1991.

This Medal is awarded to recognize distinguished achievement in any aspect of the field of Chiral Discrimination. Nominations, together with a short supporting statement, should be sent before April 30, 1993, to:

Professor A.F. Fell, *Secretary, Chirality Medal Honours Committee,*
Pharmaceutical Chemistry, University of Bradford, Bradford, UK BD7 1DP.

Future Issues will Include—

Determination of Trace Amounts of Phosphorus by Laser Excited Time-resolved Fluorimetry—**Ronghua Li and Zhauro Zhou**

Determination of Aluminium in Different Tissues of the Rat by Atomic Absorption Spectrometry With Electrothermal Atomization—**Aleksandar Radunovic, Michael W. B. Bradbury and H. Trevor Delves**

Determination of Ascorbic Acid by Flow Injection Analysis With Chemiluminescence Detection—**Abdulrahman A. Alwarthan**

Palladium–Magnesium Nitrate as a Chemical Modifier for the Determination of Lead in Mussel Slurries by Electrothermal Atomic Absorption Spectrometry—**P. Bermejo-Barrera, M. Aboal-Somoza, Rosa Maria Soto-Ferreiro and R. Domínguez-González**

Immobilization of Glutamate Oxidase on Non-porous Glass Beads. Automated Flow Injection System for the Assay of Glutamic Acid in Food Samples and Pharmaceuticals—**Stella M. Tzouwara-Karayanni, Constantine D. Stalikas and Miltiades I. Karayannis**

Novel Instrumentation and Biomedical Applications of Very Near Infrared Fluorescence—**M. B. Brown, Tony E. Edmonds, James N. Miller, D. P. Riley and Nichola J. Seare**

Enzymes for Amperometric Detection of Herbicides in Aquatic Environments—**Fiona A. McArdle and Krishna C. Persaud**

Incorporation of Hydroxamic Acid Ligands Into Nafion Film Electrodes—**Damien W. M. Arrigan, Brian Deasy, Jeremy D. Glennon, Brian Johnson and Gyula Svehla**

Determination of Zirconium and Molybdenum With 4,5-Dihydroxybenzene-1,3-disulfonic Acid Disodium Salt by Ion-pair Reversed-phase High-performance Liquid Chromatography—**Suh-Jen Jane, Tsai and Hsiao-Tzu Yan**

Molecular Recognition Using Conducting Polymers: Basis of a New Electrochemical Sensing Technology—**G. G. Wallace and P. R. Teasdale**

Determination of Iodide Ion in Impregnated Charcoals by Flow Injection—**Colin G. Taylor, Cheryl D. Monks and Duangjai Nacapricha**

Recovery of Sulphadimidine from Pig Feeds—**Peter Warwick, Neil T. Crosby and Ian M. Barwick**

An Account of Kinetic Determinations and Other Kinetic Aspects of Analytical Chemistry: from Córdoba to Erlangen—**Horacio A. Mottola**

Separation and Determination of Thiosulfate, Sulfite and Sulfide in Mixtures—**Tomozo Koh, Katsuaki Okabe and Yasuyuki Miura**

Poly(pyrrole) Based Amperometric Sensors: Theory and Characterization—**Michael E. G. Lyons, Cormac H. Lyons, Catherine Fitzgerald and Thomas Bannon**

Multi-layer Conducting Polymer Gas Sensor Arrays for Olfactory Sensing—**Jonathan M. Slater, J. Paynter and Esther J. Watt**

Evaluation of Coating Materials Used On Piezoelectric Crystals for the Detection of Dimethylsulfide in Liquefied Petroleum Gas—**K. Hawkesworth and John F. Alder**

Monitoring of Sulfur Dioxide Using a Piezoelectric Crystal Based Controller—**John J. McCallum, F. Benmakroha, T. Boudjerda, R. Boufenar, H. Allag and F. Djerboua**

Present State of Fabrication of Chemically Sensitive Field Effect Transistors—**Karel Domanský, Jiří Janata, Mira Josowicz and Danuta Petelenz**

Biosensor System Employing Acoustic Impulses in Thin Polymer Films—**P. W. Walton, P. M. Gibney, M. P. Roe, M. J. Lang and W. J. Andrews**

Sodium-selective Membrane Electrode Based on p-tert-Butylcalix[4]arene Methoxyethylester—**K. Cunningham, S. J. Harris, M. A. McKervey and Gyula Svehla**

Development of Interdigitated Acoustic Wave Transducers for Biosensor Applications—**D. Zhang, G. M. Crean, T. Flaherty and A. Shallow**

Novel Approach to the Development of Alkalinity and Acidity Detectors—**O. Lev and M. Tsionsky**

Laboratory of the Government Chemist, Past and Future—**Richard D. Worswick**

2nd National Symposium on Planar Chromatography: Modern Thin-Layer Chromatography

Co-Chairmen:
Professor Harold M. McNair and Professor Colin F. Poole

September 19-22, 1993
Research Triangle Park, North Carolina, USA

Further information may be obtained from:

Janet E. Cunningham, Barr Enterprises, P.O. Box 279,
Walkersville, MD 21793 USA
Phone: (301) 898-3772 - Fax: (301) 898-5596

ROYAL SOCIETY OF CHEMISTRY

NEW AND RECENT ANALYTICAL BOOKS

Spectrochemical Analysis by Atomic Absorption and Emission

By Lauri H.J. Lajunen
University of Oulu, Finland

This **new** book describes both the theory of atomic spectroscopy and all the major atomic spectrometric techniques (AAS, Flame-AES, Plasma AES, AFS and ICP-MS), including basic concepts, instrumentation and applications.

Spectrochemical Analysis by Atomic Absorption and Emission is very wide in scope and will be extremely useful to both undergraduates and lecturers undertaking modern analytical chemistry courses. It contains many figures and tables which illuminate the text, covers various sample preparation methods and gives suggestions for further reading.

Contents:
Introduction; Theory of Atomic Spectroscopy; Atomic Absorption Spectrometry; Flame Atomic Emission Spectrometry; Plasma Atomic Emission Spectrometry; Inductively Coupled Plasma Mass Spectrometry; Atomic Fluorescence Spectrometry; Sample Preparation; Advantages and Mutual Comparison of Atomic Spectrometric Methods; Further Reading; Subject Index.

Softcover	xii + 242 pages
ISBN 0 85186 873 8	Price £18.50
June 1992	

Analytical Ultracentrifugation in Biochemistry and Polymer Science

Edited by S.E. Harding
University of Nottingham

J.C. Horton
University of Nottingham

A.J. Rowe
University of Leicester

Analytical Ultracentrifugation in Biochemistry and Polymer Science is the first book of its kind to appear for nearly two decades and gives as comprehensive a coverage as is possible of the present state-of-the-art, from the leading experts in the field. It describes the advances currently being made and assesses to what extent 'classical' methods are still applicable, providing an up-to-date guide for potential users and experienced researcher alike.

The book divides naturally into four parts. Part I describes the state-of-the-art in instrumentation including a detailed consideration of optical systems and data capture and analysis procedures. Part II focuses on sedimentation equilibrium methods for obtaining molecular weight, polydispersity and interaction information. Part III considers transport methods (both sedimentation and diffusive) and includes a detailed consideration of rigid and flexible particle conformation analysis, polydisperse and interacting systems and concentration dependence phenomena. Part IV looks at a wide range of applications to macromolecular systems in biochemistry and polymer science, including seed and membrane proteins, polysaccharides and glycoconjugates and synthetic macromolecular systems.

This important **new** book is the consequence of an exciting resurgence of interest in the technique, will assist researchers in biochemistry and polymer science to make the most of the exciting opportunity that now exists.

Hardcover	xiv + 630 pages
ISBN 085186 345 0	Price £85.00
November 1992	

Particle Size Analysis

Edited by N.G. Stanley-Wood
University of Bradford

R.W. Lines
Coulter Electronics Limited, Luton

Particle Size Analysis reviews the development of particle characterization over the past 25 years and also speculates on its future. Interest in the subject has increased enormously over the years and this book highlights the changes and advances made within the field.

This book is comprehensive in its coverage of particle size analysis and includes contributions on such characterization techniques as microscopy using fractal analysis, light diffraction, light scattering with the phase doppler technique, light observation, and photon correlation spectroscopy. A number of chapters address the interest in on-line in-stream particle size analysis and illustrate the progress being made in achieving this long sought after ideal of *in-situ* in-process particle characterization. Applications to other technological fields are detailed by chapters covering biological systems and the pharmaceutical industry. The subject of surface area determination is considered with particular emphasis on the measurements on porosity of powders, the characterization and comparability of reference materials, and the need for standards.

Particle Size Analysis should provide stimulating reading for technologists, scientists, and engineers involved in particle characterization and powder technology worldwide.

Special Publication No. 102

Hardcover	xx + 538 pages
ISBN 0 85186 487 2	Price £57.50
June 1992	

Bioanalytical Approaches for Drugs
including Anti-asthmatics and Metabolites

Edited by Eric Reid
Guildford Academic Associates

I.D. Wilson
ICI Pharmaceutical Division, Macclesfield

Methodological Surveys in Biochemistry and Analysis
Volume 22

Series Editor Eric Reid
Guildford Academic Associates

Bioanalytical Approaches for Drugs, including Anti-asthmatics and Metabolites gives a state-of-the-art account of the subject and focuses on assaying blood and other biological samples, especially drugs which are given in low dosage or which yield metabolites that need subtle investigation. It covers advances in HPLC, SFC, CZE, MS and other detectors, NMR, and automated sample handling, as well as diverse drugs. The book also looks at problems such as analyte lability, stereoselectivity and interferants.

This book is the latest volume in the 'Analysis' sub-series of **Methodological Surveys in Biochemistry and Analysis**, which is acknowledged as an integrated reference source, and contains a cumulative analyte index. It will be essential reading for researchers involved in analytical, medicinal, pharmaceutical and bio-organic chemistry.

Special Publication No. 110

Hardcover	xiv + 356 pages
ISBN 0 85186 236 5	Price £75.00
September 1992	

Circle 004 for further information

FOLD HERE

THE ANALYST READER ENQUIRY SERVICE

MARCH'93

For further information about any of the products featured in the advertisements in this issue, please write the appropriate number in one of the boxes below.

Postage paid if posted in the British Isles but overseas readers must affix a stamp.

PLEASE USE BLOCK CAPITALS LEAVING A SPACE BETWEEN WORDS

Valid 12 months

1 NAME

2 COMPANY

PLEASE GIVE YOUR BUSINESS ADDRESS IF POSSIBLE. IF NOT, PLEASE TICK HERE ☐

3 STREET

4 TOWN

5 COUNTY
POST CODE

6 COUNTRY

7 DEPARTMENT/
DIVISION

8 YOUR JOB TITLE/
POSITION

9 TELEPHONE NO

OFFICE USE ONLY   REC'D ☐☐☐☐   PROC'D ☐☐☐☐

FOLD HERE

Postage will be paid by Licensee

Do not affix Postage Stamps if posted in Gt. Britain, Channel Islands, N. Ireland or the Isle of Man

2

BUSINESS REPLY SERVICE
Licence No. WD 106

Reader Enquiry Service
The Analyst
The Royal Society of Chemistry
Burlington House, Piccadilly
LONDON
W1E 6WF
England

ROYAL SOCIETY OF CHEMISTRY

Analyst

The Analytical Journal of The Royal Society of Chemistry

CONTENTS